University of Alberta

Transcriptional Regulation and Role of B-FABP and GFAP in Malignant Glioma

by

Jeffrey E. Coles ©

A thesis submitted to the Faculty of Graduate Studies and Research in partial fulfillment
of the requirements for the degree of

Master of Science

in

Medical Sciences - Oncology

Edmonton, Alberta

Fall 2004

Library and
Archives Canada

Published Heritage
Branch

395 Wellington Street
Ottawa ON K1A 0N4
Canada

Bibliothèque et
Archives Canada

Direction du
Patrimoine de l'édition

395, rue Wellington
Ottawa ON K1A 0N4
Canada

Your file Votre référence
ISBN: 0-612-95726-8
Our file Notre référence
ISBN: 0-612-95726-8

The author has granted a non-exclusive license allowing the Library and Archives Canada to reproduce, loan, distribute or sell copies of this thesis in microform, paper or electronic formats.

L'auteur a accordé une licence non exclusive permettant à la Bibliothèque et Archives Canada de reproduire, prêter, distribuer ou vendre des copies de cette thèse sous la forme de microfiche/film, de reproduction sur papier ou sur format électronique.

The author retains ownership of the copyright in this thesis. Neither the thesis nor substantial extracts from it may be printed or otherwise reproduced without the author's permission.

L'auteur conserve la propriété du droit d'auteur qui protège cette thèse. Ni la thèse ni des extraits substantiels de celle-ci ne doivent être imprimés ou aturement reproduits sans son autorisation.

In compliance with the Canadian Privacy Act some supporting forms may have been removed from this thesis.

While these forms may be included in the document page count, their removal does not represent any loss of content from the thesis.

Conformément à la loi canadienne sur la protection de la vie privée, quelques formulaires secondaires ont été enlevés de cette thèse.

Bien que ces formulaires aient inclus dans la pagination, il n'y aura aucun contenu manquant.

Canadä

ACKNOWLEDGEMENTS

First and foremost I would like to thank my parents, Ernie and Florence, for their support and encouragement throughout the numerous years of my university education. I firmly believe that you have instilled in me the thirst for knowledge and the drive to succeed, and for that I am grateful. I'd also like to acknowledge my younger brother Greg, who has always been one of my closest friends.

Much thanks go to my lab mates for providing an excellent work environment, including: Sachin Katyal, Mary Packer, Liz Monckton, Dr. John Rowe, Dr. Ji Hyeon Kim, and Rong Zong Liu. Without your assistance, advice and friendship, I am sure my experience as a graduate student would not nearly have been so enjoyable. As well, I would like to acknowledge Dr. Dwayne Bisgrove, who worked on the 'Malignant Glioma' project before my arrival in the lab.

Thanks also go out to my close friends: Ken Roy, Mike Fedeyko, Dawn Daley, Jennifer Freeman, David Kincade, Sachin Katyal, Sharon Barker and Holly Mewhort. Each of you has been a great friend throughout the years and I wish you all the best in your future endeavours.

I thank my committee members, Dr. Joan Turner and Dr. Gordon Chan, whose advice along the way has been very helpful and much appreciated.

Lastly, but most importantly, I would like to thank my supervisor Dr. Roseline Godbout for allowing me to work in her lab on a project that I have found both challenging and rewarding. Your guidance and encouragement was greatly appreciated (and necessary at times) and I will miss our thought provoking discussions.

TABLE OF CONTENTS

CHAPTER ONE – Introduction **1**

1.1. MALIGNANT GLIOMA AND GLIAL CELLS 1
- *1.1.1. Molecular Biology of Malignant Glioma* 2
- *1.1.2. Radial Migration and Glial Cell Differentiation* 5
- *1.1.3. Malignant Glioma Cell of Origin* 9

1.2. GLIAL FIBRILLARY ACIDIC PROTEIN (GFAP) 11
- *1.2.1. Molecular Aspects of GFAP* 12
- *1.2.2. GFAP Gene Regulation and Function* 14
- *1.2.3. GFAP and Malignant Glioma* 21

1.3. FATTY ACID BINDING PROTEINS (FABP) 24
- *1.3.1. FABPs of the Central Nervous System* 26
- *1.3.2. FABP Involvement in Growth and Differentiation* 28
- *1.3.3. FABPs: Membrane Interaction and Gene Transcription* 30
- *1.3.4. B-FABP Function* 32
- *1.3.5. B-FABP and Malignant Glioma* 33
- *1.3.6. B-FABP Gene Regulation* 34

1.4. NUCLEAR FACTOR I (NFI) 37
- *1.4.1. NFI Structure/Function Studies* 40
- *1.4.2. NFI Expression and CNS Specific Gene Regulation* 44

1.5. RESEARCH OBJECTIVES 45

Chapter 3: Characterization of B-FABP and GFAP transcriptional regulation by NFI proteins 45
Chapter 4: Effects of B-FABP and/or GFAP expression in malignant glioma cell lines 46

CHAPTER TWO – Materials and Methods **47**

2.1. GENERAL TISSUE CULTURE AND MOLECULAR BIOLOGY TECHNIQUES 47
- *2.1.1. Cell Lines and Culture Conditions* 47
- *2.1.2. Calcium Phosphate Transfection* 47
- *2.1.3. Whole Cell Extract Preparation* 48
- *2.1.4. Plasmid DNA Preparation* 48
- *2.1.5. Cesium Chloride Plasmid DNA Preparation* 49
- *2.1.6. Restriction Endonuclease Digestions* 50
- *2.1.7. DNA Insert and Oligonucleotide Purification by Electroelution* 50

2.1.8. *DNA Ligation and Bacterial Transformation* 51
2.1.9. *DNA Sequencing* 52
2.1.10. *RNA Preparation and Northern Blotting* 52
2.1.11. *Hybridization of Northern Blots and Probe Preparation* 53
2.1.12. *Western Immunoblotting and Protein Detection* 54

2.2. ANALYSIS OF THE *B-FABP* AND *GFAP* PROMOTERS 56

2.2.1. *Cloning of the* B-FABP *promoter* 56
2.2.2. *Cloning of the GFAP promoter* 56
2.2.3. *Transfection and Harvesting of the Malignant Glioma Cell Lines* 58
2.2.4. *CAT Assay* 59
2.2.5. *Preparation of Hirt DNA and Southern Blot Analysis* 59

2.3. ELECTROPHORETIC MOBILITY SHIFT ASSAY (EMSA) 60

2.3.1. *Generation of Annealed and Radiolabeled Oligonucleotides* 60
2.3.2. *Nuclear Extract Preparation* 62
2.3.3. *EMSA* 63
2.3.4. *Competition and Antibody Supershift Experiments* 64

2.4. ESTABLISHMENT OF SENSE B-FABP AND/OR GFAP STABLE TRANSFECTANTS 64

2.4.1. *Cell Lines and Plasmid Constructs* 64
2.4.2. *Transfection and Colony Selection* 65

2.5. RNA INTERFERENCE EXPERIMENTS 65

2.5.1. *Generation of the pSUPER, pSUPERDDX1 and pSUPERB-FABP Constructs* 65
2.5.2. *Cell Lines, Transfection, and Colony Selection* 67

2.6. CELL MORPHOLOGY EXPERIMENTS 67

2.7. PROLIFERATION RATE ASSAY 68

2.8. ANALYSIS OF ANCHORAGE-INDEPENDENT GROWTH 68

2.9. MATRIGEL INVASION ASSAY 69

2.9.1. *Invasion Assay for Malignant Glioma Cell Lines* 69
2.9.2. *Fixation, Staining, and Counting of Invasive Cells* 70

2.10. IMMUNOFLUORESCENCE OF TRANSFECTANTS 70

2.10.1. *Antibodies* 71
2.10.2. *Preparation of Coverslips and Antibody Staining* 71
2.10.3. *Confocal Microscopy* 72

CHAPTER THREE - Characterization of B-FABP and GFAP transcriptional regulation by NFI proteins 73

3.1 *Expression of NFI mRNA in Malignant Glioma* 73

3.2 *Protein Binding to the Putative NFI-Binding Sites in the GFAP promoter* 76

3.3 *Binding of Specific NFI Proteins to the NFI Sites in the B-FABP and GFAP promoters* 80

3.4 *Transcriptional Activation of B-FABP and GFAP by Specific NFI Proteins* 86

CHAPTER FOUR - Effects of B-FABP and/or GFAP expression in malignant glioma cell lines 92

4.1. *Isolation of the B-FABP and/or GFAP Stably Transfected T98 and U87 Malignant Glioma Clones* 92

4.2. *Immunofluorescence Analysis of B-FABP and/or GFAP in the T98 and U87 transfectants* 96

4.3. *Isolation of U251 Malignant Glioma Clones with Reduced B-FABP Levels* 103

4.4. *Morphological Alterations in the Malignant Glioma Clones* 104

4.5. *Subcellular Localization of B-FABP in the U87 Transfectants* 118

4.6. *Effects of B-FABP and/or GFAP Expression on Cell Proliferation* 118

4.7. *Correlation between B-FABP and/or GFAP Expression and Anchorage-independent Growth* 126

4.8. *Effects of B-FABP and/or GFAP Expression on the Invasive Potential of Malignant Glioma Cells* 135

CHAPTER FIVE – Discussion 151

5.1. REGULATION OF B-FABP AND GFAP EXPRESSION 151

5.1.1. NFI-binding Sites in the GFAP promoter 151
5.1.2. Role of NFI proteins in regulating B-FABP and GFAP expression 153
5.1.3. Importance of NFI phosphorylation status 158
5.1.4. B-FABP and GFAP Regulation in Glial Cells and Malignant Glioma 161

5.2. ROLE OF B-FABP AND GFAP EXPRESSION IN MALIGNANT GLIOMA 163

5.2.1. B-FABP Reduces the Growth and Invasive Potential of Malignant Glioma Cells 163
5.2.2. GFAP Reduces the Growth and Invasive Potential of Malignant Glioma Cells 167
5.2.3. Alterations in Morphology 169
5.2.4. Importance of Subcellular Localization 173

5.3. FUTURE DIRECTIONS 174

5.4. CONCLUDING REMARKS 176

CHAPTER SIX - References 177

LIST OF TABLES

Table	Title	Page
1.1	Characteristics of FABPs, their ligands and distribution	25
4.1	Doubling time for the T98, U87 and U251 cell lines and the transfectants	124
4.2	Colony counting results for the B-FABP and/or GFAP transfectants and the T98 and U87 cell lines	128
4.3	Number of cells that invaded through the Matrigel™ invasion chambers	137

LIST OF FIGURES

Figure **Title** **Page**

1.1 Classical and proposed glial and neuronal cell differentiation pathways 8

1.2 Potential *cis*- and *trans*-elements responsible for regulating *GFAP* promoter activity 16

1.3 Domains and alternative splicing of human and mouse NFI 39

2.1 Sequences of synthetic oligonucleotides 61

3.1 Northern blot analysis of 10 MG cell lines 75

3.2 Binding of NFI to G-br1, G-br2 and G-br3 78

3.3 NFI-A, -B, -C and -X binding to G-br1, G-br2 and G-br3 82

3.4 NFI-A, -B, -C and -X binding to B-br-1, B-br2 and B-br3 85

3.5 Analysis of *B-FABP* and *GFAP* promoter activity 87

3.6 Southern blot analysis of Hirt DNA from T98 cells transfected with the CAT reporter constructs 88

3.7 Transcriptional activation of B-FABP and GFAP CAT constructs by specific NFI proteins 90

4.1 Western blot analysis of B-FABP and GFAP in the T98 transfectants 95

4.2 Western blot analysis of B-FABP and GFAP in the U87 transfectants 97

4.3 Immunofluorescence analysis of B-FABP and/or GFAP in the T98 transfectants 100

4.4 Immunofluorescence analysis of B-FABP in the U87 transfectants 101

4.5 Western blot analysis of B-FABP and DDX1 in the pSUPER, pSUPER/B-FABP, and pSUPER/DDX1 transfectants 105

4.6 Morphology of the T98, U251 and U87 MG cell lines 106

4.7 Morphology of the T98-pREP4 transfectants 108

4.8 Alterations in morphology produced by the expression of B-FABP and/or GFAP in T98 cells 110

4.9 Effects of B-FABP expression on the morphology of U87 cells 114

4.10 Absence of processes in U251-pSUPER/B-FABP clones 117

4.11 Subcellular localization of B-FABP in the U87 transfectants 119

4.12 Growth rate curves for the T98 B-FABP and/or GFAP transfectants 121

4.13 Effect of B-FABP cDNA transfection on U87 MG proliferation 122

4.14 Reduced B-FABP expression in U251 MG does not affect proliferation 123

4.15 Growth of the T98 B-FABP and/or GFAP transfectants in soft agar 129

4.16 Colony forming ability of the U87 B-FABP transfectants in soft agar 132

4.17 Reduced B-FABP expression alters the growth of U251 cells in soft agar 134

4.18 Invasion of the T98 transfectants through Matrigel™ after 22 hours 136

4.19 Percentage of invasive cells for the T98 transfectants relative to the T98-pREP4-5 clone 138

4.20 Reduced B-FABP expression does not alter the invasive behaviour of U251 cells 140

4.21 Invasion of the T98 transfectants through Matrigel™ after 30 hours (Trial 1) 142

4.22 Invasion of the T98 transfectants through Matrigel™ after 30 hours (Trial 2) 143

4.23 Percentage of invasive cells for the T98 transfectants relative to the T98-pREP4-6 clone after 30 hours 145

4.24 Invasion of the U87 transfectants through Matrigel™ after 30 hours (Trial 1) 146

4.25 Invasion of the U87 transfectants through Matrigel™ after 30 hours (Trial 2) 147

4.26 Invasion of the U87 transfectants through Matrigel™ after 30 hours (Trial 3) 148

4.27 Percentage of invasive cells for the U87 transfectants relative to the U87-pREP4-3 clone 150

INDEX OF ABBREVIATIONS AND SYMBOLS

~	approximately
A	adenosine
aa	amino acid(s)
A-FABP	adipocyte-fatty acid binding protein
AMP	ampicillin
AP-1	activator protein 1
AP-2	activator protein 2
APS	ammonium persulfate
ATCC	American Type Culture Collection
ATP	adenosine-5'-triphosphate
BAC	bacterial artificial chromosome
B-br	binding region (in B-FABP promoter)
B-FABP	brain-fatty acid binding protein
bp	base pair(s)
BPB	bromophenol blue
BSA	bovine serum albumin
°C	celcius
C	cytosine
C_f	final concentration
$CaCl_2$	calcium chloride
cAMP	cyclic adenosine monophosphate
CAT	chloramphenicol acetyltransferase
cat.	catalogue
CEL	carboxyl ester lipase
cDNA	complementary DNA
C-FABP	cutaneous-fatty acid binding protein
CNS	central nervous system
CO_2	carbon dioxide
CPTS	copper phthalocyanine tetrasulfonic acid
CRABP	cellular retinoic acid-binding protein
CRBP	cellular retinol-binding protein
CRE	cAMP-responsive element
CREB	CRE binding protein
CTD	C-terminal domain
CTF	CCAAT transcription factor
CsCl	cesium chloride
C-terminal	carboxy terminal
d	day(s)
dCMP	2'-deoxycytosine-5'-monophosphate
Da	dalton(s)
DAPI	4',6-diamidino-2-phenylindole

DBD	DNA binding domain
dCTP	2'-deoxycytosine-5'-triphosphate
DDX1	DEAD box 1
DEAD	aspartic acid(D)-glutamic acid(E)-alanine(A)-aspartic acid(D)
DHA	docosahexaenoic acid
DMEM	Dulbecco's modified eagle medium
DMSO	dimethyl sulfoxide
DNA	deoxyribonucleic acid
DRGE	dorsal root ganglion enhancer
DSCS	dorsal spinal cord silencer
DTT	dithiothreitol
ECM	extracellular matrix
ED	embryonic day
EDTA	ethylenediaminetetraacetic acid
E-FABP	epidermal-fatty acid binding protein
EGF(R)	epidermal growth factor (receptor)
EMSA	electrophorectic mobility shift assay
EtBr	ethidium bromide
FA	fatty acid
FABP	fatty acid binding protein
FAT	fatty acid translocase
FCS	fetal calf serum
fmol	femtomole
fp	footprint
g	gram
g	acceleration of gravity
G	guanosine
GGF	glial growth factor
G418	geneticin 418
GBM	glioblastoma multiforme
G-br	binding region (in GFAP promoter)
GFAP	glial fibrillary acidic protein
h	hour(s)
HA	hemagglutinin
HCl	hydrochloric acid
HEPES	N-(2-hydroxyethyl)piperazine-N'-(2-ethanesulfonic acid)
H-FABP	heart-fatty acid binding protein
hgcs	human *gfa* common sequence
H_2O	water
HRE	hormone response element
IPTG	isopropylhio-β-D-galactoside
IF	intermediate filament
I-FABP	intestinal-fatty acid binding protein

IL-6	interleukin-6
iLBP	intracellular lipid-binding protein
IL-FABP	ileal-fatty acid binding protein
ITP	intrinsic transactivation potential
kb	kilobase(s) or kilobase pair(s)
KCl	potassium chloride
kDa	kilodaltons
KH_2PO_4	potassium phosphate monobasic
KO	knock out
KoAc	potassium acetate
KOH	potassium hydroxide
LB	Luria-Bertani medium
LCFA	long-chain fatty acid
L-FABP	liver-fatty acid binding protein
LOH	loss of heterozygosity
LSM	laser scanning microscope
M	molar
mA	milliamps
MDGI	mammary derived growth inhibitor
min	minute(s)
M-FABP	myelin-fatty acid binding protein
MG	malignant glioma
$MgCl_2$	magnesium chloride
MgoAc	magnesium acetate
$MgSO_4$	magnesium sulfate
mC_i	millicurie
mg	milligram
ml	milliliter
mm	millimeter
mM	millimolar
mmol	millimole
MMP	matrix metalloproteases
MOPS	3-(N-morpholino)propanesulfonic acid
mRNA	messenger RNA
MW	molecular weight
μg	microgram
μl	microliter
NaCl	sodium chloride
NaH_2PO_4	sodium dihydrogen phosphate
$Na_2HPO_4 \bullet 7\ H_2O$	sodium phosphate dibasic heptahydrate
$Na_2H_2P_2O_7$	sodium pyrophosphate dibasic
NaoAc	sodium acetate
NaOH	sodium hydroxide

NH_4oAc	ammonium acetate
NFI	nuclear factor I
ng	nanogram
nm	nanometer
nM	nanomolar
NP-40	nonidet P-40
NRG	neuregulin
NSC	neuroepithelial stem cell
N-terminal	amino terminal
nt	nucleotide(s)
NT	nick translation
OD_{260}	optical density at 260 nm
OD_{590}	optical density at 590 nm
P	postnatal day
^{32}p	radioactive phosphate
PAGE	polyacrylamide gel electrophoresis
PBS	phosphate buffered saline
Pbx	paired box protein
PCNA	proliferating cell nuclear antigen
PCR	polymerase chain reaction
PDGF(R)	platelet-derived growth factor (receptor)
pH	potential of hydrogen
pmol	picomole
PMSF	phenylmethanesulfonyl fluoride
PNK	polynucleotide kinase
PPAR	peroxisome proliferator-activated receptor
PTEN	phosphatase and tensin homology
PUFA	polyunsaturated fatty acid
PVP	polyvinylpyrrolidone
RB	retinoblastoma
RGE	radial glial enhancer
RNA	ribonucleic acid
RNAi	RNA interference
ROK	rho-associated kinase
rpm	revolutions per minute
RT	room temperature
RXR	retinoid X receptor
SDS	sodium dodecyl sulfate
sec	second(s)
siRNA	small interfering RNAs
SSC	standard saline citrate
ssDNA	single strand DNA
STAT3	signal transducer and activator of transcription 3

T	thymidine
TBE	tris-borate-EDTA
TE	tris/EDTA
TEG	tris-EDTA-glucose
TEMED	N,N,N',N'-tetramethylethylenediamine
TFIIB	transcription factor IIB
T-FABP	testicular-fatty acid binding protein
TIMP	tissue inhibitors of matrix metalloproteinases
TP53	tumour protein p53
Triton X-100	polyethylene glycol tert-octylphenylether
tRNA	transfer-RNA
U	unit(s)
uPA(R)	urokinase-type plasminogen activator (receptor)
UV	ultra-violet
V	volt(s)
vim	vimentin
WHO	World Health Organization
X-gal	5-bromo-4-chloro-3-indoyl-β-D-galactoside

CHAPTER ONE

Introduction

1.1. Malignant Glioma and Glial Cells

The mammalian central nervous system (CNS) is comprised primarily of two different cell populations: neurons and glia. While the function of the neurons is to transmit signals along the nervous system, the glial cells serve a supportive role and are essential for the normal functioning of neurons. Glial cells outnumber neurons in the CNS by approximately ten- to fifty-fold and are divided into three subpopulations based on morphology and function: astrocytes, oligodendrocytes and microglia (Louis *et al.*, 2001). Of all the glial cells, the astrocytes are the most abundant and serve several important functions including the regulation of synapse formation and synapse transmission (Hansson and Ronnback, 1994; Nakanishi *et al.*, 1994).

Neoplasms of the CNS that arise from the glial cells are called gliomas, and these tumours comprise nearly 60% of all human CNS malignancies (Dai and Holland, 2003). According to the World Health Organization (WHO), there are three main types of gliomas which are distinguished by their histological features and probable cell-type of origin: astrocytomas, oligodendrogliomas, and mixed oligoastrocytomas. The WHO has also developed a four point grading scheme according to tumour anaplasia, ranging from the most benign (grade I) to the most malignant (grade IV). Commonly, low-grade gliomas are classed as WHO grades I and II, while high-grade gliomas are WHO grades III and IV (Behin *et al.*, 2003). Astrocytomas, the most common form of gliomas in humans, include pilocytic astrocytoma (grade I), diffuse astrocytoma (grade II), anaplastic astrocytoma (grade III), and glioblastoma multiforme (GBM; grade IV).

The grades III and IV astrocytomas are commonly referred to as malignant gliomas (MGs), and these are the most common and most aggressive human brain tumours. Despite advances in treatment (surgery, radiation therapy, and/or chemotherapy) the median survival for patients diagnosed with GBM remains less than 1 year and approximately 2-3 years for those patients diagnosed with anaplastic astrocytoma. In addition, the fate of most low grade astrocytomas is to eventually undergo malignant transformation to a high grade astrocytoma. Low-grade astrocytomas that have progressed to MG are termed secondary MG, while tumours that present as MG at first diagnosis are called primary MG. The dismal failure of traditional treatment for patients with MG has prompted many studies to examine the molecular genetics of these tumours, and significant progress has been made in this area.

1.1.1. *Molecular Biology of Malignant Glioma*

Several genetic alterations have been identified in human MG tumours, most of which are associated with two important cellular processes: signal transduction and cell cycle arrest. In GBM, loss of heterozygosity (LOH) has been detected on chromosomes 6, 9, 10, 13, 17, 19, and 22, as well as amplification of parts of chromosomes 1, 5, 7, 8, 11 and 12 (reviewed in Benjamin *et al.*, 2003). Therefore, numerous genes are likely involved in the initiation and/or progression of MG. Of particular note, Kleihues and Ohgaki (1999) have reported that inactivation of *TP53* and overexpression of *PDGFR* play a crucial role in the initial steps of the evolution to secondary MG. Also, Bigner and coworkers (1988) determined that alterations in chromosomes 9p and 19q are significant events in malignant progression. Located on 9p is the tumour suppressor *p16*, a cyclin dependant kinase inhibitor that has been implicated in many different tumour types (Kamb *et al.*, 1994).

For both primary and secondary MG, LOH of chromosome 10q is present in 80-90% of glioblastomas. Several candidate genes have been identified in this region, including the *PTEN* gene which is mutated in 20-30% of glioblastomas (Zhou *et al.*, 1999). In regards to signal transduction, the *EGFR* gene is amplified in 40-50% and overexpressed in ~80% of primary glioblastomas (Libermann *et al.*, 1985), while the *PDGFR-α* gene is amplified in ~10% of secondary glioblastomas (reviewed in Benjamin *et al.*, 2003).

One of the main attributes that distinguishes high-grade gliomas from low-grade gliomas is the presence of local tissue invasion in high-grade gliomas. In high-grade astrocytomas, microscopic evidence of malignant cells can often be found well beyond the margins of the tumour (Burger, 1983). The ability of tumour cells to invade into the local environment depends on several criteria including their ability to interact with the extracellular matrix (ECM), to degrade the ECM through the release of proteolytic enzymes, and to migrate through the area of destruction. The matrix metalloproteinases (MMPs) are a family of enzymes that degrade a variety of ECM molecules such as proteoglycans, glycoproteins, and collagen (Matrisian, 1992). Interestingly, immunohistochemical studies performed by Nakagawa and coworkers (1994) have demonstrated that MG tumours express MMPs, while normal brain tissue and low-grade astrocytomas do not. Furthermore, several researchers have shown that the activity of these MMPs correlate with the destructive and invasive properties of these tumours *in vitro* and *in vivo,* with MMP-2 being the most important in glioma invasiveness (reviewed in Ware *et al.*, 2003). Also, *ex vivo* data suggest that the expression of the tissue inhibitors of matrix metalloproteinases (TIMPs) inversely correlate with the invasiveness of astrocytomas (Nakagawa, 1994; Mohanam *et al.*, 1995).

Similar to the MMPs, both the serine protease urokinase-type plasminogen activator (uPA) and its receptor (uPAR) display increased expression levels and activity with increasing glioma anaplasia (Gladson *et al.*, 1995; reviewed in Rao, 2003). The expression of uPAR in MG cell lines has been shown to contribute to their invasive potential and uPAR appears to be localized to the focal contacts at the leading edges of the tumour (Gladson *et al.*, 1995). These features have made the uPA-uPAR interaction a key target for the treatment of MG and reports have indicated that the reduced expression of uPA and uPAR leads to tumour growth inhibition (Engelhard *et al.*, 1996; reviewed in Rao, 2003).

Recently, the development of the microarray technique has provided a potential method for distinguishing different types or grades of tumours through the gene expression profiling of tumour tissue. While still in its infancy, this technique has already been used to identify distinctive molecular patterns in high-grade and low-grade gliomas (Rickmann *et al.*, 2001), and could eventually lead to the identification of signature gene sets indicative of a specific tumour grade. For instance, using microarray analysis, Wang *et al.* (2003) identified an increased expression of insulin growth factor binding protein 2 (IGFBP2) in high-grade gliomas (*i.e.* GBM). Furthermore, these researchers show that IGFBP2 expression enhances MMP-2 gene transcription and, in turn, tumour cell invasion.

While there is a correlation between specific genetic alterations with tumour grade (I-IV) and/or course of MG progression, not all tumours within a category display the same genetic changes. Prognostic values for MG based on genetic markers have met with only mixed acceptance. For example, some studies correlate *EGFR* overexpression with poor prognosis (Etienne *et al.*, 1998), while others could not substantiate these results (Newcomb *et al.*, 1998). To date, the best predictors of survival for MG patients are patient age and histologic grade. However, new insights into the parallels between glial differentiation and glioma formation indicate that the differentiation machinery is still present in MG tumours, and a target for therapy could be the induction of these differentiation pathways. Therefore, a better understanding of the mechanisms underlying glial cell differentiation may provide valuable information as to how these tumours can be treated more effectively.

1.1.2. *Radial Migration and Glial Cell Differentiation*

During the development of the CNS, the primary function of glial cells is to provide a scaffold for the directed migration of neurons (reviewed in Hatten, 1999). In fact, *in vitro* (Edmunson and Hatten, 1987) and *in vivo* (Gao and Hatten, 1993, 1994) studies indicate that 80-90% of the billions of neuronal precursor cells migrate along radial glial fibers. To perform this function, the radial glial cells, identified by their expression of brain-fatty acid binding protein (B-FABP) (Feng *et al.*, 1994) and antigens recognized by RC1 (Edwards *et al.*, 1990) and RC2 (Misson *et al.*, 1988a), extend processes that span the wall of the developing neural tube (reviewed in Hatten, 1999). Postmitotic neurons utilize these radial glial processes for migration (Rakic, 1971, 1972). Therefore, for the neurons to become fully differentiated, they must first initiate a differentiation program that allows for cell movement, and secondly, as the neurons migrate along the radial glial scaffold, they must undergo the final steps of differentiation (reviewed in Hatten, 1999).

The neuronal migration program appears to be regulated, at least in part, by members of the EGF family of growth and differentiation factors called neuregulins (NRGs). NRGs are expressed and secreted mostly by the differentiating neurons (Corfas *et al.*, 1995) and bind to the erbB receptors on the radial glial cells (Anton *et al.*, 1997). Glial growth factor (GGF), a soluble NRG, has been shown by Anton and coworkers (1997) to participate in the induction of the radial glial cell morphology, possibly through the activated expression of B-FABP. *In vitro* studies suggest that B-FABP is essential for the establishment and maintenance of radial glial fibers during neuronal migration and that B-FABP may also play a role in neuronal differentiation (Feng *et al.*, 1994; Kurtz *et al.*, 1994; Feng and Heintz, 1995). Similar to the role of NRGs in stimulating the radial glial specific phenotype, glia-derived signals have been proposed to regulate neuronal differentiation. For example, Toresson and colleagues (1999) have shown that retinoic acid produced by radial glial cells in the lateral ganglionic eminence can influence the differentiation of neurons migrating into the developing striatum. Thus, the neuron-glia relationship is very important in both neuronal migration and the differentiation of both of these cell types.

The classical view of glial cell differentiation holds that both the astroglial and neuronal cell lineages diverge early in development, prior to neuronal migration, from the multipotent, self-renewing neuroepithelial stem cells (NSC) (Levitt and Rakic, 1980). While it is still uncertain how astrocytes and neurons arise from NSCs, it is generally accepted that NSCs first produce neuronal precursors (Figure 1.1; Gage, 2000; Okano-Uchida, 2004). Whether these neuronal precursors, which are highly proliferative, give rise directly to the glial lineage, or whether the glial lineage arises from the NSCs or another precursor cell type remains controversial. Okano-Uchida and coworkers (2004) have shown that granule cell precursors, a neuronal precursor, can be induced to differentiate into astroglial cells *in vitro*. However, studies by Rao and Mayer-Proschel (1997) have shown a direct lineage relationship between NSCs and glial restricted precursor cells (reviewed in Lee *et al.*, 2000). Regardless of the origin of the glial cell lineage, the classical view of glial cell differentiation holds that after migration is complete, the radial glial cells transform into mature astrocytes through the generation of intermediary transitional astroglial forms (Schmechel and Rakic, 1979; Culican *et al.*, 1990).

However, this strict view of radial glial differentiation into astrocytes is not held by all researchers. Alvarez-Buylla and colleagues (1990) suggest that mitotically active radial glia may also give rise to neurons (reviewed in Parnavelas and Nadarajah, 2001). In support of this theory, radial glia have been shown to display characteristics unique to precursor cells, including the ability to undergo interkinetic nuclear migration (Misson *et al.*, 1988b). Also,

Figure 1.1 - Classical and proposed glial and neuronal cell differentiation pathways. The classical view (solid black arrows) holds that neuroepithelial stem cells (NSC) produce two separate pools of committed progenitor cells, glial and neuronal, each of which further differentiate to produce the mature astrocytes and neurons, respectively. However, more recently, it has become generally accepted that the NSCs first give rise to neuronal precursors (red dotted lines). It is not clear whether the neuronal precursors differentiate into glial cells, but *in vitro* data suggest that it is possible. Other proposed pathways (black dotted lines) suggest that NSCs directly produce radial glial cells, and that these radial glial cells can serve as precursor cells and divide asymmetrically to produce neurons, either directly or via the neuronal precursors. In mammals, the radial glial cells are believed to transform into astrocytes perinatally. This period coincides with neuronal migration (blue arrows), whereby postmitotic neurons migrate along radial fibers and differentiate into mature neurons. Recently, astrocytes have also been observed to have stem cell characteristics in that, prior to the mouse postnatal day 11, they can give rise to neurospheres containing multipotential precursors and to radial glial cells. However, this ability is lost in adulthood, except in the subventricular zone where astrocytes continue to produce neurons and glia.

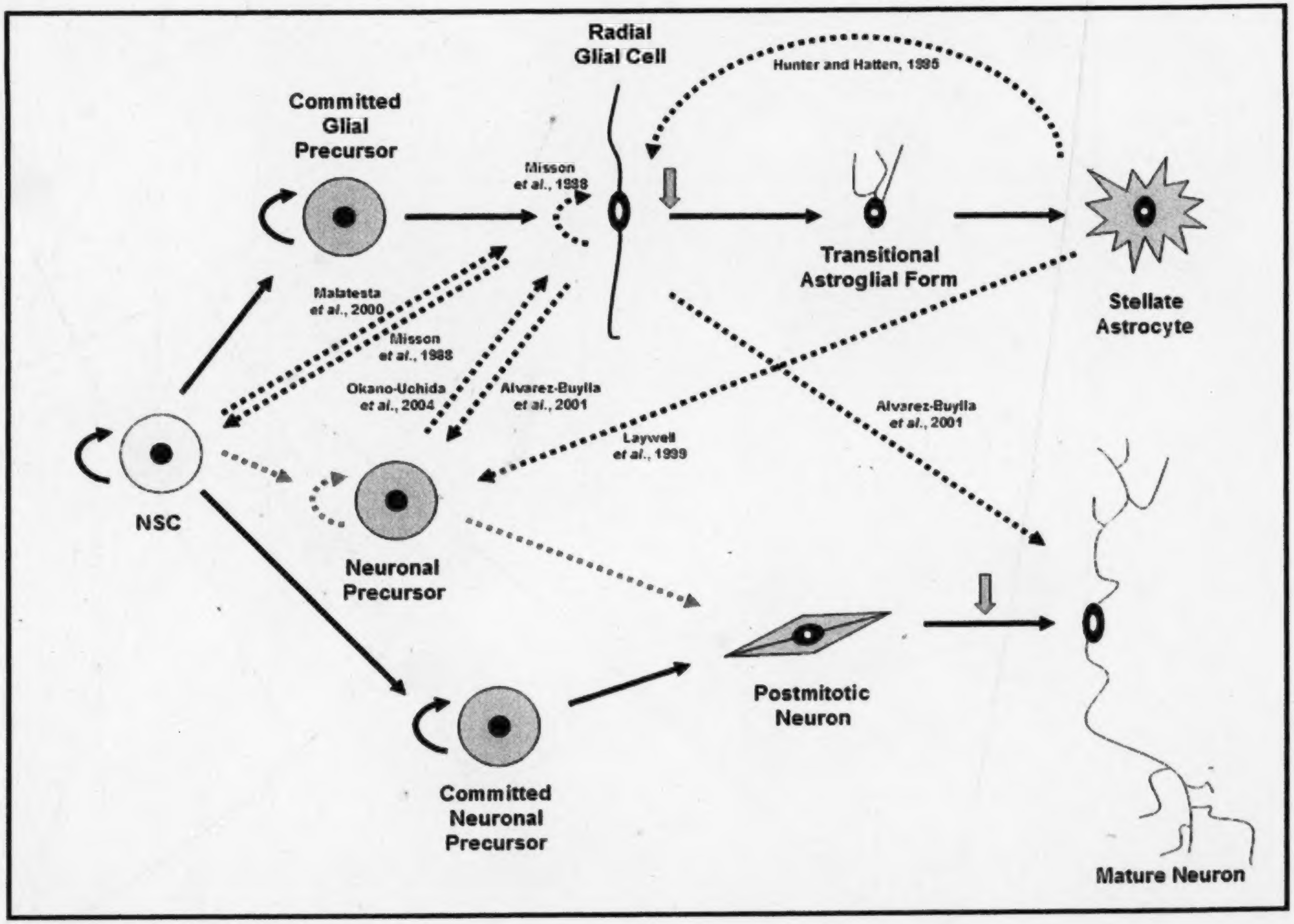
Radial
Glial Cell
Hunter and Hatten, 1985
Committed
Glial
Precursor
Misson
et al., 1988
Transitional
Astroglial Form
Stellate
Astrocyte
Malatesta
et al., 2000
Misson
et al., 1988
Okano-Uchida
et al., 2004
Alvarez-Buylla
et al., 2001
Alvarez-Buylla
et al., 2001
Laywell
et al., 1999
NSC
Neuronal
Precursor
Postmitotic
Neuron
Committed
Neuronal
Precursor
Mature Neuron

radial glia isolated from mouse cortex have the ability to produce both neurons and glial cells *in vitro* (Malatesta *et al.*, 2000), with neurons migrating along their own parent radial glial fiber (Noctor *et al.*, 2001). These findings suggest that radial glial fibers have a dual role in the development of the CNS: initially, radial glial cells serve to produce neurons (ED 14-16 in mouse); by ED18, radial glial cells provide migration guidance as neurons migrate along their own parent radial glial fiber (reviewed in Parnavelas and Nadarajah, 2001). However, these studies and others typically identify radial glial cells by their antigenic properties and/or bipolar morphology, and it should be remembered that these characteristics are shared by both radial glial cells and neuroepithelial cells (Parnavelas and Nadarajah, 2001).

While the pathways of glial cell differentiation are somewhat controversial, there is a general consensus that the expansion of the multipotent neuroepithelial stem cells and the restriction of cell fate are controlled, at least partly, by soluble factors that regulate gene expression (reviewed in Jessell and Melton, 1992; Green, 1994). For instance, Burrows and coworkers (2000) have shown that overexpression of EGFR favours astroglial differentiation and leads to an increased number of astrocytes. Furthermore, Hunter and Hatten (1995) have shown that the transformation from radial glial cell to astrocyte is reversible, and that this process is regulated by a soluble, diffusible signal, termed radializing factor (RF60) (reviewed in Chanas-Sacre *et al.*, 2000)

1.1.3. *Malignant Glioma Cell of Origin*

The bidirectional transformation of radial glial cells to astrocytes provides support for the belief that astrocytes are the cell of origin for MG. Although the cellular origin of MG is controversial, astrocytomas are believed to arise from astrocytes because they produce bundles of glial fibrillary acidic protein (GFAP), a protein specifically associated with astrocytes (Eng, 1980; Gottschalk and Szymas, 1987). As the cell of origin of MG, a mature astrocyte would have to dedifferentiate into a neoplastic version of an immature glial cell (reviewed in Linskey and Gilbet, 1995). Therefore, if mature astrocytes can readily dedifferentiate under normal physiological conditions in response to extrinsic signals, it is even more plausible that they can dedifferentiate during neoplastic transformation.

Although the majority of astrocytomas express GFAP (Gottschalk and Szymas, 1987), it is not universally believed that this is a definitive sign that the astrocytoma arose from an astrocyte. Several investigators have reported that neural stem cells either express, or have expressed GFAP at some point in development (Zhou *et al.*, 2001; Imura *et al.*, 2003). Also, recent studies indicate that GFAP expression does not necessarily correlate with that of other markers of astrocytic differentiation or function, including the Ca^{2+}-binding protein S100β (discussed in Goldman, 2003; Barres, 2003). In fact, Goldman (2003) has proposed that it may be more accurate to view GFAP as a protein expressed in immature progenitor cells of the CNS, as well as in mature astrocytes. This concept underlies a second hypothesis for the cell of origin of MG, which postulates that there remains present, in the adult CNS, a pool of dormant, undifferentiated stem cells. With the onset of cancer, these undifferentiated stem cells differentiate into a neoplastic version of a glial precursor cell with an unlimited proliferative capacity (reviewed in Linskey and Gilbert, 1995).

As a third hypothesis, one can envision MG arising from the intermediary transitional glial forms generated when radial glial cells differentiate into mature astrocytes (Hunter and Hatten, 1995). These cells are not fully differentiated, and already display several characteristics necessary for malignancy, including high proliferative and migratory capabilities. Also, since these cells are in the process of differentiating into mature astrocytes, it is likely that they would express GFAP.

While each of these three hypotheses for the cell of origin is valid, it is important to recall that astrocytes are the most abundant cell population in the CNS, and thus a very probable candidate for the cell of origin of MG.

1.2. Glial Fibrillary Acidic Protein (GFAP)

The glial fibrillary acidic protein (GFAP) is an intermediate filament (IF) protein that was initially purified by Eng and colleagues from multiple sclerosis brain tissue (1970) and fibrous astrocytes (1971). On the basis of their tissue-restricted distribution and sequence identity, IF proteins have been divided into five main classes, type I – V (reviewed in Fuchs, 1996). The type I and type II IF proteins are the keratins, type IV are the neurofilaments, and the type V IF proteins are referred to as lamins. GFAP is a member of the type III IF proteins, a group that also includes: desmin, peripherin, nestin, and vimentin. While GFAP is found almost exclusively in differentiated astrocytes of the mature CNS, several studies have also documented its expression in other cell types such as radial glial cells of cerebellum (Bergmann glia) (Eng *et al.*, 2000), neural stem cells (Zhou *et al.*, 2001; Imura *et al.*, 2003), and the majority of MG tumours (Gottschalk and Szymas, 1987).

Similar to all other members of the IF superfamily, GFAP consists of an α-helical rod domain flanked by a non-helical head (N-terminal) and tail (C-terminal) domain (Reeves *et al.*, 1989). The highly conserved structure of the rod domain allows the IF proteins to intertwine in a coiled-coil fashion to generate the dimer subunit structure of the 8-10 nm filaments (reviewed in Fuchs and Weber, 1994). With the exception of the keratins, it is typically homodimers that are formed through this interaction, but heterodimers have also been observed (Quinlan *et al.*, 1986). These dimers associate in an antiparallel fashion to form tetramers with staggered ends. At this stage in IF assembly, it has been shown that the non-helical end domains are necessary for the tetramers to form higher-order structures

(Kaufmann *et al.*, 1985; Quinlan *et al.*, 1989). More specifically, in regards to GFAP, it has been shown that an intact head domain and all but the C-terminal one fifth of the tail domain are necessary for GFAP self-assembly and for GFAP-vimentin co-assembly (Chen and Liem, 1994a).

To generate the higher-order IF structures, the tetramers link together in a head-to-tail fashion to create protofilaments, two protofilaments intertwine to form a protofibril, and four protofibrils intertwine to generate the 10 nm filament (reviewed in Fuchs, 1996). These 10 nm IFs, along with the microtubules and microfilaments, are then organized into a tridimensional scaffold in the cytoplasm where they are believed to provide mechanical stability. In addition, due to their diverse pattern of expression, it is speculated that specialized functions are still to be defined for many IF proteins (reviewed in Fuchs, 1996). In support of this theory, the expression of vimentin and GFAP is tightly regulated during development (Lazarides, 1982). Vimentin is expressed in radial glial cells and immature astrocytes, but as astrocyte differentiation takes place, its expression is replaced by GFAP (Dahl *et al.*, 1981; Bignami *et al.*, 1982). This switch from one type III IF to another suggests a specific role for each in astrocyte differentiation. In an attempt to determine specialized roles for the *GFAP* genes, several studies have been performed examining their molecular structure.

1.2.1. *Molecular Aspects of GFAP*

GFAP is present as a single copy in the human genome, located on chromosome 17q21. The sequence of the human *GFAP* gene shows strong homology (~85%) to that of other species including: mouse, rat, and pig (Geisler and Weber, 1983; Balcarek and Cowan, 1985; Reeves *et al.*, 1989; Brenner *et al.*, 1990; Isaacs *et al.* 1998). In addition, intron sizes and the 5'-flanking sequence (*i.e.* promoter region) are similar in mouse and human *GFAP*

(Isaacs *et al.* 1998). While nearly all studies thus far examining transcriptional regulation and function have explicitly measured the dominant GFAP isoform, GFAPα (typically referred to as GFAP), four other *GFAP* transcripts have been identified: *GFAP*-β, -γ, -δ, -ε. Each of the *GFAP* transcripts appears to be generated by the usage of alternative transcriptional start sites and/or differential splicing (discussed in Condorelli *et al.*, 1999; Nielsen *et al.*, 2002).

The transcriptional start site of *GFAPα* is located 14 bp upstream of the translation start site. The *GFAPα* transcript is 2.9 kb long and produces a 432-amino acid-long polypeptide of 55 kDa (Brenner *et al.*, 1990). This transcript is encoded by 9 exons spread over a 10-kb genomic region (Isaacs *et al.*, 1998). The *GFAPβ* transcript is similar to the *GFAPα* transcript except its transcriptional start site is located 169 nucleotides upstream to that of *GFAPα* (Feinstein *et al.*, 1992). Zelenika *et al.* (1995) identified the third transcript of 2.4 kb, called *GFAPγ*, which lacks all of exon I but contains the last 126 nucleotides of intron I linked to the remaining 8 exons. The fourth *GFAP* transcript (*GFAPδ*), generating a mRNA of 4.2 kb, is the product of alternative splicing of a novel exon (VII+) located in intron VII of *GFAP* (Condorelli *et al.*, 1999). Similar to *GFAPδ*, the most recently identified *GFAP* transcript (*GFAPε*) is also alternatively spliced to include a novel exon (VIIa) located in intron VII (Nielson *et al.*, 2002). However, inclusion of exon VIIa results in the replacement of exon VIII and IX with 42 amino acids encoded by exon VIIa, generating an mRNA of 1.8 kb (Nielson *et al.*, 2002).

The astrocyte-specific GFAP isoform (GFAPα) represents the dominant form of GFAP in the human CNS. In fact, to date, the *GFAP*-β, -γ, and -δ transcripts have only been reported in the rodent CNS, where the mRNA is present at extremely low levels relative to *GFAPα*. In addition, no studies have examined whether a functional GFAP protein is expressed from these three *GFAP* transcripts, and quantitative reverse transcription-polymerase chain reaction (RT-PCR) or northern blot analysis indicates that they may be more prominent outside the CNS (discussed in Condorelli *et al.*, 1999). However, human *GFAPε* transcript and protein has been identified in the CNS, although mRNA levels were 20-fold lower than that of *GFAPα* (Nielsen *et al.*, 2002).

The GFAPε isoform was identified due to its ability to interact with presenilin-1 (PS-1), a protein that has been shown to interact with cytoskeletal proteins (Zhang *et al.*, 1998; Johningh *et al.*, 2000) and has been found to have increased expression in astrocytomas (Miake *et al.*, 1999). Interestingly, GFAPε has a unique tail domain that shows little homology to GFAPα or any other IF protein, and this tail is indispensable for PS-1 binding and cannot be replaced by the tail of GFAPα (Nielsen *et al.*, 2002). These findings suggest that it may be relevant to study the GFAPε isoform in regards to MG; however, the studies presented here will examine only GFAPα expression in MG, and this isoform will be referred to as GFAP. Also, the transcriptional regulation studies reported in this thesis will not distinguish between the different forms of *GFAP* mRNA, primarily because the mechanisms involving alternative splicing and alternative transcription start site usage have not been elucidated.

1.2.2. *GFAP Gene Regulation and Function*

Several studies have focused on examining the regulatory mechanisms underlying astrocyte-specific gene expression in the hope that a cassette could be identified that would drive astrocyte-specific transcription. Miura and coworkers (1990) were the first group to study the *GFAP* promoter, and since this time many other studies have contributed to our current understanding of *GFAP* gene regulation (Figure 1.2). Experiments using the mouse

Figure 1.2 – Potential *cis*- and *trans*-elements responsible for regulating *GFAP* promoter activity. Genomic organization of the *GFAP* gene is diagrammed at the top. Black boxes, white boxes, and the black hatched box indicate exons, introns, and 3' untranslated region, respectively. *Cis*-elements are shown for both the -1980/-1489 and -155/-79 regions. The binding sites include NFI (red), AP-1 (green hatched), AP-2 (blue), Sp1 (purple), STAT3 (brown), CRE (green). Negative *cis*-elements (gray boxes) are shown and include: a negative CRE (- CRE), a neuronal-specific element, and a glial-specific element. The positions of the hgcs sequences (yellow) are also shown. (**A**) In nonneural tissues it has been proposed that a ubiquitous repressor (UbR) that is expressed in nonneural tissues, but not in neural tissues, binds to the neural-specific element to repress GFAP expression (Kaneko *et al.*, 1993). (**B**) The ubiquitous repressor is absent, but neural stem cells that differentiate to neuronal cell types may synthesize a negative factor (neuronal downstream repressor, NDR) that binds to the glial-specific element to repress *GFAP* transcription (Kaneko *et al.*, 1993). Also, low cAMP levels permit a repressor (CR) to bind to the –CRE element (Kaneko *et al.*, 1994). (**C**) As cells progress down the glial lineage cAMP levels rise and CR no longer binds to –CRE. Instead, CREB is able to bind to the CRE. Glial specific cells do not produce either the UbR or NDR, or they produce other factors that inhibit the repressors from functioning (Kaneko *et al.*, 1993). Thus, the neuronal- and glial-specific elements are free of repressors. Potential *trans*-activating factors including NFI, AP-1, AP-2, and STAT3 may bind to their *cis*-elements to activate transcription. Also, the hgcs sequences may serve to bring the regulatory regions close to one another for efficient activation (Besnard *et al.*, 1991).

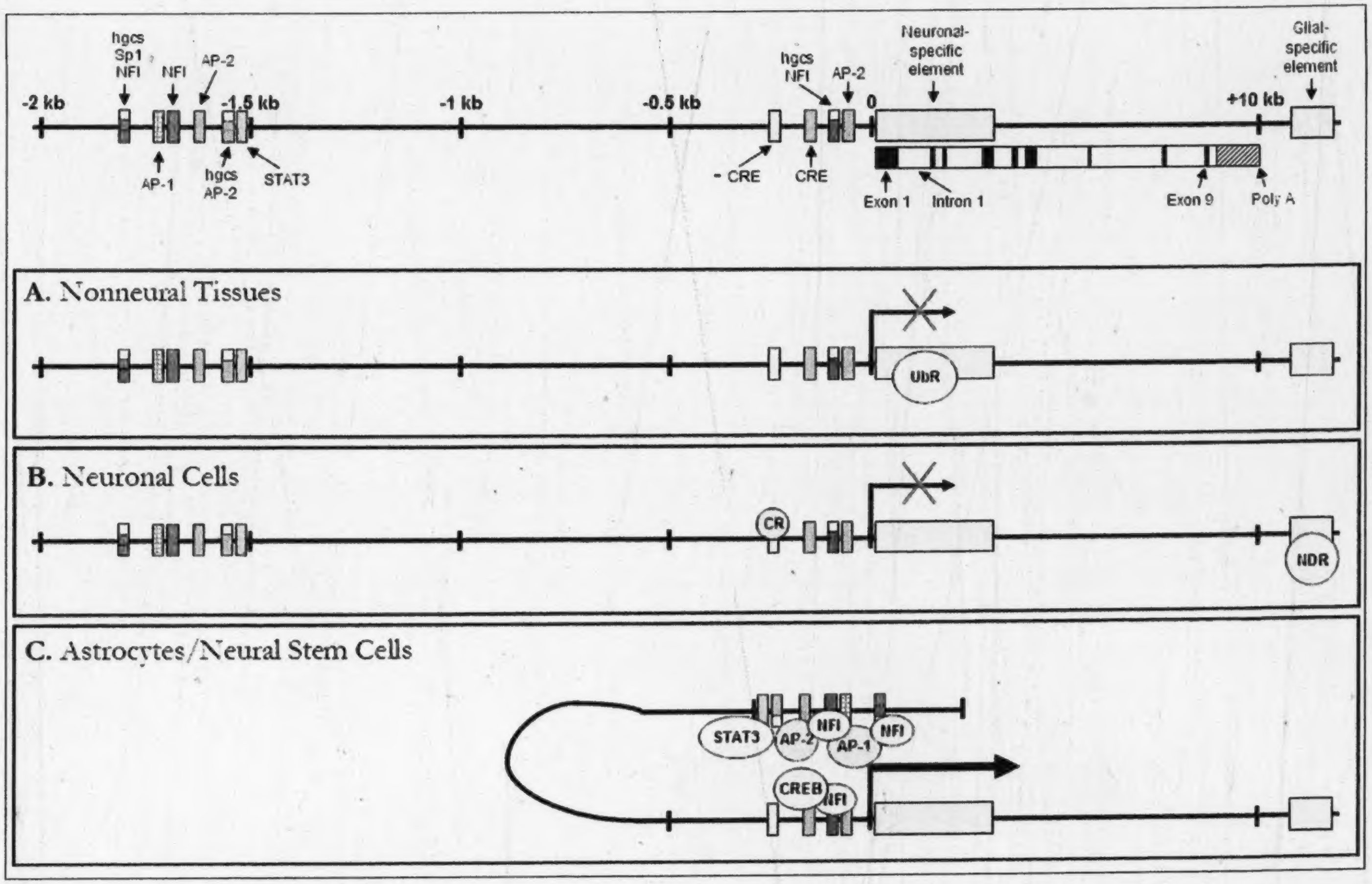
hgcs
Sp1
NFI
NFI
AP-2
-2 kb
-1.5 kb
-1 kb
-0.5 kb
AP-1
hgcs
AP-2
STAT3
hgcs
NFI
AP-2
0
- CRE
CRE
Neuronal-specific element
Exon 1
Intron 1
Exon 9
Poly A
+10 kb
Glial-specific element
A. Nonneural Tissues
UbR
B. Neuronal Cells
CR
NDR
C. Astrocytes/Neural Stem Cells
STAT3
AP-2
NFI
AP-1
NFI
CREB
NFI

GFAP promoter by Miura *et al.* (1990) demonstrated that, in relation to the transcription start site, there are at least two negative regulatory regions located at -2567/-1980 and -681/-155, and two positive regulatory regions located at -1980/-1489 and -155/-79. These results were confirmed for the human *GFAP* promoter (Besnard *et al.*, 1991), which also has a basal promoter region at -30/+47 that is important for efficient transcription (Nakatani *et al.*, 1990a,b).

Upon further analysis of the -155/-79 region, Miura and coworkers (1990) characterized several *cis*-acting elements, including binding sites for activator protein-2 (AP-2), nuclear factor I (NFI), and cAMP-responsive element binding protein (CREB). Mutation studies revealed that the NFI binding site was the most critical *cis* element for efficient activation of GFAP expression from the -155/-79 region (Miura *et al.*, 1990). Interestingly, NFI binding sites have also been identified in the promoters of other glial specific genes such as myelin basic protein (MBP) (Tamura *et al.*, 1988), which is one of the best characterized marker proteins for oligodendrocytes (Shiota *et al.*, 1989). For MBP transcription regulation, it has been proposed that the ability of NFI to activate transcription is modulated by cAMP (Zhang and Miskimins, 1993) and that NFI-B may be the primary NFI protein involved in activating MBP expression (Inoue *et al.*, 1990).

Since the NFI binding site in the -155/-79 region of the *GFAP* promoter is flanked by a cAMP-responsive element (CRE) binding site, it is reasonable to expect that *GFAP* transcription activation is also regulated by cAMP. In support of this theory, Kaneko and colleagues (1994) have reported a functional positive CRE within the -170/-110 region that corresponds with the CRE motif identified by Miura *et al.* (1990). However, Kaneko and colleagues (1994) also identified a functional negative CRE motif within the -240/-170 region. These researchers have hypothesized that when cAMP levels are low, a repressor binds to the -240/-170 region to maintain GFAP expression at a minimal level. Then, during astrocytic differentiation when extracellular signals have been proposed to upregulate cAMP levels (Vallejo and Vallejo, 2002), a cAMP-modulating factor (non cell-type specific) inactivates the repressor and a positive regulatory factor (glial cell-type specific) binds to the positive CRE motif. Thus, GFAP expression is only activated in glial cells, and not in the neuronal cells that are present in the same microenvironment. In this model, one can speculate that a specific NFI protein expressed in glial cells, but not neuronal cells, may serve as the positive regulatory factor. Furthermore, in support of the concept of cell-type specific positive regulators, much evidence now suggests that even in different populations of astroglial (*i.e.* midbrain vs cerebellar), distinct *cis-* and *trans-*acting factors differentially regulate GFAP expression (discussed in de Oliveira *et al.*, 2004).

More recent analyses of the role of cAMP in the regulation of the *GFAP* gene have identified an alternative mechanism of activation via the interleukin-6 (IL-6) family of cytokines (Takanaga *et al.*, 2004). In these studies, cAMP was shown to activate IL-6 expression in rat C6 glioma cells. The autocrine IL-6 signal then induced these cells to activate signaling pathways leading to the activation of a downstream transcription factor, STAT3 (signal transducer and activator of transcription 3). STAT3 has previously been shown to activate transcription of the *GFAP* promoter from a STAT3 binding element located at -1518/-1510 (Nakashima *et al.*, 1999). Binding of STAT3 appears to be mediated by the regulated methylation of lysine residues on histone H3 at the STAT-binding site (Song and Ghosh, 2004). In support of this cAMP/STAT3-mediated GFAP activation pathway, several reports have demonstrated the ability of members of the IL-6 family to induce GFAP expression through STAT3 (Yanagisawa *et al.,* 1999; Ochiai *et al.*, 2001).

In addition to the STAT3 binding element at -1518/-1510, the -1980/-1489 region also has two DNase I footprints located at -1634/-1614 and -1596/-1543 (Besnard *et al.*, 1991). Within the -1634/-1614 footprint lie potential binding sites for Sp1 and NFI, while the -1596/-1543 footprint has potential binding sites for activating protein-1 (AP-1), AP-2, and NFI. Masood and coworkers (1993) have shown that the AP-1 site in the -1596/-1543 region is the most potent activator of transcription in the *GFAP* promoter; however, they suggest that for glial-specific activation the cooperative interactions of multiple factors are likely necessary. These authors speculate that the neighboring NFI and AP-1 binding sites cooperatively regulate GFAP expression, and note that several genes in the CNS have flanking AP-1 and NFI sites (Amemiya *et al.*, 1992; Masood *et al.*, 1993).

While at first glance the spacing between regions -1634/-1489 and -155/-79 appears insignificant, it is likely to have a functional role in *GFAP* regulation since there is evidence for its active maintenance. For example, the human, but not the mouse, *GFAP* gene contains an *alu* insertion at bp -291 (Schmid and Jelinek, 1982). Compensatory deletions have occurred in human to preserve the spacing of this region in the mouse and human *GFAP* promoters (Besnard *et al.*, 1991). A potential reason for this conserved spacing emerges upon closer examination of three activating regions of the *GFAP* promoter: -1634/-1614, -1596/-1489, and -155/-79. In each of these activating regions, a novel 12-bp motif has been identified which is referred to as the human *gfa* common sequence (hgcs) (Besnard *et al.*, 1991). Interestingly, a related motif has also been recognized in another astrocyte specific marker protein, S100β (Allore *et al.*, 1990). In the *GFAP* promoter, Besnard *et al.* (1991) have proposed that the hgcs element participates in interactions between the *cis* regulatory elements. For instance, they speculate that the main function of the -1634/-1614 region may be to position the -1596/-1489 activating region close to the -155/-79 activating region.

The identification of *GFAP* promoter elements that serve as astrocyte-specific regulatory elements remains controversial. The first region claimed to be necessary for astrocyte-specific expression was identified as the 256 bp directly upstream of the transcription start site (Miura *et al.*, 1990). However, Masood and colleagues (1993) contend that the -1596/-1489 region contains the astrocyte-specific transcription activation elements. The difference in these two reports may simply be that one study examined the human *GFAP* promoter, while the other the rat *GFAP* promoter. Other studies by Kaneko and coworkers (1993) contradict both of these views, and present evidence that the astrocyte-specific elements lie downstream of the *GFAP* transcription start site. They claim there is a neural-specific expression element located in a 2.7-bp region that spans exon I-V of the rat genome and a glial-specific element located 1.7 kb downstream of the rat *GFAP* polyadenylation site (Figure 1.2; Kaneko *et al.*, 1993).

Several studies have focused on understanding the role of GFAP in astrocytes. For example, *GFAP*-null mice (*GFAP*-/-) have been used in an attempt to determine the function of GFAP. Surprisingly, these mice have provided little insight as they are viable, and have a normal life span, reproduction capacity, and gross motor behaviour (reviewed in Messing and Brenner, 2003). One explanation for this is that vimentin, the IF typically expressed in radial glial cells and immature astrocytes, has at least some degree of functional overlap with GFAP and can substitute for its loss. This hypothesis is supported by gene knock-out (KO) studies that have shown that astrocytes in mice deficient for both GFAP and vimentin (*GFAP*-/-vimentin-/-) cannot form IFs, but *GFAP*-/- or vimentin-/- mice are still able to form IFs (Pekny *et al.*, 1999). A closer examination of astrocyte morphology in

GFAP-null mice has been difficult due to the absence of the traditional marker (GFAP) used in immunohistochemical experiments. However, the loss of GFAP does appear to impair blood-brain barrier maintenance (Pekney *et al.*, 1998), myelination (Liedtke *et al.*, 1996), and synaptic transmission (Shibuki *et* al., 1996). Also, it has been demonstrated that the absence of GFAP leads to subtle changes in astrocyte processes (reviewed in Messing and Brenner, 2003).

GFAP is believed to be involved in the extension of glial processes (Weinstein *et al.*, 1991; Chen and Liem, 1994b; Linksey and Gilbert, 1995), but to inhibit neurite extension (Menet *et al.*, 2000). The loss of GFAP expression in astrocytes enhances neurite outgrowth in neurons grown on these astrocytes (Menet *et al.*, 2000). These findings have led to the hypothesis that the absence of GFAP, typical of radial glial cells, is permissive to the adhesion of immature neurons to radial glial cells and subsequent neurite extension (Gasser and Hatten, 1990). In addition, others have shown, using the U373 MG cell line, that transfections of antisense GFAP constructs leads to reduced GFAP expression and increased cell motility (Murphy *et al.*, 1998; Zhou and Skalli, 2000). This suggests that GFAP is not essential for the migratory capacity of normal radial glia, but that its loss may be instrumental to MG progression. Overall, to date, the specific function of GFAP remains unclear, but general roles in cytoskeletal organization have been observed, mostly through the study of MG cell lines.

1.2.3. *GFAP and Malignant Glioma*

Tumour cell transformation involves several phenotypic alterations which include increases in proliferation, cell motility and invasiveness, the loss of anchorage-independent growth and cell adhesion, and changes in cell shape. As expected for an astrocytic differentiation marker, there is an inverse correlation between GFAP expression and the degree of MG anaplasia, with the more malignant tumours expressing lower levels of GFAP than the benign tumours (Eng and Rubinstein, 1978; van der Meulen *et al.*, 1978; Velasco *et al.*, 1980). This reduced GFAP expression in MG has been suggested to play a direct role in the establishment of tumour cell transformation. *In vitro* studies transfecting antisense *GFAP* cDNA into the GFAP-positive MG cell line, U251, led to a loss in the ability of these cells to form long complex processes (Weinstein *et al.*, 1991). These phenotypic alterations could be reversed by reexpression of GFAP (Chen and Liem, 1994b). In addition, cells transfected with the antisense GFAP construct displayed a greater degree of cell crowding and piling at confluence, had a 2-3 fold increase in proliferation rate, formed larger and more numerous colonies in soft agar (a test for anchorage-independent growth), and were more invasive as determined by their ability to penetrate Matrigel-coated filters (Rutka *et al.*, 1994). In contrast, the expression of GFAP in GFAP-deficient MG cell lines inhibited their growth and resulted in the formation of stellate processes that are indicative of differentiated astrocytes (Rutka and Smith, 1993; Toda *et al.*, 1994). More recently, *in vivo* experiments performed by Toda and coworkers have confirmed these *in vitro* observations (Toda *et al.*, 1999). These researchers found that the tumour growth of GFAP-transfected rat astrocytoma C6 cells injected into mice was significantly reduced when compared to that of the control C6 cells.

The inverse correlation of GFAP levels and MG anaplasia suggests that the loss of GFAP may represent a progression event from lower to higher grade gliomas. However, the loss of GFAP could simply represent the secondary loss of an astrocytic differentiation factor. In support of the latter, Wilhelmsson and colleagues (2003) have demonstrated, by crossing p53-negative (p53-/-) with GFAP-negative (GFAP-/-) mice, that the loss of GFAP does not contribute to the development or progression of astrocytomas. When the p53-/-

mice, which frequently develop astrocytomas, were crossed with GFAP-/- mice or GFAP+/+ controls, approximately the same percentage of mice in each group developed tumours (41% and 34%, respectively) and the age of onset, tumour histology, and tumour progression were similar for both groups. To reconcile this finding with the *in vitro* data that suggest that the loss of GFAP provides cells with a proliferative advantage over GFAP-positive cells, Wilhelmsson *et al.* (2003) postulate that the absence of GFAP may cause an increase in proliferation by increasing the accessibility of cell cycle components to kinases. This is supported by the fact that the phosphorylation of IFs during depolymerization requires some of the same kinases involved in the cell cycle (Tsujimura *et al.*, 1994). Thus, cultured cells devoid of GFAP, and the GFAP-negative cells in an astrocytoma would divide more rapidly, while the absence of GFAP *in vivo* would not result in an increased malignant potential.

Regardless of whether the loss of GFAP expression directly contributes to tumour progression or whether it is a secondary consequence, the reexpression of GFAP and/or other genes involved in glial differentiation may represent a novel method of treating gliomas. Towards this purpose, and to study the regulatory elements important for astrocyte-specific gene expression, Brenner and colleagues (1994) designed a *GFAP*-lacZ transgene that has the bacterial *lacZ* reporter gene linked to a 2.2 kb 5'-flanking sequence derived from upstream region of the human *GFAP* gene. This construct has provided a wealth of information regarding astrocyte differentiation and several groups have used this *GFAP* promoter construct for glioma gene therapy studies (Andæ *et al.*, 2001; Zamorano *et al.*, 2003). Although still in its infancy, differentiation therapy may represent a promising approach for glioma treatment. One potential candidate for such differentiation therapy is B-FABP, which is a member of the fatty acid-binding protein (FABP) family and a potential regulator of cell growth and differentiation. It has been shown that B-FABP, normally found in the radial glial cells of the developing CNS, is co-expressed with GFAP in MG cell lines (Godbout *et al.*, 1998).

1.3. Fatty Acid Binding Proteins (FABPs)

The uptake and utilization of long-chain fatty acids (LCFAs) is an essential requirement for most mammalian cells. LCFAs serve many diverse functions including precursors for signaling molecules, metabolic substrates, membrane phospholipid constituents, and mediators of gene expression. However, since fatty acids (FAs) have a low aqueous solubility they require specific and efficient transport mechanisms within the cell (reviewed in Glatz and Storch, 2001). The cytoplasmic fatty acid-binding proteins (FABPs) have been postulated to play a pivotal role in FA uptake and intracellular trafficking, and have been implicated in modulating signal transduction, gene transcription, cell growth and differentiation (reviewed in Zimmerman and Veerkamp, 2002). FABPs are members of the intracellular lipid-binding protein (iLBP) family, which also includes the cellular retinol-binding protein (CRBP) and the cellular retinoic acid-binding protein (CRABP). Thus far, the expression of this gene family, which dates back to one billion years ago, seems to be confined to the animal kingdom (Schaap *et al.*, 2002).

The first FABP was discovered by Ockner and coworkers (1972) as a cytosolic protein that is capable of binding LCFAs (C_{16}-C_{22}) with high affinity. Subsequent studies have revealed a large family of *FABP* genes that encode at least nine distinct proteins which are named after their first tissue of identification (Table 1.1). Members of this family are 14- to 15-kDa proteins that have a highly conserved three-dimensional structure despite an amino acid sequence similarity ranging from 22-73% (reviewed in Zimmerman and Veerkamp, 2002). All FABPs are composed of 10 antiparallel β-strands (βA-βJ) that form a

Table 1.1 - Characteristics of FABPs, their ligands and distribution.

Gene[a] (Locus[b])	Protein Name	Ligand(s)	Tissue Occurrence[c]
FABP1 (2p11)	Liver (L)-FABP	LCFA, cholesterol, heme	liver, intestine, kidney, stomach
FABP2 (4q28-q31)	Intestinal (I)-FABP	LCFA	intestine, stomach
FABP3 (1p32-p33)	Heart (H)-FABP or Mammary Derived Growth Inhibitor (MDGI)	LCFA	heart, kidney, skeletal muscle, adrenals, placenta, brain, testes, lung, mammary gland, stomach, aorta, ovary
FABP4 (8q21)	Adipocyte (A)-FABP	LCFA, retinoic acid	adipose
FABP5 (15q12-q24.3)	Epidermal (E)-FABP or cutaneous (C)-FABP	LCFA, eicosanoids	skin, brain, lens, capillary, retina, endothelium
FABP6 (5q23-q35)	Ileal (IL)-FABP	LCFA, bile salts	intestine, ovary, adrenals, stomach
FABP7 (6q22-q23)	Brain (B)-FABP or retinal (R)-FABP	LCFA	brain, retina
FABP8 (8q21-q22)	Myelin (M)-FABP	LCFA, retinoiods	peripheral nervous system
FABP9 (8q21)	Testicular (T)-FABP	?	testes

[a] Gene nomenclature according to human genome database conventions. [b] Chromosome location according to locus in human genome.
[c] The presence of a FABP in a specific tissue type does not mean it is present in all cell types of that tissue. Expression may be limited to specific developmental periods and/or cell types

Table adapted from Schaap *et al.* (2002) and Zimmerman and Veerkamp (2002).

β-barrel, and 2 α-helices that form a helix-turn-helix motif that serves as a lid to the β-barrel (reviewed in Coe and Bernlohr, 1998). The β-barrel forms a large, water-filled cavity that is capable of binding specific ligands based on the amino acid sidechains buried within the cavity. For instance, in intestinal (I)-FABP, the positively charged arginine residue at position 106 has been shown to interact with the carboxyl group of the FA to provide binding specificity (Jakoby *et al.*, 1993). It is hypothesized that FABPs have developed these distinct binding sites to allow them to perform specific functions within the different tissues in which they are expressed.

1.3.1. *FABPs of the Central Nervous System*

To date, three FABP types have been detected in the central nervous system: heart (H)-FABP, epidermal (E)-FABP, and brain (B)-FABP (Heuckeroth *et al.*, 1987; Bennett *et al.*, 1994; De Leon *et al.*, 1996). These three FABPs and myelin (M)-FABP, a peripheral nervous system FABP, share the highest amino acid sequence similarity of any in the family, with approximately 70% identity (Veerkamp and Zimmerman, 2000).

Despite this strong identity, Lipidex assay experiments have shown that the binding affinity for each CNS FABP varies with different FAs. H-FABP has a strong affinity for oleic acid (C18:1) and arachadonic acid (C20:4), but not palmitic acid (C16:0), while B-FABP has a strong affinity for all three FAs and E-FABP has a lower affinity for all three (Veerkamp and Zimmerman, 2000). Additional experiments have shown that B-FABP preferentially binds polyunsaturated LCFAs. Xu and colleagues (1996) demonstrated that bacterially produced B-FABP readily bound unsaturated FAs such as oleic acid and arachadonic acid, but failed to bind the saturated FAs palmitic acid and arachidinic acid (C20:0) with high affinity. Furthermore, B-FABP has been shown to bind docosahexaenoic acid (DHA; C22:6) with the highest affinity yet reported for any FABP-ligand pair (Xu *et al.*, 1996; Balendiran *et al.*, 2000). This high affinity suggests that DHA is an endogenous ligand for B-FABP and is supported by the fact that DHA is enriched in the developing brain. Thus, it is possible that by binding different ligands, each FABP type in the brain may have distinct functions.

In support of the possibility that each CNS FABP has a specific function in the developing and mature brain, Owada *et al.* (1996) have shown a spatiotemporal differential expression pattern of these FABPs. In the rat brain, H-FABP expression is localized to neurons and is first detected at ED19. H-FABP expression then increases until postnatal day (P)14 and remains abundant in the adult brain (Sellner *et al.*, 1995; Owada *et al.*, 1996). E-FABP is also expressed in neurons, but at an earlier stage than H-FABP, with highest expression levels in the prenatal and perinatal rat brain (Owada *et al.*, 1996; Liu *et al.*, 1997). B-FABP expression is primarily restricted to radial glial cells in the developing rat and mouse embryo (detailed below), but is also present at low levels in the neuroepithelial precursor cells of the developing brain and immature astrocytes (Feng *et al.*, 1994; Kurtz *et al.*, 1994; Owada *et al.*, 1996).

Feng and coworkers (1994) found that murine *B-FABP* mRNA levels in the CNS rose from ED12-14, peaked from ED14 to P0/P5, and then decreased to undetectable levels in the adult cerebral cortex. Interestingly, this elevated B-FABP expression pattern coincides with neuronal migration along radial glial fibers. Postnatally, B-FABP expression is localized to astrocytes which typically derive from radial glial cells. Although not as extensively characterized as mouse, human *B-FABP* mRNA has been detected in both the fetal and adult brain, as well as in fetal retina (Shimizu *et al.*, 1997; Godbout *et al.*, 1998).

In regards to the function of each FABP in the CNS, B-FABP expression is required for glial cell differentiation and neuronal migration (Kurtz *et al.*, 1994; Liu *et al.*, 2000). The addition of anti-B-FABP antiserum to primary cerebellar cell cultures blocks the extension of radial glial cell processes thereby inhibiting neuronal and glial cell differentiation (Feng *et al.*, 1994). E-FABP and H-FABP have both been implicated in neurite outgrowth, neurogenesis, and neuronal migration (Owada *et al.*, 1996; Liu *et al.*, 1997, 2000). However, only E-FABP has been shown to have a direct effect on these processes in the brain. In fact, depletion of E-FABP abolishes neurite outgrowth in PC12 cells (Allen *et al.*, 2000) and, in mature neurons, E-FABP expression is up-regulated during axon regeneration after nerve damage, but H-FABP is not (De Leon *et al.*, 1996; Owada *et al.*, 1997). From these data, it can be hypothesized that, in neurons, E-FABP is the main FABP involved in neuronal migration and initiating neurite outgrowth and neurogenesis, while H-FABP plays more of a maintenance/maturation role.

1.3.2. *FABP Involvement in Growth and Differentiation*

For the most part, the specific functions of FABPs remain unclear; however, it is generally accepted that FABPs are involved in intracellular lipid metabolism. Such a role is supported by the fact that FABPs are involved in FA uptake and storage, as well as by *FABP* knockout mice which show abnormalities in FA uptake, transport, and metabolism resulting in altered FA oxidation, fuel selection, and metabolic homeostasis (reviewed in Zimmermann and Veerkamp, 2002). As an example, Schaap and coworkers (1999) have demonstrated that *H-FABP*-null mice display reduced uptake and oxidation of palmitate in resting and contracting cardiomyocytes.

In addition to their roles in lipid metabolism, several FABPs have been implicated in modulating cell growth and differentiation, and their actions tend to be both FABP-type and cell-type specific. An example of FABP-type specificity is demonstrated by the effect of H-FABP and adipocyte (A)-FABP expression in L6 muscle cells. Transfection of L6 muscle cells with H-FABP had no effect on their proliferation, while A-FABP transfection led to an increase in proliferation (Prinsen and Veerkamp, 1998). Thus, different FABPs can generate a different growth response in the same cell line, likely due to their ligand specificty. In regards to cell-type specifity, L-FABP has been shown to increase the proliferation rate of rat liver cells (Keler *et al.*, 1992), but decrease the proliferation rate of mouse embryonic stem cells (Schroeder *et al.* 2001). A possible explanation for these opposite effects is that L-FABP expression in liver cells increases the efficacy of the utilization of unsaturated FAs leading to an increase in proliferation, while in embryonic stem cells L-FABP acts as a differentiation factor, thereby inhibiting proliferation (reviewed in Zimmermann and Veerkamp, 2002).

Other FABPs that have been implicated in differentiation include H-FABP, E-FABP, and B-FABP. While the roles of E-FABP and B-FABP in differentiation have mainly been speculative based on their spatiotemporal distribution patterns in the CNS (*i.e.* B-FABP in radial glial cells), H-FABP has actually been purified as a differentiation factor called mammary derived growth inhibitor (MDGI) (Böhmer, 1984). MDGI has been shown to inhibit proliferation and to cause the functional and morphological differentiation of mouse mammary gland explants (Yang *et al.*, 1994).

The finding that FABPs can induce differentiation or serve as differentiation markers has led to the suggestion that they could also be used as tumour markers (reviewed in Zimmermann and Veerkamp, 2002). In support of this theory, the level of L-FABP and I-FABP have been found to decrease with the dedifferentiation and progression of human colon carcinoma (Davidson *et al.*, 1993). Similar findings have been observed for H-FABP in ductal mammary gland carcinoma (Huynh *et al.*, 1995) and A-FABP in bladder transitional cell carcinoma (Celis *et al.*, 1996). Furthermore, while B-FABP has not been directly correlated with tumour progression, it has been found to be co-expressed with GFAP in MG cell lines, and when GFAP is absent, B-FABP expression is also lost (Godbout *et al.*, 1998).

1.3.3. *FABPs: Membrane Interactions and Gene Transcription*

It has been postulated that the ability of FABPs to mediate growth and differentiation likely lies in their ability to strictly regulate the uptake and transport of specific FAs to specific cellular locations (reviewed in Storch and Thumser, 2000). In this regard, while LCFA uptake into a cell can occur via passive diffusion (Hamilton and Kamp, 1999), recent studies have suggested the need for a protein-mediated uptake component (Abumrad *et al.*, 1999; reviewed in Kleinfeld, 2000). In support of protein-mediated LCFA uptake, integral membrane proteins, such as fatty acid translocase (FAT/CD36), have been shown to increase the rate of FA uptake (Baillie *et al.*, 1996; reviewed in Abumrad *et al.*, 1999). With these protein-mediated uptake systems, it is possible to hypothesize that cells may be able to selectively regulate their FA content. Also, specific FABPs may be able to directly interact with the plasma membrane to assist in the uptake of specific FAs (reviewed in Glatz and Storch, 2001).

For FA transport within the cell, two different mechanisms of FA transfer to and from membranes have been proposed to date: aqueous solubility (diffusion) and collisional transfer (reviewed in Storch and Thumser, 2000). The aqueous solubility mechanism involves FA transfer from a FABP to an acceptor membrane by dissociation of the FA from the FABP followed by aqueous diffusion. Collisional transfer involves a direct interaction between the FABP and the membrane, resulting in an increased rate of FA transfer. The majority of the FABPs studied (A-, I-, H-, and M-FABP) are able to perform collision-mediated FA transfer (Kim and Storch, 1992a; Wootan *et al.*, 1993; Hsu and Storch, 1996).

For these FABPs, the FA transfer rate was shown to increase when membranes contained anionic phospholipids, thus indicating that positively charged residues on the FABP surface are likely involved in the membrane interaction (Wootan and Storch, 1994; Smith and Storch, 1999).

The helix-turn-helix motifs of A-, I, H, and M-FABP display a net positive potential. When a lysine residue located within the helix-turn-helix domain (Lys21) of H-FABP and A-FABP was either mutated or neutralized by acetylation, collision-mediated transfer was abolished (Herr *et al.*, 1996; Liou and Storch, 1998). Thus, the helix-turn-helix motif is likely involved in FABP-membrane interactions. Interestingly, the helix-turn-helix motif of L-FABP has a net negative charge and this is the only FABP shown to transfer FAs entirely by aqueous solubility (Kim and Storch, 1992b). These results suggest that, in contrast to L-FABP, most FABPs may target FAs to anionic membranes or protein domains.

Many genes in mammals are regulated by specific LCFAs in an either positive or negative manner (reviewed in Zimmermann and Veerkamp, 2002). FABPs have been implicated in specifically modulating the effects of LCFAs on gene transcription by delivering specific FAs to the nucleus or by trafficking ligands to peroxisome proliferator-activated receptors (PPARs) (reviewed in Duplus *et al.*, 2000). PPARs are a family of three (PPAR-α,-β,-γ) nuclear hormone receptors that heterodimerize with the retinoid X receptor (RXR) to exert their transcriptional control over genes containing PPAR-response elements (PPREs). Importantly, FABPs localize to both the cytoplasm and nucleus, and therefore may function in translocating specific FAs to the nucleus, and delivering these ligands to PPARs *via* direct interaction between the FABP and PPAR. However, to date, only L-FABP and PPARα/γ, and A-FABP and PPARβ/γ, have been shown to directly interact (Wolfrum *et al.*, 2001; Tan *et al.*, 2002). None of the CNS FABPs, including B-FABP, have been directly implicated in delivering specific FAs to the nucleus. Therefore, the CNS FABPs may have a more general role in regulating gene expression, possibly by passively modulating unbound FA levels.

1.3.4. *B-FABP Function*

A function for B-FABP was first proposed twenty years ago by Bass and colleagues (1984). These researchers proposed that FABPs isolated from the rat brain served as a FA sink to protect synaptosomal trans-membrane proteins (*i.e.* Na^+-dependent uptake systems) from inhibition by these FAs. Since brain-isolated FABPs were shown to relieve the inhibition of neurotransmitter amino acid uptake, it was suggested that B-FABP may potentially regulate synapse function. However, more recent experiments have localized B-FABP to the radial glial cells of the developing brain, not to neurons where B-FABP would be required to perform this function (Feng *et al.*, 1994; Kurtz *et al.*, 1994). Thus, this function may be more applicable to FABPs expressed in neurons, such as E-FABP and H-FABP.

Since 1984, numerous studies have implicated FABPs in FA metabolism and *FABP* knockout mice have specifically identified L-, E-, I-, A-, and H-FABP as being intimately involved in this process (reviewed in Zimmermann and Veerkamp, 2002; Martin *et al.*, 2003). However, since the primary source of energy in the brain is glucose, B-FABP is unlikely to serve as important a role in the energy requirement of the cell as other FABPs expressed in tissues where FAs are the primary source of energy, such as adipose tissue and cardiomyocytes.

New potential functions for B-FABP were formulated in 1994. The first was based on a study by Sellner and coworkers (1994) who proposed that R-FABP, the chicken ortholog of B-FABP, was involved in enriching developing and mature retinal membranes with polyunsaturated FAs (PUFAs). From ED6-9, the chick retina undergoes enormous growth and there is a great expansion in membrane area (Prada *et* al., 1991) producing a need for large amounts of PUFAs. Sellner *et al.* (1994) proposed that R-FABP acts as a storage depot for these PUFAs thereby facilitating the incorporation of PUFA into the rapidly expanding embryonic CNS. This hypothesis is consistent with the fact that the retina and brain are both enriched in PUFAs (Fliesler and Anderson, 1983) and that B-FABP does predominantly bind PUFAs (Xu *et al.*, 1996). Also, our lab has identified high levels of R-FABP, nearly 1% of total cytosolic protein, in the chick retina and brain as early as ED3.5, suggesting a role in early retinal differentiation (Godbout, 1993).

A second role for B-FABP, introduced in 1994 and still widely accepted, stipulates that B-FABP is involved in the establishment and maintenance of the radial glial fiber system (Feng *et al.*, 1994). Feng and coworkers (1994) found that the addition of B-FABP antibodies to mixed neuronal-radial glial primary cell cultures from mice prevented both glial and neuronal differentiation. It was proposed that the effects of B-FABP on neuronal differentiation were a secondary consequence of the prevention of glial process formation and differentiation. Since Feng and coworkers (1994) identified B-FABP in the tissue culture media in which these cells were grown, they concluded that B-FABP functions as an extracellular signaling molecule in establishing the radial glial fiber system. While this is the best characterized function of B-FABP to date, how it mediates these effects is still unknown. However, to this day, B-FABP remains one of the most potent differentiation markers of radial glial cells.

1.3.5. *B-FABP and Malignant Glioma*

Our lab was first to demonstrate the presence of B-FABP in human MG cell lines (Godbout *et al.*, 1998). In these studies, both B-FABP and GFAP expression was analyzed in a panel of fifteen MG cell lines. Of these cell lines it was found that five expressed high levels of both *B-FABP* and *GFAP* mRNA, eight expressed neither *B-FABP* nor *GFAP*, and two expressed very low levels of *B-FABP* mRNA and no *GFAP* mRNA. The co-expression of B-FABP and GFAP in these cell lines is interesting because *in vivo* these proteins are normally only expressed together in very select cell types including: cerebellar Bergmann glial, radial glia of the hippocampal dentate gyrus, and gomori-positive astrocytes (Kurtz *et al.*, 1994; Young *et al.*, 1996). Generally, it is believed that in the transition from the radial glial cell type to the mature astrocyte, B-FABP-postive/GFAP-negative radial glia become B-FABP-negative/GFAP-positive astrocytes (Hatten, 1999). Co-expression of these proteins in MG suggests the following possibilities: i) MG tumours may arise from cells that express both of these proteins, ii) MG tumours may arise from cells that are in transition between radial glial cells and astrocytes, and/or iii) the expression of the *B-FABP* and *GFAP* genes may be mediated by similar *cis*-acting elements and *trans*-acting factors.

1.3.6. *B-FABP Gene Regulation*

The differential spatiotemporal distribution of B-FABP in the developing CNS has fueled an interest in its gene regulation. Sequence analysis of B-FABP orthologs from mouse (Kurtz *et al.*, 1994; Feng and Heitz, 1995), human (Godbout *et al.*, 1998) and chick (Bisgrove *et al.*, 1997) indicate that the murine and human promoter regions are highly conserved and thus it is likely that their regulatory elements are also conserved. However, the chick *R-FABP* and mammalian *B-FABP* promoters have diverged significantly. The chick promoter region contains a G-C rich region, in contrast to mammalian *B-FABP* genes. Since the chick *R-FABP* 5'-flanking sequence has diverged from that of the human and mouse genes, only the mammalian *B-FABP* regulatory elements will be discussed here.

Feng and coworkers (1995) were the first to show that *B-FABP* transcription *in vivo* involves multiple regulatory elements and that the 1.6 kb of sequence upstream of the *B-FABP* transcription start site is sufficient for correct spatiotemporal distribution. They identified the following regulatory elements: a silencer element [dorsal spinal cord silencer (DSCS)] located at -1.6 to -1.2 kb, a positive element [dorsal root ganglion enhancer (DRGE)] located at -1.2 to -0.8 kb, and a radial glial enhancer (RGE) that was localized to the -0.8 to -0.3 kb region. The DSCS element was found to repress transcription in cells of the dorsal spinal cord, while the enhancer elements, DRGE and RGE, directed *B-FABP* expression in the dorsal root ganglion cells and radial glial cells (including Bergmann glia), respectively. Transgenic mice carrying the -300/+72 bp *B-FABP*/lacZ reporter construct did not express the reporter gene, indicating that this region is not sufficient for correct spatiotemporal expression. In contrast, a -800/+72 *B-FABP*/lacZ reporter construct directed reporter gene expression in radial glial and Bergmann glial throughout the developing CNS. This finding suggests that while B-FABP expression in the developing CNS involves multiple elements, radial glial expression is determined by a single radial glial cell specific element, RGE. Further characterization of the DSCS, DRGE, and RGE elements has not been reported.

Josephson and colleagues (1998) performed a more in depth analysis of the proximal promoter region (-800 to +72 bp) identified by Feng *et al.* (1995) as being sufficient for radial glial expression. They identified three DNA binding sites within the region by deletion analysis, DNase I footprinting and *in vitro* gel shift assays. These sites corresponded to a POU protein (Brn1 and Brn2) binding site located between -370 to -362 bp, a paired box protein (Pbx-1) binding site overlapping the same region, and a hormone response element (HRE) located at -286 to -275 bp. Analysis of transgenic mice carrying various mutant *B-*

FABP/lacZ reporter constructs demonstrated that both the POU binding sites and HRE are functional since mutation of these sites led to reduced lacZ expression in the CNS, particularly in the telencephalon. However, deletion of the Pbx site (leaving the POU site intact) had no effect on lacZ expression. The presence of a POU binding site in the *B-FABP* promoter is particularly interesting since POU family members have been implicated in neuronal cell type specification and/or cell survival (Xiang *et al.*, 1996). While the role of the POU binding site in B-FABP expression in the developing CNS has not been further characterized, it is noteworthy that a POU binding domain is also observed in the chick *R-FABP* promoter (Bisgrove *et al.*, 1997).

Our lab is the only group to date that has characterized the *cis-* and *trans-*acting elements that regulate the expression of the human *B-FABP* gene (Bisgrove *et al.*, 2000). These studies have revealed that the human *B-FABP* transcription start site is located 81 bp upstream of the translation initiation codon and that there is a putative TATA box at -22/-28 bp relative to the transcription start site. Furthermore, through the use of sequencing, DNase I footprinting and *in vitro* gel shift assays, two NFI-binding sites have been identified in the *B-FABP* promoter located between at -54/-40 bp and -257/-243 bp. A third potential NFI-binding site was identified at -171/-157 bp; however, this region failed to bind NFI when used in gel shift assays.

While NFI proteins from both B-FABP-positive (U251) and B-FABP-negative (T98) MG cell lines were able to bind to the -54/-40 and -257/-243 NFI-binding sites, the NFI proteins in the B-FABP-positive cell lines appeared hypophosphorylated in relation to those in T98. Thus, it has been postulated that the hyperphosphorylated form of NFI may be unable to activate *B-FABP* transcription. In support of a role for phosphorylation in regulating NFI-mediated transactivation, Yang *et al.* (1993) have shown that phosphorylated forms of NFI are able to transactivate NFI-dependent promoters less effectively than dephosphorylated forms. Our data indicate that B-FABP expression is regulated by NFI; however, which of the NFI proteins mediate its transactivation has yet to be elucidated.

1.4. Nuclear Factor I (NFI)

The CCAAT transcription factor/nuclear factor I (CTF/NFI) family was initially identified as two separate entities (NFI and CTF) from human HeLa cell nuclear extracts, but Jones and coworkers (1987) later determined that these proteins were identical. In addition, the TGGCA protein identified in chicken (Nowock and Sippel, 1982) was also found to substitute for NFI proteins and has since been classified as a homologous NFI protein (Leegwater *et al.*, 1986). NFI was originally isolated as a protein that assisted in the formation of a covalent complex between the adenovirus terminal protein (pTP) and dCMP, a key step in adenovirus DNA replication (Nagata *et al.*, 1982). In contrast, the CCAAT-binding protein (CTF) was purified as the result of *in vitro* transcription studies of the herpesvirus thymidine kinase gene Jones *et al.* (1985). However, it has since been discovered that NFI/CTF proteins do not bind the CCAAT sequence (Zorbas *et. al.*, 1992), but rather bind the DNA sequence $^{T}/_{C}\mathrm{TGG}^{A}/_{C}(\mathrm{N}_{5})\mathrm{GCCAA}$ with high affinity and individual half sites (TTGGC or GCCAA) with somewhat reduced affinity (Meisterernst *et al.*, 1988a).

Through the isolation of NFI-encoding cDNAs from rat (Paonessa *et al.*, 1988), human (Santoro *et al.*, 1988), hamster (Gil *et al.*, 1988), mouse (Inoue *et al.*, 1990) and pig (Meisterernst *et al.*, 1988b, 1989) four closely related genes have been identified [*NFI-A*, *-B*, *-C*, and *-X* (also called *-D*)]. The four *NFI* genes are distributed across three chromosomes in both the human and mouse genomes, with *NFI-C* and *-X* on the same chromosome in humans and *NFI-A* and *-B* on the same chromosome in mice (Figure 1.3; Qian *et al.*, 1995; reviewed in Gronostajski, 2000). These genes generate multiple alternatively spliced

Figure 1.3 - Domains and alternative splicing of human and mouse NFI. Shown on top is a schematic diagram of the general organization of the NFI transcription factor. Numbers above the schematic are approximate amino acid positions and those below are exon numbers. The general gene structure consists of 11 exons (boxes) with the DNA-binding and dimerization domain encoded predominantly by exon 2 (gray box). Within exon 2 there are four conserved cysteine residues (labeled in red with amino acid position below) required for DNA-binding and redox regulation of binding that lie within a sequence-specific DNA-binding region (labeled Site-specific DNA binding). Also, there is a basic alpha-helical domain within exon 2 (labeled Basic helix) that functions in non-specific DNA interactions. The C-terminal region of NFI encodes the transactivation/repression domain. Within this region there is a specialized proline-rich activation domain (labeled Proline-rich). For each gene (*NFI-A*, *-B*, *-C*, and *-X*), both the human and mouse chromosome locations are shown below the gene name (right). Of note, in the human genome the *NFI-C* and *NFI-X* genes are located on the same chromosome, while in the mouse the *NFI-A* and *NFI-B* genes are on the same chromosome. Isoforms generated by alternative splicing are shown for each species (h, human; m, mouse). An alternative polyadenylation site between exons 2 and 3 of NFI-B (labeled Ter) yields the short human NFI-B3 protein (hB3). Alternative first exons (E1b, E1c) are shown by boxes or lines connected to exon 2. The heptamers above NFI-A and NFI-C are regions homologous to the C-terminal domain (CTD) repeat of RNA polymerase. N: amino terminus; C: carboxy terminus.

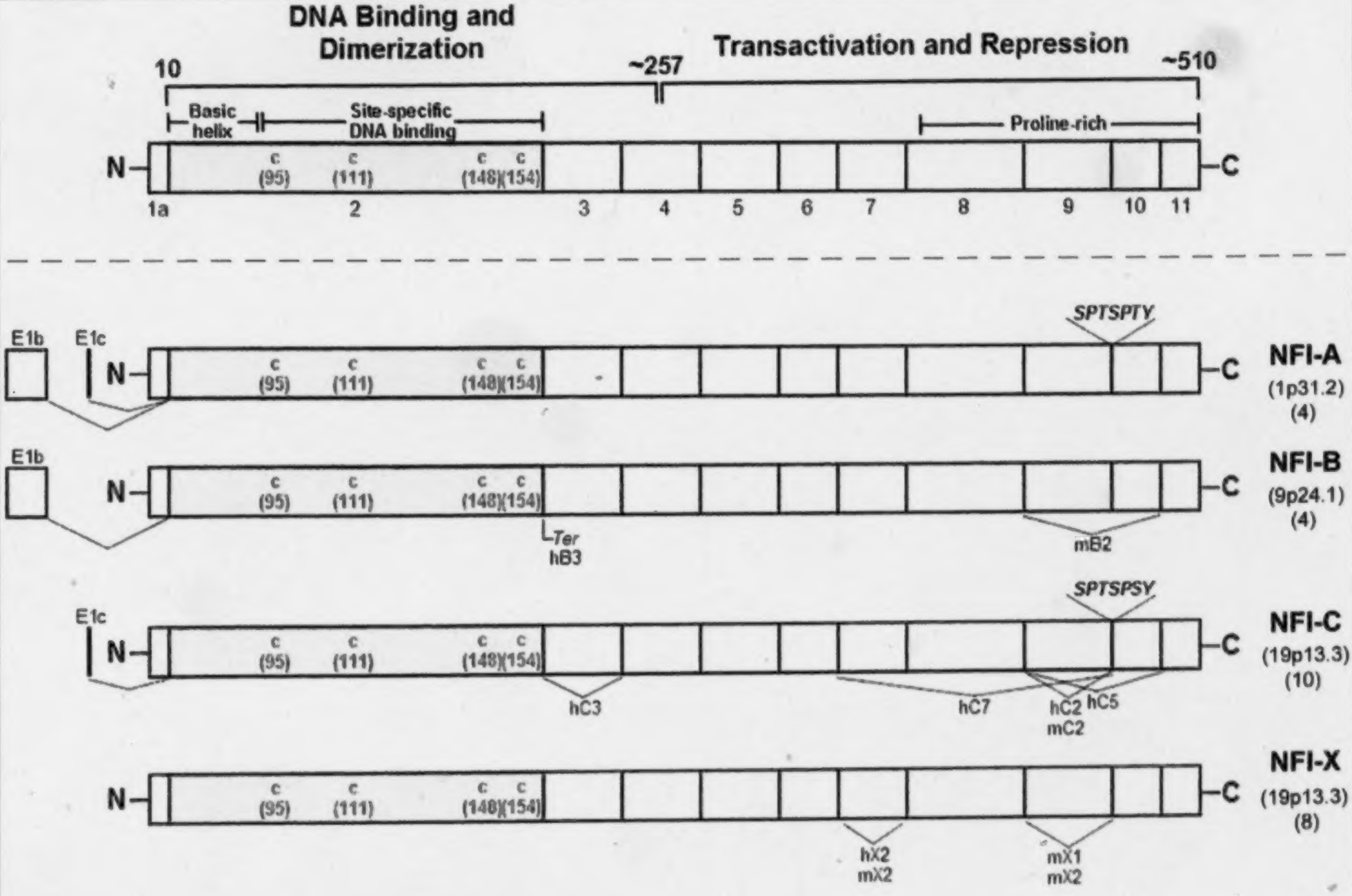
DNA Binding and Dimerization
Transactivation and Repression
10
~257
~510
Basic helix
Site-specific DNA binding
Proline-rich
N
C
c (95)
c (111)
c (148)
c (154)
1a
2
3
4
5
6
7
8
9
10
11
E1b
E1c
SPTSPTY
NFI-A
(1p31.2)
(4)
NFI-B
(9p24.1)
(4)
Ter
hB3
mB2
SPTSPSY
NFI-C
(19p13.3)
(10)
hC3
hC7
hC2
mC2
hC5
NFI-X
(19p13.3)
(8)
hX2
mX2
mX1
mX2

Figure adapted from Gronostajski, 2000

mRNAs that encode proteins ranging from 52-66 kDa (reviewed in Gronostajski, 2000). While each of the four *NFI* genes is highly conserved across vertebrate species, the four *NFI* genes differ significantly from each other with only ~61% sequence similarity (Meisterernst *et al.*, 1989; reviewed in Gronostajski, 2000). In particular, while the N-terminal DNA binding domain is well-conserved in all four *NFI* genes (~91%), the C-terminal transactivation domain is highly variable (~39%) (reviewed in Gronostajski, 2000).

1.4.1 ***NFI Structure/Function Studies***

DNA Binding:

Gronostajski (1986, 1987) has performed several studies on the DNA binding properties of NFI proteins and has identified strong, weak, and non-binding sequences. The strongest binding sequence was identified as $^{T}/_{C}$TGG$^{A}/_{C}$(N$_5$)GCCAA where even the addition or subtraction of 1 bp from the 5 bp internal spacer drastically reduced NFI binding affinity. Within the internal (N$_5$) spacer, stronger binding was observed when the second residue was a C or G and the last residue was a G or T. Weak NFI binding sequences typically had a G or T in the last position before the internal spacer (Gronostajski, 1987) and it has been postulated that the exclusive presence of G-C base pairs within the internal spacer disrupts NFI binding (Gronostajski *et al.*, 1985). Furthermore, DNase I protection studies suggest that the important DNA-protein contacts probably occur 5' to the final two A residues, and features other than sequence alone likely affect NFI binding (Gronostajski *et al.*, 1985).

The DNA binding domain (DBD) of NFI proteins is located at the N-terminus and displays little sequence similarity to any other transcription factor DBD and therefore may be structurally distinct (reviewed in Gronostajski, 2002). By over-expressing various parts of human *NFI-C* cDNAs in bacteria, Mermod and coworkers (1989) have shown that the N-terminal 220 amino acids of NFI are sufficient for the DNA binding activity and the stimulation of adenovirus DNA replication. However, data from Meisterernst *et al.* (1989) indicate that the N-terminal 257 amino acids are required for full NFI binding activity. Closer examination of this region using NFI-A and NFI-C deletion mutants has revealed that the first 11 amino acids are dispensible (Meisterernst *et al.*, 1989; Gounari *et al.*, 1990). Thus, the functionally active DNA binding domain of NFI appears encompass amino acids 11-257, the most highly conserved region amongst the NFI family.

Additional work detailing the functional aspects of the DNA binding domain of NFI has led to the identification of two subdomains within this region: a highly basic region (amino acids 1-78) and a NFI sequence-specific DNA binding region (amino acids 75-236) (Dekker *et al.*, 1996). The highly basic region appears to fold into a stable α-helical structure to provide a low-affinity interaction with the DNA in a non-sequence-specific manner. The sequence-specific region, which contains four highly conserved cysteine residues (cys-95, -111, -148, and -154) (Novak *et al.* 1992), increases the binding affinity of NFI to their consensus sites by ~100-fold when fused to the highly basic region (Dekker *et al.*, 1996). Deletion analysis of the four cysteine residues have shown that the cys-95, -148, and -154 are required for DNA binding, while cys-111 is not required but renders NFI proteins sensitive to oxidative inactivation (Bandyopadhyay and Gronostajski, 1994). It has been proposed that the highly basic region interacts with the phosphates of the DNA providing a weak interaction. When the sequence-specific region encounters an NFI consensus site, the protein forms a high-affinity interaction with the DNA (Meisterernst *et al.*, 1989).

Dimerization:

As with most transcription factors, NFI proteins bind to DNA as dimers (and exist in solution as dimers). The dimerization domains of the NFI proteins lie within the N-terminal DNA binding domain and are therefore highly conserved (Mermod *et al.*, 1989). As demonstrated by *in vitro* transcription/translation experiments, the NFI proteins can form either homodimers or heterodimers; however, NFI proteins need to be cotranslated in order to form heterodimers (Kruse and Sippel, 1994). The mixing of pre-formed homodimers does not result in the formation of heterodimers. The potential formation of heterodimers increases the complexity of transcriptional control mediated by NFI proteins since the heterodimers may have a different transactivation potential relative to the homodimers. In support of this theory, Chaudry and colleagues (1998) co-transfected an NFI-X expression plasmid with increasing amounts of an NFI-C expression plasmid and found that transcription activation decreased with increasing NFI-C. This decrease in transcription activation was not observed when NFI-C or NFI-X were separately transfected. Thus, the *in vivo* situation is most likely very complex considering the presence of four distinct *NFI* genes and the numerous NFI splice forms generated by alternative splicing.

Transactivation/Repression:

The transactivation/repression function of NFI transcription factors resides within the C-terminal half of the protein. To date, only a fraction of the numerous NFI splice forms has been tested for functional activity. One of the more interesting functional aspects of the NFI transactivation domain is the presence of a proline-rich (~25% proline) activation domain (amino acids 399-499) (Figure 1.3). This region was characterized by Mermod and coworkers (1989) through the use of deletion mutants. These researchers discovered that the removal of the C-terminal 62 amino acids reduced NFI transactivation capacity and the removal of 100 residues completely abolished activity. In addition, when this proline-rich activation domain was linked to heterologous DBDs (*i.e.* Sp1) a strong induction of reporter gene expression was observed (Mermod *et al.*, 1989; Seipel *et al.*, 1992).

Further support for this proline-rich domain being an activation domain comes from Gerber and colleagues (1994) who showed that homopolymeric stretches of proline are sufficient to cause transactivation.

However, others have postulated that the proline-rich region may simply serve as a flexible linker for the real transactivation regions encoded by exons 4-6 (domain I) and exons 10-11 (domain II) (Altmann *et al.*, 1994). Through the use of an *NFI-C* cDNA that lacks exons 7-9 (Figure 1.3, hC7), these investigators have found that hC7 has a higher transactivation capacity than full length NFI-C (exons 1-11). Thus, removal of the proline-linker and the increased proximity of domains I and II leads to an increase in transactivation.

NFI proteins have also been implicated in the repression of transcription from several promoters (reviewed in Gronostajski, 2000), but this function is poorly characterized. Repression domains have been localized to amino acids 318-509 of rat NFI-A (Osada *et al.*, 1997) and amino acids 190-280 of rat NFI-X (Nebl and Cato, 1995). However, there is no apparent sequence similarity between these domains which suggests that repression may be mediated through a different mechanism for each of these NFIs. Importantly, both repression and activation by NFI proteins is cell-type and promoter specific indicating that other *cis-* and *trans-*acting factors may be involved (reviewed in Gronostajski, 2000).

While the mechanism of NFI activation or repression remains poorly understood, three prevalent mechanisms have been postulated (reviewed in Gronostajski, 2000). The first mechanism suggests that NFI proteins serve to recruit co-activators, co-repressors, or RNA polymerase components upon binding to their consensus site. In support of this theory, NFI-A and NFI-C contain a copy of the heptapeptide repeat found in the C-terminal domain (CTD) of RNA polymerase II (Figure 1.3). This domain has been shown to interact with human transcription factor IIB (TFIIB) to activate transcription (Kim and Roeder, 1994). The second mechanism of NFI function suggests that specific NFI proteins, and splice forms, are recruited to promoters by proteins bound to sites adjacent to NFI consensus sites. These cooperative interactions would allow cell-specific proteins to cooperatively recruit specific NFI proteins and thereby mediate NFI activation or repression of promoters in a cell-specific manner. Finally, NFI proteins may displace activators, repressors or nucleosomes upon binding to generate an overly positive or negative environment for transcription.

1.4.2. *NFI Expression and CNS Specific Gene Regulation*

In the developing and mature mouse CNS, the expression of NFI proteins appears to be both spatially and temporally regulated (Chaudhry *et al.*, 1997). At ED11.5 in mouse embryos, NFI-A, -B, and -X are expressed in the neocortex region of the telencephalon, and NFI-B and -X are highly expressed in the cerebral cortex, while NFI-C is ubiquitously expressed at very low levels. Postnatally, NFI-X is expressed primarily in the grey matter of the cerebral cortex, whereas NFI-A and -B are concentrated in the white matter. This pattern of expression suggests a glial distribution for NFI-A and -B, and a neuronal distribution for NFI-X. In contrast, NFI-C is expressed at low levels in a more ubiquitous manner throughout the mature mouse brain. The spatiotemporal expression patterns of NFI proteins in the human CNS has not been determined, but studies by Krebs and coworkers (1996) suggest that NFI-A is expressed in glial cells and that it has a greater transactivation potential than the ubiquitously expressed NFI-C. In addition, through the use of human fetal glial cells and HeLa cells, Sumner *et al.* (1996) have postulated that NFI-X levels are elevated in glial cells.

The localization of specific members of the NFI family to glial cells is not surprising since these transcription factors have been implicated in regulating the expression of several genes in a glial cell-lineage specific manner, including human JC papovavirus genes (Amemiya *et al.*, 1992), *MBP* (Tamura *et al.*, 1988), *GFAP* (Miura *et al.*, 1990; Besnard *et al.*, 1991), and most recently, *B-FABP* (Bisgrove *et al.*, 2000). Interestingly, while NFI-B has been implicated in the transcriptional activation of the *MBP* gene in oligodendrocytes (Inoue *et al.*, 1990), NFI-A has been proposed to regulate *GFAP* expression. Recent studies have demonstrated that GFAP levels, but not S100β levels, are reduced in *NFI-A-/-* mice (das Neves *et al.*, 1999). This reduction in GFAP has been speculated to lead to abnormal development of midline glial structures due to the inability of astrocytes to adequately extend their processes (Shu *et al.*, 2003).

It is likely that the spatiotemporal distribution of the different NFI proteins is one of the more important mechanisms underlying activation or repression of NFI-responsive genes. However, cell-specific co-factors are also important. For instance, NFI-X represses *PDGF* basal transcription by binding to an NFI binding site in the *PDGF* promoter, but NFI-X can also repress Sp1-induced *PDGF* transcription activation by interacting with Sp1 and preventing its binding to the *PDGF* promoter (Rafty *et al.*, 2002). In regards to glial cell differentiation, this is particularly interesting because PDGF signaling is known to promote oligogliogenesis (Calver *et al.*, 1998). Thus, a better understanding of the transcription factors mediating glial-specific gene expression may provide greater insight into glial-cell differentiation and the malignancies that arise within the CNS.

1.5. Research Objectives

***Chapter 3*: Characterization of B-FABP and GFAP transcriptional regulation by NFI proteins.**

In light of the evidence that NFI family members (NFI-A, -B, -C, and –X) display distinct spatiotemporal distribution patterns in the developing and mature CNS, and the fact that specific NFI proteins have been implicated in the regulation of glial cell-specific genes, we hypothesize that *B-FABP* and *GFAP* transcription is regulated by specific NFI proteins. We also contend that in MG the loss of GFAP and B-FABP expression may correlate with the altered expression of one of more NFI family members. Here, we study the expression patterns of the four *NFI* genes in both B-FABP/GFAP-positive and B-FABP/GFAP-negative MG cell lines. In addition, we characterize the ability of each NFI protein to bind to NFI consensus DNA binding sites located in both the *B-FABP* and *GFAP* promoters and use the CAT reporter system to assess the biological activity of each NFI.

Chapter 4: Effects of B-FABP and/or GFAP expression in malignant glioma cell lines.

Previous work in our lab has led to the identification of a glial cell differentiation factor, B-FABP, that is co-expressed with GFAP in MG cell lines. While several groups have characterized the effects of GFAP expression in MG and glial cell differentiation, B-FABP expression in MG has not been examined. To address this issue, we expressed B-FABP and/or GFAP in two B-FABP/GFAP-negative MG cell lines, T98 and U87. Stable transfectants have been examined for proliferation rate, morphology, anchorage-independent growth, and invasion. To further examine the role B-FABP expression in MG, the RNA interference approach was used to reduce B-FABP expression in the B-FABP/GFAP-positive cell line, U251. Transfectants were examined for proliferation rate, morphology, anchorage-independent growth, and invasion. Although the abnormalities within MG are unquestionably complex and multiple, we hope that studying B-FABP and GFAP expression in these tumours will lead to new approaches for the treatment of MG, possibly by inducing their terminal differentiation.

CHAPTER TWO

Materials and Methods

2.1. General Tissue Culture and Molecular Biology Techniques

2.1.1. *Cell Lines and Culture Conditions*

All human malignant glioma cell lines (T98, U251MG, and U87MG) were obtained from Drs. Rufus Day III and Joan Turner, Department of Oncology, University of Alberta and Cross Cancer Institute. The source of these cell lines are: T98 (Walter Nelson-Rees, Naval Biomedical Research Station, Oakland, CA, USA); U87MG and U251MG (Jorgen Fogh, Sloane Kettering Institute, Rye, NY, USA). Unless otherwise stated, each cell line was grown as monolayers and passaged every 4 d in culture medium (DMEM supplemented with 10% FCS (GibcoBRL), 100 U/ml penicillin and 100 μg/ml streptomycin). The cell lines were grown in a humidified environment containing 5% CO_2 at 37°C.

2.1.2. *Calcium Phosphate Transfection*

All transfections of the malignant glioma cell lines were performed using the calcium phosphate DNA precipitation method as described by Graham and van der Eb (1973). Briefly, 10 μg of plasmid DNA for single transfectants and between 15-20 μg of total plasmid DNA for double transfectants were used for each 100-mm tissue culture dish (Sarstedt). The DNA in 250 mM $CaCl_2$ was mixed with an equal volume of 2X HEPES solution (50 mM HEPES, 280 mM NaCl, 1.5 mM NaH_2PO_4; pH 7.12) with constant bubbling. The precipitate was allowed to form over a period of 30 min and then added evenly to the 100-mm tissue culture dish containing approximately 2 x 10^6 cells that had been plated the previous day. After a 16 h incubation, the DNA precipitate was removed, the cells were washed twice with PBS (137 mM NaCl, 2.7 mM KCl, 4.3 mM $Na_2HPO_4 \bullet 7$

H_2O, 1.4 mM KH_2PO_4), and 10 ml of fresh culture medium was added. The cells were then incubated at 37°C for 48 h and either harvested for whole cell extract, nuclear extract or CAT analysis, or drug selected to obtain stable transfectants.

2.1.3. *Whole Cell Extract Preparation*

Near confluent 100-mm tissue culture plates were washed twice with 10 ml PBS, trypsinized, and resuspended in 10 ml of culture medium to inactivate the trypsin. Cell pellets were obtained by centrifugation at 1400 rpm for 7 min at RT. The pellets were washed twice with PBS and stored at -80°C overnight. The whole cell extracts were prepared on ice. Briefly, the cell pellet was resuspended in an equal volume (*i.e.* 50-100 µl) of buffer A (10 mM HEPES-NaOH pH 7.9, 1.5 mM $MgCl_2$, 10 mM KCl, and freshly added 0.5 mM DTT and 0.5 mM PMSF). An equal volume of 50 mM Tris-HCl pH 8.0/1% SDS solution was then added and the cells were syringed with a 23-gauge needle until the solution reached a viscosity that could be pipetted. 1-2 µl of extract was quantified using the Bradford assay (Bradford, 1976) and extracts were stored at -20°C or used immediately for western blot analysis.

2.1.4. *Plasmid DNA Preparation*

In all instances, except when the plasmid DNA was required for transfections, plasmid DNA was prepared using a protocol similar to the lysis by boiling method described by Sambrook *et al.* (1989). Briefly, 5 ml LB cultures were inoculated from a single bacterial colony and grown overnight at 37°C in a shaking incubator. Cultures were centrifuged at 2000 rpm for 10 min at 15°C and the bacterial pellet was resuspended in 700 µl of lysis buffer (8% sucrose, 0.5% Triton® X-100, 5 mM EDTA pH 7.5, 50 mM Tris-HCl pH 7.5). Lysozyme was then added to a final concentration of 1.5 µg/µl and the cells were vortexed briefly and incubated for 5 min at RT. To lyse the cells, the samples were boiled for 50 sec and then centrifuged for 10 min at RT. The DNA in the supernatant was precipitated in 700 µl of cold isopropanol, pelleted at 11000 rpm for 10 min at 4°C and washed with 75% ethanol. The pellet was resuspended in 100 µl TE followed by the addition of 100 µl of 7.5 M NH_4oAc and 500 µl of 100% ethanol. The centrifugation and 75% ethanol wash were repeated and the pellets were dried in a SpeedVac® (Savant Instruments Inc.) and resuspended in 80 µl of TE.

2.1.5. *Cesium Chloride Plasmid DNA Preparation*

All DNA to be used for transfections was generated using a method similar to that described by Sambrook *et al.* (1989) whereby lysis by alkali was used in conjunction with equilibrium centrifugation in CsCl-EtBr gradients. A 330 ml LB culture inoculated with 200 µl of a log phase bacterial culture was grown overnight at 37°C with shaking. Bacterial cells were pelleted at 7000 rpm for 15 min at 4°C in a GS-3 rotor (Sorvall) and the bacterial pellet was resuspended in 30 ml of cold TEG buffer (25 mM Tris-HCl pH 7.5, 10 mM EDTA, 50 mM glucose). Lysozyme was added to a final concentration of 2 mg/ml and incubated at RT for 10 min. To lyse the bacteria, 67 ml of lysis buffer (0.2 M NaOH, 0.1% SDS) was added with intermittent swirling on ice for 10 min. The bacterial DNA, high-MW RNA, and membranes were then precipitated by adding 50 ml of 3 M KoAc (adjusted to pH 4.8 with glacial acetic acid), inverting several times, and incubating the tube on ice for 15 min. The lysed bacterial solution was pelleted at 8000 rpm for 20 min at 4°C and the supernatant was poured through a gauze filter into a 500 ml centrifuge bottle. 100 ml of cold isopropanol was added and the solution was placed at -20°C for at least 1 h. Precipitated plasmid DNA was pelleted by centrifugation at 8000 rpm for 20 min at 4°C and the pellet was resuspended in 3.8 ml TE. 7.8 ml of CsCl saturated TE and 0.38 ml of EtBr (10 mg/ml) were then added to obtain a final CsCl density of 1.55 g/ml (refractive index = 1.393). The DNA/CsCl solution was centrifuged at 60000 rpm for 20 h at 20°C in a Sorvall T-127 rotor and the plasmid DNA band was collected using a pasteur pipette and subjected to a second round of CsCl purification. The twice-purified band was collected using a pasteur pipette and the ethidium bromide removed by extraction with 1-butanol. CsCl was removed by dialysis (MW cut off of 12000-14000 Da) with four changes of TE (pH 8.0) over a period of a least 4 h. The OD_{260} was measured and the DNA was diluted to ~1 μg/μl and stored in aliquots at -20°C.

2.1.6. *Restriction Endonuclease Digestions*

Plasmid DNA was analyzed by restriction endonuclease digestion. Generally, each digest contained ~1 μg of DNA, a 3-fold molar excess of restriction enzyme(s), the appropriate digestion buffer, and, if required, BSA in a total volume of 20 μl. Reactions were incubated at 37°C for at least 1 h. After the digestion, 3 μl of loading dye (50% sucrose in TE with 0.3% BPB) was added to each reaction and, if necessary, 50 ng/μl RNase A was added to degrade any residual RNA. The digests were then run on a 1% agarose gel in Howley buffer (40 mM Tris, 33 mM NaoAc, 1 mM EDTA; pH 7.2 with glacial acetic acid) and stained with ethidium bromide for visualization on a UV light box. Photographs of gels were taken using Alpha Imager™ 2000 (Alpha Innotech Corporation).

2.1.7. *DNA Insert and Oligonucleotide Purification by Electroelution*

For insert purification, 25-100 μg of plasmid DNA was digested with an appropriate restriction endonuclease(s) and purified by electroelution. For the purification of double-stranded oligonucleotides, the entire solution of annealed product (see **2.3.1**) was purified by electroelution. The DNA was loaded onto a polyacrylamide gel in TBE (4.5 mM Tris, 3.5 mM boric acid, 4 mM EDTA; pH 8.1) and electrophoresed for ~3 h at 170V in TBE. Bands of interest were visualized under UV light, excised, and electroeluted in TBE using dialysis tubing with a MW cut-off of 12000-14000 Da (3500 Da for oligonucleotide purification). Following electroelution, the DNA was collected by rinsing the inside of the dialysis tubing with ~2 ml of TE. This volume was transferred to a polypropylene tube, a 1/10 volume of 5 M NaCl was added, and the DNA was extracted with equal volumes of organic solvents (*i.e.* 1X chloroform:isoamyl alcohol (24:1), 1X phenol, 1X chloroform:isoamyl alcohol (24:1), and 1X ether). To precipitate the DNA, 2.5 volumes of 100% ethanol were added and the tube was incubated overnight at -20°C. The DNA was then pelleted by centrifugation at 8000 rpm for 30 min at 4°C and the pellet was washed with 75% ethanol. Once the pellet was dried, it was resuspended in an appropriate volume of H_2O or TE and the sample was stored at -20°C. Typically, 50-100 ng was run on an agarose gel to verify DNA purity and quantity.

2.1.8. *DNA Ligation and Bacterial Transformation*

DNA ligations were performed in a total reaction volume of 20 μl consisting of ligation buffer (50 mM Tris-HCl pH 7.5, 10 mM $MgCl_2$, 10 mM DTT), 1 mM ATP, 0.1 μg/μl BSA, a suitable volume of insert DNA, an appropriate volume of digested vector DNA[*], and 1U of T4 DNA ligase. The reactions were incubated overnight at 16°C. For bacterial transformation, 10 μl of the ligation reaction was diluted 1/5 with TE and 100 μl of chemically competent DH5α cells (thawed on ice from -80°C) were added to the diluted DNA. The mixture was incubated on ice for 20 min and then placed at 37°C for 5 min. 5 ml of LB was then added and the tube was incubated at 37°C for 30 min with shaking. After the incubation, the cells were plated on LB-agar plates containing the appropriate drug selection (*i.e.* ampicillin or kanomycin) and incubated overnight at 37°C.

---

[*] Generally, if the vector backbone DNA was cut with a single restriction endonuclease, the 5' phosphate was removed with calf intestinal alkaline phosphatase to prevent the vector from re-ligating. Briefly, 0.5 μl of calf intestinal alkaline phosphatase was added to the digested DNA and incubated for 45 min at 37°C.

2.1.9. *DNA Sequencing*

DNA sequencing was performed by capillary gel electrophoresis using the ABI PRISM® 310 Genetic Analyzer (Applied Biosystems). The sequencing reactions consisted of ~500 ng of plasmid DNA, 10 pmol of an appropriate primer, 4 μl of BigDye3™ terminator mix, and H_2O to a final volume of 10 μl per reaction. The sequencing products were generated in a GeneAmp® 2400 thermal cycler (Perkin Elmer). Amplification conditions consisted of 25 cycles of 96°C for 10 sec, 50°C for 5 sec, and 60°C for 4 min. Reaction products were precipitated by adding 1/10 volume of 3 M NaoAc pH 5.2 and 2.5X volume of 100% ethanol for 15 min[*] at RT. After precipitation, the reactions were centrifuged at 14000 rpm for 20 min at RT, the pellets were washed twice in 75% ethanol and then dried in a SpeedVac®. At this point, samples were either immediately prepared for sequencing or stored at -80°C until sequencing was to be performed. To prepare the reactions for sequencing, the dried pellets were resuspended in 12.5 μl of formamide (Fluka), boiled for 5 min, chilled on ice for 10 min, and then transferred to sequencing tubes and loaded on the ABI PRISM® Genetic Analyzer. Sequence data were collected with the ABI PRISM® 310 Collection Software (version 3.0.0), and were subjected to BLAST analysis (www.ncbi.nlm.nih.gov/BLAST) to verify conformity with published sequence data.

2.1.10. *RNA Preparation and Northern Blotting*[†]

RNA was prepared from frozen cell pellets. Briefly, the frozen pellets were resuspended in 500 μl of 50 mM NaoAc pH 5.2. To extract the RNA, 6 ml of 50 mM NaoAc/1% SDS and 6 ml 60°C phenol (equilibrated with 50 mM NaoAc pH 5.2) were added to the tube and vortexed. The tube was then incubated at 60°C for 15 min with frequent inversion, and placed on ice for 5 min. Organic and aqueous phases were separated by centrifugation at 3000 rpm for 10 min at 4°C and the phenol was removed. The aqueous phase was re-extracted with phenol followed by extraction with chloroform:isoamyl alcohol (24:1). The aqueous phase was then brought to a final concentration of 0.5 M NaCl and the RNA was precipitated with two volumes of 100% ethanol. After overnight incubation at -20°C, the RNA was pelleted at 3000 rpm for 50 min at 4°C. The supernatant was removed and the pellet was dried at RT. Poly(A)$^+$ RNA was purified by oligo dT-cellulose chromatography and stored at -80°C.

---

[*] Longer incubations should be avoided as it will lead to the precipitation of unincorporated dye terminator nucleotides.

[†] The RNA and northern blots were kindly prepared by Dr. Roseline Godbout.

To generate the northern blots, 2 μg of poly(A)$^+$ RNA for each sample were resuspended in sample buffer (C_f of 50% formamide, 17.5% formaldehyde, and 1X MOPS). Prior to loading, RNA samples were heat-shocked at 65°C for 15 min and then 3 μl of loading buffer (1X MOPS, 50% glycerol, and 0.1% BPB) was added. The RNA samples were loaded in a 1.5% agarose gel prepared in MOPS buffer (20 mM MOPS, 5 mM NaoAc, 1 mM EDTA; pH 7.2) with 6.3% formaldehyde. Gel electrophoresis was performed for 3-4 h at 40 mA in 1X MOPS. The RNA was transferred to a nitrocellulose membrane by capillary action for 20 h in 20X SSC. After transfer, the membrane was washed in 2X SSC, air-dried, and baked in a vacuum oven at 80°C for 2.5 h.

2.1.11. *Hybridization of Northern Blots and Probe Preparation*

Northern blot filters were incubated at 42°C for 4-16 h in pre-hybridization buffer (50% formamide, 5X SSC, 5X Denhardt's[*], 50 mM NaH_2PO_4 pH 6.5, and 125 μg/ml denatured salmon sperm DNA). The DNA probe was radiolabeled by nick translation. Briefly, a 25 μl nick translation reaction was set up on ice by combining ~500 ng of DNA, dGAT (C_f of 0.08 mM for each nucleotide), 7 μl of [α-^{32}P]dCTP (800 Ci/mmol, Amersham),

---

[*] A 100X Denhardt's stock solution contains 2 g of PVP, 2 g of BSA, and 2 g of Ficoll® in 100 ml of H_2O. This solution is filter sterilized prior to use.

DNase I (C_f of 0.016 ng/μl) and 7.5U of Kornberg DNA polymerase (Boehringer Mannheim) all in NT buffer (5 mM Tris-HCl pH 7.2, 10 mM $MgSO_4$, 0.1 mM DTT, 50 μg/ml BSA). The reaction was incubated for 30 min in a 16°C water bath and then terminated by adding 10 μl of stop buffer (125 mM EDTA, 10 mM Tris-HCl pH 7.5, 0.1% SDS, 10 μg/ml salmon sperm ssDNA and 0.1% phenol red). The probe was then heat-shocked at 65°C for 10 min and loaded onto a Bio-Gel® A-1.5m Bead Slurry (Bio-Rad) column to separate the radiolabeled probe from the unincorporated nucleotides. The probe was collected into a tube containing 150 μl of salmon sperm DNA (10 mg/ml), boiled for 10 min, and then put on ice for at least 5 min. The denatured probe was then combined with 10 ml hybridization mix for a final concentration of 50% formamide, 5X SSC, 3X Denhardt's, 20 mM NaH_2PO_4 pH 6.5, and 10% dextran sulfate. This mixture was inverted thoroughly and added to the blot. Filters were hybridized overnight at 42°C and then washed in 0.1% SDS, 2X SSC at RT followed by high stringency washes in 0.1% SDS, 0.1X SSC at 55-60°C. The blot was then dried and exposed to film. If the blot was to be re-probed, the membrane was stripped using 0.05X Thomas buffer (10X Thomas buffer: 0.5 M Tris-HCl pH 8.0, 20 mM EDTA, 5% $Na_2H_2P_2O_7$, 0.2% BSA, 0.2% Ficoll®, 0.2% PVP) at 60°C for 2-3 h.

2.1.12. *Western Immunoblotting Protein Detection*

SDS-PAGE was performed using the Mini-PROTEAN®II electrophoresis apparatus (Bio-Rad). For each gel, 7.5 ml of separating solution containing an appropriate concentration (10-15%) of acrylamide:bis (30:0.8) in separating buffer (0.1% SDS, 375 mM Tris-HCl pH 8.8, 37.5 μl 10% APS, 3.75 μl TEMED) was poured into the gel casting apparatus and overlayed with ~500 μl of isopropanol. The separating gel was allowed to polymerize for 30-60 min, the isopropanol was removed, and a 2.5 ml stacking gel consisting of 5.5% acrylamide:bis (30:0.8) in stacking buffer (0.1% SDS, 125 mM Tris-HCl pH 6.8, 37.5 μl 10% APS, 3.75 μl TEMED) was poured on top of the separating gel. Typically, 50 μg of whole cell extract or 20-25 μg of nuclear extract were run in each lane. The samples were prepared by adding an appropriate volume of loading dye (5X loading dye: 25% glycerol, 0.5% SDS, 1.25X stacking buffer, 0.0075% BPB, and 125 mM DTT) and boiling the samples for ~3 min prior to loading. 10 μl of broad range protein standards (Bio-Rad) were also boiled and included in one lane on each gel. The gels were generally electrophoresed at 120V in Laemmli buffer (25 mM Tris, 192 mM glycine, 0.1% SDS; adjusted to a final pH of 8.3) until the dye front had run off the bottom of the gel (~2 h). Proteins were transferred to a nitrocellulose membrane using the wet-transfer method as described by Sambrook *et al.* (1989). The transfer was performed for 2 h at 150 mA in transfer buffer (20% methanol, 25 mM Tris, 192 mM glycine; adjusted to a final pH of 8.3). To assess protein transfer, the blot was placed in 0.005% CPTS (in 12 mM HCl) for 5 min with shaking to visualize protein bands. The membrane was then washed twice in TBS (150 mM NaCl, 50 mM Tris-HCl pH 7.5) for 10 min and blocked in 10% milk powder (in TBS) for 30 min with shaking.

For immunoblotting, the membrane was placed in a sealed bag with an appropriate dilution of antibody in 5 ml of 5% milk powder (in TBS) and the blot was rotated overnight at 4°C on a platform shaker. After ~16 h, the membrane was washed 3X for 10 min each in TBS with 1% Tween-20 and then 1X for 10 min in TBS. To probe the blot with an HRP-conjugated secondary antibody, the membrane was placed in 50 ml of 5% milk powder (in TBS) containing a suitable secondary antibody diluted 1/50000. The blot was shaken for 4 h, the TBS with 1% Tween-20 and TBS washes were repeated, and protein detection was performed using the ECL™ western blotting detection reagents (Amersham-Pharmacia).

2.2. Analysis of the *B-FABP* and *GFAP* promoters

The CAT reporter system (Gorman *et al.*, 1982) was used to examine *B-FABP* and *GFAP* promoter activity in malignant glioma cells co-transfected with different isoforms of NFI.

2.2.1. *Cloning of the B-FABP promoter*[*]

The promoter of the *B-FABP* gene was cloned into the pCAT-basic vector (Promega) as previously described by Godbout *et al.* (1998) and Bisgrove *et al.* (2000). Briefly, a 3 kbp *Eco*RI fragment containing 1.8 kb of 5'-flanking DNA, *B-FABP* exon I, and *B-FABP* exon II was obtained from a human placenta genomic library (Clontech), subcloned into pBluescript® (Stratagene), and sequenced to generate pBluescript/B-FABP. A series of pCAT-basic/B-FABP constructs were then generated by linking different amounts 5'-flanking DNA to the CAT reporter gene. This was performed using a *Pst*I site located 20 bp downstream of the *B-FABP* transcription start site and another restriction site upstream of *Pst*I. The pCAT/B-FABP-160 construct, containing the 140 bp immediately proximal to the *B-FABP* transcription start site, was generated by restriction endonuclease digestion of pBluescript/B-FABP with *Xho*I and *Pst*I and subcloning into the MCS of pCAT-basic. In a similar manner, pCAT/B-FABP-440, with 420 bp of 5'-flanking sequence, was generated by digesting the DNA with *Eco*0109I and *Pst*I digest.

2.2.2. *Cloning of the GFAP Promoter*

The *GFAP* promoter fragments used to generate the pCAT/GFAP-176 and pCAT/GFAP-1716 constructs were obtained through PCR amplification of BAC clone RP11-975005 kindly provided by Dr. Stephen Scherer (Center for Applied Genomics, Hospital for Sick Children, Toronto, ON). This BAC clone contains human genomic DNA corresponding to positions 43414760-43482120 of chromosome 17. The *GFAP* transcription start site lies at position 43453402, so this BAC clone contains approximately 67 kbp of 5'-flanking DNA and the entire coding sequence for *GFAP*.

---

[*] The pCAT-basic/B-FABP constructs were generated by Dr. Dwayne Bisgrove.

Briefly, the BAC clone was obtained as an agar stab and was streaked on LB plates containing 20 μg/ml of chloramphenicol to isolate single colonies. To purify BAC DNA, a single colony was used to inoculate 5 ml of LB containing 20 μg/ml chloramphenicol. After overnight culture at 37°C with shaking, the bacteria was pelleted at 3000 rpm for 10 min at RT, resuspended in 300 μl of chilled P1 buffer (15 mM Tris-HCl pH 8.0, 10 mM EDTA, 100 μg/ml RNase A), and lysed by adding 300 μl of P2 buffer (0.2 M NaOH, 1% SDS). Samples were incubated for 5 min at RT, 300 μl of 3 M KoAc pH 5.5 was added, and the samples were placed on ice for 5 min. After centrifugation at 14000 rpm for 10 min at RT, 750 μl of supernatant (containing BAC DNA) was transferred to another tube and BAC DNA was precipitated in an equal volume of cold isopropanol. The DNA was then pelleted by centrifugation at 14000 rpm for 20 min and resuspended in 30 μl of H_2O.

The primers used to generate pCAT/GFAP-176 from BAC clone RP11-975005, in relation to the *GFAP* transcription start site (+1) were: primer 1 (5'-CTGGCTCTGCTGCT CGCT-3') corresponding to positions +8 to -10 and primer 2 (5'-CCTCTGGGCACAGTG ACC-3') corresponding to positions -168 to -150. The PCR amplification using these primers generated a 176 bp fragment with 168 bp of sequence upstream of the transcription start site. To generate pCAT/GFAP-1716, primer 1 was used along with primer 3 (5'-TGGAGTAGGGGACGCTGC-3') corresponding to positions -1755 to -1728. The PCR products were then re-amplified with a nested primer (primer 4) corresponding to positions -1708 to -1691 (5'-CCTGAGCTGGCTCTGTGA-3') and with primer 1. The final PCR product was 1716 bp with 1708 bp of sequence upstream of the transcription start site.

Each *GFAP* promoter fragment was ligated into the TOPO-TA vector® (Invitrogen) directly from the PCR reaction. For each *GFAP* fragment, a 6 µl TOPO® cloning reaction was performed consisting of approximately 25-100 ng of amplified DNA product (typically 1 µl of the PCR reaction), 0.2 M NaCl, 10 mM $MgCl_2$, and 0.5 µl of pCR®II-TOPO® reagent[*]. The reaction was incubated for 20 min at RT and then placed on ice. For the transformation, 2 µl of the ligation reaction was added to 25 µl of TOP10 one-shot competent cells (Invitrogen). Cells were thawed on ice for 30 min and then heat-shocked at 42°C for 30 sec. 250 µl of SOC medium (2% tryptone, 0.5% yeast extract, 10 mM NaCl, 2.5 mM KCl, 10 mM $MgCl_2$, 10 mM $MgSO_4$, 20 mM glucose) was then added and the cells were incubated at 37°C for 1 h with shaking. After the incubation, half the cells were plated on LB/AMP plates (100 µg/ml AMP) coated with 3 ml of 1% top agar containing X-gal (0.3 mg/ml) and IPTG (0.3 mg/ml) for colour selection. The plates were incubated overnight at 37°C and the next day white colonies were selected, and plasmid DNA was prepared and sequenced to ensure that there were no mutations introduced during PCR amplification. Each *GFAP* promoter fragment was then subcloned into the multiple cloning site of the pCAT-basic vector.

2.2.3. *Transfection and Harvesting of the Malignant Glioma Cell Lines*

Transfections were performed using the calcium phosphate DNA precipitation protocol (see **2.1.2**). For each transfection, 10 µg of the appropriate CAT vector (pCAT-basic, pCAT/B-FABP-160, pCAT/B-FABP-440, pCAT/GFAP-176, or pCAT/GFAP-1716) was used along with 0.5 µg of a specific NFI construct (pCHNFI-A, -B, -C, or -X) or control (pCH). The pCHNFI expression plasmids express HA-tagged mouse NFI-A1.1,

---

[*] The pCR®II-TOPO® reagent contains 10 ng/µl of linearized, topoisomerase-linked, pCR®II-TOPO® plasmid DNA in 50% glycerol, 50 mM Tris-HCl pH 7.4, 1 mM EDTA, 1 mM DTT, 0.1% Triton X-100, 100 µg/ml BSA.

NFI-B2, NFI-C2, and NFI-X2 (kindly provided by Dr. R.M. Gronostajski, Lerner Institute, Cleveland, OH, USA). Transfected cells were harvested by scraping in PBS and centrifugation at 1400 rpm for 7 min at RT to pellet. Pelleted cells were resuspended in 2 ml of PBS and divided into two aliquots: a 1.6 ml aliquot for the CAT assay and a 400 μl aliquot for Hirt DNA purification (Hirt, 1967).

2.2.4. *CAT Assay*

Cells were pelleted at 14000 rpm for 7 min at 4°C and the pellet was resuspended in 800 μl of TEN buffer (40 mM Tris-HCl pH 7.5, 1 mM EDTA pH 8.0, 150 mM NaCl) and incubated at RT for 5 min. The cells were then centrifuged for 2 min at RT and the pellet was resuspended in 120 μl of 0.25 M Tris-HCl pH 8.0. Extracts were prepared by subjecting the cells to three freeze-thaw cycles using liquid nitrogen and a 37°C water bath. After the freeze-thaw cycles, cell extracts were incubated at 60°C for 10 min, centrifuged at 14000 rpm for 2 min at RT, and the supernatant was transferred to a 1.5 ml eppendorf tube. To perform the CAT assay, 125 μl reactions containing 20 μl of the cell extract, 0.05 mCi/ml D-threo-[dichloroacetyl-1,2-^{14}C]-chloramphenicol (57 mCi/mmol, Dupont-NEN), and 0.2 mg/ml n-butyryl coenzyme A (Sigma) all in 0.25 M Tris-HCl pH 8.0 were incubated at 37°C for 3 h*.

2.2.5. *Preparation of Hirt DNA and Southern Blot Analysis*

To purify the episomal (Hirt) DNA, the 400 μl aliquot was centrifuged at 14000 rpm for 7 min at 4°C and the pellet was resuspended in 200 μl of Hirt buffer (10 mM Tris-HCl pH 7.5, 10 mM EDTA, 0.6% SDS). The genomic DNA was then precipitated in 1 M NaCl by adding 50 μl of 5 M NaCl and incubating the tube at 4°C overnight. Samples were then centrifuged at 14000 rpm for 20 min at 4°C and the supernatant (containing the episomal DNA) was collected and digested with proteinase K (C_f of 0.8 μg/μl) for 16 h at 37°C. The Hirt DNA was then extracted with equal volumes of organic solvents (*i.e.* 1X chloroform:isoamyl alcohol (24:1), 1X phenol, 1X chloroform:isoamyl alcohol (24:1), and 1X ether) and precipitated with two volumes of 100% ethanol. Hirt DNA was pelleted by centrifugation at 14000 rpm for 20 min at 4°C and the pellet was resuspended in 40 μl of TE.

---

* Incubation times can be adjusted to ensure values obtained are within the linear scale and to avoid CAT activity saturation. The CAT assay is linear for up to 20 h for samples with low levels of CAT activity.

For southern blot analysis, 3 μl of the Hirt DNA sample was linearized by restriction endonuclease digestion and electrophoresed on a 1% agarose gel for ~3 h at 45V. The DNA was transferred to a nitrocellulose membrane by capillary action for 20 h in 20X SSC. After transfer, the membrane was washed in 2X SSC, air-dried, and baked in a vacuum oven at 80°C for 2.5 h. For plasmid DNA detection, southern blots were probed with radiolabeled pCAT-basic vector in a similar fashion as described for the hybridization of northern blots (see **2.1.11**).

2.3. Electrophoretic Mobility Shift Assay (EMSA)

The mobility shift assay was carried out using a protocol similar to that described by O'Brien *et al.* (1995).

2.3.1. *Generation of Annealed and Radiolabeled Oligonucleotides*

Complementary oligonucleotides representing the three consensus NFI binding sites in the *B-FABP* promoter (either bp -62 to -33 [*B**-FABP* promoter NFI binding region 1 {B-br1}], bp -174 to -155 [B-br2], or bp -263 to -238 [B-br3]) and the *GFAP* promoter (either bp -126 to -100 [*G**FAP* promoter NFI binding region 1{G-br1}], bp -1591 to -1564 [G-br2], or bp -1639 to -1613 [G-br3]; Figure 2.1) were annealed and radiolabeled. Briefly, 2000 pmol of each pair of complementary oligonucleotides were incubated in annealing buffer (10

NFI Consensus Binding Site Sequence → $\frac{T}{C}$TGG$\frac{A}{C}$NNNNNGCCAA

```
A  B-br1    TTA AAT CAC TGG ATT TTT GCC CAC C
                  A GTG ACC TAA AAA CGG GTG GGA GAA

   B-br2    GGC CTG AGC CAA TCA CAA AG
              G GAC TCG GTT AGT GTT TC

   B-br3    AGC CCC ATT GAA TCC CTG CCG AG
                GGG TAA CTT AGG GAC GGC TCG AAA

B  G-br1    CCA TAG CTG GGC TGC GGC CCA AC
                    GAC CCG ACG CCG GGT TGG GGT

   G-br2    CTC ACC TTG GCA CAG ACA CAA TG
                  G AAC CGT GTC TGT GTT ACA AGC C

   G-br3    ATT GGG CTG GCC GCC CCC CAG GG
                  C GAC CGG CGG GGG GTC CCG GAG

C  G-br1*   CCA TAG CTA AGC TGC GGC CCA AC
                    GAT TCG ACG CCG GGT TGG GGT

   G-br2*   CTC ACC TTA ACA CAG ACA CAA TG
                  G AAT TGT GTC TGT GTT ACA AGC C

   G-br3*   ATT GGG CTA ACC GCC CCC CAG GG
                  C GAT TGG CGG GGG GTC CCG GAG

   NFI      ATT TTG GCT TGA AGC CAA TAT G
            TAA AAC CGA ACT TCG GTT ATA C

   Sp1      GAT CGA TCG GGG CGG GGC GAT C
            CTA GCT AGC CCC GCC CCG CTA G

   AP-2     GAT CGA ACT GAC CGC CCG CGG CCC GT
            CTA GCT TGA CTG GCG GGC GCC GGG CA
```

Figure 2.1 - Sequences of synthetic oligonucleotides. Oligonucleotides used to test NFI binding are shown. A, NFI binding regions in the B-FABP promoter: B-br1from bp -62 to -33, B-br2 from bp -172 to -155, and B-br3 from -263 to -238. B, NFI binding regions in the GFAP promoter: G-br1 from -126 to -100, G-br2 from -1591 to -1564, and G-br3 from -1639 to -1613. C, Competitor oligonucleotides including NFI, Sp1, AP-2, and mutated GFAP NFI binding regions (G-br1*, G-br2*, and G-br3*). The G-br1, G-br2, and G-br3 oligonucleotides were also used as competitors in some experiments. Putative NFI binding sites are shown in red and the mutated nucleotides are shown in blue.

mM Tris-HCl pH 7.5, 2 mM $MgCl_2$, 50 mM NaCl, 1 mM EDTA) at 95°C for 10 min. Reactions were then cooled slowly by placing the tubes at 72°C for 7 min followed by RT for 2 h and then 4°C for 16 h. The annealed oligonucleotides were purified by PAGE and electroelution. 4 pmol of this PAGE-purified DNA was used for each 20 μl labeling reaction. Labeling reactions were performed in NT buffer (5 mM Tris-HCl pH 7.2, 10 mM $MgSO_4$, 0.1 mM DTT, 0.05 μg/μl BSA) and contained approximately 500 ng of probe DNA, dAGT (C_f of 0.25 mM of each oligonucleotides), 7 μl of [α-^{32}P]dCTP (800 Ci/mmol, Amersham), and 2U of Klenow DNA polymerase (Boehringer Mannheim). Each reaction was incubated at RT for 15 min, cold chased with dCTP (C_f of 0.25 mM) for 5 min at RT, and then quenched by adding 40 μl of TE. The reactions were then loaded onto a Bio-Spin® disposable chromatography column (Bio-Rad) containing packed Biogel P-6 to remove any unincorporated label. Loaded columns were centrifuged for 4 min at 2600 rpm and the flow-through containing the labeled probe was collected. The radiolabeled oligonucleotides in the flow-through were precipitated by adding 1/10 volume of 3 M NaoAc pH 5.2 and two volumes of 100% ethanol. The next day, the tubes were centrifuged at 14000 rpm for 20 min at 4°C. The pellet was washed in 75% ethanol, dried, and resuspended in 100 μl TE. To estimate the amount of radioactivity incorporated into each probe, 2 μl was added to a scintillation vial containing 5 ml of Ready Safe™ Scintillation Cocktail (Beckmann) and counted in a scintillation counter. Probes were stored at -20°C.

2.3.2. *Nuclear Extract Preparation*

Nuclear extracts from T98, U251, and T98 cells transiently transfected with 10 μg pCH control or pCHNFI-A, -B, -C, or –X expression plasmids were prepared using the technique described by Dignam *et al.* (1983). After transfection, cells were grown to approximately 90% confluence in 100-mm tissue culture dishes, washed twice in PBS, harvested in a small volume of PBS by scraping with a rubber policeman, pelleted by centrifugation at 1400 rpm for 7 min, and stored at -80°C. For nuclear extract preparation, all the following steps were performed at 4°C. The cell pellets were thawed on ice and then incubated for 10 min in a small volume (100 µl - 250 µl depending on pellet size) of buffer A (10 mM HEPES-NaOH pH 7.9, 1.5 mM $MgCl_2$, 10 mM KCl, and freshly added 0.5 mM DTT and 0.5 mM PMSF). The cells were then homogenized in a 1 ml dounce homogenizer with 15 strokes of a pestle and the mixture was centrifuged at 1000*g* for 10 min. The supernatant was discarded, and the remaining pellet (*i.e.* the crude nuclear extract) was centrifuged at 25000*g* for an additional 20 min. Residual supernatant was removed and the pellet was resuspended in a small amount (typically 50 µl) of buffer C (20 mM HEPES-NaOH pH 7.9, 25% glycerol, 0.42 M KCl, 1.5 mM $MgCl_2$, 0.2 mM EDTA, and freshly added 0.5 mM DTT and 0.5 mM PMSF). Resuspension took place over a 1 h period with periodic (every 10 min) pipetting. The suspension was then centrifuged at 25000*g* for 30 min and the supernatant was collected. Protein concentrations were determined using the Bradford assay (Bradford, 1976) by combining 2 µl of nuclear extract, 800 µl of H_2O, and 200 µl of Bradford reagent (Bio-rad), vortexing briefly, and reading OD_{590} in a DU® 7400 spectrophotometer (Beckmann) against a programmed standard curve. Nuclear extracts were stored at -80°C.

2.3.3. *EMSA*

Before the addition of labeled oligonucleotides, the nuclear extracts were pre-incubated with 1.25 µg of poly [dI-dC] in binding buffer (20 mM HEPES pH 7.9, 20 mM KCl, 1 mM spermidine, 10 mM DTT, 10% glycerol, and 0.1% NP-40) for 10 min at RT. For the T98 and U251 nuclear extracts, 4 µg of total nuclear protein was used for the pre-incubation. For the nuclear extracts generated from the T98 cells transiently transfected with pCH or pCHNFI expression plasmids, 1 μg of nuclear extract was used. After the pre-incubation, labeled oligonucleotides (approximately 40 fmol in 1-2 μl) were added and incubated for 20 min at RT. DNA-protein complexes were loaded onto a pre-run 0.5X TBE 6% polyacrylamide gel (29:1 acrylamide:bis) and electrophoresed for 100 min at 150V.

2.3.4. *Competition and Antibody Supershift Experiments*

For competition experiments, a 100-fold molar excess (4 pmol) of unlabeled oligonucleotide was added during the pre-incubation stage. Competitor oligonucleotides included consensus binding sites for AP-2, NFI, and Sp1, as well as, G-br1, G-br2, and G-br3 oligonucleotides (Figure 2.1). Mutated G-br oligonucleotides (G-br*) were also used as competitors (Figure 2.1). For supershift experiments, 1 μl of anti-HA antibody (clone H7, Sigma) was included in the pre-incubation reaction.

2.4. Establishment of sense *B-FABP* and/or *GFAP* Stable Transfectants

2.4.1. *Cell Lines and Plasmid Constructs*

The U87 and T98 human malignant glioma cell lines were derived from glioblastoma multiforme tumour tissue (Pontén and MacIntyre, 1968; Stein, 1979). These cell lines lack B-FABP and GFAP expression at both the mRNA and protein levels (Godbout *et al.*, 1998). The expression vector constructs used to express B-FABP and/or GFAP in these cell lines were pREP4/B-FABP, pREP4/GFAP, and pcDNA3/B-FABP[*]. The pREP4/B-FABP expression plasmid carries the gene for hygromycin resistance and a 467 bp insert containing the entire human *B-FABP* coding region. The pcDNA3/B-FABP construct also contains this 467 bp human *B-FABP* insert, but carries the neomycin resistance cassette. The pREP4/GFAP expression vector contains a 2.3 kbp *GFAP* cDNA insert obtained from ATCC (Clone HHCPF23).

---

[*] The B-FABP and GFAP expression constructs were generated by Dr. Dwayne Bisgrove.

2.4.2. *Transfection and Colony Selection*

Transfections were performed as described earlier (see **2.1.2**). When the T98 or U87 cell lines were transfected with only pREP4/B-FABP or pREP4/GFAP, 10 μg of plasmid DNA was used for the transfection. When T98 was co-transfected with pREP4/GFAP and pcDNA3/B-FABP, 7.5 μg of each expression plasmid was used. Transfected cells were selected in culture medium containing 400 μg/ml hygromycin (Roche), while double transfectants were selected in culture medium containing 400 μg/ml hygromycin and 800 μg/ml Gibco G418 (Invitrogen). After 3 weeks, single colonies containing 250-500 cells were trypsinized within a cloning ring and transferred to a single well of a Falcon® 24-well plate tissue culture plate (BD Biosciences). Approximately six clones were selected for each transfectant. Each colony was expanded as a separate clone in culture medium containing hygromycin (200 μg/ml) and/or G418 (400 μg/ml) until two confluent 100-mm plates were generated. At this time, each clonal population was frozen in DMEM containing 20% FCS and 10% DMSO. Control transfectants for both the T98 and U87 cell lines were generated through the transfection of the pREP4 vector.

2.5. RNA Interference Experiments

To reduce the levels of B-FABP in the U251 malignant glioma cell line, the pSUPER RNAi system (Oligoengine™) was used to generate stable expression of *B-FABP* siRNA (Brummelkamp *et al.*, 2002).

2.5.1. *Generation of the pSUPER, pSUPERDDX1, and pSUPERB-FABP Constructs*

The pSUPER vector was kindly provided by Dr. Gordan Chan (Cross Cancer Institute, Edmonton, AB). The general strategy for generating the pSUPER/B-FABP and pSUPER/DDX1* constructs involved subcloning a 64 bp inverted repeat into pSUPER within the *Bgl*II/*Hin*dIII sites. The 64 bp inverted repeat contained both a sense and anti-sense copy of a 19-nt gene-specific sequence derived from either the *B-FABP* or *DDX1* coding region. The 19-nt sequences were empirically determined, but are flanked in the mRNA with AA at the 5'-end and were analyzed by BLAST searches to verify that they did not have any significant sequence homology with other genes. The PAGE-purified 64-nt oligonucleotides used to generate pSUPER/B-FABP, with the 19-nt gene-specific sequence in bold, were 5'-GATCCCC**CCAACGGTAATTATCAGTC**TTCAAGAGA**GACTGATAATTACCGTTGG**TTTTTGGAAA-3' (forward primer) and 5'-AGCTTTTCCAAAAA**CCAACGGTAATTATCAGTC**TCTCTTGAA**GACTGATAATTACCGTTGG**GGG-3' (reverse primer). For the pSUPER/DDX1 construct, the gene-specific portion of the 64-nt primers consisted of 5'-**TTGGGTCAGATGGTCTTTG**-3' and 5'-**CAAAGACCATCTGACCCAA**-3'. The 19-nt gene-specific sequence for the pSUPER/B-FABP 64-nt primers corresponds to nucleotides 114-133 of the *B-FABP* coding region, while the targeted region for the pSUPER/DDX1 64-nt primers corresponds to nucleotides 597-616 in the *DDX1* coding region.

To ligate the oligonucleotides into the pSUPER vector, 1 nM of each gene-specific oligonucleotide was annealed in 100 mM KoAc, 30 mM HEPES-KOH pH 7.4, 2 mM MgoAc in a total volume of 50 μl. Annealing reactions were incubated at 95°C for 4 min, 70°C for 10 min, and then 4°C overnight. Annealed oligonucleotides were phosphorylated by combining 2 μl of annealed oligonucleotides with 1 mM ATP and 1 U T4 PNK (New England Biolabs) in T4 PNK buffer (70 mM Tris-HCl pH 7.6, 10 mM $MgCl_2$, 5 mM DTT) in a total volume of 10 μl. Reactions were incubated at 37°C for 30 min and heat-inactivated at 70°C for 10 min. For the ligation, 2 μl of the annealed phosphorylated oligonucleotides and approximately 500 ng of pSUPER (*Bgl*II/*Hin*dIII digested) were used. The ligation products were transformed into DH5α cells, and vectors containing the 64 bp insert were identified by *Eco*RI/*Hin*dIII restriction enzyme digestion and verified by sequencing.

---

* pSUPER/DDX1 is a construct that produces siRNA for the DEAD box 1 (DDX1) gene. In these experiments it was used as a control.

2.5.2. *Cell Lines, Transfection, and Colony Selection*

The U251 cell line was derived from a patient with malignant astrocytoma (Westermark *et al.*, 1973). This cell line expresses both B-FABP and GFAP at high levels (Godbout *et al.*, 1998). To generate stable U251-pSUPER, -pSUPER/DDX1, and -pSUPER/B-FABP cell lines, U251 cells were co-transfected with 7.5 μg of one of these pSUPER constructs and 7.5 μg of pREP4. Transfected cells were cultured in medium containing hygromycin (400 μg/ml) and, after 2 weeks, six colonies for each transfectant were selected and expanded as a separate clonal population in culture medium containing hygromycin (200 μg/ml).

2.6. Cell Morphology Experiments

Cell morphology was analyzed by phase contrast microscopy using a Nikon Diaphot 300 microscope and photos were taken using a mounted Nikon F50 camera. Briefly, cells were grown to confluence in culture medium containing the appropriate selection drugs (*i.e.* 200 μg/ml of hygromycin and/or 400 μg/ml of G418). To allow time for the cells to attach to the surface of the plate and develop their phenotypic characteristics, cell lines were analyzed for cell morphology 48 h after plating. Morphology was analyzed at various stages of confluence and photos were typically taken when the cells had reached 60-80% confluence.

2.7. Proliferation Rate Assay

To measure proliferation rate, cells were grown to confluence on 100-mm tissue culture plates in culture medium containing drug selection (200 μg/ml of hygromycin, 400 μg/ml of G418), and then passaged to new 100-mm tissue culture plates in the absence of any drug selection. When the cells reached approximately 80% confluence they were trypsinized, resuspended in approximately 8 ml of fresh culture medium, and counted using a Coulter Particle and Size Analyzer (Beckman Coulter). For the proliferation rate experiments, 15000 cells were plated out in triplicate in 35-mm tissue culture wells for each time point (typically 48 h, 96 h, 120 h, 144 h, and 168 h). At the appropriate time points, the number of cells in each well was counted using a Coulter Particle and Size Analyzer. The triplicate values were averaged[*] and plotted to generate growth rate curves from which the doubling time for each cell line was calculated.

2.8. Analysis of Anchorage-Independent Growth

Anchorage-independent growth was analyzed using the soft agar assay first introduced by MacPherson and Montagnier (1964) and described by Freshney (1983). Each cell line was tested as early as possible using an aliquot of cells frozen at an early passage. After two passages and when the cells reached 80% confluence, the cells were counted using a Coulter Particle and Size Analyzer and diluted in culture medium to a concentration of 2×10^4 cell/ml in a 10 ml volume.

A 1.2% agarose stock was prepared by adding 1.2 g of agarose to 100 ml of H_2O. The 1.2% agarose stock was autoclaved and placed in a 45°C water bath. The 1.2% agarose was mixed 1:1 with warmed (45°C) 2X DMEM supplemented with 20% FCS, 200 U/ml penicillin and 200 μg/ml streptomycin sulfate. 2 ml of this 0.6% agarose-medium was plated into 35-mm Falcon® petri dishes (BD Biosciences) and placed at 4°C for 5 min followed by a 10 min incubation at 37°C in a CO_2 incubator. Briefly, 5 ml of a 1 x 10^4 cell/ml 0.3% agarose-medium solution was generated by mixing 2.5 ml of a 2 x10^4 cell/ml cell suspension with 2.5 ml of 0.6% agarose-medium and 1 ml of this 1 x 10^4 cell/ml 0.3% agarose-medium solution was layered over the 0.6% agarose-medium basal layer in quadruplicate plates. The plates were incubated for 4 weeks and colonies were counted using a Nikon Diaphot 300 light microscope with a 4X objective. A colony greater than 50 cells[*] was scored as positive and counted. Low magnification photographs were taken using an Olympus OM-4T Camera mounted on a Leica MZ95 Dissecting Microscope with a 0.63X objective.

---

[*] None of the individual counts at any time point differed significantly from one another within any triplicate group, so values were averaged rather than generating error bars on the growth rate curves.

2.9. Matrigel™ Invasion Assay

BD Biocoat™ Matrigel™ invasion chambers (BD Biosciences, Cat. #354480) were used to study the invasive potential of malignant glioma parent cell lines and transfectants. The protocol was provided by BD Biosciences (www.bdbiosciences.com). Each cell line was started fresh from a frozen aliquot. After two passages in culture medium and when the cells reached 80% confluence, the cells were counted using a Coulter Particle and Size Analyzer. Cells were then diluted in serum-free DMEM to a concentration of 1 x 10^5 cell/ml in a 5 ml volume for the matrigel invasion assay.

2.9.1. *Invasion Assay for Malignant Glioma Cell Lines*

Matrigel invasion chamber inserts (stored at -20°C) were brought to RT by placing the inserts in a new 24-well Falcon® tissue culture plate. To rehydrate the matrigel, the inserts were transferred to a well containing 0.5 ml of 37°C serum-free DMEM medium and

---

[*] Typically, a colony of 50 cells corresponds to about 100 μm. However, the size of individual cells between each cell line was not identical so an estimation of the number of cells in a colony was deemed a more accurate method of scoring colonies.

0.5 ml of serum-free medium was added to the upper chamber of the matrigel insert. Rehydration took place at 37°C for 2 h in a humidified environment containing 5% CO_2. After rehydration, the medium in the upper chamber was removed and the insert was transferred to a new well containing 750 µl of DMEM with chemoattractant (*i.e.* 10% FCS). 250 µl of the 1 x 10^5 cell/ml cell suspension was immediately added, in triplicate wells, to the upper chamber of the matrigel invasion inserts. The inserts were then placed in a CO_2 incubator at 37°C for 22 h or 30 h.

2.9.2. *Fixation, Staining, and Counting of Invasive Cells*

To quantify the invasive potential of each cell line, the medium was removed from the upper well of each matrigel insert and a cotton-tipped swab moistened with warm serum-free DMEM was used to remove any cells in the upper chamber that had not passed through the filter. This process was repeated twice with a fresh swab. The insert was then placed in a new well containing 1 ml of 100% methanol to fix the cells. After 2 min, the insert was transferred to a well with 1 ml of 1% crystal violet stain (prepared in 100% methanol) for 5 min. The insert was then washed by dipping the insert into a beaker filled with H_2O. When the residual stain had been washed off the insert, it was placed in an empty well of a 24-well plate and allowed to air-dry. Once the insert had dried, a photograph was taken using an Olympus OM-4T Camera mounted on a Leica MZ95 Dissecting Microscope with a 1X objective. The photographs were used to count the number of cells on the insert.

2.6. Immunofluorescence of Transfectants

Immunofluorescence analysis was performed on the T98 and U87 transfectants to study the relative levels of B-FABP and/or GFAP in each of the T98 or U87 transfectants and to determine the percentage of cells expressing B-FABP and/or GFAP.

2.10.1. *Antibodies*

The primary antibodies used in these experiments were a rabbit polyclonal anti-B-FABP antibody (produced by our laboratory) and a mouse monoclonal anti-GFAP antibody cocktail[*] (Cat. #60311D, PharMingen). The rabbit anti-B-FABP antiserum (batch 2292) was prepared by Mary Packer, a technician in our laboratory, using native B-FABP (amino acids 1-132). The antiserum was affinity-purified by Dr. John Rowe, a research associate in our laboratory, using B-FABP recombinant protein and a HiTrap NHS-activated Sepharose column. The fluorescent secondary antibodies used included Alexa 488 goat anti-mouse and Alexa 555 goat anti-rabbit (Cedarlane Laboratories).

2.10.2. *Preparation of Coverslips and Antibody Staining*

Coverslips were seeded with 25000 cells in a single well of a Falcon® 24-well plate tissue culture plate in culture medium containing the appropriate selection drugs (*i.e.* 200 μg/ml of hygromycin and/or 400 μg/ml of G418). When the cells on the coverslips had reached approximately 60-80% confluence, they were washed 2X in PBS, fixed in 1% paraformaldehyde in PBS for 10 min, and permeabilized in 0.5% Triton® X-100 in PBS for 5 min. The cells were double-stained with rabbit polyclonal anti-B-FABP (1:100) and mouse monoclonal anti-GFAP (1:1000) antibodies in blocking buffer (3% BSA in PBS). After a 2 h incubation, the coverslips were washed 3X with PBS and then incubated for 2 h with the fluorescent secondary antibodies (Alexa 488 and Alexa 555) (1:200). Following three washes in PBS, the coverslips were mounted on slides using glycerol containing 1 mg/ml p-phenylenediamine + 1 μg/ml 4',6-diamidino-2-phenlyindole (DAPI).

---

[*] The anti-GFAP antibody cocktail contains a mixture of three monoclonal anti-GFAP antibodies (4A11, 1B4, and 3E1). Each antibody is at an equal concentration in the cocktail.

2.10.3. *Confocal Microscopy*

Images were collected on a Zeiss LSM 510 confocal microscope. To compare B-FABP and/or GFAP expression between each of the transfectants, a 25X/0.8 immersion correction lens was used. B-FABP subcellular localization in each of the U87-BFABP transfectants was examined using a 40X/1.3 oil immersion lens. Argon and helium (HeNe) lasers were used sequentially to scan at wavelengths of 488 nm and 543 nm, respectively. A UV laser was used to excite DAPI stained cells. Laser scanning parameters (*i.e.* laser strength, detector gain, amplitude offset, and pinhole size) were kept constant throughout the image collection using the 25X/0.8 immersion correction lens to ensure the collected images could be compared quantitatively. For the single cell images with the 40X/1.3 oil immersion lens, laser scanning parameters were optimized for each image to prevent signal saturation.

CHAPTER THREE

Characterization of B-FABP and GFAP transcriptional regulation by NFI proteins.

3.1. Expression of *NFI* mRNA in Malignant Glioma

Members of the NFI family of transcription factors (NFI-A, -B, -C, and -X) are expressed in a spatiotemporal dependent manner during CNS development. In postnatal mouse, NFI-A and NFI-B are localized primarily to the white matter of the cerebral cortex, suggesting a glial distribution, while NFI-C is ubiquitously expressed throughout the mouse brain (Chaudhry *et al.*, 1997). In humans, NFI-A and NFI-X are expressed in glial cells where these two NFI proteins appear to have a greater transactivation capacity than other NFI proteins (*i.e.* NFI-C) (Krebs *et al.*, 1996; Sumner *et al.*, 1996).

Expression of NFI-A and NFI-X in glial cells may be of significance as NFI family members have been implicated in mediating glial cell-specific gene transcription. Of note, reduced levels of GFAP have been observed in *NFI-A*-/- mice, suggesting a role for NFI-A in the activation of *GFAP* transcription (das Neves *et al.*, 1999). Furthermore, studies from our lab have shown that NFI proteins are important for the regulation of B-FABP expression in MG (Bisgrove *et al.*, 2000). However, the specific NFI proteins that contribute to B-FABP and GFAP regulation in MG have not yet been identified. We therefore screened five B-FABP/GFAP-positive and five B-FABP/GFAP-negative MG cell lines (Godbout *et al.*, 1998; Bisgrove *et al.*, 2000) to determine if quantitative or qualitative differences in NFI could account for the pattern of B-FABP and GFAP expression in these cell lines.

A northern blot loaded with RNA prepared from B-FABP/GFAP-positive (M016, M049, M103, U251 and U373) and B-FABP/GFAP-negative (A172, CLA, M021, T98 and

U87) MG cell lines was sequentially hybridized with radiolabeled probes for NFI-A, -B, -C, -X, B-FABP, GFAP and actin. As shown in Figure 3.1, M016, M049, M103, U251 and U373 expressed both *B-FABP* and *GFAP* mRNA, with *B-FABP* being highest in M103 and U251 and *GFAP* being highest in M103. A172, CLA, M021, T98, and U87 produced neither *B-FABP* nor *GFAP* mRNA.

Analysis of *NFI-A*, *-B*, *-C* and *-X* mRNA did not reveal a direct correlation with *B-FABP* and/or *GFAP* expression (Figure 3.1). All four *NFI* genes were typically expressed in the MG cell lines, albeit at different levels. *NFI-B* and *NFI-C* were expressed in all the MG cell lines analyzed. *NFI-A* was primarily expressed in M049 and M103, while *NFI-X* was predominant in M103 and M021. Overall, levels of *NFI-A*, *NFI-X* and possibly *NFI-B* were higher in the B-FABP/GFAP-positive cell lines compared to the B-FABP/GFAP-negative cell lines. Interestingly, the M103 cell line, which expressed the highest levels of both *B-FABP* and *GFAP*, also expressed the highest levels of *NFI-A* and *NFI-X*.

As antibodies specific to each NFI protein are not yet available, we were not able to corroborate our northern blot results by western blot analysis. From the mRNA data, we hypothesize that factors or events other than the presence or absence of NFI proteins are likely involved in the regulation of *B-FABP* and *GFAP* in MG. These factors/events may include the post-translational modification of NFI proteins, including phosphorylation and/or glycosylation (Jackson and Tjian, 1988; Jackson *et al.*, 1990). In support of this concept, our lab has previously shown that the NFI proteins in B-FABP/GFAP-positive MG cell lines are hypophosphorylated in comparison to the NFI proteins in the B-FABP/GFAP-negative MG cell lines (Bisgrove *et al.*, 2000). In addition, other researchers have speculated that NFI-C binds to the promoter of the carboxyl ester lipase (CEL) gene as a phosphoprotein (Kannius-Janson *et al.*, 2002).

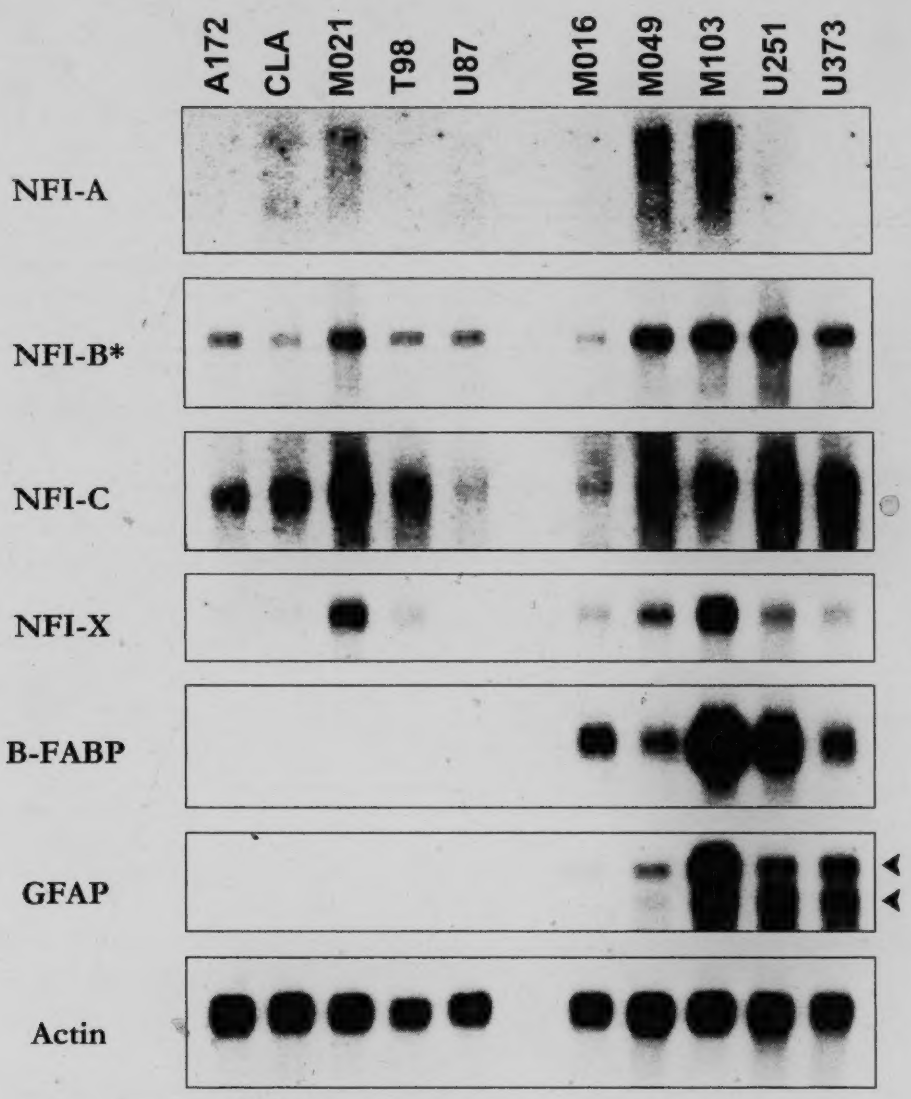
A172
CLA
M021
T98
U87
M016
M049
M103
U251
U373
NFI-A
NFI-B*
NFI-C
NFI-X
B-FABP
GFAP
Actin

Figure 3.1 - Northern blot analysis of 10 MG cell lines. A northern blot was prepared by transferring 2 μg of poly(A)$^+$ RNA derived from five B-FABP/GFAP-negative (A172, CLA, M021, T98, and U87) and five B-FABP/GFAP-positive (M016, M049, M103, U251, and U373) MG cell lines onto nitrocellulose. The blot was sequentially hybridized with ^{32}P-labeled DNA probes specific for NFI-A, -B, -C, -X, B-FABP, GFAP, and actin. After each hybridization, the blot was stripped as described in Materials and Methods. Two different size *GFAP* transcripts are indicated with arrowheads.

* Preliminary data shown for NFI-B were obtained using an oligonucleotide specific for NFI-B rather than a cDNA probe. We are in the process of preparing a cDNA probe for NFI-B to confirm these data.

3.2. Protein Binding to the Putative NFI-Binding Sites in the *GFAP* promoter

Previous studies from our lab characterizing the *cis*- and *trans*-acting elements that regulate the expression of the human *B-FABP* gene have led to the identification of two NFI-binding sites located at -54/-40 bp and -257/-243 bp in relation to the transcription start site (Bisgrove *et al.*, 2000). A third NFI-like binding site at -171/-157 bp failed to bind NFI when used in gel shift assays. Similarly, three putative NFI binding sites have been identified in the human *GFAP* promoter, located at -120/-106 bp, -1585/-1571 bp and -1633/-1619 bp (Besnard *et al.*, 1991). While each of these putative NFI-binding sites corresponds to a site of DNA-protein interactions based on DNase I footprinting studies (Besnard *et al.*, 1991), experiments have not been performed to definitively prove that these footprints were formed as the result of NFI-DNA interactions.

To determine whether the putative NFI-binding sites in the *GFAP* promoter are able to bind NFI, we used the electrophoretic mobility shift assay (EMSA). Double-stranded oligonucleotides were generated for each of the *GFAP* promoter NFI-binding regions (G-br1, G-br2 and Gbr3). The oligonucleotides consisted of the putative NFI-binding site as well as ~6 bp of sequence on each side of the NFI site. The double-stranded oligonucleotides synthesized are shown in Figure 2.1 and include: bp -126 to -100 (G-br1), bp -1591 to -1564 (G-br2), and bp -1639 to -1613 (G-br3). These oligonucleotides were radiolabeled and used as probes in the EMSAs. In addition to these oligonucleotides, competitor oligonucleotides were generated and are shown in Figure 2.1. Competitor oligonucleotides included unlabeled G-br1, G-br2 and G-br3, as well as consensus binding sites for AP-2, NFI, and Sp1. Mutated G-br oligonucleotides (G-br*) were also used as competitors for their respective G-br to verify that mutations in the NFI-binding site would eliminate the DNA-protein interaction. For the EMSAs, nuclear extracts from either B-

FABP/GFAP-negative T98 cells or B-FABP/GFAP-positive U251 cells were pre-incubated alone or with a 100-fold excess of unlabeled G-br1, Gbr2, Gb3, Sp1, NFI, AP-2 or the appropriate G-br*. After this pre-incubation period, each reaction was incubated with radiolabeled oligonucleotides corresponding to G-br1, G-br2 or G-br3.

Results from these experiments are shown in Figure 3.2. One major DNA-protein band was obtained when G-br1, G-br2 or G-br3 was used as the ^{32}P-labeled probe with the T98 nuclear extract (Figure 3.2, panel A). This complex was specifically competed out by unlabeled G-br1, G-br2, G-br3 and NFI oligonucleotides, but not by Sp1, AP-2 or G-br1*, indicating that the protein that bound G-br1, G-br2 and G-br3 is NFI or NFI-like. Although all the cold competitors (G-br1, G-br-2 and G-br3) were effective in reducing the intensity of the protein-DNA band, optimal competition was observed when competitor and probe oligonucleotides were of the same species.

Interestingly, the DNA-protein complex in the lane with no competitor was more intense than the lane where G-br1*, G-br2* or G-br3* was used as a competitor. This was especially apparent for G-br3 and suggests that either NFI proteins are able to bind to the mutated NFI site with low affinity or that there are other proteins in the T98 nuclear extract that are able to bind to the G-br1, G-br2 and G-br3 oligonucleotides. In support of the latter, the G-br1, G-br2, G-br-3 or NFI cold competitors were not always able to completely eliminate the DNA-protein complex. In addition, the intensity of the complex obtained with G-br3 was reduced upon the addition of Sp1 and AP-2 competitor oligonucleotides. Results obtained with the G-br3 probe can be partially explained by the presence of Sp1- and AP-2-like sites in the G-br3 oligonucleotide (Besnard *et al.*, 1991).

When the G-br1 and G-br2 probes were used in gel shift experiments with the U251 nuclear extract, one major DNA-protein band was observed (Figure 3.2, panel B). This

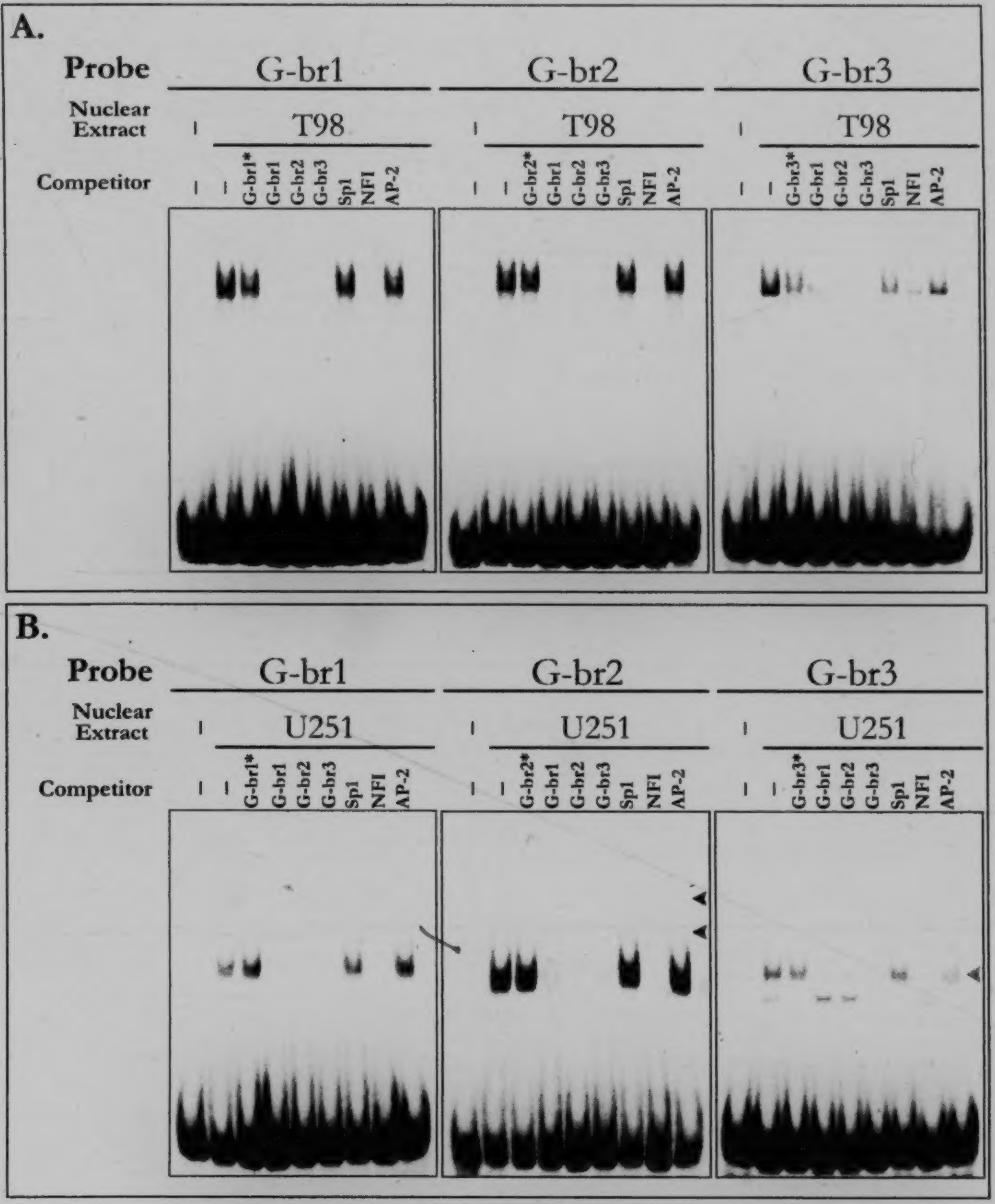
A.
Probe
G-br1
G-br2
G-br3
Nuclear Extract
T98
Competitor
G-br1*
G-br1
G-br2
G-br3
Sp1
NFI
AP-2
G-br2*
G-br3*
B.
U251

Figure 3.2 - Binding of NFI to G-br1, G-br2 and G-br3. Gel shifts were carried out by pre-incubating T98 (panel A) or U251 (panel B) nuclear extracts alone or with a 100-fold excess of unlabeled competitor oligonucleotides for G-br1, G-br2, G-br3, Sp1, NFI, AP-2 or the appropriate G-br*. The reactions were then incubated with radiolabeled G-br1, G-br2 or G-br3 oligonucleotides. DNA binding reactions were electrophoresed in a 0.5X TBE 6% polyacrylamide gel to separate unbound (free) DNA and DNA-protein complexes.

band was specifically competed out by G-br1, G-br2, G-br3 and NFI, indicating that both G-br1 and G-br2 oligonucleotides can bind NFI or NFI-like proteins. In addition, two minor DNA-protein complexes were observed with the G-br2 probe (Figure 3.2, blue arrowheads). These complexes were competed out by G-br2* and G-br2 only, suggesting that the minor bands are not simply different phosphorylation states of NFI proteins since they were not competed out by consensus NFI oligonucleotides. Instead, it is possible that other proteins bind G-br2, such as AP-1 whose binding site is immediately upstream of the NFI binding site and which is not affected by mutation of the NFI site.

In contrast to the single band observed when the G-br3 probe was incubated with the T98 nuclear extract, three distinct DNA-protein complexes were observed with the U251 nuclear extract (Figure 3.2, panel B). Only one of these three bands was specifically competed out by G-br1, G-br2, G-br3 and NFI (indicated with a red arrowhead). The intensity of this band did not change upon addition of G-br3* competitor, suggesting that it represents a bona fide NFI-DNA complex. The other two bands were competed out with G-br3*. These data demonstrate that members of the NFI family are able to bind to G-br3; however, other proteins are also able to interact with G-br3. Of note, both AP-2 and Sp1 competitor oligonucleotides were able to compete with the fastest migrating DNA-protein complex, suggesting that AP-2 and Sp1 are able to bind G-br3. As mentioned earlier, a similar effect was observed when the G-br3 probe was incubated with T98 nuclear extract in the presence of excess G-br3*, Sp1 or AP2 competitor oligonucleotides. In support of Sp1 binding to G-br3, Besnard and coworkers (1991) have shown that the NFI site in G-br3 overlaps with a Sp1 site. As for AP-2, the N_5 spacer region of the NFI-binding site in G-br3 consists exclusively of G-C base pairs. Since AP-2 consensus binding sites are G-C rich (*i.e.*

5'-GCCCACGGCCC-3'), this G-C rich spacer region represents a potential AP-2 binding site.

The results obtained from these gel shift experiments demonstrate that NFI and probably other transcription factors such as AP-1, AP-2 and Sp1, likely interact with the *GFAP* promoter to mediate transcription. Importantly, NFI is able to bind each of the three consensus NFI-binding sites in the *GFAP* promoter. However, one of the most interesting features of our gel shift experiments is the difference in the migration of the protein-DNA complexes obtained with the T98 versus U251 nuclear extracts. As shown in Figure 3.2, complexes formed in the presence of T98 nuclear extracts migrated at much slower rate than those formed in the presence of U251 nuclear extracts. These differences in gel shift patterns suggest differences in the type or nature of NFI proteins expressed in these cells. Previous results from our lab have demonstrated that the NFI proteins that regulate B-FABP expression in T98 cells are hyperphosphorylated in comparison to those in U251 cells, thereby causing them to migrate at a slower rate (Bisgrove *et al.*, 2000). Similarly, phosphorylation likely accounts for the difference in migration observed for the NFI proteins that bind to the *GFAP* promoter in T98 versus U251 cells. In combination, our results indicate that the transcriptional activation of both *B-FABP* and *GFAP* is mediated by hypophosphorylated forms of NFI proteins.

3.3. Binding of Specific NFI Proteins to the NFI Sites in the *B-FABP* and *GFAP* promoters

Our results indicate that each of the NFI-binding sites in the *GFAP* and *B-FABP* promoters are able to bind NFI proteins, and *NFI* genes (*NFI-A*, *-B*, *-C*, and *-X*) are widely expressed in MG cell lines. We therefore sought to determine whether specific NFI proteins preferentially bind to the NFI-binding sites in the *GFAP* and *B-FABP* promoters. The hypothesis underlying these experiments is that since different NFI proteins have been shown to have different transactivation capabilities, specific NFI proteins will bind to these sites better than others to mediate *GFAP* and/or B-FABP transcription. In support of this hypothesis, other researchers have recently shown that NFI-C2 has a higher affinity for NFI-binding sites in the *CEL* promoter than NFI-A1, and that NFI-C2 is the specific NFI protein responsible for *CEL* promoter activity (Kannius-Janson *et al.*, 2002). Thus, through these studies we hope to identify the specific NFI proteins responsible for GFAP and/or B-FABP transcriptional activation.

To address our hypothesis, we transfected T98 cells with expression vectors containing HA-tagged mouse *NFI* cDNAs (pCHNFI-A, -B, -C or -X) as well as empty vector (pCH). Nuclear extracts were prepared from transfected cells and examined for NFI binding activity by EMSA. Because the NFI proteins are highly conserved within vertebrates (reviewed in Gronostajski, 2000), we expect the mouse NFI proteins to have the same DNA-binding characteristics as their human counterparts. The T98 cell line was chosen for these experiments because it has relatively low levels of endogenous NFIs and because we found that it can be more efficiently transfected than other MG cell lines such as U251 and U87.

GFAP promoter studies:

To ensure that the transfected cells produced similar amounts of exogenous NFI proteins, 10 µg of nuclear extracts were run on SDS-PAGE gels and immunostained with anti-HA antibody. As shown in Figure 3.3 (panel A), there was some variation in NFI signal intensity in each of the nuclear extracts prepared from the T98 cells transfected with the NFI-A, -B, -C or -X expression plasmids. Compared to NFI-B and NFI-X which were of equal intensity, NFI-C produced a slightly stronger signal, while the NFI-A signal was 2 to 3-

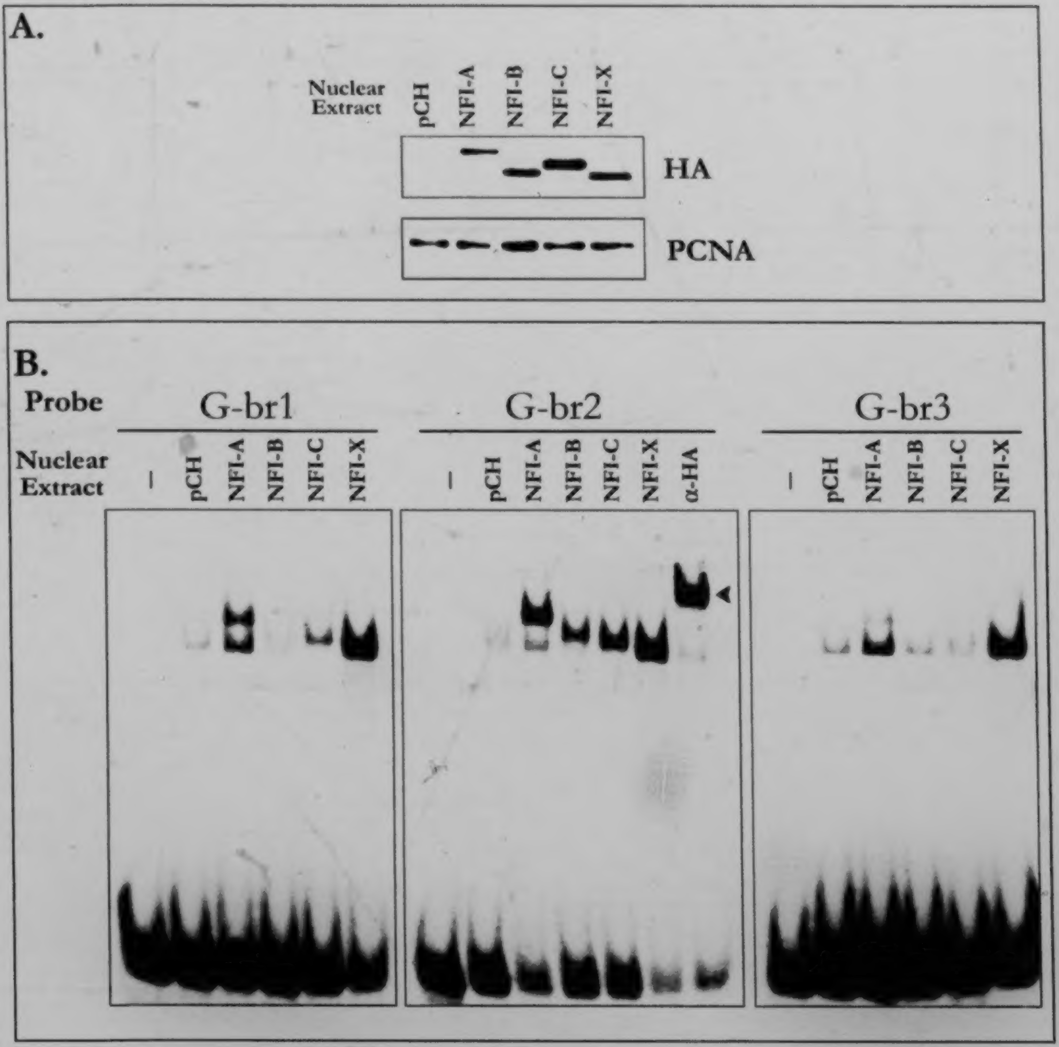
A.
Nuclear Extract
pCH
NFI-A
NFI-B
NFI-C
NFI-X
HA
PCNA
B.
Probe
G-br1
G-br2
G-br3
Nuclear Extract
–
pCH
NFI-A
NFI-B
NFI-C
NFI-X
–
pCH
NFI-A
NFI-B
NFI-C
NFI-X
α-HA
–
pCH
NFI-A
NFI-B
NFI-C
NFI-X

Figure 3.3 - NFI-A, -B, -C and -X binding to G-br1, G-br2 and G-br3. Nuclear extracts were prepared from T98 cells transfected with control (pCH) or NFI expression constructs (NFI-A, -B, -C or -X). **A**, 10 μg of nuclear extracts were analyzed by western blot using anti-HA and anti-PCNA antibodies. **B**, gel shift assays were carried out with radiolabeled G-br1, G-br2 and G-br3 oligonucleotides and ~1 μg of the nuclear extracts. DNA binding reactions were electrophoresed in a 0.5X TBE 6% polyacrylamide gel to separate unbound (free) DNA and DNA-protein complexes. A supershift experiment was peformed by incubating anti-HA antibody (α-HA) with the nuclear extract prepared from T98 cells transfected with NFI-X. The red arrowhead shows the supershifted complex.

fold weaker. An equal amount (~1 μg) of each of these extracts was used to study NFI-binding to G-br1, G-br2 and G-br3.

NFI-A and NFI-X showed the highest level of binding to the G-br1-, G-br2 and G-br3 oligonucleotides (Figure 3.3, panel B). Of these two NFIs, NFI-X generated the stronger signal; however, in light of the lower abundance of NFI-A in the nuclear extracts, we predict that NFI-A and NFI-X may have similar affinities for G-br1, G-br2 and G-br3. NFI-C showed weak binding to G-br1 and barely detectable binding to G-br3 while NFI-B did not appear to bind to either G-br1 or G-br3. In contrast, all four NFIs were able to bind to G-br2 relatively efficiently.

An antibody supershift experiment was performed to verify that the complexes produced in the EMSA experiments did indeed contain NFI. For the supershift experiment, nuclear extract obtained from the T98 cells transfected with pHNFI-X was incubated with anti-HA antibody prior to the addition of labeled G-br2 oligonucleotide. As shown in Figure 3.3, a supershifted band (indicated by the red arrowhead) was observed.

The enhanced binding properties observed for NFI-A and NFI-X compared to the other NFI proteins suggest that NFI-A and NFI-X are the most potent NFIs involved in mediating *GFAP* transcription. In addition, the elevated levels of NFI binding to G-br2 compared to G-br1 and G-br3 indicates that G-br2 represents the most active site for NFI binding and possibly for the activation of *GFAP* transcription. In support of these observations, Besnard *et al.* (1991) have used *GFAP* promoter deletion constructs to demonstrate that the region from which our G-br2 oligonucleotide derives has a high level of activator activity, while relatively little activation was observed from constructs containing G-br1 and/or G-br3.

B-FABP promoter studies:

To determine the ability of each NFI protein to bind to the NFI-binding sites in the *B-FABP* promoter, double-stranded oligonucleotides were generated to each of the *B-FABP* promoter NFI-binding regions (B-br1, B-br2 and B-br3). The double-stranded oligonucleotides synthesized are shown in Figure 2.1 and include: bp -62 to -33 (B-br1), bp -172 to -155 (B-br2), and bp -263 to -238 (B-br3). Of note, B-br2 was included in this analysis even though previous studies from our lab have failed to demonstrate NFI binding activity in this region (Bisgrove *et al.*, 2000). Our goal was to substantiate our previous results using individual NFI proteins.

As shown in Figure 3.4 (panel A), the amount of NFI protein in each of the nuclear extracts used for the EMSA experiments was nearly identical. EMSA analysis using radiolabeled B-br1, B-br2 and B-br3 revealed significant differences in the level of NFI binding (Figure 3.4, panel B). All four NFI proteins were able to bind to B-br1, with NFI-C and NFI-X binding at the highest level. As expected based on previous results, none of the NFI proteins were able to bind B-br2. A wide variation in signal intensity was observed with B-br3, with the strongest signal obtained with NFI-X followed by NFI-C. NFI-A and NFI-B displayed very low levels of binding to B-br3. These results suggest that the NFI-C and NFI-X proteins bind to the NFI-binding sites in the *B-FABP* promoter more readily than NFI-A and NFI-B. In addition, since all four NFI proteins bind to B-br1, this region appears to represent the most active site for NFI binding and possibly for the activation of *B-FABP* transcription. In support of this, our lab has previously shown by mutation of the NFI-binding site located at -54/-40 bp that this NFI-binding site is essential for *B-FABP* promoter activity (Bisgrove *et al.*, 2000).

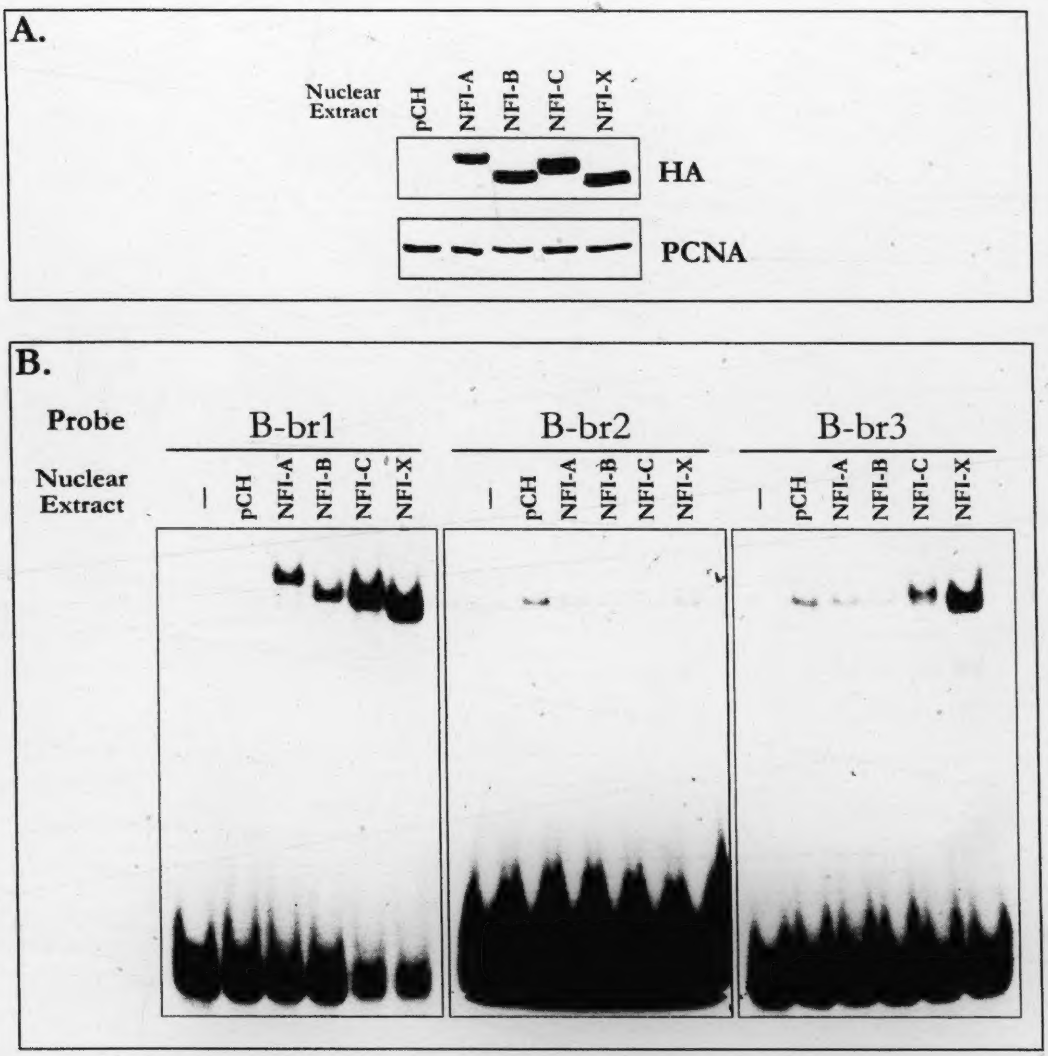
A.
Nuclear Extract
pCH
NFI-A
NFI-B
NFI-C
NFI-X
HA
PCNA
B.
Probe
B-br1
B-br2
B-br3
Nuclear Extract
–
pCH
NFI-A
NFI-B
NFI-C
NFI-X

Figure 3.4 - NFI-A, -B, -C and -X binding to B-br1, B-br2 and B-br3. Nuclear extracts were prepared from T98 cells transfected with control (pCH) or NFI expression constructs (NFI-A, -B, -C or -X). **A**, 10 μg of nuclear extracts were analyzed by western blot using anti-HA and anti-PCNA antibodies. **B**, gel shift assays were carried out with radiolabeled B-br1, B-br2 and B-br3 oligonucleotides and ~1 μg of the nuclear extracts. DNA binding reactions were electrophoresed in a 0.5X TBE 6% polyacrylamide gel to separate unbound (free) DNA and DNA-protein complexes.

3.4. Transcriptional Activation of *B-FABP* and *GFAP* by Specific NFI Proteins

Having determined the *in vitro* ability of each NFI protein to bind to the NFI elements in both the *B-FABP* and *GFAP* promoters, we next analyzed the transactivation capacity of each NFI protein on these promoters using a reporter gene assay in cultured cells. For this work, we tested CAT reporter constructs containing different amounts of *B-FABP* and *GFAP* 5'-flanking DNA (Figure 3.5, panel A and B). Each of the CAT constructs (pCAT/B-FABP-160, pCAT/B-FABP-440, pCAT/GFAP-176 or pCAT/GFAP-1716) or pCAT-basic was co-transfected into T98 cells along with pCH or an NFI expression plasmid (pCHNFI-A, -B, -C or -X). Transfection efficiency from plate to plate was determined by southern blot analysis of Hirt DNA. Shown in Figure 3.6 is the Hirt DNA analysis results from a single set of transfections (three sets of independent transfections were performed). Importantly, Hirt DNA analysis revealed no significant differences in transfection efficiency. Of note, the amount of pCAT construct transfected was 20X higher than the amount of the pCHNFI expression constructs (red and blue arrows in Figure 3.6). This ratio was determined by titrating the amount of pCHNFI used to transfect the cells. At levels higher than 1 μg, non-specific inhibition of CAT activity was observed, likely due to the presence of elevated levels of a potent transcription factor.

As shown in Figure 3.5 (panel C), the basal level of transcription (*i.e.* without exogenous NFI expression) for each of these constructs differs significantly. A 1.5-fold and 3.5-fold increase in CAT activity was observed for the pCAT/B-FABP-160 and pCAT/B-FABP-440 constructs, respectively. For the pCAT/GFAP-176 and pCAT/GFAP-1716 constructs, a 12-fold and 13.5-fold increase in CAT activity was observed, respectively. Of note, there was little difference in basal CAT activation between the two GFAP CAT constructs. This is interesting because we have shown that NFI proteins bind with high

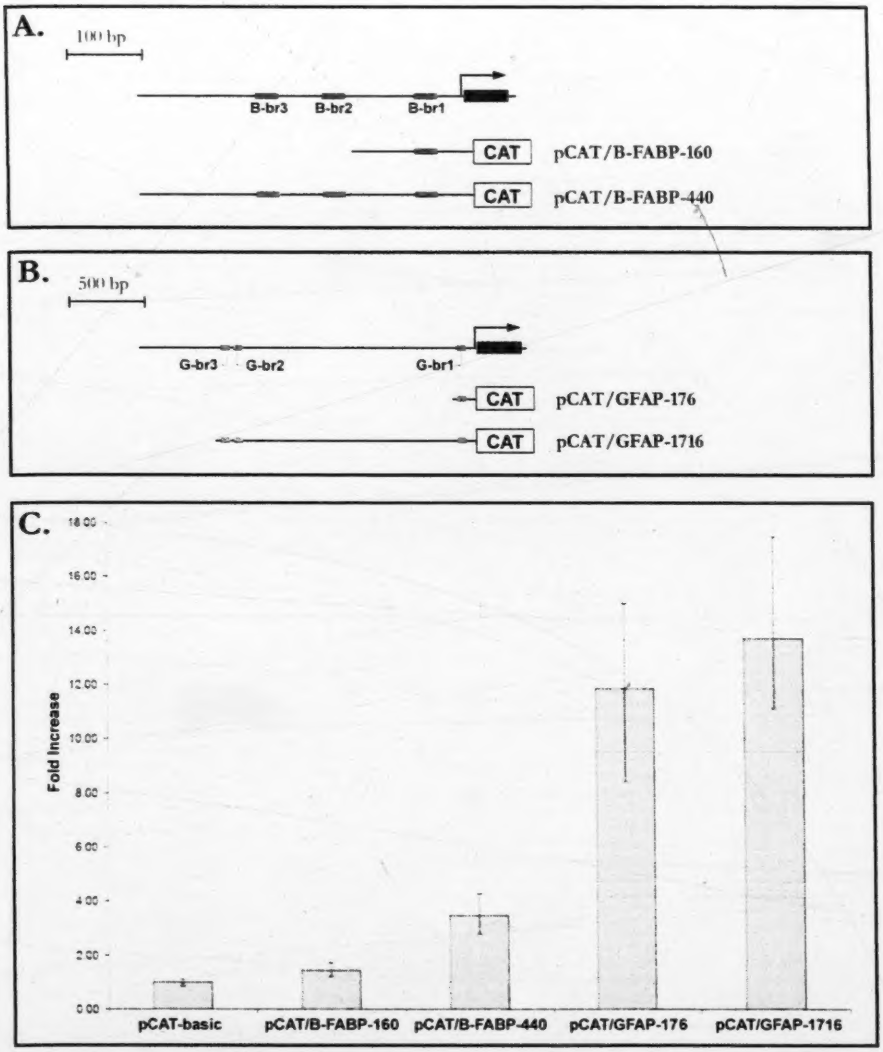

Figure 3.5 - Analysis *B-FABP* and *GFAP* promoter activity. Schematic diagrams of the B-FABP (panel A) and GFAP (panel B) CAT reporter constructs are shown indicating the transcription start site (arrow), exon I (black filled box), and the locations of the NFI-binding regions (B-FABP: B-br1, B-br2, and B-br3 or GFAP: G-br1, G-br2 and G-br3; red filled box). In relation to the transcription start site, the B-FABP CAT constructs extend from +20 bp to -140 bp (pCAT/B-FABP-160) or +20 to -420 bp (pCAT/B-FABP-440), while the GFAP CAT constructs extend from +8 bp to -168 bp (pCAT/GFAP-176) or +8 to -1708 (pCAT/GFAP-1716). 10 µg of pCAT-basic, pCAT/B-FABP-160, pCAT/B-FABP-400, pCAT/GFAP-176, or pCAT/GFAP-1716 were co-transfected with 0.5 µg of pCH into T98 cells. Extracts prepared from transfected cells were assayed for CAT activity by monitoring the level of $[^{14}C]$chloramphenicol butyrylation. The results shown are an average of at least three independent experiments with standard deviation indicated by the error bars.

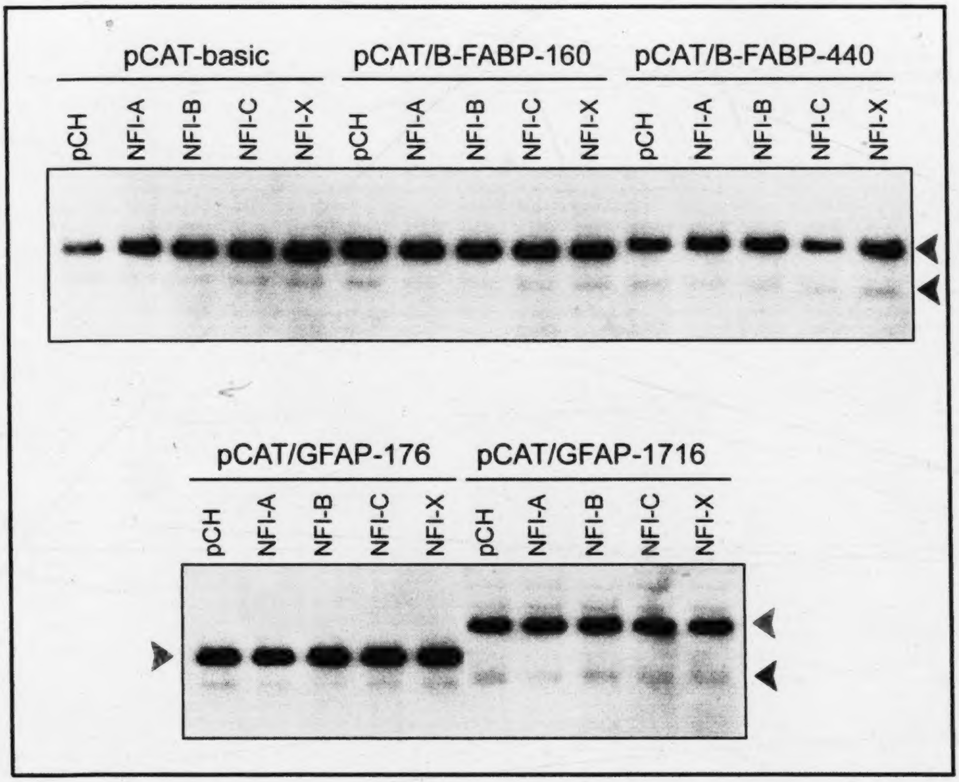
pCAT-basic
pCAT/B-FABP-160
pCAT/B-FABP-440
pCH
NFI-A
NFI-B
NFI-C
NFI-X
pCAT/GFAP-176
pCAT/GFAP-1716

Figure 3.6 - Southern blot analysis of Hirt DNA from T98 cells transfected with the CAT reporter constructs. Whole cell extracts were prepared from T98 cells co-transfected with the CAT reporter constructs (pCAT-basic, pCAT/B-FABP-160, pCAT/B-FABP-440, pCAT/GFAP-176 or pCAT/GFAP-1716) and pCH or the pCHNFI expression constructs (NFI-A, -B, -C or -X). Hirt DNA was prepared from a set fraction (one fifth) of the whole cell lysate from each plate of cells. The DNA was restriction enzyme digested and electrophoresed in a 1% agarose gel, transferred to nitrocellulose, and probed with radiolabeled plasmid DNA. The band indicated by the red arrow represents the CAT construct. The band indicated by the blue arrow represents the pCH or NFI expression plasmid.

levels to the G-br2 region that is present in pCAT/GFAP-1716 but absent in pCAT/GFAP-176. In addition, Besnard and coworkers (1991) have shown that when introduced into U251 cells, a CAT construct containing -1660 bp of GFAP 5'-flanking DNA generates a 15-fold increase in activity compared to a construct containing -210 bp of GFAP 5'-flanking DNA. These differences can be explained by our observation that NFIs in U251 cells are hypophosphorylated and active, whereas in T98 cells the hyperphosphorylated NFIs are inactive (Bisgrove *et al.* 2000). Thus, in T98 cells we would not expect to observe a large difference in CAT activity between pCAT/GFAP-176 and -1716 or between pCAT/B-FABP-160 and -440 when no exogenous NFIs are present.

In Figure 3.7, the level of CAT activity generated when each B-FABP or GFAP CAT construct was co-transfected with pCHNFI-A, -B, -C or -X is represented as a fold increase over its respective basal CAT activity (*i.e.* co-transfection with pCH). With the pCAT/B-FABP-160 construct, NFI-A and NFI-X expression generated a 5.8-fold and 11.6-fold increase in CAT activity, respectively, while NFI-B and NFI-C had a negligible (2-fold and 2.5-fold increase, respectively) effect on CAT activity. Similar values were observed with the pCAT/B-FABP-440 construct except that the increase observed with NFI-X expression dropped to 6.1-fold. These data suggest that NFI-A and NFI-X are involved in the transactivation of *B-FABP*. In addition, it appears that the NFI-binding site located at -257/-243 bp (B-br3) is not essential for the transcriptional activation caused by NFI-A and NFI-X. Instead, possibly by acting as a repression element or as a sink for NFI-X, the NFI-binding site at -257/-243 bp reduces *B-FABP* transactivation. These results support our previous conclusion that the NFI-binding site located at -54/-40 bp (B-br1) is the essential NFI-binding site for *B-FABP* promoter activity (Bisgrove *et al.*, 2000).

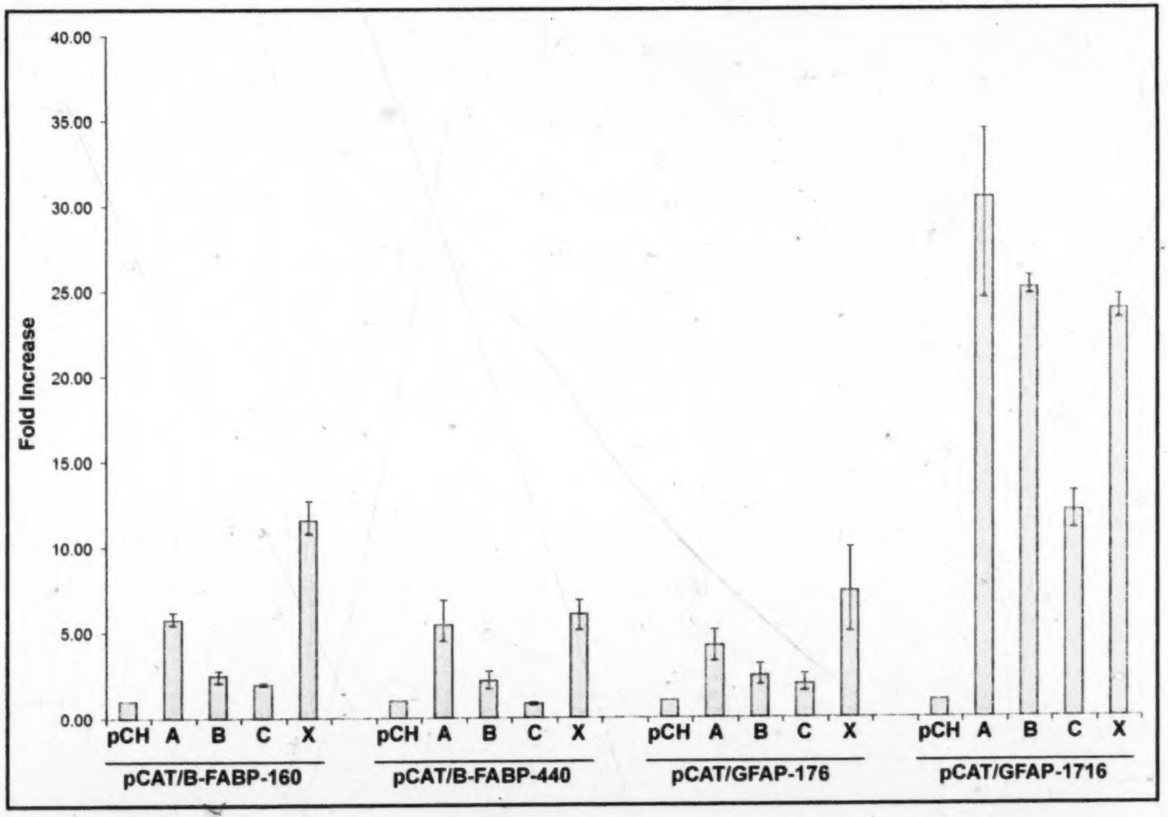

Figure 3.7 - Transcriptional activation of B-FABP and GFAP CAT constructs by specific NFI proteins. T98 cells were transiently transfected with 10 μg of each of the CAT constructs (pCAT/B-FABP-160, pCAT/B-FABP-440, pCAT/GFAP-176, or pCAT/GFAP-1716) and 0.5 μg of pCH or NFI expression plasmids (NFI-A, -B, -C or -X). Extracts prepared from transfected cells were assayed for CAT activity by monitoring the level of [^{14}C]chloramphenicol butyrylation. The results shown are an average of at least three independent experiments with standard deviation indicated by the error bars. The fold increase in CAT activity is represented relative to the basal CAT activity shown in Figure 3.5 for each CAT construct.

The pattern of CAT activation observed for the pCAT/GFAP-176 construct was nearly identical to that of the B-FABP CAT constructs. NFI-A and NFI-X expression generated a 4.2-fold and 7.4-fold increase in CAT activity, respectively, while NFI-B and NFI-C had a lesser effect (Figure 3.7). However, a drastic increase in CAT activity was observed for each NFI construct with the pCAT/GFAP-1716 construct. This is not surprising since it has been postulated that the -1612/-1489 bp region of the *GFAP* promoter is the most important for *GFAP* transcriptional activation (Besnard *et al.*, 1991). Overall, our results suggest that the NFI site within this region is primarily responsible for the dramatic increase CAT activity observed here and reported by Besnard and coworkers (1991).

Unlike the other CAT constructs which displayed CAT activation only upon NFI-A and NFI-X expression, all four NFIs activated transcription from pCAT/GFAP-1716 (Figure 3.7). This is interesting because NFI proteins have been implicated in both transcriptional activation and repression (reviewed in Gronostajski, 2000). However, our results indicate that for the *GFAP* gene, each NFI protein appears to activate transcription. Of note, a reduction in transcriptional potential was never observed upon transfection of T98 cells with any of the NFI expression constructs. Therefore, it is possible that all four NFI proteins serve to activate *GFAP* transcription, but due to DNA-binding affinities and *in vivo* expression patterns (discussed earlier) only certain NFIs have actually mediate *B-FABP* and/or *GFAP* transcription *in vivo.*

CHAPTER FOUR

Effects of B-FABP and/or GFAP expression in malignant glioma cell lines.

Malignant gliomas (MGs) are the most common and most aggressive human brain tumours. Despite advances in treatment, the prognosis for patients with these tumours remains dismal. The failure of traditional therapy for patients with MG has prompted many studies to examine the mechanisms of glial cell differentiation in the hope that it will lead to the development of novel therapies designed to induce MG tumour cells to undergo differentiation. MGs are believed to arise from the astrocyte lineage because they express glial fibrillary acidic protein (GFAP), a cytoskeletal protein expressed specifically in mature astrocytes. Interestingly, there is an inverse correlation between levels of GFAP and malignancy, with the number of GFAP positive cells decreasing with increased malignancy (van der Meulen *et al.*, 1978). Furthermore, Rutka and coworkers (1993) have shown that the introduction of GFAP expression constructs into the GFAP-negative MG cell line SF-126 results in decreased cell proliferation and growth in soft agar.

We have recently identified another marker of glial cell differentiation, brain-fatty acid binding protein (B-FABP), that is co-expressed with GFAP in MG cell lines (Godbout *et al.*, 1998). B-FABP is normally expressed in the radial glial cells that form the fiber network that guides the migration of neurons in the developing brain. Members of the FABP family (Table 1.1) are involved in the uptake, storage and/or delivery of fatty acids (FAs) and have been implicated in modulating cell growth and differentiation. FABPs function in both a cell-type and FABP-type specific manner to exert their effect on proliferation and differentiation. For example, L-FABP has been shown to increase the proliferation rate of rat liver cells (Keler *et al.*, 1992), but decrease the proliferation rate of mouse embryonic stem cells (Schroeder *et al.*, 2001). In addition, FABPs have recently been shown to serve as markers for certain cancers. For example, L-FABP and A-FABP are expressed at higher levels in lower grade colon carcinoma and bladder carcinoma, respectively, compared to their higher grade counterparts (reviewed in Zimmerman and Veerkamp, 2002).

Since B-FABP is co-expressed with GFAP in MG cell lines and since the levels of other FABPs have been shown to correlate with tumour progression, we were interested in determining if B-FABP expression in MG cell lines is associated with a less aggressive phenotype. Here, we describe the effects of B-FABP expression on proliferation, cell morphology, anchorage-independent growth, and invasion in two B-FABP/GFAP-negative MG cell lines (T98 and U87) that have been stably transfected with a B-FABP expression plasmid. In addition, we examine growth properties of a B-FABP/GFAP-positive MG cell line (U251) after reduction of B-FABP levels by RNA interference (RNAi).

4.1. Isolation of the B-FABP and/or GFAP Stably Transfected T98 and U87 Malignant Glioma Clones

The T98 MG cell line was transfected with the following B-FABP and/or GFAP expression constructs: pREP4 (control), pREP4/B-FABP, pREP4/GFAP, or both pREP4/GFAP and pcDNA3/B-FABP. The U87 MG cell line was transfected with pREP4 or pREP4/B-FABP. Transfected cells were selected in culture medium containing hygromycin and/or G418 and at least six independent clones were isolated and expanded for each construct. To verify that the clones expressed the appropriately transfected gene(s), western blot analysis was performed using whole cell extracts prepared from each transfectant (data not shown).

T98 transfectants:

For T98, we selected the three transfected clones expressing the highest levels of B-FABP and/or GFAP, as well as three control (pREP4) transfected clones. These clonal cultures were labeled: T98-B-FABP-1, -2 and -4; T98-GFAP-1, -2 and -3; T98-B/G-1, -6 and -8 (B-FABP/GFAP transfectants); and T98-pREP4-4, -5 and -6. Western blot analyses of the B-FABP transfected clones revealed that B-FABP levels were highest in clones 1 and 2, with approximately 2-fold lower levels in clone 4 (Figure 4.1). No GFAP expression was detected in these three clones. In the GFAP transfectants, GFAP expression was highest in clone 3 followed by clone 2, with clone 1 having the lowest levels. B-FABP was not detected in these clones. All three double transfectants showed high levels of GFAP (generally higher than that observed in GFAP transfected cells). However, B-FABP expression was highly variable in the double transfectants with elevated B-FABP levels in clone 1 and barely detectable levels in clones 6 and 8. The B-FABP/GFAP-positive MG cell line (U251) and B-FABP/GFAP-negative parent T98 cell line are shown for comparison. Of note, B-FABP and GFAP levels in the transfectants were lower than those observed in U251.

U87 transfectants:

For U87, we analyzed B-FABP levels in seven B-FABP transfected clones and found that each clone expressed B-FABP at much higher levels than the T98 B-FABP transfectants. Of these seven U87-B-FABP clones, the five transfectants expressing the highest levels of B-FABP (U87-B-FABP-1, -2, -3, -5, -7) were selected for further studies. In addition, we selected four control clones (U87-pREP4-1, -3, -6, -7). For the five U87-B-FABP clones, highest levels of B-FABP were observed in clones 3 and 7, intermediate levels in clones 1 and 2, and lowest levels in clone 5 (Figure 4.2). Consistent with the

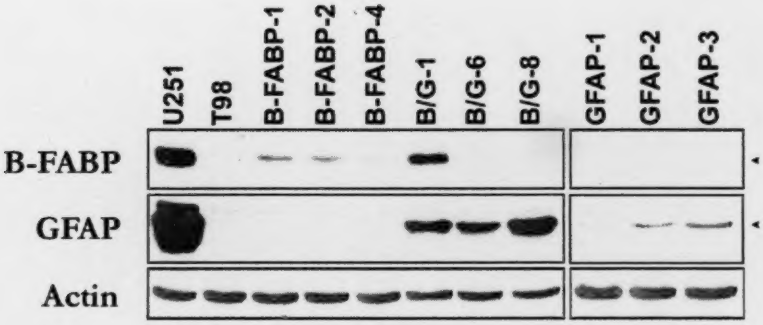

U251
T98
B-FABP-1
B-FABP-2
B-FABP-4
B/G-1
B/G-6
B/G-8
GFAP-1
GFAP-2
GFAP-3
B-FABP
GFAP
Actin

Figure 4.1 - Western blot analysis of B-FABP and GFAP in the T98 transfectants. Whole cell extracts were prepared from the MG cell lines U251 and T98, B-FABP transfectants (B-FABP-1, -2, and -4), B-FABP/GFAP transfectants (B/G-1, -6, and -8), and GFAP transfectants (GFAP-1, -2, and -3). Equal amounts of protein (50 μg) were loaded in each lane and electrophoresed in a 15% SDS-PAGE gel. Proteins were transferred to nitrocellulose, blocked and incubated sequentially with anti-B-FABP, anti-GFAP and anti-actin antibodies. The arrowheads denote the position of the bands representing B-FABP and GFAP immunoreactivity.

previous results in T98, GFAP expression was not detected in the U87-B-FABP transfectants. These results indicate that B-FABP, while often co-expressed with GFAP in MG, does not by itself play a role in regulating GFAP expression.

4.2. Immunofluorescence Analysis of B-FABP and/or GFAP in the T98 and U87 transfectants

Some of the transfected clones had low B-FABP and/or GFAP levels which might mean that either a low percentage of cells within these clones express the transfected gene(s) or a high percentage of cells express the gene(s) but at low levels. To address these two possibilities, immunofluorescence analysis was performed on each of the T98 and U87 transfectants previously discussed (T98-B-FABP-1, -2 and -4; T98-GFAP-1, -2 and -3; T98-B/G-1, -6 and -8; and U87-B-FABP-1, -2, -3, -5 and -7). In addition, one control for each set of transfectants (T98-pREP4-4 and U87-pREP4-7) was analyzed. The goals of these studies were twofold: i) to examine the relative levels of B-FABP and/or GFAP in each of the transfectants and, ii) to determine the approximate percentage of cells expressing B-FABP and/or GFAP.

For these experiments, each transfectant was plated on coverslips and grown to ~60-80% confluence. Cells were double-stained with anti-B-FABP and anti-GFAP primary antibodies followed by fluorescent secondary antibodies and visualized using a confocal microscope. To determine the percentage of cells expressing B-FABP and/or GFAP, a total of four images were collected for each transfectant. Importantly, laser scanning parameters were kept constant for all images to ensure that the data collected could be compared quantitatively. To calculate the percentage of cells expressing B-FABP and/or GFAP, the total number of cells expressing B-FABP and/or GFAP was divided by the total number of cells as determined by DAPI staining to identify each cells nucleus. A representative image

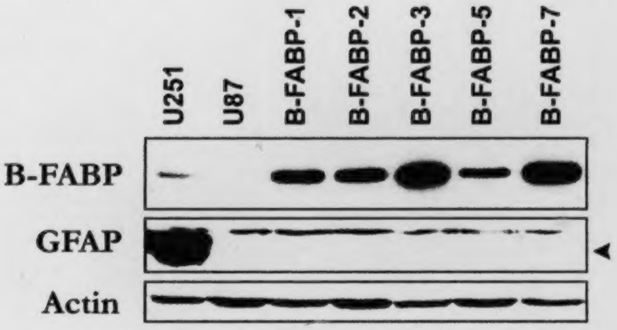
U251
U87
B-FABP-1
B-FABP-2
B-FABP-3
B-FABP-5
B-FABP-7
B-FABP
GFAP
Actin

Figure 4.2 - Western blot analysis of B-FABP and GFAP in the U87 transfectants. Whole cell extracts were prepared from the MG cell lines U251 and U87, and B-FABP transfectants (B-FABP-1, -2, -3, -5 and -7). Equal amounts of protein (50 μg) were loaded in each lane and electrophoresed in a 15% SDS-PAGE gel. Proteins were transferred to nitrocellulose, blocked and incubated sequentially with anti-B-FABP, anti-GFAP and anti-actin antibodies. The arrowhead denotes the position of the band representing GFAP immunoreactivity.

for each T98 B-FABP and/or GFAP transfectant is shown in Figure 4.3 and for each U87 B-FABP transfectant in Figure 4.4.

T98 transfectants:

For the T98 transfectants, B-FABP expression was observed in 100% of the cells for T98-B-FABP-1, -4 and T98-B/G-1 (Figure 4.3). The remaining B-FABP and B-FABP/GFAP transfectants showed a slight reduction in the percentage of cells expressing B-FABP at 96%, 92% and 85% for T98-B-FABP-2, T98-B/G-6 and -8, respectively. Thus, the percentage of cells expressing B-FABP in each clone likely has little to do with the difference in B-FABP levels observed by western blot analysis. Interestingly, while B-FABP expression appeared to be almost absent in the T98-B/G-6 and -8 clones by western blot analysis, it was easily detected by immunofluorescence. This is most probably due to the increased low-signal sensitivity of the immunofluorescence technique compared to western blotting. In agreement with the western blot data, the most intense B-FABP immunofluorescence signal was observed in T98-B/G-1, followed by the three T98-B-FABP transfectants. A less intense B-FABP immunofluorescence signal was observed in the T98-B/G-6 and -8 clones. Overall, these data suggest that the differences in B-FABP expression observed by western blot were due to low intracellular B-FABP expression levels rather than a low percentage of cells expressing B-FABP.

Of note, differences in B-FABP levels are difficult to assess in Figure 4.3 since the laser scanning parameters in this experiment were optimized to analyze the percentage of cells expressing B-FABP and/or GFAP rather than to quantitate protein levels. When laser scanning parameters were adjusted for quantitative measurement, by appearance, protein levels were found to correlate with the pattern observed by western blot analysis (data not shown).

Figure 4.3 - Immunofluorescence analysis of B-FABP and/or GFAP in the T98 transfectants. Each transfectant was plated on coverslips, grown to 60-80% confluence, fixed, permeabilized and double-stained with rabbit anti-B-FABP and mouse anti-GFAP antibodies. Fluorescent secondary antibodies [Alexa 488 (anti-mouse) and Alexa 555 (anti-rabbit)] allowed image collection using a confocal microscope. Laser scanning parameters were kept constant to ensure that the images could be quantitatively compared. Four images were collected for each transfectant and a representative image is shown. **A)** B-FABP (Alexa 555; green) and DAPI (white) channels are shown for T98-B-FABP-1 (B1), -2 (B2), and -4 (B4). **B)** GFAP (Alexa 488, red) and DAPI channels are shown for T98-GFAP-1 (G1), -2 (G2), and -3 (G3). **C)** B-FABP, GFAP and DAPI channels are shown for T98-B/G-1 (B/G-1), -6 (B/G-6), and -8 (B/G-8). **D)** B-FABP and DAPI channels are shown for T98-pREP4-4 (pREP4). No GFAP signal was detected in the T98-pREP4-4 and T98-B-FABP transfectants. Similarly, no B-FABP signal was detected in the T98-GFAP transfectants. The name of the cell line is indicated in the top left corner. The antibody or nuclear stain (DAPI) used for image collection is indicated in the bottom left corner. The percentage of cells expressing B-FABP or GFAP is indicated in the bottom right corner. Of note, immunofluorescence analysis with secondary antibody alone produced a background signal similar to that of T98-pREP4 in panel D.

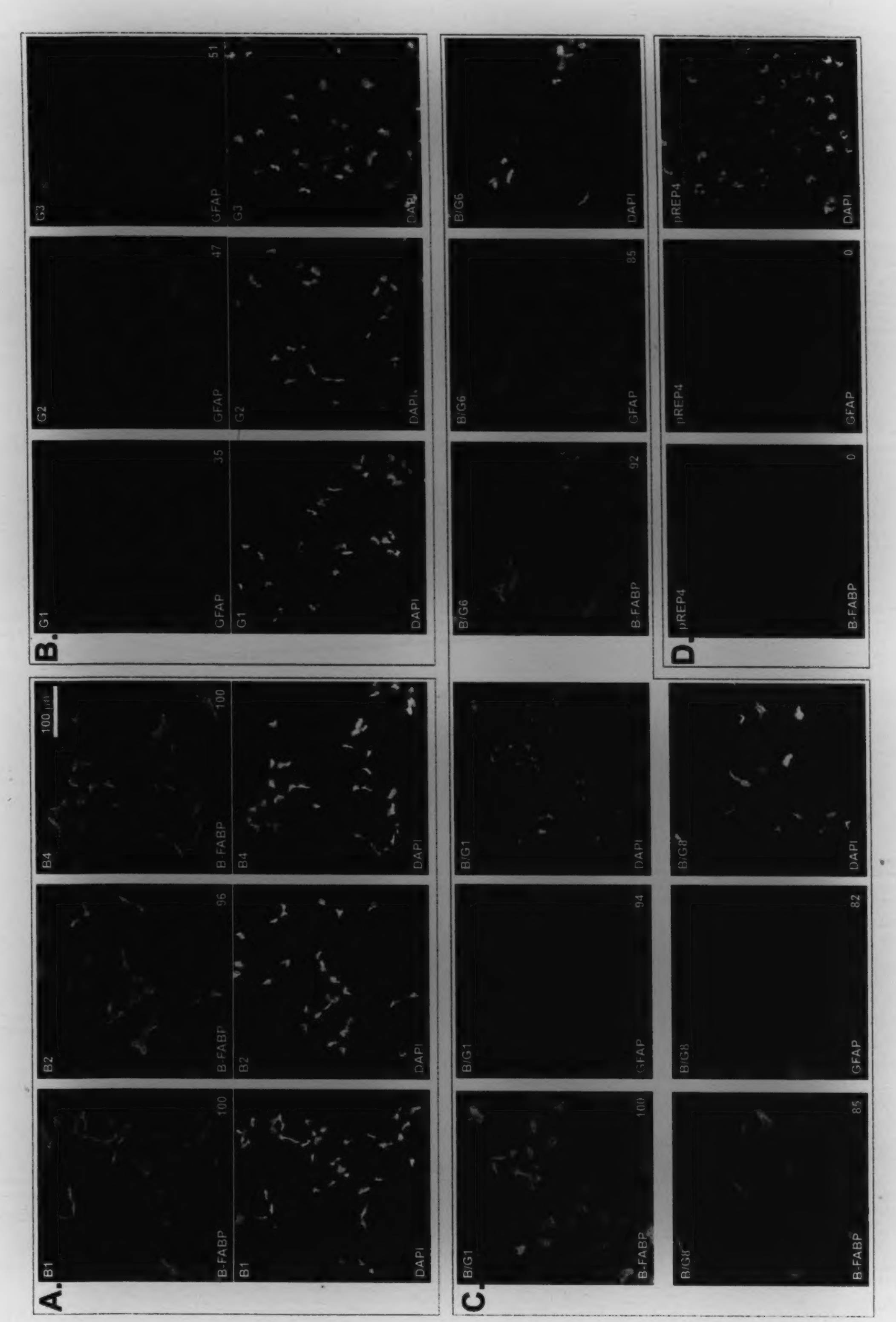
A.
B1
B-FABP
100
B1
DAPI
B2
B-FABP
96
B2
DAPI
B4
B-FABP
100
100 µm
B4
DAPI
B.
G1
GFAP
35
G1
DAPI
G2
GFAP
47
G2
DAPI
G3
GFAP
51
G3
DAPI
C.
B/G1
B-FABP
100
B/G1
GFAP
94
B/G1
DAPI
B/G8
B-FABP
85
B/G8
GFAP
82
B/G8
DAPI
B/G6
B-FABP
92
B/G6
GFAP
85
B/G6
DAPI
D.
pREP4
B-FABP
0
pREP4
GFAP
0
pREP4
DAPI

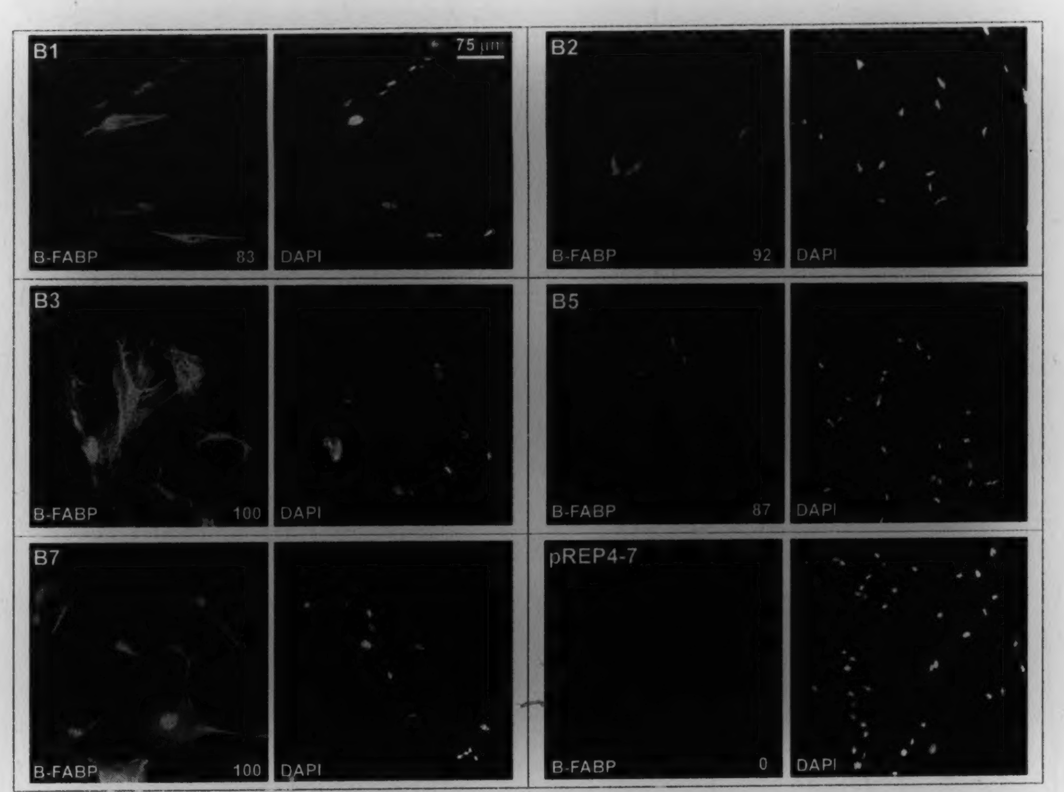

Figure 4.4 - Immunofluorescence analysis of B-FABP in the U87 transfectants. Each transfectant was plated on coverslips, grown to 60-80% confluence, fixed, permeabilized and double-stained with rabbit anti-B-FABP and mouse anti-GFAP antibodies. Fluorescent secondary antibodies [Alexa 488 (anti-mouse) and Alexa 555 (anti-rabbit)] allowed image collection using a confocal microscope. Laser scanning parameters were kept constant to ensure that the images could be quantitatively compared. Four images were collected for each transfectant and a representative image is shown for each transfectant: U87-B-FABP-1 (B1), -2 (B2), -3 (B3), -5 (B5), -7 (B7) and U87-pREP4-7 (pREP4-7). The B-FABP (green) and DAPI (white) channels are shown for each image. No GFAP signal was detected for any image collected. The name of the cell line is indicated in the top left corner. The antibody or nuclear stain (DAPI) used for image collection is indicated in the bottom left corner. The percentage of cells expressing B-FABP or GFAP is indicated in the bottom right corner.

In contrast to the results obtained for B-FABP, a relatively low percentage of cells in the T98-GFAP-1, -2, -3 transfectants expressed GFAP (~35%, 47% and 57%, respectively). GFAP signal intensity in T98-GFAP-1 was lower than that observed in T98-GFAP-2 and -3. These patterns correspond to the data obtained by western blot, suggesting that the low levels of GFAP expression in the T98-GFAP clones is due to both low GFAP levels and a relatively low percentage of GFAP-expressing cells. A correlation with western blot data was also observed for the T98-B/G clones, with 94%, 85% and 82% of cells expressing GFAP in T98-B/G-1, -6 and -8, respectively. In addition, GFAP expression in the double transfectants appeared to be slightly higher than that observed in the T98-GFAP clones. The latter was determined by adjusting the laser scanning parameters to eliminate immunofluorescence signal saturation (data not shown).

U87 transfectants:

A B-FABP signal was observed in ~100% of the cells in the clones expressing the highest levels of B-FABP (U87-B-FABP-3 and -7), whereas ~83%, 92% and 87% of the cells in the U87-B-FABP-1, -2 and -5 clones, respectively, were B-FABP-positive (Figure 4.4). Although most of the cells in each clone were B-FABP-positive, the percentage of cells expressing B-FABP in each clone may partly explain the western blot data showing lower levels of B-FABP in the U87-B-FABP-1, -2 and -5 clones compared the U87-B-FABP-3 and -7 clones. However, significant differences in the intensity of the B-FABP signal were also observed by immunofluorescence with the strongest signal in U87-B-FABP-1, -3 and -7, a significantly weaker signal in U87-B-FABP-2, and the weakest signal in U87-B-FABP-5. These results indicate that there is significant cell-to-cell variation in B-FABP levels in the different clonal populations.

4.3. Isolation of U251 Malignant Glioma Clones with Reduced B-FABP Levels

The pSUPER RNA interference (RNAi) technique was used to reduce B-FABP levels in the B-FABP/GFAP-positive MG cell line, U251. This technique allows stable production of small (21- to 22-nucleotide) interfering RNAs (siRNA) that can mediate a strong and specific suppression of gene expression (Brummelkamp *et al.*, 2002). Unlike transient siRNA transfection, the pSUPER system generates long-term loss-of-function, which typically becomes more pronounced over time due to the persistent intracellular synthesis of siRNA (www.oligoengine.com). In eukaryotic cells, these siRNAs generate a response whereby the host cells destroy mRNAs that share the same sequence as the siRNA.

We designed two pSUPER constructs for this work, one that produced siRNA specific to B-FABP (pSUPER/B-FABP) mRNA and another that produced siRNA specific to DEAD box 1 (DDX1) mRNA (pSUPER/DDX1). The pSUPER/DDX1 construct served as a control to ensure that any changes observed with pSUPER/B-FABP were caused by a specific reduction in B-FABP levels and not by a non-specific effect caused by the production of siRNA. In addition, the pSUPER vector (without insert) served as an empty vector control. The pSUPER/B-FABP and pSUPER/DDX1 constructs were generated by inserting a double-stranded 64-nt synthetic oligonucleotide containing two 19-nt reverse complement sequences specific to a portion of the target gene. The 19-nt gene-specific sequence for pSUPER/B-FABP corresponds to nucleotides 114-133 of the B-FABP coding region, while the targeted region for pSUPER/DDX1 corresponds to nucleotides 597-616 in the DDX1 coding region.

The U251 MG cell line was co-transfected with pSUPER, pSUPER/B-FABP or pSUPER/DDX1 as well as pREP4, and the cells were selected in culture medium containing hygromycin. At least six independent clones were isolated and expanded for each construct.

To examine the level of gene-specific suppression in each of the clones, western blot analysis was performed using whole cell extracts prepared from each transfectant immediately after clonal expansion. No reduction in B-FABP levels was observed in any of the U251-pSUPER or U251-pSUPER/DDX1 clones. Thus, for each of these transfectants, clones 1, 2 and 3 were randomly selected for further studies. B-FABP and DDX1 expression in these clones is shown in Figure 4.5A. While DDX1 levels were reduced by ~70-80% in U251-pSUPER/DDX1-1 and -2, no change in DDX1 levels detected in U251-pSUPER/DDX1-3.

The seven U251-pSUPER/B-FABP clones analyzed showed variable B-FABP expression. The clones with the most significantly reduced levels of B-FABP (U251-pSUPER/B-FABP-1, -4 and -7) showed a 40-60% reduction immediately after clonal expansion (Figure 4.5A). Because loss-of-phenotype is predicted to develop over longer periods of time, whole cell extracts were prepared from U251-pSUPER-1, -2 and -3, and U251-pSUPER/B-FABP-1, -4 and -7 after an additional six passages (1 passage = 1:6 dilution every 4 days). As shown in Figure 4.5B, a 90% or greater reduction in B-FABP levels was observed in the U87-B-FABP-1, -4 and -7 clones compared to controls. The lag in B-FABP suppression may have been due to the high abundance of B-FABP in U251 and/or protein stability. Regardless, B-FABP levels were sufficiently reduced in the U251-pSUPER/B-FABP-1, -4 and -7 clones to allow further characterization of growth and invasive properties.

4.4. Morphological Alterations in the Malignant Glioma Clones

The parent MG cell lines (T98, U87, U251) used for these analyses display significantly different morphological characteristics. Before confluence, T98 cells (B-FABP/GFAP-negative) are typically flat and polygonal-shaped, with smooth boundaries (Figure 4.6, top panel). U87 cells (B-FABP/GFAP-negative) are smaller, stellate-shaped,

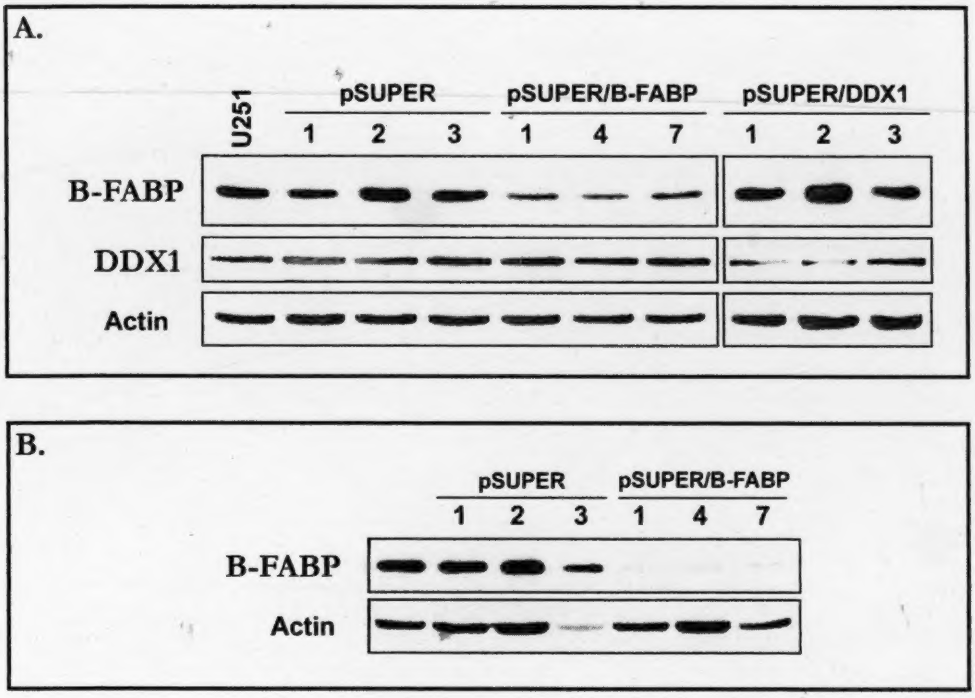
A.
U251
pSUPER
pSUPER/B-FABP
pSUPER/DDX1
1
2
3
1
4
7
1
2
3
B-FABP
DDX1
Actin
B.
pSUPER
pSUPER/B-FABP
1
2
3
1
4
7
B-FABP
Actin

Figure 4.5 - Western blot analysis of B-FABP and DDX1 in the pSUPER, pSUPER/B-FABP and pSUPER/DDX1 transfectants. Whole cell extracts were prepared from the MG cell line U251, U251-pSUPER transfectants (pSUPER-1, -2, and -3), U251-pSUPER/B-FABP transfectants (pSUPER/B-FABP-1, -4, and -7), and U251-pSUPER/DDX1 transfectants (pSUPER/DDX1-1, -2, and -3). Equal amounts of protein (50 µg) were loaded in each lane and electrophoresed in a 12% SDS-PAGE gel. Proteins were transferred to nitrocellulose, blocked and incubated sequentially with anti-B-FABP, anti-DDX1 and anti-actin antibodies. **A)** Whole cell extracts were prepared immediately after clonal expansion. **B)** Whole cell extracts from U251-pSUPER and U251-pSUPER/B-FABP transfectants were prepared after an additional six passages compared to (A).

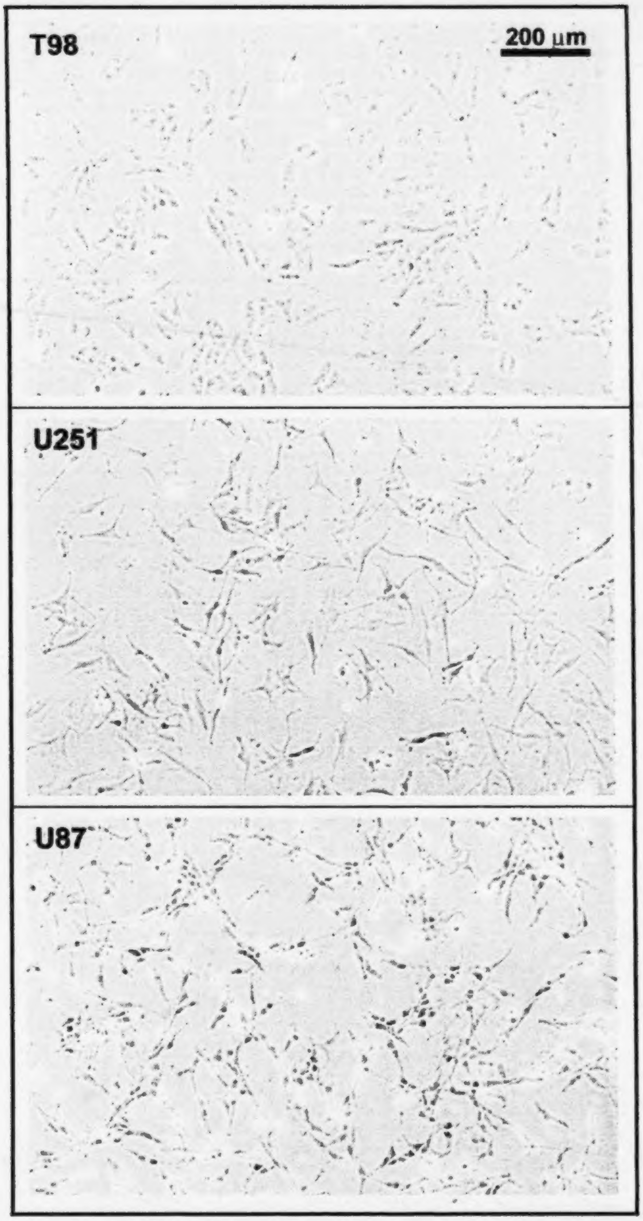

Figure 4.6 - Morphology of the T98, U251 and U87 MG cell lines. Phase contrast microscopy was used to photograph the cell lines when they had reached approximately 60-80% confluence. T98 cells (top panel) are flat, polygonal-shaped with smooth boundaries. U251 cells (middle panel) are similar to T98 in size, but display a stellate-shaped morphology and have numerous processes. U87 cells (bottom panel) are morphologically similar to U251 cells except they have a slightly smaller cell body and fewer processes. All microscopy images were taken using a 10X objective lens.

and have short but well defined processes (Figure 4.6, bottom panel). U251 cells (B-FABP/GFAP-positive) are morphologically similar to U87 cells, except that they tend to have slightly larger cell bodies and more numerous processes (Figure 4.6, middle panel). At confluence, all three cell lines display a high degree of cell crowding and piling, especially the U87 cell line which typically forms tight balls of cells that are easily shed into the medium.

T98 transfectants:

As expected, the T98-pREP4 cells were morphologically indistinguishable from the T98 cell line (Figure 4.7), indicating that neither transfection nor growth in selection medium (hygromycin and/or G418) was sufficient to induce a change in morphology. However, cells transfected with B-FABP and/or GFAP displayed significant changes in morphology compared to the pREP4 transfectants.

Although there was some variability in the morphology of the T98-B-FABP clones, these clones were generally comprised of cells that were more stellate-shaped than the T98-pREP4 cells (Figure 4.8). In addition, most of the B-FABP transfected cells no longer had smooth cell boundaries and formed thin cytoplasmic processes (as indicated by the arrows in Figure 4.8). Before confluence, these processes were abundant (typically 3-5/cell) and often quite long, forming lines of contact between numerous cells. At confluence the majority of the processes appeared to shorten as the cells packed closer together. The short processes were most obvious in the small gaps that the cells tended to leave between each other instead of crowding and piling up like the controls. While this is the first report of B-FABP inducing process formation in MG cell lines, Feng and coworkers (1994) have shown that B-FABP expression is important for the development of glial processes in radial glial cells and coincides with radial glial cell differentiation. Thus, it is possible that the formation of processes in these MG cell lines is a step towards a more differentiated state.

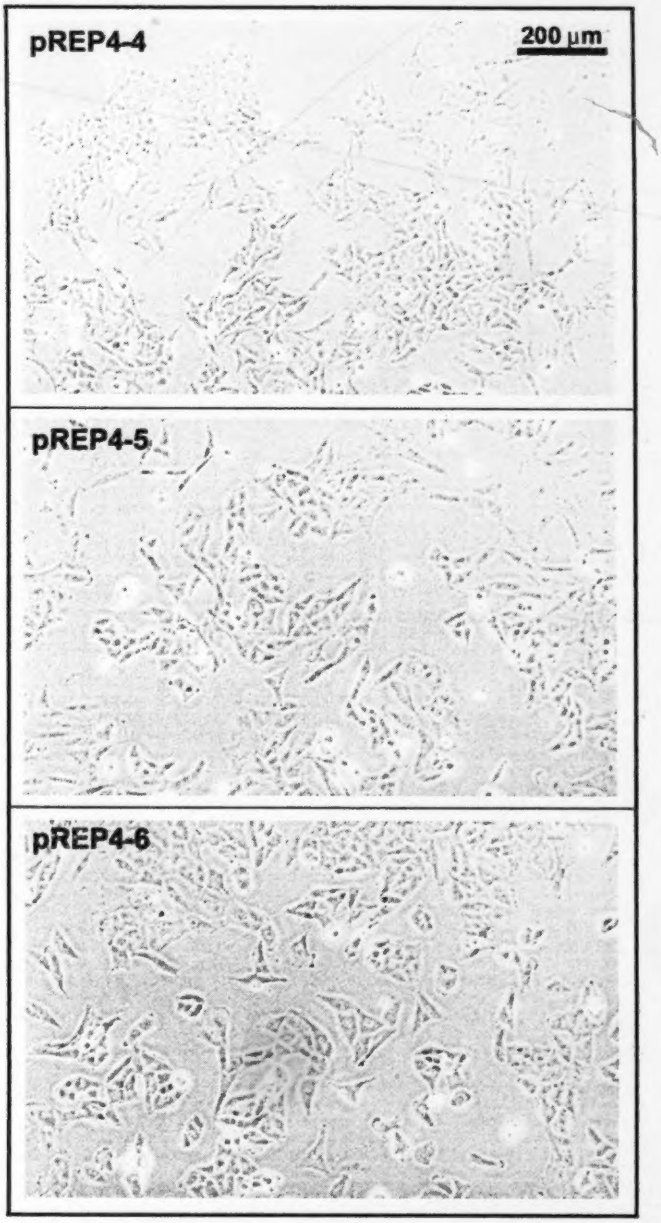

Figure 4.7 - Morphology of the T98-pREP4 transfectants. Phase contrast microscopy was used to photograph the cell lines when they had reached approximately 60-80% confluence. The T98-pREP4-4 (top panel), -5 (middle panel), and -6 (bottom panel) cells all display a morphology similar to that of the parent T98 cell line. The cells are flat, polygonal-shaped with smooth cell boundaries. All microscopy images were taken using a 10X objective lens.

Figure 4.8 - Alterations in morphology produced by the expression of B-FABP and/or GFAP in T98 cells. Phase contrast microscopy was used to photograph the cell lines when they had reached approximately 60-80% confluence. The T98-BFABP-1 (B1), -2 (B2), -4 (B4) clones are comprised of cells that are stellate-shaped and have extended thin cytoplasmic processes (indicated by arrowheads). Unlike the T98-B-FABP transfectants, the T98-GFAP-1 (G1), -2 (G2), and -3 (G3) clones have an elongated appearance and processes formation is absent. There is no predominant morphology for the T98-B-FABP/GFAP-1 (B/G1), -6 (B/G6), and -8 (B/G8) clones. The cells within these clones display phenotypes similar to that of the T98-pREP4, -B-FABP, and -GFAP transfectants. However, one morphological feature common to all the T98-B/G clones is that the cells tend to grow in clumps. Also, the T98-B/G clones that express higher levels of B-FABP have more pronounced processes. All microscopy images were taken using a 10X objective lens.

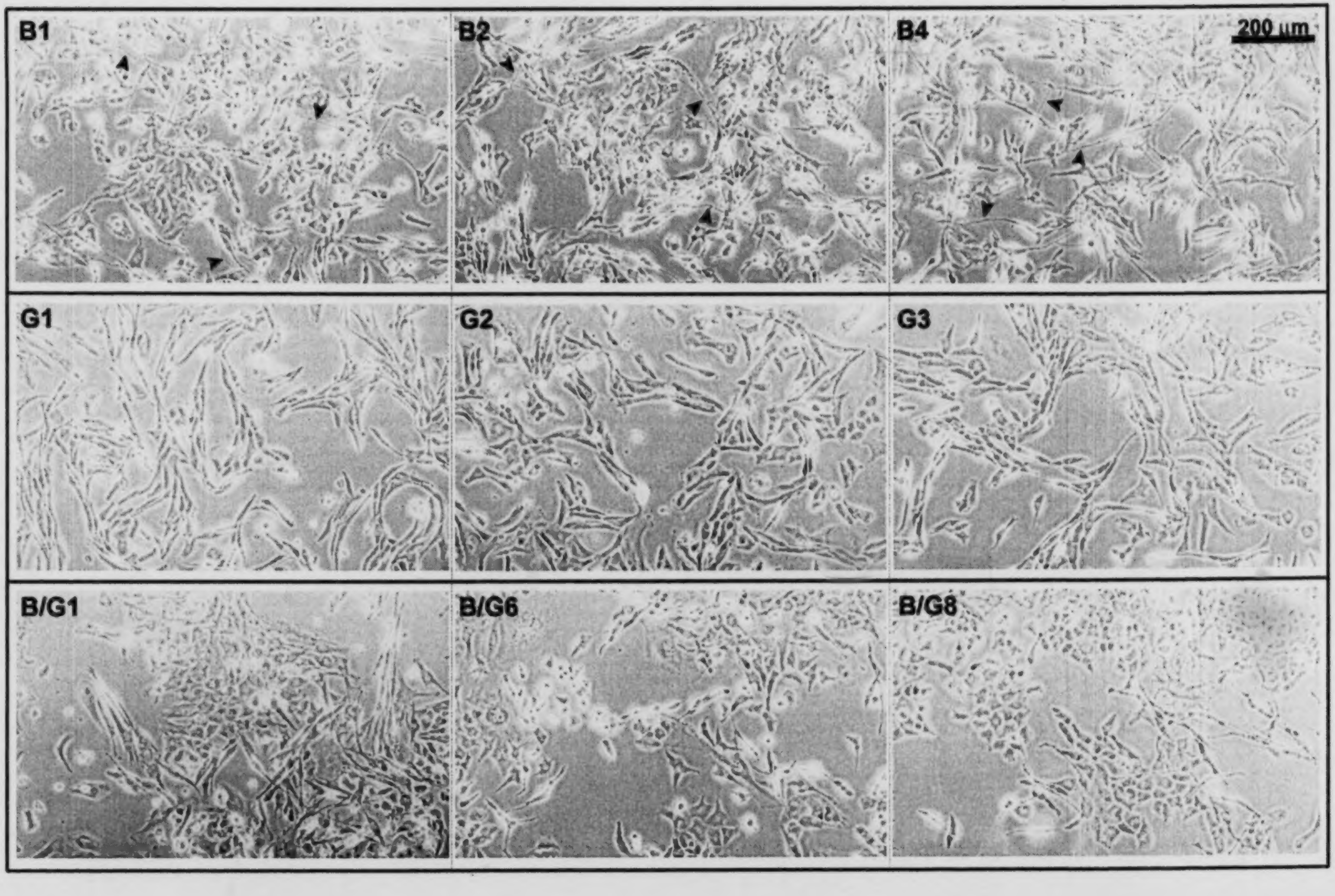
B1
B2
B4
200 µm
G1
G2
G3
B/G1
B/G6
B/G8

The most striking difference between the T98-GFAP clones and the T98-B-FABP clones was the elongated appearance and the absence of processes in the T98-GFAP transfectants (Figure 4.8). This elongated morphology was observed prior to confluence as well as at confluence, and seemed to be associated with an increased cytoplasmic:nuclear ratio. Since GFAP is a cytoplasmic intermediate filament (IF), its overexpression might be expected to change the structure and/or volume of the cytoplasm. Rutka and Smith (1993) have observed a similar effect upon transfection of the astrocytoma cell line SF-126 with a GFAP expression construct. In accordance with these findings, others have postulated that GFAP is involved in maintaining astrocyte cell shape via interactions with the nuclear and plasma membranes (Duffy *et al.*, 1982; Goldman and Chiu, 1984). The absence of processes in the GFAP transfected cells is not surprising since it has previously been demonstrated that GFAP only leads to process formation in astrocytes when these cells are co-cultured with neurons (Weinstein *et al.*, 1991; Chen and Liem, 1994).

Of note, there was little clone-to-clone morphological variation for both the T98-B-FABP and T98-GFAP transfectants even though B-FABP and GFAP expression was variable in these clones. For example, the T98-GFAP-1 clone expressed very low levels of GFAP compared to the T98-GFAP-3 clone, yet the cells in these two clonal populations were morphologically similar. These results suggest that even low levels of B-FABP or GFAP expression are sufficient to mediate the morphological changes observed in the transfected T98 cells.

In contrast to the T98-B-FABP and T98-GFAP transfectants, the T98-B/G clones did not display a predominant morphology (Figure 4.8). The cells within each clone appeared to be a mixture of the phenotypes displayed by the T98-B-FABP and T98-GFAP clones. However, the clones in which B-FABP expression could be detected by western blot analysis (T98-B/G-1 and -8) did tend to have more processes than did T98-B/G-6. Also, the T98-B/G clones tended to grow as clumps, with individual clumps expanding to form a monolayer. Since GFAP is expressed at high levels in all three T98-B/G clones compared to the T98-GFAP clones, and because GFAP has previously been found to inhibit mobility in another MG cell line (U373) (Zhou and Skalli, 2000), we can speculate that this strong overexpression of GFAP inhibited the migration of the cells, leading to cell clumping.

U87 transfectants:

Examination of the morphology of the U87-B-FABP clones provided further evidence of a role for B-FABP in process formation. In these transfectants, numerous long and thin cytoplasmic processes were readily apparent in 4/5 of the U87-B-FABP transfectants (U87-B-FABP-1, -2, -3 and -7) (as indicated by arrowheads in Figure 4.9). However, these processes were not evident in U87-B-FABP-5 cells. One possible explanation for absence of long processes in the U87-B-FABP-5 clone may be the lower levels of B-FABP observed in this clone by western blot (Figure 4.2). It is possible that, unlike the T98 cell line, relatively high levels of B-FABP are required for the formation of processes in U87 cells. Another possibility is that the subcellular localization of B-FABP in U87-B-FABP-5 is altered compared to that of the other four clones. As expected, the U87-pREP4 clones looked similar to the parent U87 cell line, with a stellate-shaped cell body and relatively short cytoplasmic processes (Figure 4.9).

In addition to process formation, a few other morphological changes were observed in the U87-B-FABP-1, -2, -3 and -7 clones, but not in U87-B-FABP-5. First, the U87-B-FABP-1, -2, -3 and -7 clones showed an increase in cell size compared to the U87-pREP4 clones. This change in cell size was most evident in those transfectants expressing the highest levels of B-FABP (U87-B-FABP-3 and -7) (Figures 4.4 and 4.9). Interestingly,

Figure 4.9 - Effects of B-FABP expression on the morphology of U87 cells. Phase contrast microscopy was used to photograph the cell lines when they had reached approximately 60-80% confluence. The morphology of the cells in the U87-pREP4-1 (C1), -3 (C3), -6 (C6), and -7 (C7) clones is similar to that observed for the U87 parent cell line. These cells are stellate-shaped and extend relatively short processes. U87-B-FABP-5 (B5) cells also have this morphology. In contrast, the clones with higher levels of B-FABP, U87-B-FABP-1 (B1), -2 (B2), -3 (B3), and -7 (B7) have a markedly different phenotype. These B-FABP transfectants extend very long processes (indicated by arrowheads), some stretching over 200 μm, and have an increased cell size. All microscopy images were taken using a 10X objective lens.

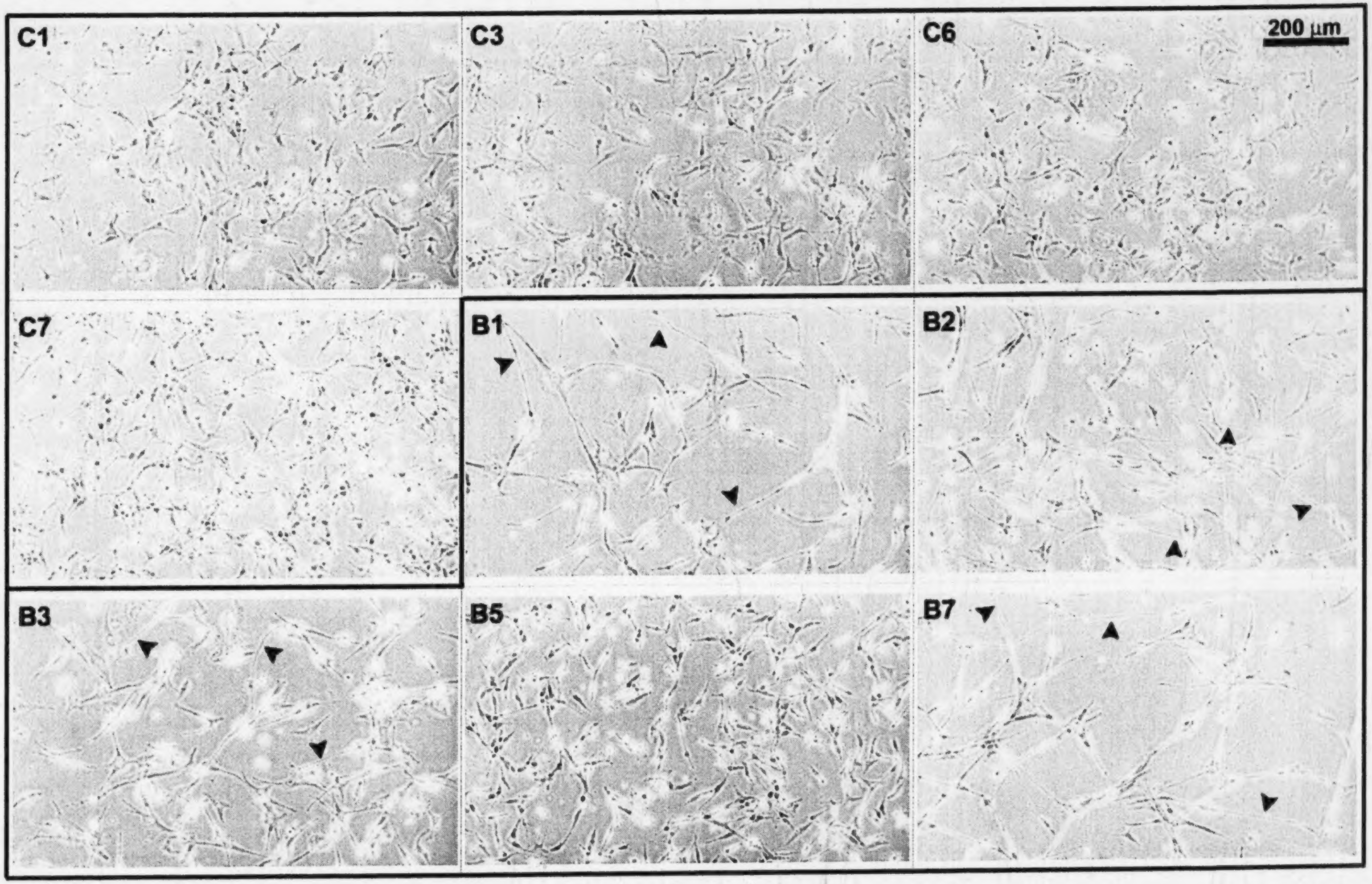
C1
C3
C6
200 µm
C7
B1
B2
B3
B5
B7

both the nucleus and cytoplasm were generally larger in these cells (Figure 4.4), but overall an increase in the cytoplasmic:nuclear ratio was evident. Thus, it appears that both GFAP expression in T98 cells and B-FABP expression in U87 cells increase the cytoplasmic:nuclear ratio in these MG cell lines. Second, at confluence none of the U87-B-FABP-1, -2, -3 and -7 clones displayed a high degree of cell crowding, and there was no piling up of cells. In contrast, the U87-B-FABP-5 and U87-pREP4 clones displayed cell crowding and mild cell piling; however, they no longer formed the tight balls of piled up cells observed in the parent line. The absence of piled-up cells could be due to the decreased proliferation rate observed for the U87-pREP4 clones compared to the parent U87 cell line (discussed in section 4.4).

U251 transfectants:

Yet additional evidence supporting a role for B-FABP in process formation comes from the U251-pSUPER/B-FABP clones, where B-FABP expression was reduced by ~90%. Lower levels of B-FABP in U251 were generally accompanied by a reduction in the number of processes. As shown in Figure 4.10, U251 cells transfected with pSUPER (panel A-C) and pSUPER/DDX1 (panel D-F) had a similar morphology as the U251 parent cell line. These cells were stellate-shaped and had numerous short cytoplasmic processes. In contrast, cells transfected with pSUPER/B-FABP (panel G-I) typically failed to develop processes, and displayed fan-like structures (indicated by arrows). One possible explanation for this finding is that the reduction in B-FABP expression enhances cell motility since the fan-like structures resemble the characteristic structure of the leading-edge in migrating cells. At confluence, these fan-like structures disappeared and the U251-pSUPER/B-FABP clones looked much like the U251-pSUPER and U251-pSUPER/DDX1 clones. Of note, no increase in cell crowding or piling was observed for any of the U251 transfectants at confluence.

Figure 4.10 - Absence of processes in U251-pSUPER/B-FABP clones. Phase contrast microscopy was used to photograph the cell lines when they had reached approximately 60-80% confluence. The morphology of the cells in the control transfectants U251-pSUPER-1 (A), -2 (B), and -3 (C) is similar to that observed for the U251 parent cell line. These cells are stellate-shaped and have relatively short processes. U251-pSUPER/DDX1-1 (D), -2 (E) and -3 (F) clones also displayed this morphology. In contrast, the U251-pSUPER/B-FABP clones which showed a ~90% reduction in B-FABP levels based on western blotting, exhibit drastic morphological alterations. The cells in these pSUPER/B-FABP transfectants typically fail to develop processes, and instead display fan-like structures (indicated by arrowheads) similar to migratory leading-edge structures. All microscopy images were taken using a 10X objective lens.

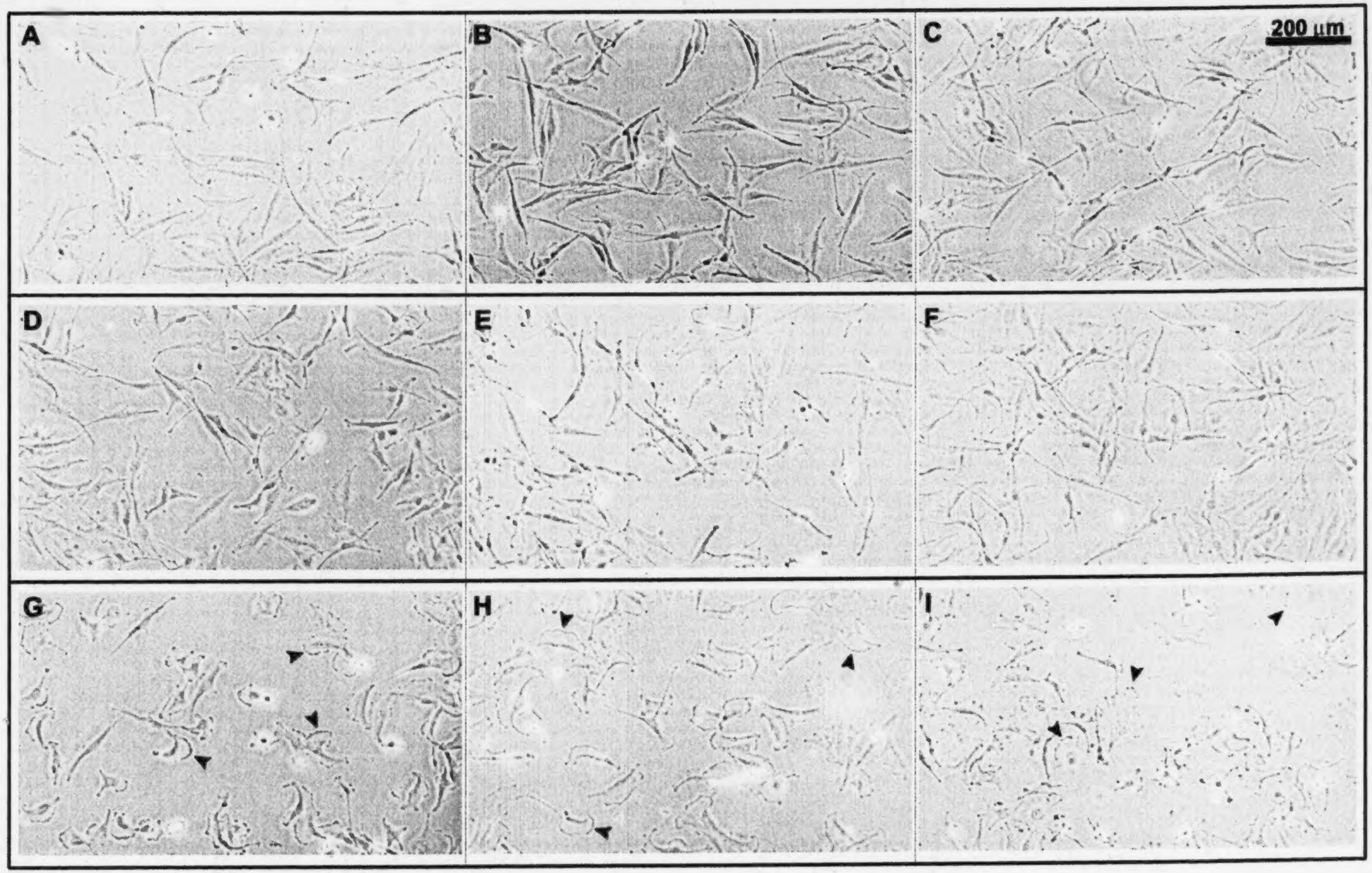
A
B
C
200 µm
D
E
F
G
H
I

4.5. Subcellular Localization of B-FABP in the U87 Transfectants

As mentioned in section 4.4, the morphology of the U87-B-FABP-5 clone was different from that of U87-B-FABP-1, -2, -3 and -7. We reasoned that this difference could be due to either the lower levels of B-FABP or a difference in the subcellular localization of B-FABP in U87-B-FABP-5. To address the latter, confocal microscopy studies were performed on each of the U87-B-FABP transfectants. The experimental design was identical to that described in section 4.2 except that the laser scanning parameters were adjusted between images to prevent signal saturation. Also, a 40X/1.3 oil immersion lens was used rather than a 25X/0.8 immersion correction lens to allow a more detailed subcellular analysis. We examined a minimum of five images for each of the five transfectants. From the images captured, a strong nuclear B-FABP signal was detected in U87-B-FABP-1, -2, -3 and -7; however, nuclear B-FABP was virtually absent in U87-B-FABP-5 clone. A representative image for each transfectant is shown in Figure 4.11.

These findings suggest that the morphological alterations observed in the U87-B-FABP clones may be mediated, at least partly, by a function for B-FABP in the nucleus. In support of this idea, other researchers have demonstrated an involvement of FABPs in regulating gene transcription and differentiation by delivering FAs to the nucleus and/or by interacting with PPARs in the nucleus (reviewed in Zimmermann and Veerkamp, 2000). While we have not addressed the role of B-FABP in the nucleus in these studies, our results indicate that B-FABP may play a role in mediating cell morphology and probably cell differentiation.

4.6. Effects of B-FABP and/or GFAP Expression on Cell Proliferation

To determine the proliferation rate of each of the transfectants and the parent lines, 15000 cells were plated in triplicate in 35-mm tissue culture plates. At specific time points

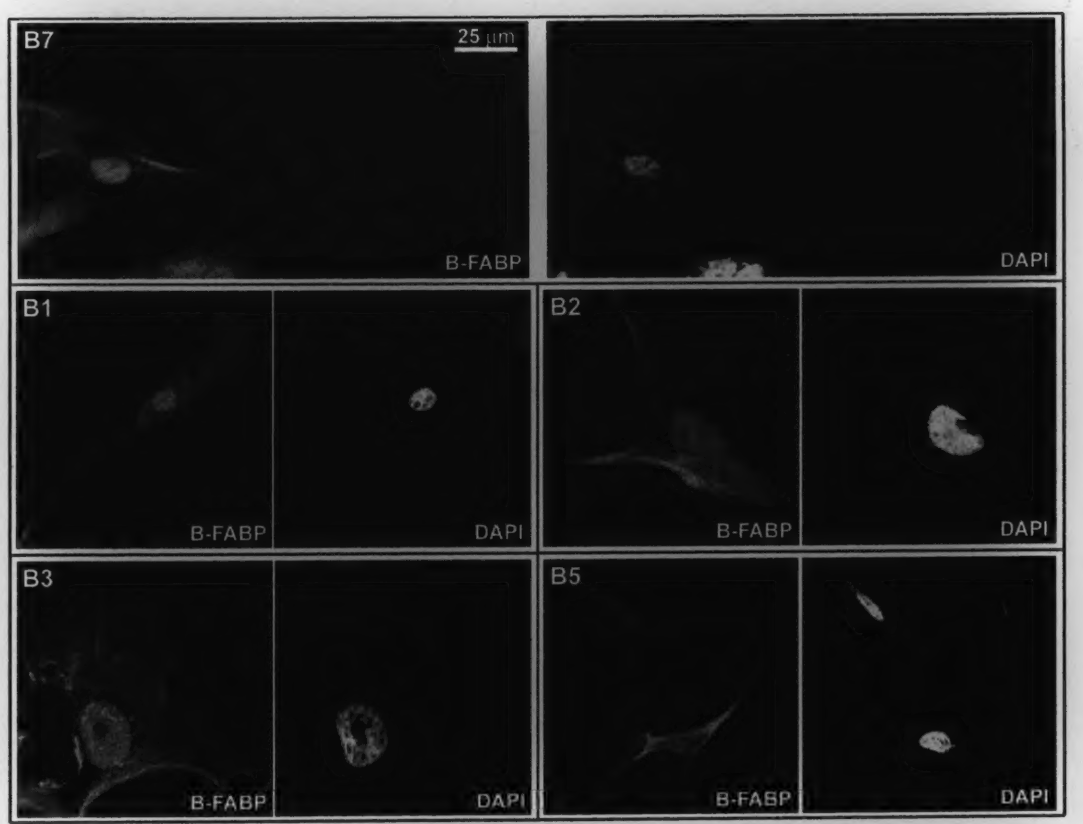

Figure 4.11 - Subcellular localization of B-FABP in the U87 transfectants. Each transfectant was plated on coverslips, grown to 60-80% confluence, fixed, permeabilized and double-stained with rabbit anti-B-FABP and mouse ~~anti-GFAP~~ antibodies. Fluorescent secondary antibodies [Alexa 488 (anti-mouse) and Alexa 555 (anti-rabbit)] allowed image collection using a confocal microscope. DAPI was used to stain the nucleus. At least five images were collected for each transfectant, U87-B-FABP-1 (B1), -2 (B2), -3 (B3), -5 (B5), and -7 (B7). A representative image is shown for the B-FABP (green) and DAPI (white) channels. Interestingly, the U87-B-FABP clones that displayed distinct morphological alterations (B1, B2, B3, and B5) exhibited a strong nuclear staining pattern for B-FABP, while U87-B-FABP-5, similar in morphology to the controls, showed little B-FABP nuclear staining.

the number of cells in each plate was counted to generate a growth rate curve for each cell line. The growth rate curves for the T98 transfectants are shown in Figure 4.12, the U87 transfectants in Figure 4.13, and the U251 transfectants in Figure 4.14. From the growth rate curves, the doubling time for each cell line was calculated during a period when the cells were undergoing exponential growth. The doubling times calculated for each of the cell lines and clones are shown in Table 4.1.

T98 transfectants:

The proliferation rate of the T98-B-FABP transfectants was similar to that observed for T98 and the T98-pREP4 transfectants (Figure 4.12), with doubling times of 19 hours for T98 and the T98-pREP4 clones, and 20 hours for the T98-B-FABP clones (Table 4.1). Thus, B-FABP appears to have very little influence on the proliferation rate of T98 cells. In contrast, T98 cells transfected with GFAP demonstrated significant alterations compared to the control cells, with doubling times of 24, 25.5 and 27 hours for T98-GFAP-1, -2 and -3, respectively. Interestingly, the rate of proliferation inversely correlated with GFAP expression in these clones. For instance, the clone with the highest level of GFAP, T98-GFAP-3, had the slowest proliferation rate. This is as expected as others have previously described an inverse correlation between GFAP expression and proliferation rate (Rutka and Smith, 1993; Rutka *et al.*, 1994)

The T98-B/G clones demonstrated an even greater reduction in proliferation rate than the T98-GFAP clones, with doubling times of 36 and 55 hours observed for T98-B/G-1 and -8, respectively. While much of this effect on proliferation may be mediated by the high levels of GFAP in the double transfectants, it is noteworthy that the T98-B/G-6 clone, which has levels of GFAP nearly as high as those observed in T98-B/G-1 and -8, but undetectable B-FABP, has a proliferation rate similar to that of T98-GFAP transfectants

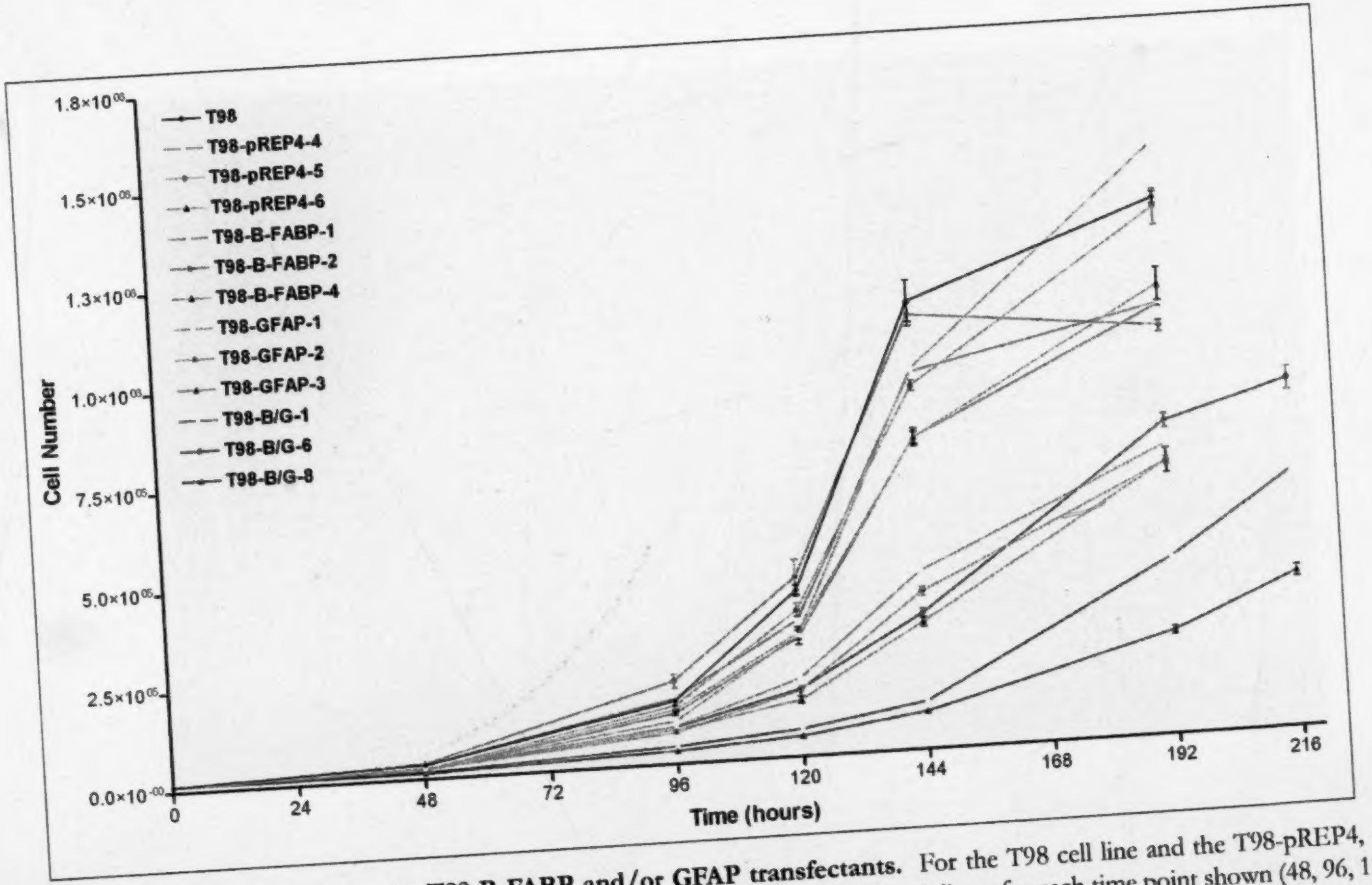

Figure 4.12 - Growth rate curves for the T98 B-FABP and/or GFAP transfectants. For the T98 cell line and the T98-pREP4, -GFAP, -B-FABP and -B/G transfectants, 15000 cells were plated in 35-mm tissue culture plates in triplicate for each time point shown (48, 96, 120, 144, 192, and 216 hours). Cells were counted at each time point and growth rate curves were plotted for each cell line. Error bars depict the standard deviation for each count; however, many lie within the time point label and cannot be seen. When compared to the control transfectants (T98-pREP4), the growth rate of T98 cells did not appear to be affected by B-FABP cDNA transfection, while GFAP expression significantly reduced the proliferation rate of these cells.

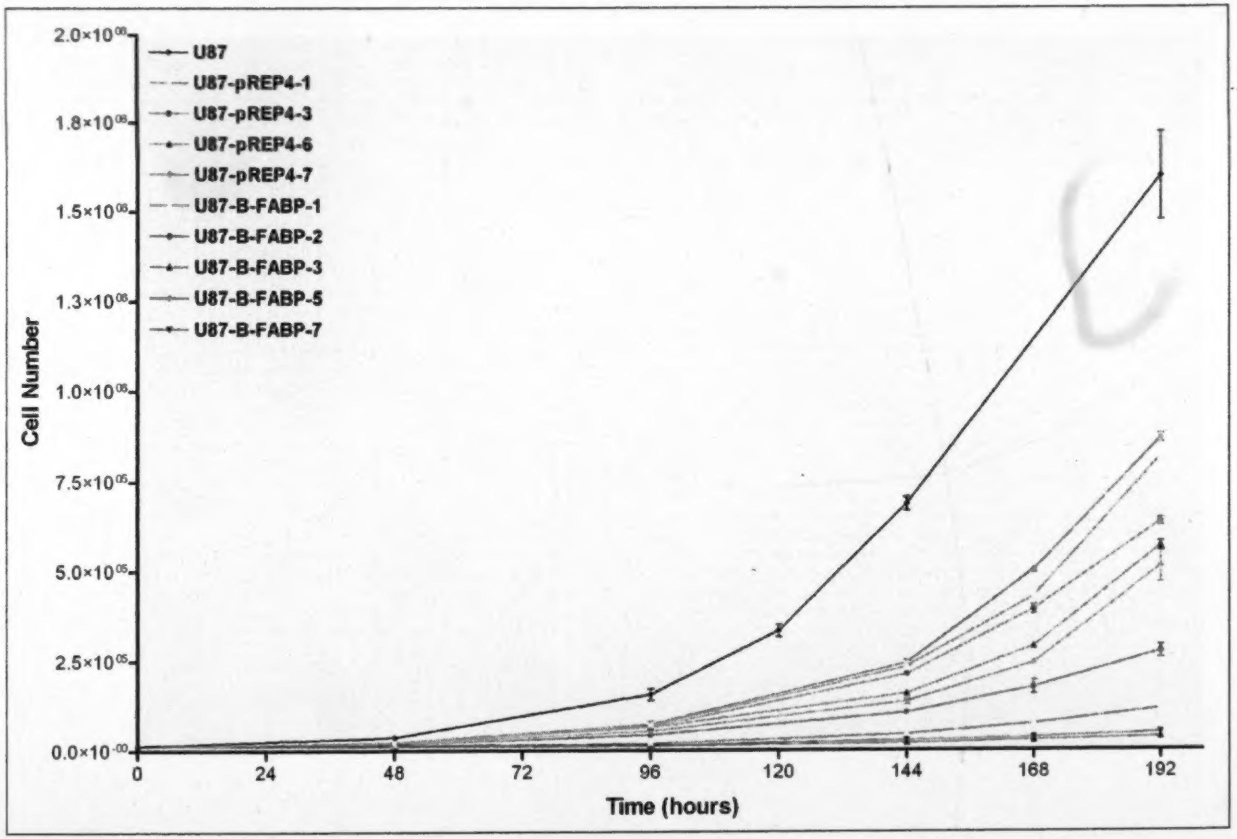

Figure 4.13 - Effect of B-FABP cDNA transfection on U87 MG proliferation. For the U87 cell line and the U87-pREP4 and U87-B-FABP transfectants, 15000 cells were plated in 35-mm tissue culture plates in triplicate for each time point shown (48, 96, 120, 144, 168, and 192). Cells were counted at each time point and growth rate curves were plotted for each cell line. Error bars depict the standard deviation for each count; however, many lie within the time point label and cannot be seen. When compared to the control transfectants (U87-pREP4), the growth rate of the U87-B-FABP-1, -2, 3, and -7 clones is significantly reduced, while that of U87-B-FABP-5 is not. Unexpectedly, the U87-pREP4 clones showed a markedly reduced proliferation rate compared to the U87 parent cell line.

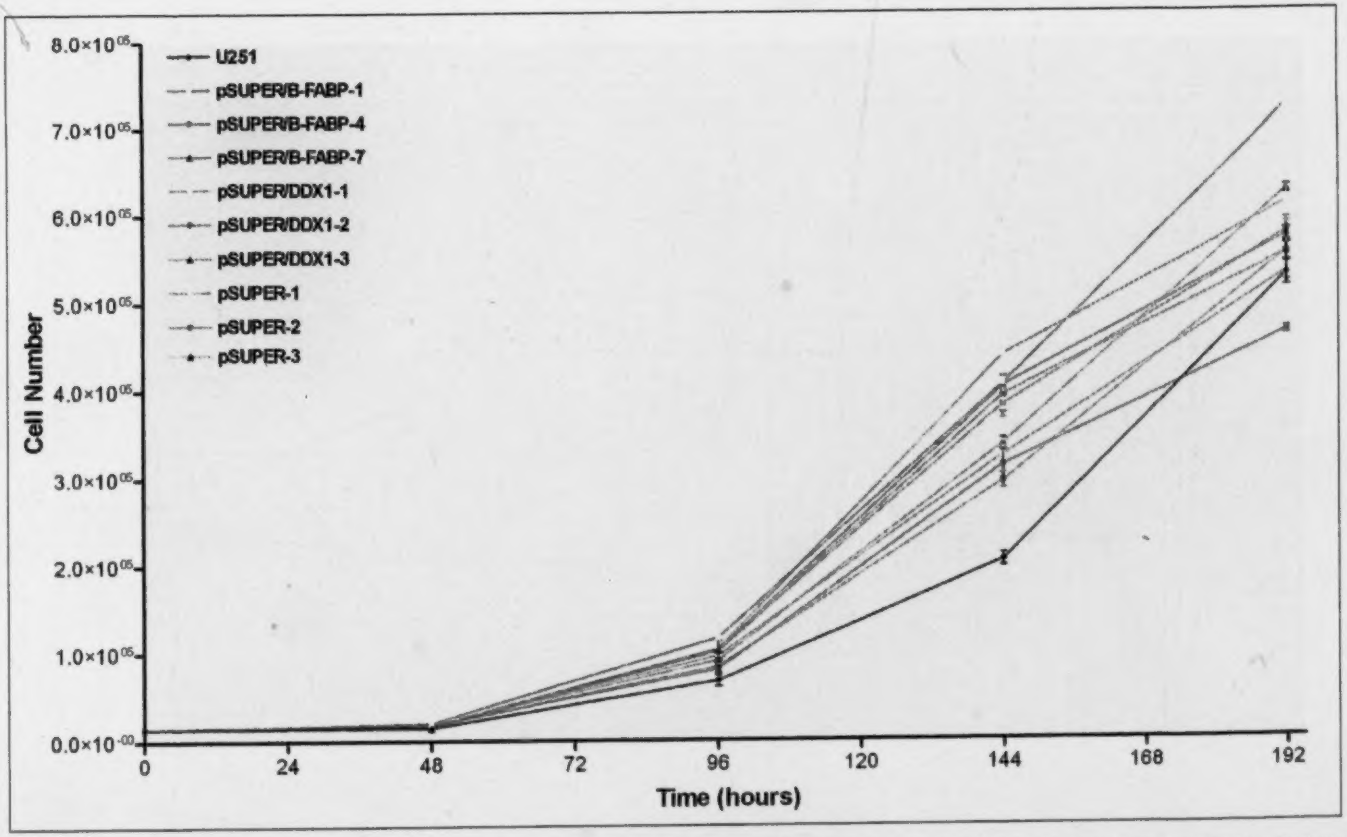

Figure 4.14 - Reduced B-FABP expression in U251 MG does not affect proliferation. For the U251 cell line and the U251-pSUPER, U251-pSUPER/B-FABP, and U251-pSUPER/DDX1 transfectants, 15000 cells were plated in 35-mm tissue culture plates in triplicate for each time point shown (48, 96, 144, and 192 hours). Cells were counted at each time point and growth rate curves were plotted for each cell line. Error bars depict the standard deviation for each count; however, many lie within the time point label and cannot be seen. When compared to the control transfectants (U251-pSUPER-1, -2, and -3), the growth rate of U251 cells did not appear to be significantly affected by reduced B-FABP or DDX1 expression.

Table 4.1 - Doubling time for the T98, U87 and U251 cell lines and the transfectants.

Cell Line	Doubling Time (hours)
T98	19.0
T98-pREP4-4	19.0
T98-pREP4-5	19.0
T98-pREP4-6	19.0
T98-B-FABP-1	20.5
T98-B-FABP-2	20.0
T98-B-FABP-4	19.0
T98-GFAP-1	24.0
T98-GFAP-2	25.5
T98-GFAP-3	27.0
T98-B/G-1	36.0
T98-B/G-6	27.0
T98-B/G-8	35.0
U87	21.0
U87-pREP4-1	28.0
U87-pREP4-3	32.5
U87-pREP4-6	31.0
U87-pREP4-7	35.5
U87-B-FABP-1	49.0
U87-B-FABP-2	49.5
U87-B-FABP-3	77.0
U87-B-FABP-5	28.0
U87-B-FABP-7	64.5
U251	26.0
U251-pSUPER-1	23.0
U251-pSUPER-2	24.0
U251-pSUPER-3	23.0
U251-pSUPER/DDX1-1	21.0
U251-pSUPER/DDX1-2	23.5
U251-pSUPER/DDX1-3	20.5
U251-pSUPER/B-FABP-1	23.0
U251-pSUPER/B-FABP-4	24.0
U251-pSUPER/B-FABP-7	21.0

expressing low levels of GFAP. Therefore, we speculate that B-FABP expression in the T98-B/G-1 and -8 clones may be responsible for the greater reduction in proliferation rate observed in these cells. Alternatively, the difference in proliferation rate between the T98-B/G clones may simply be a function of clonal variation.

U87 transfectants:

In support of a role for B-FABP in mediating the proliferation rate of MG cells, we observed a strong reduction in the proliferation rate of U87 cells expressing B-FABP (Figure 4.13). The U87 cells had a doubling time of 21 hours, while the U87-pREP4 transfectants had doubling times of 28, 32.5, 31 and 35.5 hours for U87-pREP4-1, -3, -6 and -7, respectively (Table 4.1). Four of the five U87-B-FABP clones had doubling times of 49, 49.5, 77 and 64.5 hours for U87-B-FABP-1, -2, -3 and -7, respectively. Using the average doubling time for the controls (~32 hours), we calculated a 1.5-fold increase in doubling time for U87-B-FABP-1 and -2, a 2.4-fold increase for U87-B-FABP-3, and a 2.2-fold increase for U87-B-FABP-7. The U87-B-FABP-5 clone, with a doubling time of 28 hours, did not exhibit any reduction in proliferation. The U87-B-FABP-5 results suggest that either there must be a threshold level of B-FABP necessary to generate an effect on proliferation or that nuclear B-FABP is required to affect proliferation.

Unexpectedly, the U87-pREP4 control clones showed a markedly reduced proliferation rate compared to the U87 parent cell line (Figure 4.13; Table 4.1). This observation suggests that clonal selection in hygromycin influenced the growth characteristics of the U87 cells. However, since the B-FABP transfectants are always compared to the similarly generated control transfectants, this should not affect our overall conclusions as to the role of B-FABP in these cells.

U251 transfectants:

Analysis of the U251 transfectants indicated that even a 90% reduction in B-FABP levels did not have an effect on proliferation rate. The U251 cell line and each of the U251-pSUPER, -pSUPER/B-FABP and -pSUPER/DDX1 transfectants all had similar growth rate curves (Figure 4.14) and doubling times (Table 4.1). In explanation of this, it is possible that the reduction in B-FABP observed in the pSUPER/B-FABP transfected cells is primarily from the cytoplasmic pool of B-FABP, with the nuclear pool remaining intact. Extending this explanation further, it could be hypothesized that without a change in nuclear B-FABP levels, as was observed for U87-B-FABP-5 where B-FABP was not localized to the nucleus, MG cell proliferation is not affected.

4.7. Correlation between B-FABP and/or GFAP Expression and Anchorage-Independent Growth

Anchorage-independent growth is one of the most stringent assays used to distinguish transformed cells and tumour cells from normal cells (Shin *et al.*, 1975). A common method of assessing anchorage-independent growth is to determine the ability of cells to form colonies in soft agar. In regards to MG, Bigner and coworkers (1981) examined fifteen MG cell lines for several criteria including: cell piling at confluence, nuclear:cytoplasmic ratio, percentage of colony formation in soft agar, saturation density, population doubling time, and absolute plating efficiency. These researchers found the best *in vitro* correlation for *in vivo* tumourigenicity was colony formation in soft agar. These results have been corroborated by several investigators who have analyzed *in vitro* (soft agar) and *in vivo* (nude mice) tumourigenic properties of MG cell lines transfected with various cancer promoting/inhibiting genes (Huang *et al.* 1998; Sehgal *et al.* 1999; Zhang *et al.*, 2002).

Therefore, soft agar studies represent a valuable *in vitro* technique to study the tumourigenic properties of MG cell lines.

To assess the anchorage-independent growth capacity of our stably transfected clones and parent cell lines, each cell line was plated in quadruplicate on 35-mm petri dishes containing a 0.6% agarose bottom layer. A cell suspension containing 10000 cells in 0.3% agarose was then plated on top of this bottom layer and the plates were incubated for four weeks at 37°C. Colonies of greater than ~50 cells (100-250 μm) were scored as positive. Colonies were further divided into three groups based on their size: i) 50-100 cells/colony (100-250 μm), ii) 100-1000 cells/colony (250-750 μm), and iii) >1000 cells/colony (>750 μm). Results are summarized in Table 4.2 and low magnification representative photographs are shown in Figures 4.15-4.17. The counts for each individual plate for each cell line were nearly identical so the value shown represents the average of the quadruplicate plates.

T98 transfectants:

Several trends were detected in the T98 transfectants (Table 4.2; Figure 4.15). First, in comparing the control transfectants to the parent T98 cell line, a slight decrease in both colony number and colony size was observed for the T98-pREP4 clones. The majority (~75%) of colonies in T98 had greater than 1000 cells and few colonies were smaller than ~100 cells. In the T98-pREP4 clones, the majority of colonies had greater than 100 cells and an increase was observed in the number of colonies with 50-100 cells. This difference in colony formation between T98 and the T98-pREP4 clones may be a consequence of growing the T98-pREP4 transfectants in drug selection media and/or clonal variability.

Second, for each of the T98-B-FABP, -GFAP, and -B/G clones a moderate reduction in colony number was observed when compared to the T98-pREP4 clones (Table

Table 4.2 - Colony counting results for the B-FABP and/or GFAP transfectants and the T98 and U87 cell lines.

Cell Line	2 - 10 cells/colony[*][τ] 50 - 100 µm	Soft Agar (Colonies/plate[*]) 50 - 100 cells/colony 100 - 250 µm	100 - 1000 cells/colony 250 - 750 µm	> 1000 cells/colony > 750 µm	Total
T98	0	11	44	165	220
T98-pREP4-4	0	24	64	131	219
T98-pREP4-5	0	28	101	40	169
T98-pREP4-6	0	56	73	18	147
T98-B-FABP-1	0	51	9	5	65
T98-B-FABP-2	0	59	17	11	87
T98-B-FABP-4	0	48	43	15	106
T98-GFAP-1	0	34	29	22	85
T98-GFAP-2	0	27	6	1	34
T98-GFAP-3	0	44	18	13	75
T98-B/G-1	0	61	17	0	78
T98-B/G-6	0	27	61	45	133
T98-B/G-8	0	82	9	3	94
U87	0	0	50	284	334
U87-pREP4-1	0	18	127	36	181
U87-pREP4-3	0	47	231	23	301
U87-pREP4-6	0	33	139	30	202
U87-pREP4-7	0	17	28	134	179
U87-B-FABP-1	0	66	8	4	78
U87-B-FABP-2	0	90	38	12	140
U87-B-FABP-3	0	32	3	11	46
U87-B-FABP-5	0	11	17	82	110
U87-B-FABP-7	0	36	6	2	44
U251-pSUPER-2	23	8	0	0	8
U251-pSUPER/B-FABP-7	271	31	0	0	31

[*] The value shown represents the average of quadruplicate plates of a single experiment.

[τ] Clusters of 2 - 10 cells were not scored as a colony, but were recorded to note the differences between the U251-pSUPER-2 and -pSUPER/B-FABP-7 transfectants.

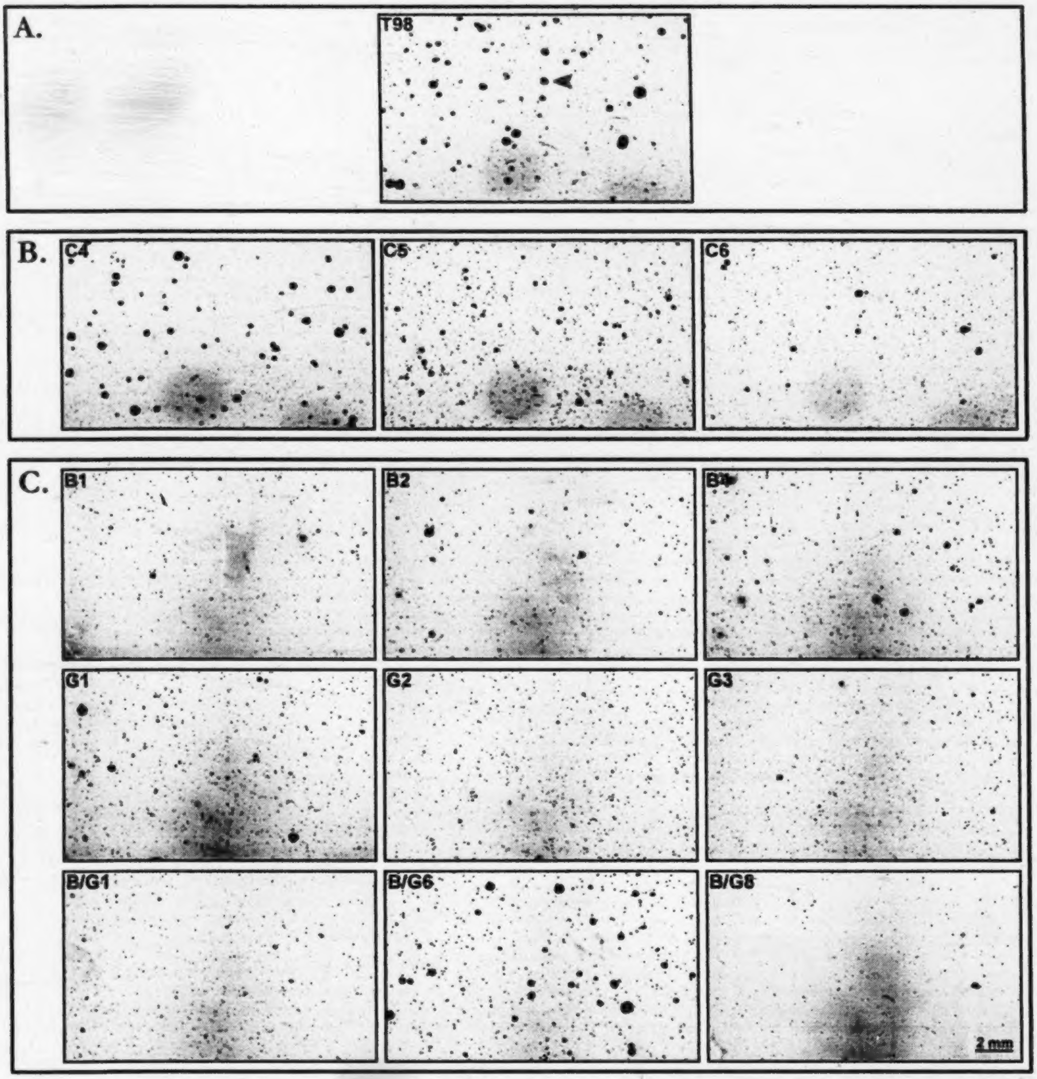

Figure 4.15 - Growth of the T98 B-FABP and/or GFAP transfectants in soft agar. For each cell line/clone, 10000 cells were plated in quadruplicate on agarose containing petri dishes. At four weeks, colonies were counted and a representative low magnification photograph was taken (shown above) for each cell line/clone. The photographs shown include: the T98 cell line (T98), the T98-pREP4-4 (C4), -5 (C5), and -6 (C6) transfectants, the T98-B-FABP-1 (B1), -2 (B2), and -4 (B4) transfectants, the T98-GFAP-1 (G1), -2 (G2), and -3 (G3) transfectants, and the T98-B/G-1 (B/G1), -6 (B/G6), and -8 (B/G-8) transfectants. The parent T98 cell line (panel A) showed numerous large and well formed colonies. The control transfectants (panel B) displayed a slight reduction in colony number and size compared to T98, and the B-FABP and/or GFAP transfectants typically exhibited an even greater reduction in colony number and size (panel C). A representative colony of 100-1000 cells/colony is indicated with a yellow arrowhead, and a colony of >1000 cells/colony with a red arrowhead. Colonies of 50-100 cells cannot be distinguished at this magnification.

4.2; Figure 4.15). For the T98-B-FABP clones this reduction ranged from ~1.7 to 2.7-fold with the clones expressing the highest levels of B-FABP (T98-B-FABP-1 and -2) showing a more pronounced reduction in colony number. The T98-GFAP clones also showed a reduction in colony formation compared to the T98-pREP4 clones with ~2.1 to 5.2-fold decreases observed. Interestingly, the T98-B/G clones, which expressed higher levels of GFAP than the T98-GFAP clones, had the least dramatic reduction in colony formation, ranging from ~1.3 to 2.3-fold. Of note, the T98-B/G-6 clone, in which B-FABP is undetectable, formed a similar number of colonies as the control lines. While this may simply be a consequence of clonal variability, it suggests that B-FABP has an important role in reducing anchorage-independent growth in the double transfectants.

Third, a reduction in colony size was observed in the B-FABP and/or GFAP transfectants compared to the controls. Within an individual category (*i.e.* 50-100, 100-1000 or >1000 cells/colony), the T98-pREP4 clones consistently displayed the highest number of colonies in either the 100-1000 cells/colony or >1000 cells/colony group (Table 4.2). However, for the B-FABP and/or GFAP transfectants (except T98-B/G-6), the highest number of colonies fell within the 50-100 cells/colony group. This is evident in the low magnification images shown in Figure 4.15 where very few colonies of 100-1000 cells (size indicated by yellow arrow) and even fewer of >1000 cells (size indicated by red arrow) were observed in the T98 B-FABP and/or GFAP transfectants. Although the low magnification photograph of T98-pREP4-6 resembles that of T98-B-FABP-4 and T98-GFAP-1, colony counts indicate that colonies of greater than 100 cells were more abundant in T98-pREP4-6.

While the reduction in colony size for the T98-GFAP and T98-B/G clones can be explained, at least in part, by their reduced proliferation rate, this does not explain the reduction in colony size observed for the T98-B-FABP clones since the proliferation rate of the B-FABP transfected clones was similar to that of the controls. Furthermore, it is interesting that of the T98-B-FABP clones and the T98-B/G clones, those that express B-FABP at higher levels are the ones that show the greatest reduction in colony size. Thus, while the effect of GFAP on colony size may be primarily due to a reduction in proliferation rate, the effect of B-FABP likely has more to do with its ability to reduce the tumourigenic properties of these cells. Nevertheless, similar to Rutka and Smith (1993) who demonstrated that GFAP expression in the SF-126 MG cell line reduced the colony forming ability of these cells, we did observe a decrease in colony formation by the T98-GFAP clones. Therefore, our data indicate that both B-FABP and GFAP expression results in a decreased capacity for anchorage-independent growth in the T98 cell line.

U87 transfectants:

U87 cells transfected with B-FABP also showed a reduced ability to form colonies in soft agar when compared to the U87-pREP4 clones and U87 parent cell line. The colonies generated by the U87-pREP4 clones were slightly smaller than those of U87, most probably due to the slower proliferation rate of the U87-pREP4 transfectants. However, whereas the U87-pREP4 control transfectants formed numerous large colonies (>100 cells) in soft agar, the U87-B-FABP clones (U87-B-FABP-1, -2, -3 and -7) had significantly smaller and fewer colonies with the exception of U87-B-FABP-5 (Table 4.2; Figure 4.16). As mentioned earlier, the results observed for U87-B-FABP-5 may be explained by the lack of B-FABP in the nucleus. This possibility is supported by the observation that the T98 transfectants expressing much lower levels of B-FABP than seen in U87-B-FABP-5 still showed a reduction in colony formation.

Results observed with the U87-B-FABP transfectants (excluding U87-B-FABP-5) were similar to those observed for the T98-B-FABP transfectants in that very few colonies

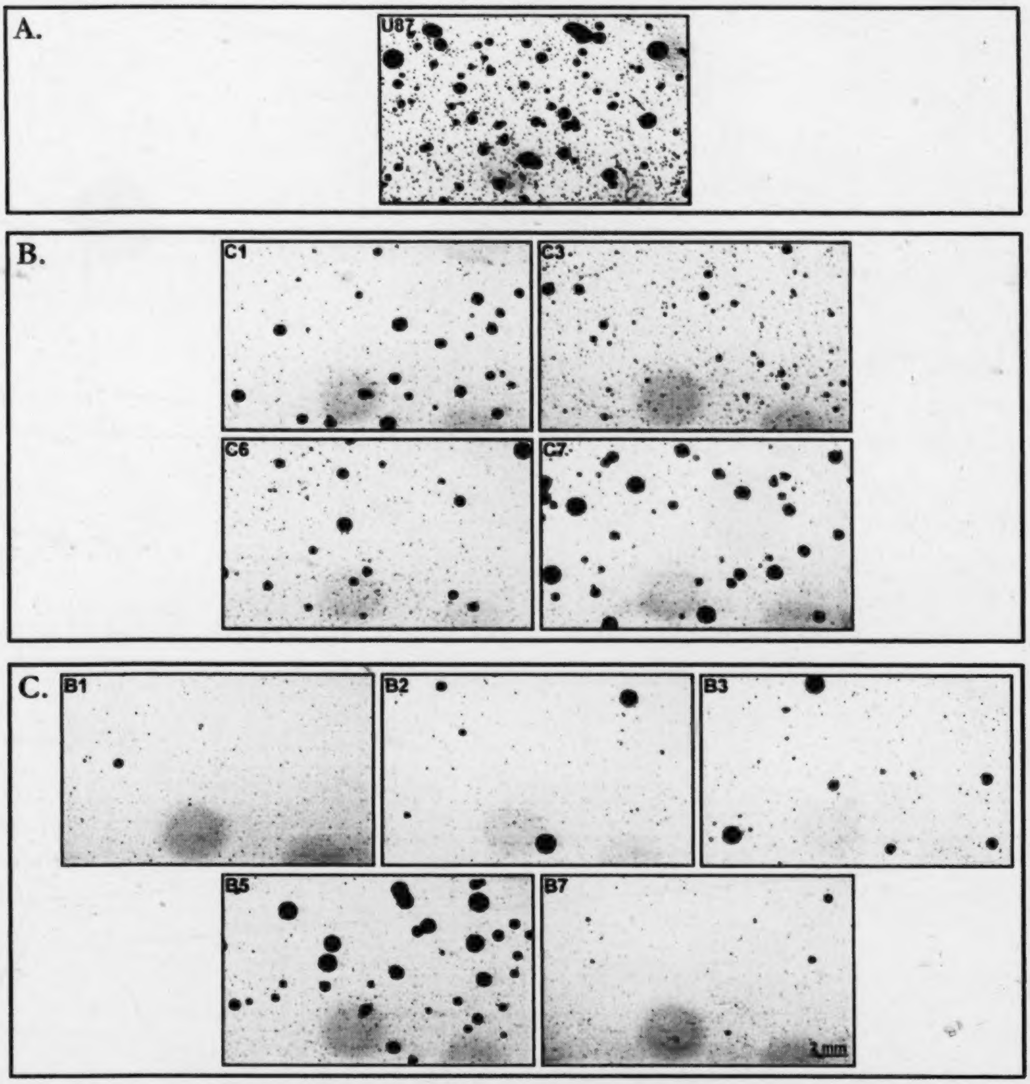

Figure 4.16 - Colony forming ability of the U87 B-FABP transfectants in soft agar. For each cell line/clone, 10000 cells were plated in quadruplicate on agarose containing petri dishes. At four weeks, colonies were counted and a representative low magnification photograph was taken (shown above) for each cell line/clone. The photos shown include: the U87 cell line (U87), the U87-pREP4-1 (C1), -3 (C3), -6 (C6) and -7 (C7) transfectants, and the U87-B-FABP-1 (B1), -2 (B2), and -3 (B3), -5 (B5) and -7 (B7) transfectants. Both the parent U87 cell line (panel A) and the U87-pREP4 control transfectants (panel B) display numerous large and well formed colonies. Compared to the control transfectants, the U87-B-FABP clones (panel C) exhibit a drastic reduction in colony size and number, with the exception of U87-B-FABP-5. Of note, colonies of 50-100 cells cannot be distinguished at this magnification.

had more than 100 cells, while the majority of colonies observed for the U87-pREP4 clones had greater than 100 cells. We can speculate that this reduction in colony size is due, at least partly, to the increased doubling time observed for the U87-B-FABP transfectants, but this does not explain the reduction in colony number. Using the average number of colonies for the controls (216 colonies), we calculated a 2.8-, 1.5-, 4.7- and 4.9-fold decrease in colony number for U87-B-FABP-1, -2, -3 and -7, respectively, compared to controls. Importantly, while U87-B-FABP-2 only showed a 1.5-fold reduction in colony number, the colonies were much smaller than those of the controls with ~65% having only 50-100 cells/colony. It is also interesting that the highest B-FABP expressing clones (U87-B-FABP-3 and -7) displayed the greatest reduction in colony number.

U251 transfectants:

U251 cells transfected with pSUPER/B-FABP were also tested for their ability to form colonies in soft agar. Since the U251 cell line generated very few colonies in soft agar (data not shown), only the U251-pSUPER-2 and U251-pSUPER/B-FABP-7 clones were analyzed to determine if a decrease in B-FABP expression would permit colony formation. Even though very few colonies, 8 and 31, were observed in U251-pSUPER-2 and U251-pSUPER/B-FABP-7, respectively, a reduction in B-FABP levels resulted in a significant increase in the presence of small cell clusters (2-10 cells/cluster) (Figure 4.17, red arrowhead). We counted an average of 271 cell clusters per plate for the U251-pSUPER/B-FABP-7 clone and an average of 23 cell clusters per plate for the U251-pSUPER-2 clone. This indicates that cells in the U251-pSUPER/B-FABP-7 clone underwent one or more cell divisions; however, the cells were not able to maintain anchorage-independent growth beyond this point. As B-FABP was still present at very low levels in U251-pSUPER/B-FABP-7, it is possible that the residual B-FABP prevented the formation of large colonies.

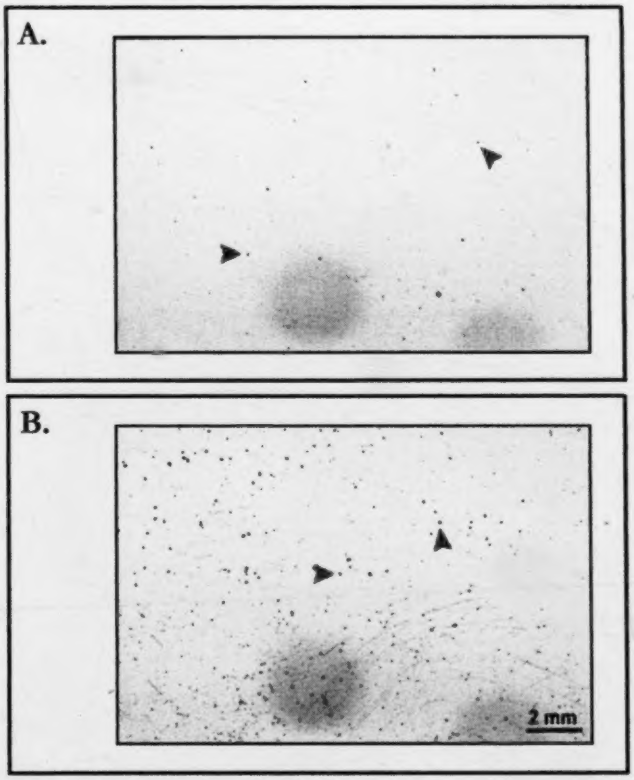

Figure 4.17 - Reduced B-FABP expression alters the growth of U251 cells in soft agar. For each transfectant, U251-pSUPER-2 (panel A) and U251-pSUPER/B-FABP-7 (panel B); 10000 cells were plated in quadruplicate on agarose containing petri dishes. At four weeks, colonies were counted and a representative low magnification photograph was taken (shown above) for each transfectant. While few colonies were found in either of the transfectants, the U251-pSUPER/B-FABP-7 clone formed numerous small clusters of 2-10 cells. These clusters, some of which are indicated with a red arrowhead, are too small to be scored as a colony; however, they do indicate that the cells divided one or more times after plating.

4.8. Effects of B-FABP and/or GFAP Expression on the Invasive Potential of Malignant Glioma Cells

The invasiveness of the MG stable transfectants was measured using BD BioCoat™ Matrigel™ invasion chambers. The matrigel matrix acts as a reconstituted basement membrane that is coated over a porous filter (8 μm pore size) at the bottom of an insert chamber. This matrix prevents non-invasive cells from migrating through the porous filter. Many researchers have successfully used Matrigel™ invasion chambers to study the invasiveness of glioblastoma cells in response to various stimuli, including: i) stable suppression of MMP-9 (Kondraganti *et al.* 2000; Lakka *et al.*, 2002), ii) stable suppression of uPA (Mohanam *et al.*, 2001), and iii) stable enhanced expression or suppression of GFAP (Rutka and Smith, 1993; Rutka *et al.*, 1994). Importantly, the significance of this *in vitro* assay for measuring the invasive properties of malignant cells has been validated by *in vivo* assessment of invasiveness by intracranial implantation (Kondraganti *et al.*, 2000).

T98 transfectants (22 hour time point):

To determine the invasiveness of the T98 transfectants, we initially followed the manufacturers' recommended protocol by adding 25000 cells (250 μl of a 1 x 10^5 cell/ml suspension) to the upper chamber of the matrigel invasion inserts and incubating these inserts for 22 hours. After 22 hours, a photograph of each insert was taken (Figure 4.18) and the number of cells that had passed through the matrigel insert was counted [Table 4.3; Trial 1 (22 hour) column]. The T98 B-FABP and/or GFAP transfectants all showed a drastic inhibition of invasion when compared to the T98-pREP4 controls.

The percentage of invasive cells for each of the T98 transfected clones is ~~shown~~ in Figure 4.19. Percent values are relative to T98-pREP4-5 (*i.e.* 789 cells set at 100%), which had the lowest level of invasion of the three controls tested. Compared to T98-pREP4-5, the T98-pREP4-4 and T98-pREP4-6 controls had relative percentage values of 146% and

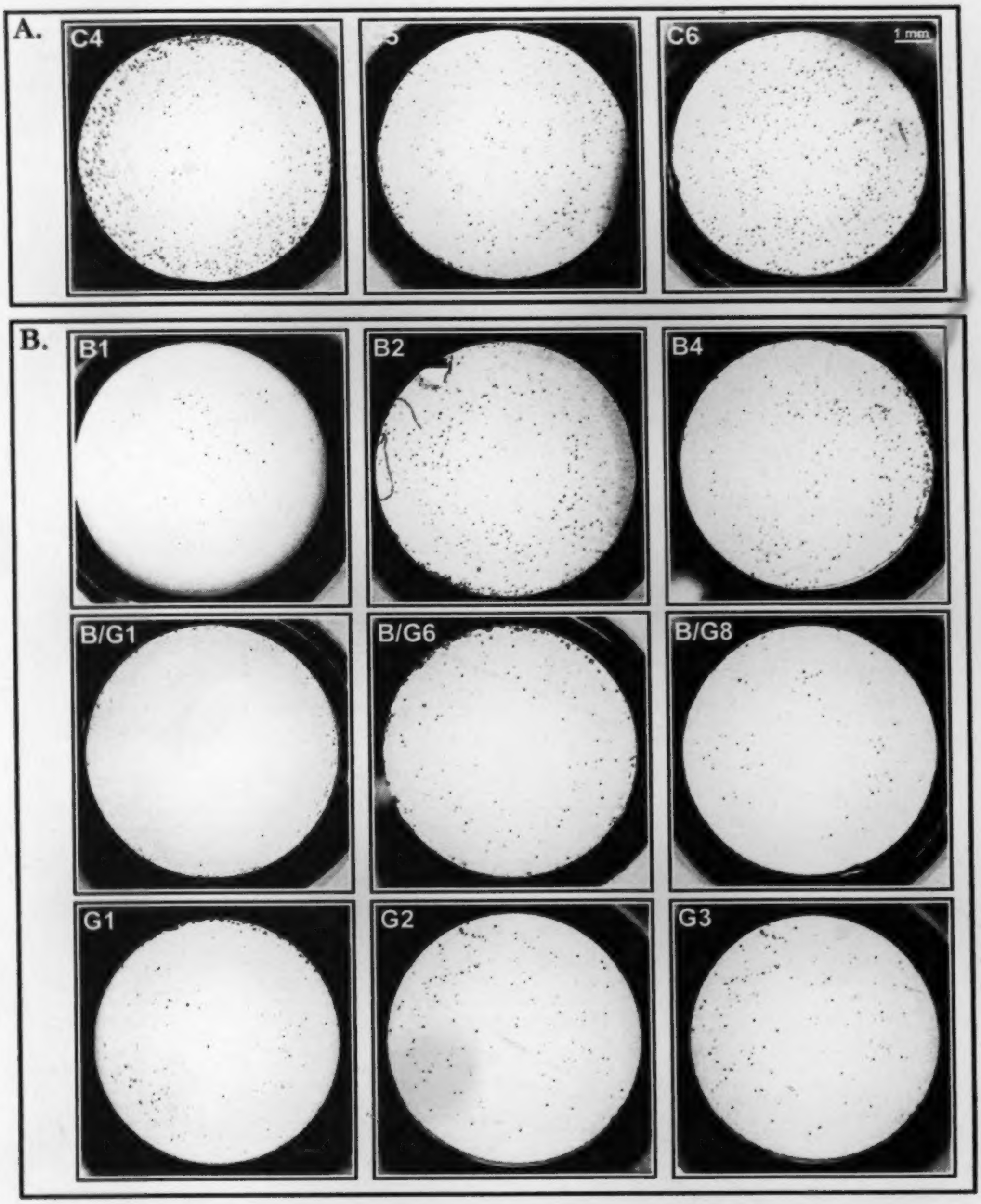

Figure 4.18 - Invasion of the T98 transfectants through Matrigel™ after 22 hours. 25000 cells were plated in the upper wells of individual transwell inserts containing an 8 μm pore size filter. Cells were allowed to invade for 22 h, at which time cells on the upper side of the filter were removed with a cotton swab and cells on the bottom side were fixed and stained with 1% crystal violet. Inserts for the T98-pREP4-4 (C4), -5 (C5) and -6 (C6), T98-B-FABP-1 (B1), -2 (B2) and -4 (B4), T98-B/G-1 (B/G1), -6 (B/G6) and -8 (B/G8), and T98-GFAP-1 (G1), -2 (G2) and -3 (G3) transfectants were photographed using a dissecting microscope. The B-FABP and/or GFAP transfectants (panel B) had reduced invasiveness compared to the T98-pREP4 control transfectants (panel A).

Table 4.3 - Number of cells that invaded through the Matrigel™ invasion chambers.

Cell Line	Matrigel (# cells invaded/insert)			
	Trial 1 (22 hour)	Trial 1 (30 hour)	Trial 2 (30 hour)	Trial 3 (30 hour)
T98-pREP4-4	1156	5254	4386	N/A
T98-pREP4-5	789	3191	2652	N/A
T98-pREP4-6	1092	751	974	N/A
T98-B-FABP-1	168	66	137	N/A
T98-B-FABP-2	317	218	229	N/A
T98-B-FABP-4	427	234	261	N/A
T98-GFAP-1	439	N/A	N/A	N/A
T98-GFAP-2	254	N/A	N/A	N/A
T98-GFAP-3	212	240	349	N/A
T98-B/G-1	85	83	71	N/A
T98-B/G-6	214	156	155	N/A
T98-B/G-8	147	256	395	N/A
U87-pREP4-3	N/A	1077	1020	1384
U87-pREP4-6	N/A	1564	1425	1822
U87-pREP4-7	N/A	1188	1412	1636
U87-B-FABP-1	N/A	74	170	304
U87-B-FABP-2	N/A	280	531	383
U87-B-FABP-3	N/A	163	147	103
U87-B-FABP-7	N/A	247	346	226
U251-pSUPER-2	1194	N/A	N/A	N/A
U251-pSUPER/B-FABP-7	1382	N/A	N/A	N/A

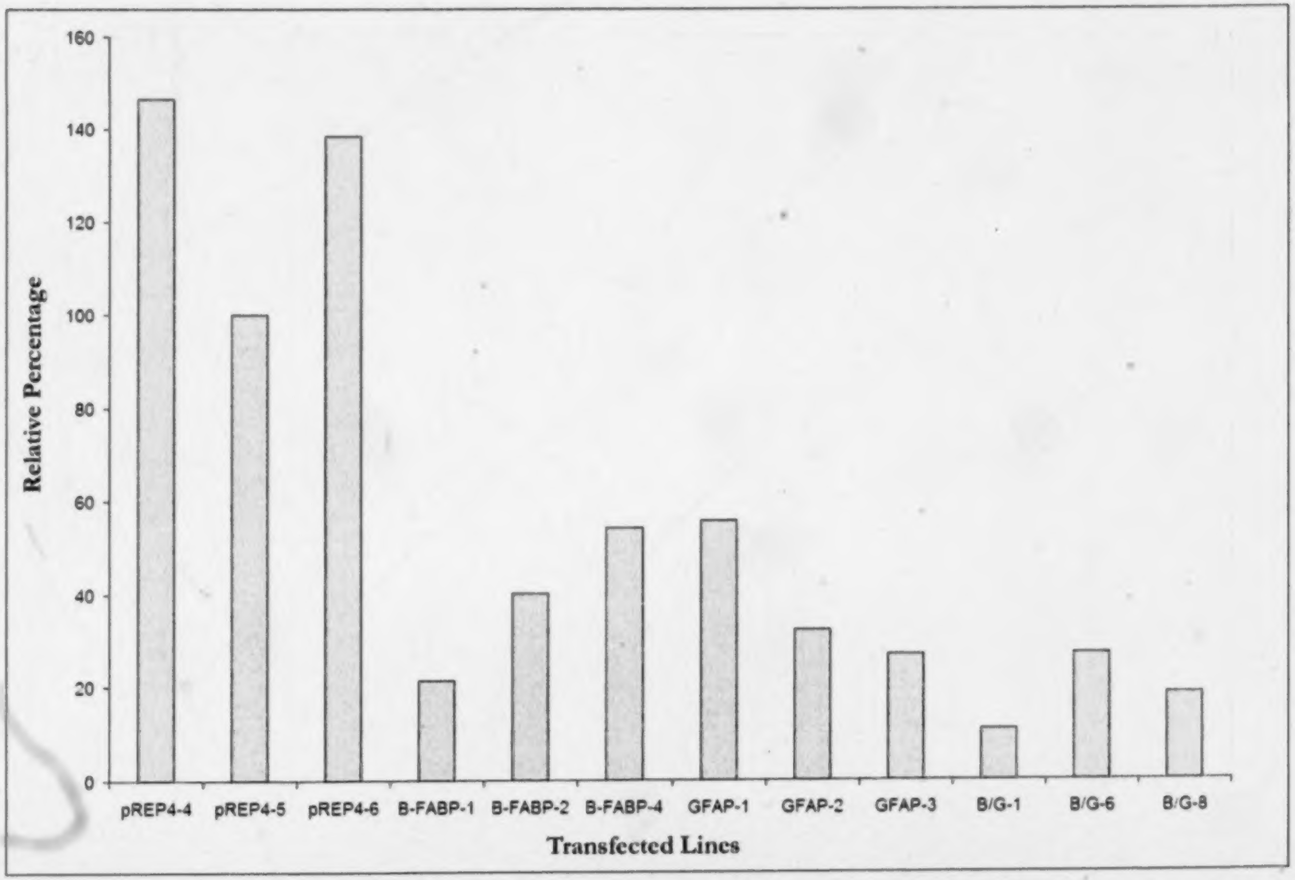

Figure 4.19 - Percentage of invasive cells for the T98 transfectants relative to the T98-pREP4-5 clone. The number of cells that passed through the matrigel insert for each T98 transfectant (pREP4-4, -5 and -6, B-FABP-1, -2 and -4, GFAP-1, -2 and -3, and B/G-1, -6 and -8) [Table 4.3; Trial 1 (22 hour) column] were compared with the T98-pREP4-5 clone and the relative percentage of invasive cells was calculated.

138%, respectively. The relative percentage of invading cells for the T98-B-FABP-1, -2 and -4 clones was 21%, 40% and 54%, respectively. Thus, B-FABP expression in T98 cells resulted in a decrease in invasiveness. Furthermore, there was an inverse correlation between B-FABP levels and the degree of invasiveness, with T98-B-FABP-4 showing the lowest levels of B-FABP and the highest percentage of invading cells. Similar results were obtained for the T98-GFAP transfectants with values of 55%, 32% and 26% obtained for T98-GFAP-1, -2 and -3, respectively. Again, an inverse correlation was noted, this time between GFAP levels and the percentage of invading cells. The most dramatic inhibition of invasion was observed in the double transfectants, with values of 11%, 27% and 18% for T98-B/G-1, -6 and -8, respectively. This greater reduction in invasiveness may be due to the higher levels of GFAP in the T98-B/G clones; however, it is of note that the T98-B/G clones that also expressed B-FABP (T98-B/G-1) displayed the greatest reduction in invasiveness. Thus, expression of B-FABP and GFAP may have a combined effect in reducing invasiveness in these clones.

U251 transfectants (22 hour time point):

The effect of reducing levels of B-FABP in U251 was tested using the same parameters described in the previous section (25000 cells plated; 22 hour incubation period). Comparison of the U251-pSUPER-2 and U251-pSUPER/B-FABP-7 clones revealed no significant differences in invasiveness (Table 4.3; Figure 4.20). A total of 1194 cells passed through the matrigel insert for U251-pSUPER-2 and 1392 cells for U251-pSUPER/B-FABP-7. Thus, a ~90% reduction in B-FABP levels resulted in only a ~15% increase in invasiveness. The failure of reduced B-FABP levels to affect invasiveness suggests that either residual B-FABP levels are still too high to permit invasion or B-FABP has no effect on U251 cell invasion.

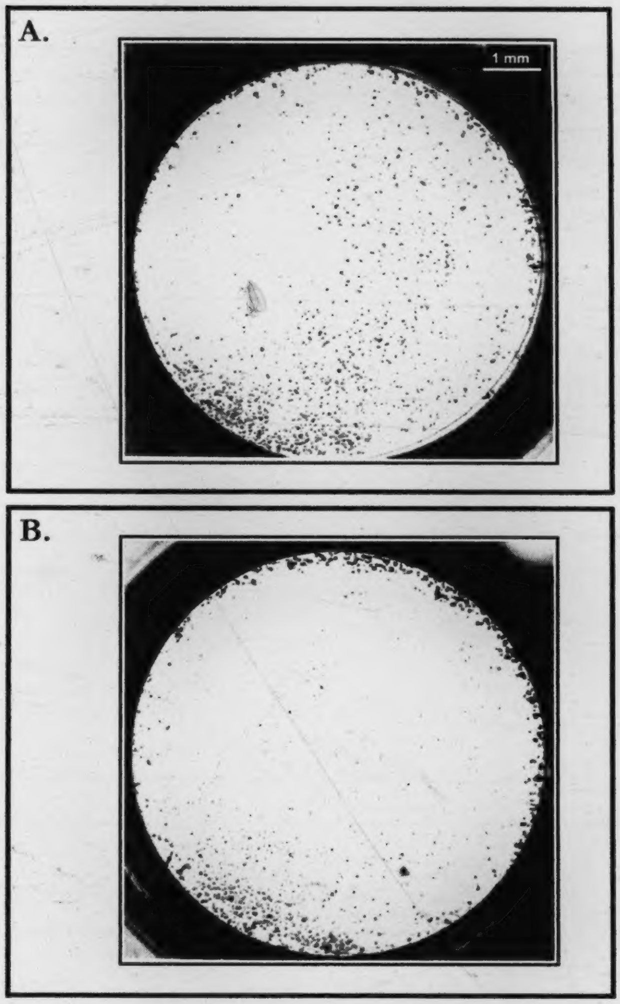

Figure 4.20 - Reduced B-FABP expression does not alter the invasive behaviour of U251 cells. 25000 cells were plated in the upper wells of individual transwell inserts containing an 8 μm pore size filter. Cells were allowed to invade for 22 h, at which time cells on the upper side of the filter were removed with a cotton swab and cells on the bottom side were fixed and stained with 1% crystal violet. Inserts for the U251-pSUPER-2 (panel A) and U251-pSUPER/B-FABP-7 (panel B) transfectants were photographed using a dissecting microscope. The invasive behaviour of each of the transfectants was similar indicating that a ~90% reduction in B-FABP levels does not affect the invasive properties of U251 cells.

T98 transfectants (30 hour time point):

Numerous studies have investigated MG cell invasion in matrigel, with invasion times typically ranging from 24 hours (Kondraganti *et al.*, 2000) to 72 hours (Rutka *et al.*, 1994). We therefore decided to examine a longer invasion time in order to determine how this would affect our relative percentage of invasion values. To ensure that cell division did not significantly alter our results, we chose an invasion time of 30 hours. Since Rutka and coworkers (1994) have already analyzed the effect of GFAP expression on the invasive behaviour of MG tumour cells, we concentrated on the B-FABP transfectants and only included our strongest GFAP expressing clone (T98-GFAP-3) in this analysis.

Two individual trials were performed for each transfectant. Photographs of the inserts were taken after 30 hours (Figures 4.21-4.22). The number of cells that passed through each matrigel insert is indicated in Table 4.3 [Trial 1 & 2 (30 hour) column]. Interestingly, while the control transfectants T98-pREP4-4 and -5 exhibited a dramatic increase (~4 to 5-fold) in invasion at 30 hours compared to 22 hours, the number of invasive cells remained similar for T98-B-FABP-1, -2, -4, T98-GFAP-3, T98-B/G-1, -6 and -8, as well as for T98-pREP4-6. Therefore, the 22 hour invasion period appears to have been sufficient for the invasion of the B-FABP and/or GFAP transfectants, but not for two of the control transfectants. It is possible that through membrane interactions and alterations in cytoplasmic architecture, B-FABP and/or GFAP expression may enhance the ability of glioma cells to penetrate through the small 8 μm pores in the insert filter. Thus, while B-FABP and/or GFAP expression may inhibit ECM degradation and cell migration, generating an overall reduction in invasiveness, invasive cells that do reach the filter are able to efficiently pass through the filter during the 22 hours permitted. In contrast, the control lines may be able to efficiently digest the matrigel and migrate to the filter, but penetration

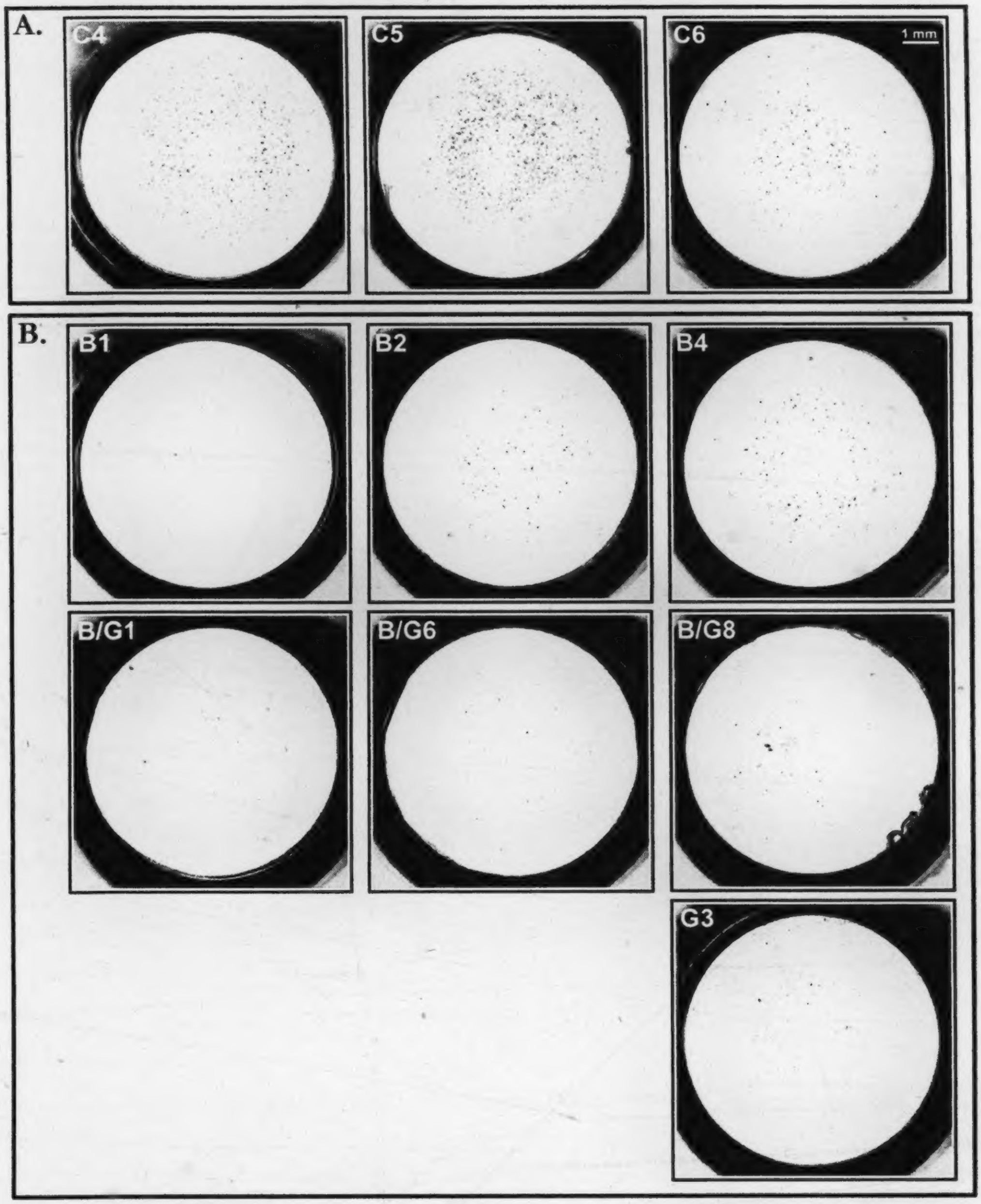

Figure 4.21 - Invasion of the T98 transfectants through Matrigel™ after 30 hours (Trial 1). 25000 cells were plated in the upper wells of individual transwell inserts containing an 8 μm pore size filter. Cells were allowed to invade for 30 h, at which time cells on the upper side of the filter were removed with a cotton swab and cells on the bottom side were fixed and stained with 1% crystal violet. Inserts for the T98-pREP4-4 (C4), -5 (C5) and -6 (C6), T98-B-FABP-1 (B1), -2 (B2) and -4 (B4), T98-B/G-1 (B/G1), -6 (B/G6) and -8 (B/G8), and T98-GFAP-3 (G3) transfectants were photographed using a dissecting microscope. The B-FABP and/or GFAP transfectants (panel B) showed reduced invasiveness compared to the T98-pREP4 control transfectants (panel A).

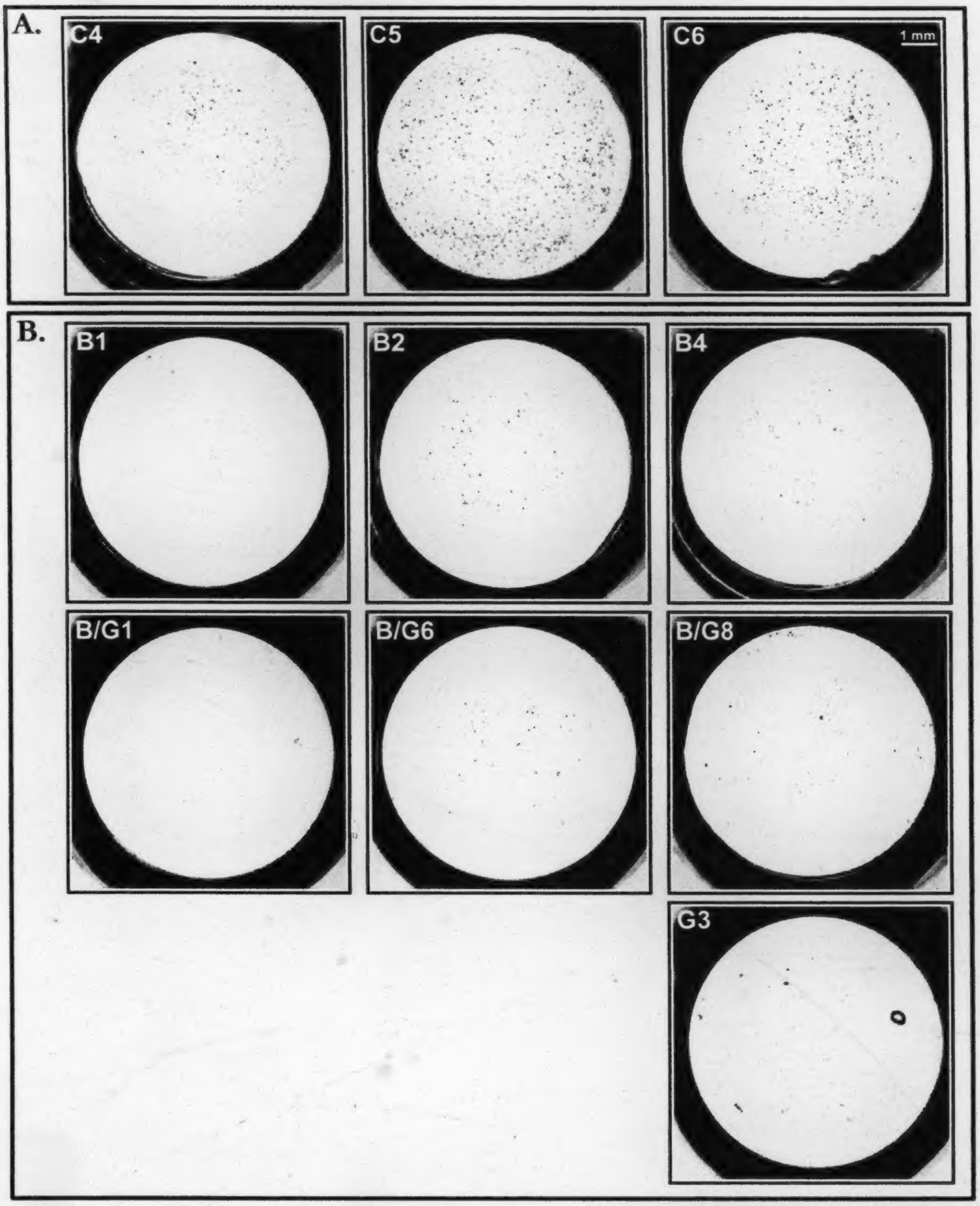

Figure 4.22 - Invasion of the T98 transfectants through Matrigel™ after 30 hours (Trial 2). 25000 cells were plated in the upper wells of individual transwell inserts containing an 8 μm pore size filter. Cells were allowed to invade for 30 h, at which time cells on the upper side of the filter were removed with a cotton swab and cells on the bottom side were fixed and stained with 1% crystal violet. Inserts for the T98-pREP4-4 (C4), -5 (C5) and -6 (C6), T98-B-FABP-1 (B1), -2 (B2) and -4 (B4), T98-B/G-1 (B/G1), -6 (B/G6) and -8 (B/G8), and T98-GFAP-3 (G3) transfectants were photographed using a dissecting microscope. The B-FABP and/or GFAP transfectants (panel B) showed reduced invasiveness compared to the T98-pREP4 control transfectants (panel A).

through the 8 μm pores is slower than that of the B-FABP and/or GFAP transfectants. Thus, the 30 hour invasion period allows a greater number of control cells to pass through the pores compared to the 22 hour invasion period.

The percentage of invasive cells for each of the T98 transfected clones is shown in Figure 4.23. Percent values are relative to T98-pREP4-6 (set at 100%), which had the lowest level of invasion of the three controls tested. The lower value obtained for trial 1 and 2 is plotted, and the higher value is indicated by the error bar. Compared to T98-pREP4-6, T98-pREP4-4 and T98-pREP4-5 had relative percentage values ranging from 353-700%, while invasion for the T98-B-FABP-1, -2 and -4 clones was reduced to ~8%, 29% and 31%, respectively. Thus, as observed in the 22 hour trial, B-FABP levels inversely correlated with the reduced invasive behaviour of the T98 cells. In addition, as described before, the invasiveness of T98-GFAP-3 and the T98-B/G-1, -6 and -8 clones were significantly reduced compared to the control transfectants. These results strongly support a role for both B-FABP and GFAP in reducing the *in vitro* invasive behaviour of T98 MG cells.

U87 transfectants (30 hour time point):

The ability of B-FABP to reduce invasiveness was also investigated using the U87 MG cell line and a 30 hour invasion period. Three of our U87 control transfectants (U87-pREP4-3, -6 and -7) and four of our U87-B-FABP transfectants (U87-B-FABP-1, -2, -3 and -7) were analyzed. U87-B-FABP-5 was not included because B-FABP expression in this clone had previously been shown to have no effect on morphology, proliferation, and anchorage-independent growth. Experiments were performed in triplicate, a photograph of each insert was taken after 30 hours (Figures 4.24-4.26), and the number of cells that had passed through each matrigel insert was counted [Table 4.3; Trial 1-3 (30 hour) column].

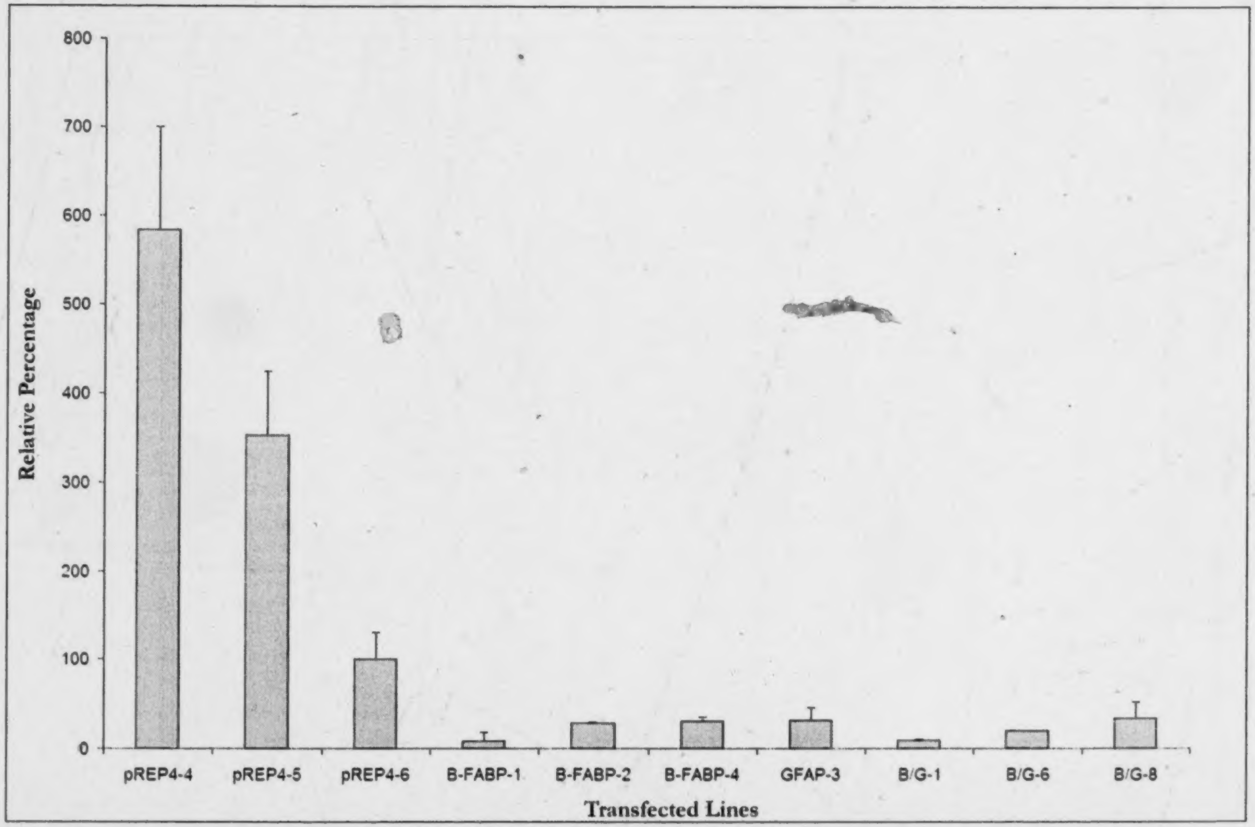

Figure 4.23 - Percentage of invasive cells for the T98 transfectants relative to the T98-pREP4-6 clone after 30 hours. The number of cells that passed through the matrigel inserts for each T98 transfectant (pREP4-4, -5 and -6, B-FABP-1, -2 and -4, GFAP-3, and B/G-1, -6 and -8) [Table 4.3; Trial 1 & 2 (30 hour) column] was compared with that of T98-pREP4-6 and the relative percentage of invasive cells was calculated. The lower value obtained from the duplicate inserts for each clone is plotted, and the higher value is indicated by the error bar.

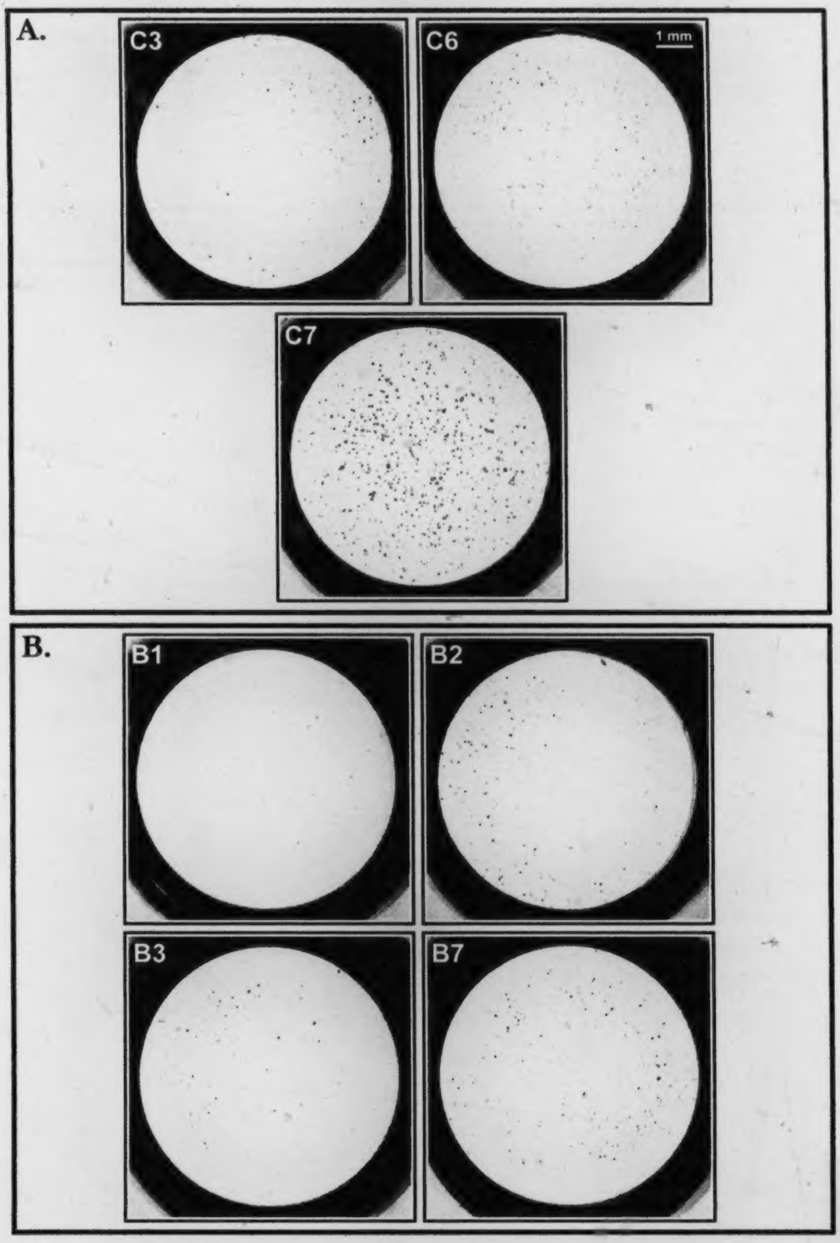

Figure 4.24 - Invasion of the U87 transfectants through Matrigel™ after 30 hours (Trial 1). 25000 cells were plated in the upper wells of individual transwell inserts containing an 8 μm pore size filter. Cells were allowed to invade for 30 h, at which time cells on the upper side of the filter were removed with a cotton swab and cells on the bottom side were fixed and stained with 1% crystal violet. Inserts for the U87-pREP4-3 (C3), -6 (C6) and -7 (C7), and U87-B-FABP-1 (B1), -2 (B2) and -3 (B3) and -7 (B7) transfectants were photographed using a dissecting microscope. The B-FABP transfectants (panel B) had a reduced invasiveness compared to the T98-pREP4 control transfectants (panel A).

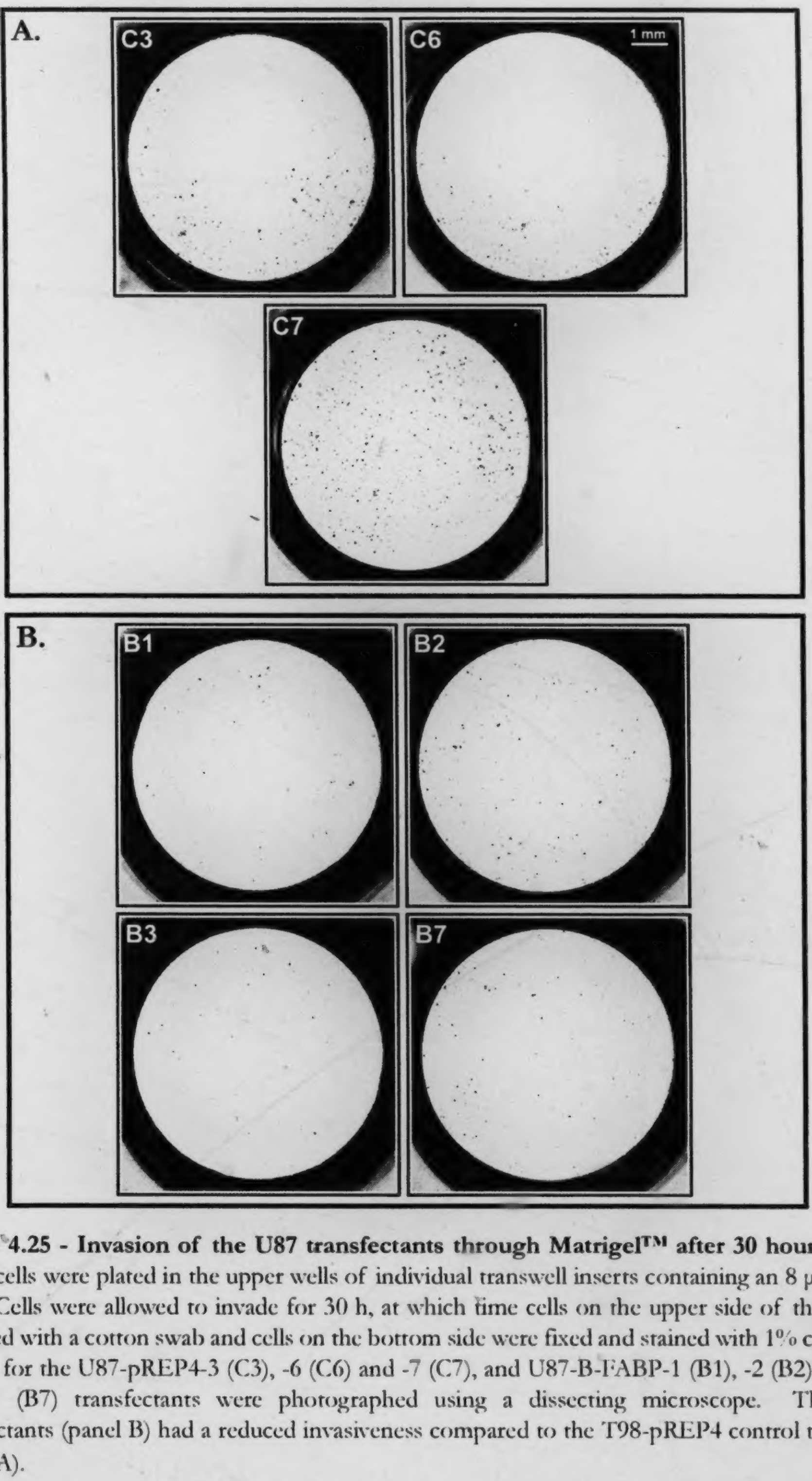

Figure 4.25 - Invasion of the U87 transfectants through Matrigel™ after 30 hours (Trial 2). 25000 cells were plated in the upper wells of individual transwell inserts containing an 8 μm pore size filter. Cells were allowed to invade for 30 h, at which time cells on the upper side of the filter were removed with a cotton swab and cells on the bottom side were fixed and stained with 1% crystal violet. Inserts for the U87-pREP4-3 (C3), -6 (C6) and -7 (C7), and U87-B-FABP-1 (B1), -2 (B2) and -3 (B3) and -7 (B7) transfectants were photographed using a dissecting microscope. The B-FABP transfectants (panel B) had a reduced invasiveness compared to the T98-pREP4 control transfectants (panel A).

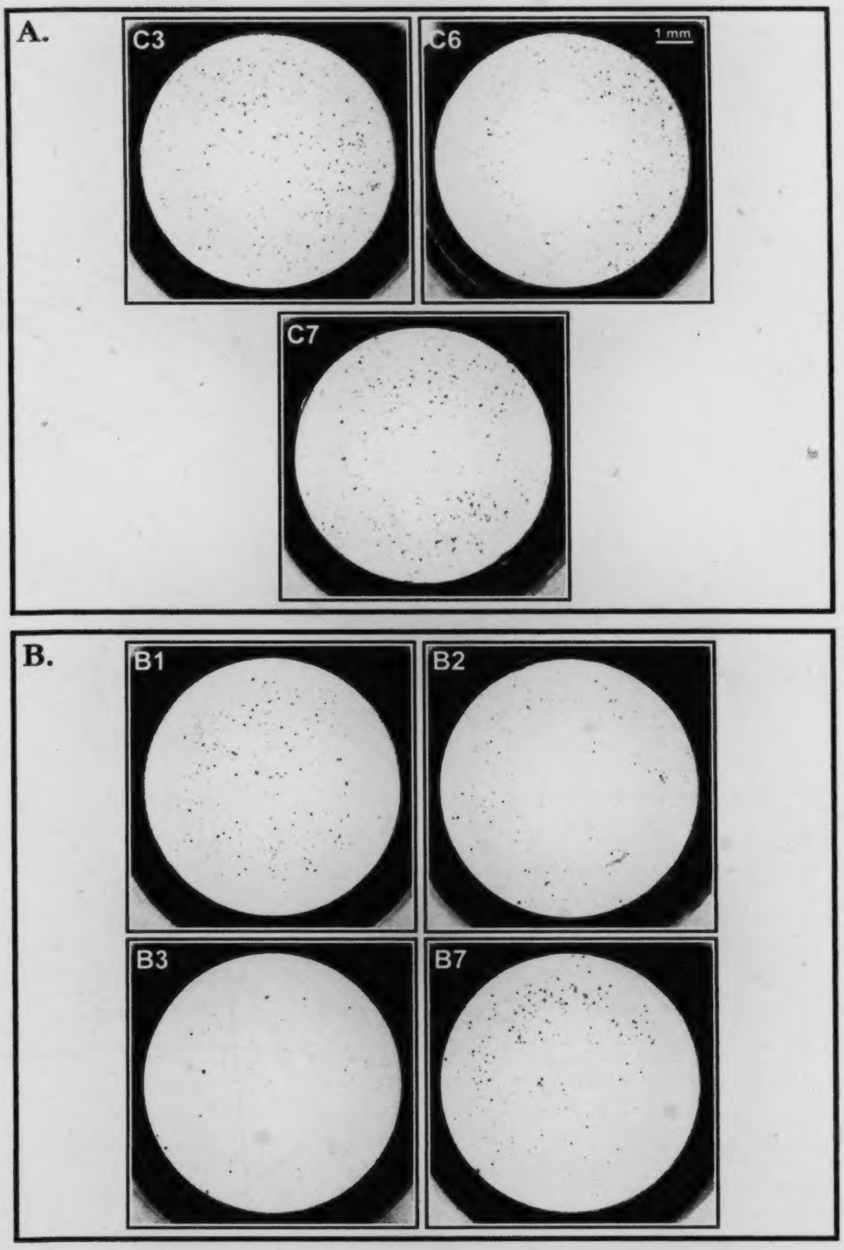

Figure 4.26 - Invasion of the U87 transfectants through Matrigel™ after 30 hours (Trial 3). 25000 cells were plated in the upper wells of individual transwell inserts containing an 8 μm pore size filter. Cells were allowed to invade for 30 h, at which time cells on the upper side of the filter were removed with a cotton swab and cells on the bottom side were fixed and stained with 1% crystal violet. Inserts for the U87-pREP4-3 (C3), -6 (C6) and -7 (C7), and U87-B-FABP-1 (B1), -2 (B2) and -3 (B3) and -7 (B7) transfectants were photographed using a dissecting microscope. The B-FABP transfectants (panel B) had a reduced invasiveness compared to the T98-pREP4 control transfectants (panel A).

Each of the U87-B-FABP transfectants showed a dramatic decrease in matrigel invasion when compared to the U87-pREP4 controls.

The percentage of invasive cells for each of the U87 transfected clones is shown in Figure 4.27. Percent values are relative to U87-pREP4-3 (set at 100%), which had the lowest level of invasion of the three controls tested. The lowest value obtained for the three trials is plotted, and the highest value is indicated by the error bar. Compared to U87-pREP4-3, the relative percentage of invasive cells in the U87-pREP4-6 and U87-pREP4-7 controls ranged from 116-179%. The relative percentage of invasive cells for U87-B-FABP-1, -2, -3 and -7 ranged from 7-30%, 27-52%, 10-16% and 22-34%, respectively. Thus, each of the B-FABP transfectants showed a dramatic inhibition of invasion compared to the controls, with U87-B-FABP-1 and U87-B-FABP3 showing the greatest reduction. Of note, while invasiveness in the T98 transfectants was inversely correlated with B-FABP levels, no such correlation was observed for the U87-B-FABP clones. This may be due to the fact that each U87-B-FABP clone expressed such high levels of B-FABP that the threshold level for reduced invasiveness was reached even in the lowest B-FABP expresser. Thus, the effect of B-FABP on invasive behaviour may be related to subcellular localization and functional activity rather than absolute expression level. Regardless, each of the U87-B-FABP transfectants did exhibit a reduction in invasiveness compared to the control transfectants.

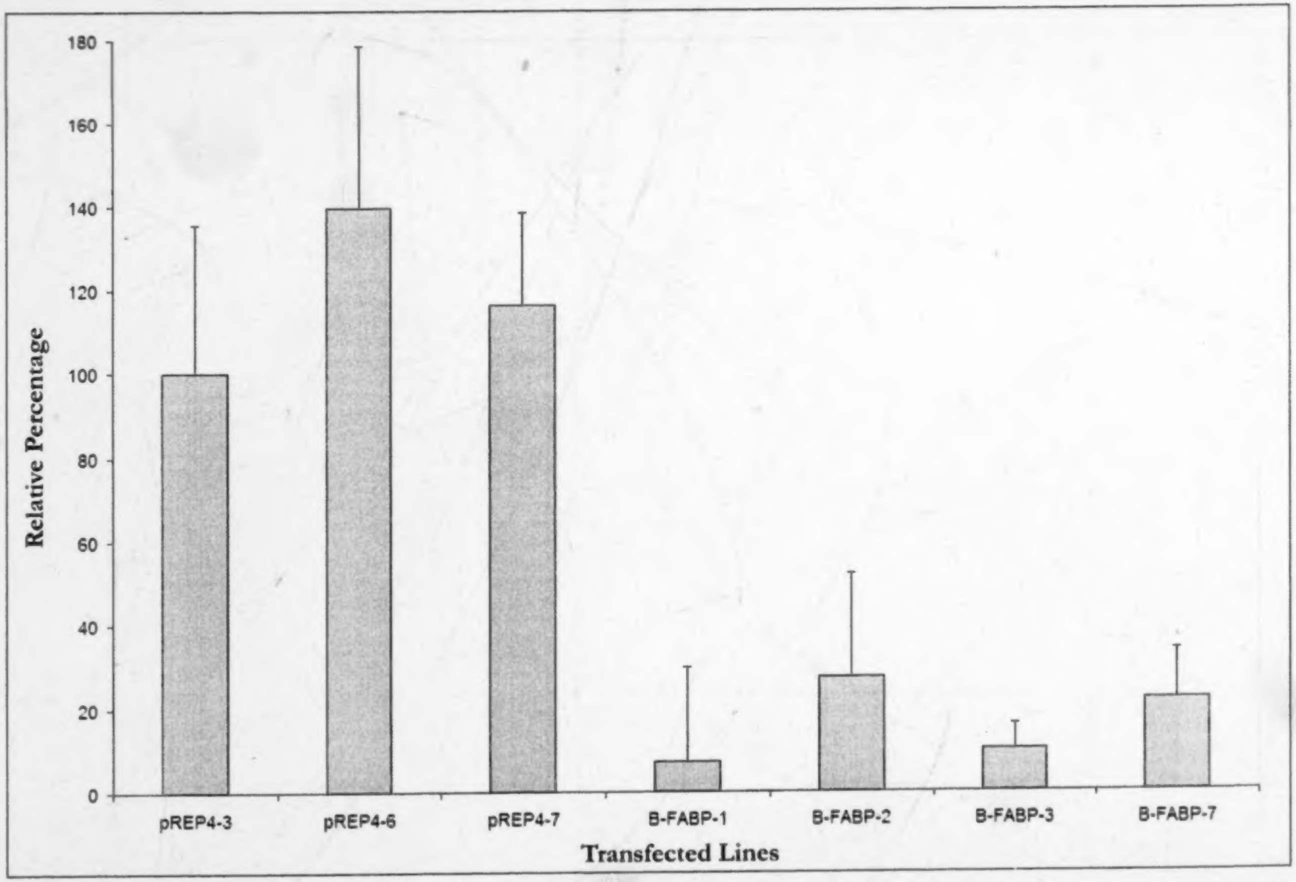

Figure 4.27 - Percentage of invasive cells for the U87 transfectants relative to the U87-pREP4-3 clone. The number of cells that passed through the matrigel inserts for the U87-pREP4-3, -6 and -7 transfectants and U87-B-FABP-1, -2, -3 and -7 transfectants [Table 4. 3; Trial 1-3 (30 hour) column] were compared with that of U87-pREP4-3 and the relative percentage of invasive cells was calculated. The lowest value obtained from the triplicate inserts for each clone is plotted, and the highest value is indicated by the error bar.

CHAPTER FIVE

Discussion

5.1. Regulation of B-FABP and GFAP expression

In the mammalian CNS, B-FABP and GFAP are both expressed in the glial cell lineage, but at different developmental stages. B-FABP is typically expressed in radial glial cells, the precursor cells of mature astrocytes, while GFAP is specifically expressed in mature astrocytes. The expression of both of these proteins in the same cell has been observed in only a few cell types *in vivo* including: Bergmann glia, radial glia of the hippocampal dentate gyrus and gomori-postive astrocytes (Kurtz *et al.*, 1994; Young *et al.*, 1996). In addition, our lab has demonstrated that B-FABP and GFAP are co-expressed in MG cell lines (Godbout *et al.*, 1998). As discussed in section 1.3.6, the co-expression of these proteins in MG cell lines suggests the following possibilities: i) MG tumours may arise from cells that express both of these proteins, ii) MG tumours may arise from cells that are in transition between radial glial cells and astrocytes, and/or iii) the expression of B-FABP and GFAP is mediated by similar *cis*- and *trans*-acting elements. In support of a similar mechanism of *B-FABP* and *GFAP* gene regulation, the NFI family of transcription factors has been implicated in the regulation of glial cell-specific genes. NFI-B has been proposed to regulate *MBP* expression in oligodendrocytes (Inoue *et al.* 1990) and NFI-A has been associated with the reduced expression of GFAP in *NFI-A*-null mice (das Neves *et al.*, 1999). In addition, NFI-binding sites have been identified in many glial cell-specific genes, including B-FABP and GFAP.

5.1.1. NFI-binding Sites in the GFAP promoter

As described in section 1.2.2, Besnard *et al.* (1991) have identified three putative NFI-binding sites in the *GFAP* promoter located at -120/-106 bp, -1585/-1571 bp and

-1633/-1619 bp in relation to the transcription start site. In Chapter 3, we demonstrate by gel shift assays that these three putative NFI-binding sites (G-br1, G-br2 and G-br3) are bound by NFI (Figures 3.2 and 3.3). Thus, each NFI-binding site in the *GFAP* promoter is capable of binding one or more of the NFI family members (NFI-A, -B, -C and -X). We propose that the NFI-binding site within G-br3 has the lowest overall affinity for NFI proteins since significant binding was only observed with NFI-X and to a lower extent NFI-A, while the NFI-binding site within G-br2 has the highest overall affinity for NFI proteins. This is supported by the gel shift assays shown in Figure 3.3 where all four NFIs were able to bind G-br2 at high levels, but only NFI-X was able to bind G-br3 at high levels. Additional support for the G-br3 NFI-binding site having less overall affinity for NFI comes from the fact that the N_5 spacer in the G-br3 NFI-binding site consists exclusively of G-C base pairs. Gronostajski and colleagues (1985) have shown that the exclusive presence of G-C base pairs within the internal spacer disrupts NFI binding.

Another possible explanation for the reduced levels of NFI binding observed for G-br3 is that Sp1 and/or AP-2 binding competes with NFI binding. In the *GFAP* promoter an Sp1-binding site overlaps the NFI-binding site located at -1633/-1619 bp (Besnard *et al.*, 1991), and the N_5 spacer region of this NFI-binding site is similar to the G-C rich AP-2 consensus binding sites. Evidence of Sp1 and AP-2 binding to G-br3 was observed in these studies (Figure 3.2) and we predict that this would likely prevent NFI proteins from accessing the NFI-binding site. A similar mechanism of regulated DNA binding has been suggested for the murine collagen α1(I) gene whereby Sp1-binding interferes with NFI-binding and inhibits transactivation (Nehls *et al.*, 1991). Further studies on the collagen α1(I) gene have revealed that an increase in AP-2 binding to a site adjacent to the NFI-binding site leads to the suppression of NFI-dependent gene activation (Chen *et al.*, 1996).

The high level of NFI binding to the NFI-binding site located at -1585/-1571 bp may also be associated with the presence of adjacent transcription factor binding sites, such as AP-1 (Besnard *et al.*, 1991). Masood *et al.* (1993) have proposed that the AP-1 site located at -1592/-1586 bp is the most potent activator of *GFAP* transcription. However, because AP-1 is a relatively ubiquitous transcription factor and cell types that do not express GFAP have active AP-1 factors, these authors suggest that cooperative interactions of multiple transcription factors are likely necessary for the cell-specific transcriptional activation of *GFAP* (Masood *et al.*, 1993). Thus, we can speculate that through cooperative interactions between AP-1 and NFI proteins, NFI binding is enhanced at the NFI-binding site within G-br2. Additional studies will need to be performed to confirm this hypothesis, especially since the AP-1 site in our G-br2 oligonucleotide is not complete and may not even permit AP-1 binding; however, it is interesting that neighboring NFI and AP-1 sites have been observed in several genes expressed in the CNS (Amemiya *et al.*, 1992).

From our data and studies performed by other researchers, we expect NFI binding in the *GFAP* promoter to be a dynamic event mediated by several other transcription factors including AP-1, AP-2 and Sp1. Importantly though, we have shown that at least one or more of the NFI proteins can bind to each of the NFI-binding sites in the *GFAP* promoter.

5.1.2. Role of NFI proteins in regulating B-FABP and GFAP expression

The transcriptional activation and repression of many ubiquitous and tissue-specific genes is mediated, at least in part, by a complex network of specialized transcription factors. However, the ability of these transcription factors to relay signals to specific gene targets relies on several features such as their differential expression, DNA binding ability, and transactivation or repression capacity. The identification of bona fide NFI-binding sites in the *B-FABP* promoter (Bisgrove *et al.*, 2000) and *GFAP* promoter (discussed earlier), the co-expression of B-FABP and GFAP in MG cell lines (Godbout *et al.*, 1998), and the observation that specific NFI proteins (NFI-A, -B, -C and -X) have different DNA binding and transactivation capacities (Kannius-Janson *et al.*, 2002) suggests that different NFI proteins may serve to mediate B-FABP and GFAP expression in a differentiation-dependent manner in the glial cell lineage. Differentiation-related changes in NFI proteins have already been described for preadipocyte differentiation (Singh *et al.*, 1998) as well as the differentiation of hematopoietic cell lines (Kulkarni *et al.*, 1996) and the mouse mammary gland (Kannius-Janson *et al.*, 2002).

By northern blot analysis we found no definitive correlation between *B-FABP* or *GFAP* expression with any of the *NFI* transcripts when we examined five B-FABP/GFAP-positive and five B-FABP/GFAP-negative MG cell lines (Figure 3.1). However, there was a general trend towards higher levels of *NFI-A* and *NFI-X* in the B-FABP/GFAP-positive lines compared to the B-FABP/GFAP-negative lines. Because even slight variations in the presence of a transcription factor can produce a dramatic alteration in the expression profile of a cell, the slightly higher level of NFI-A and NFI-X in these MG cell lines may be significant. However, it is also possible that factors other than the differential expression of NFI proteins govern the ability of specific NFIs to regulate B-FABP and/or GFAP expression. These factors may include: i) the presence or absence of co-activator or co-repressor proteins, ii) the binding affinity of each NFI protein for their binding sites in the *B-FABP* and *GFAP* promoters, iii) the transactivation capacity of each NFI, and/or iv) the post-translational modification of NFI.

Interestingly, while it was previously believed that all four NFI proteins had identical DNA binding affinities (Goyal *et al.*, 1990; Kruse and Sippel, 1994), more recent studies have demonstrated that the DNA binding affinity of each NFI protein can differ (Osada *et al.*, 1999). Our results clearly support the latter as we have shown that NFI-A and NFI-X bind to the G-br1, G-br2 and G-br3 oligonucleotides at higher levels than NFI-B and NFI-C (Figure 3.3). In addition, NFI-C and NFI-X bind to the B-br1 and B-br3 oligonucleotides at higher levels than NFI-A and NFI-B (Figure 3.4). That there is a difference in DNA binding affinity is somewhat surprising since the DNA binding domain of NFI proteins is highly conserved (~91% similar). However, Roulet and coworkers (1995) have used different alternatively spliced forms of NFI-X to demonstrate the ability of a novel repressor domain in the C-terminal region of NFI proteins to inhibit DNA binding *in vitro*. This inhibition was not observed *in vivo* leading these authors to propose that the repressor domain may interact with a regulatory factor that prevents DNA binding inhibition. Nevertheless, these studies suggest that it is possible for the highly variable C-terminal domain of NFI proteins to contribute to their DNA binding affinity.

In correlation with our DNA binding studies that demonstrate high levels of NFI-A and NFI-X binding to the most proximal NFI-binding site (G-br1) in the *GFAP* promoter, the CAT reporter assay experiments reveal that NFI-A and NFI-X are also the most potent activators of transcription using the pCAT/GFAP-176 construct which contains only the most proximal NFI-binding site (Figure 3.7). Furthermore, the large increase in transcriptional activation demonstrated by each of the NFI proteins with the pCAT/GFAP-1716 construct corresponds with our observation that all NFIs are able to bind at high levels to the NFI-binding site within G-br2. These results imply that the NFI proteins act as transcriptional activators for the *GFAP* gene. Also, the data indicate that transactivation of the *GFAP* gene may be regulated by the DNA binding affinity of each NFI rather than their intrinsic transactivation potential (ITP). This is an interesting observation since it has been predicted that the ITP of each NFI will be different due to the low sequence similarity of the

C-terminal domain (reviewed in Gronostajski, 2000). As well, alternative splicing has been postulated to influence the ITP of each NFI. As mentioned earlier, it is possible that the C-terminal domain plays a role in mediating the DNA binding capacity of NFIs. Thus, one could envision that through the association of the C-terminal domain with co-activators or co-repressors, different NFI family members may acquire different DNA binding capabilities. While this concept is beyond the scope of the work presented in this thesis, it would be an interesting avenue to investigate.

While the DNA binding potential of the NFIs appears to play a major role in their ability to activate transcription from the *GFAP* promoter, we cannot completely exclude the possibility that the NFIs have differences in their ITP. Firstly, the ability of the NFIs to bind the G-br oligonucleotides may differ from their ability to bind the larger promoter fragments in the CAT constructs. The larger fragments may provide an environment that is more in context with the *in vivo* situation. Secondly, we did observe differences in NFI DNA binding capacity and *GFAP* transactivation. For example, NFI-B bound to the G-br1 and G-br2 oligonucleotides at lower levels than NFI-C; however, CAT reporter activity observed for NFI-B was higher than that of NFI-C. These results indicate that the ITP of NFI-B is greater than that of NFI-C. This is interesting because as the most extensively characterized NFI protein, NFI-C has been implicated in the transactivation of many genes (Kane *et al.*, 2002; Kannius-Janson, 2002; Prado *et al.*, 2002; Elateri *et al.*, 2003). However, to our knowledge NFI-C has not been implicated in the transactivation of glial cell-specific genes, while NFI-B enhances the activation of the MBP (Inoue *et al.*, 1990), an oligodendrocyte differentiation marker.

Similar to *GFAP*, we propose that both the DNA binding capacity and the ITP of each NFI protein contributes to the transactivation of *B-FABP*. DNA binding studies using the B-br oligonucleotides revealed that NFI-C and NFI-X are able to bind to the NFI-binding sites in the *B-FABP* promoter at the highest levels, with NFI-X binding at higher levels than NFI-C (Figure 3.4). However, NFI-C did not stimulate CAT activity when co-transfected with either pCAT/B-FABP-140 or -440 (Figure 3.7). These results suggest that while NFI-C readily binds to NFI sites in the *B-FABP* promoter, its ITP on *B-FABP* is negligible. In contrast, NFI-A and NFI-X displayed a strong ITP when co-transfected with pCAT/B-FABP-140 or -440 even though NFI-A was only able to bind to B-br1 in gel shift assays. These results suggest that NFI-A and NFI-X are the most potent NFIs involved in mediating *B-FABP* transcription.

The transactivation capacity of each NFI protein on *B-FABP* appears to be mediated predominantly through the most proximal NFI-binding site. As mentioned in section 3.4, the fold increase in CAT activity observed with the pCAT/B-FABP-160 and -440 constructs was nearly identical for each NFI, except for NFI-X where CAT activity decreased by approximately two-fold with the larger construct. On the basis of these observations we can speculate that the most distal NFI-binding site is not essential for NFI-mediated activation of *B-FABP* transcription. Rather, this NFI site may act as a repression element or a sink for NFI-X. In support of this theory, mutation of the NFI-binding sites in the *B-FABP* promoter have shown that the most proximal NFI-binding site is essential for *B-FABP* promoter activity, while the most distal NFI site is not (Bisgrove *et al.*, 2000).

It is plausible that the most distal NFI-binding site in the *GFAP* promoter (G-br3) also acts as a repression element or as a sink for NFI-X. Besnard *et al.* (1991) have shown that this NFI-binding site is not critical for *GFAP* promoter activity. In addition, we have shown that the only NFI that is able to bind to this site is NFI-X. However, due to the inability to distinguish between G-br2 and G-br3 in our CAT experiments, our hypothesis on the functional aspects of this NFI-binding site remains purely speculative.

Overall, these studies have revealed that for both the *B-FABP* and *GFAP* promoters, NFI-A and NFI-X are potent activators of transcription. In addition, NFI-B has a very strong ITP on the *GFAP* promoter, but not on the *B-FABP* promoter. While all the NFI consensus sites in the *GFAP* promoter are able to bind NFI proteins, it is most likely the sites located at -120/-106 bp (G-br1) and -1585/-1571 bp (G-br2) that are the most important. In contrast, only the NFI-binding site located at-62/-33 bp (B-br1) in the *B-FABP* promoter appears to be involved in the NFI-mediated activation of the *B-FABP* promoter. Although further studies are needed to determine the mechanisms by which NFI proteins modulate the transcriptional activation of the *B-FABP* and *GFAP* promoters, we believe that additional complexity will be imposed by the post-translational modification of NFI proteins.

5.1.3. Importance of NFI Phosphorylation Status

Several independent reports have demonstrated that the activity of NFI is mediated by phosphorylation (Jackson *et al.*, 1990; Yang *et al.*, 1993; Cooke and Lane, 1999; Bisgrove *et al.*, 2000). These reports have all revealed a similar trend in that an increase in NFI phosphorylation results in a decrease in transactivation capacity. Interestingly, no significant difference in DNA binding affinity has ever been observed between the dephosphorylated and phosphorylated forms of NFI. Thus, phosphorylation appears to mediate its effect on NFI-dependent promoters by alterations in the ITP of NFI proteins. Previous studies from our lab have revealed that the NFI proteins that activate *B-FABP* expression in the U251 B-FABP/GFAP-positive MG cell line are hypophosphorylated compared the NFI proteins in the T98 B-FABP/GFAP-negative MG cell line (Bisgrove *et al.*, 2000).

Gel shift experiments described in Chapter 3 reveal a similar trend in the phosphorylation status of the NFI proteins that bound to the NFI-binding sites in the *GFAP* promoter (Figure 3.2). NFI proteins in the U251 cells were hypophosphorylated compared to those in the T98 cells. In combination with our previous findings (Bisgrove *et al.*, 2000), our results suggest that the transcriptional activation of both *B-FABP* and *GFAP* is mediated by hypophosphorylated forms of NFI proteins. To date, the molecular mechanisms underlying NFI phosphorylation have not been elucidated. However, it is interesting that the cdc2 kinase, which has been found to phosphorylate NFI proteins *in vitro* (Kawamura *et al.* 1993), has also been implicated in the phosphorylation of GFAP (Tsujimura *et al.*, 1994). Thus, one might speculate that when GFAP is abundant, cdc2 is engaged in the phosphorylation of GFAP and the accessibility of cdc2 to NFI proteins is reduced. In this scenario, hypophosphorylated forms of NFI would be more available to NFI-dependent promoters and genes such as *B-FABP* and *GFAP* would be expressed.

With NFI phosphorylation status in mind, we selected the T98 cell line for the CAT experiments presented in this report because we wanted to study the ability of the exogenous NFI proteins to activate *B-FABP* and *GFAP* promoter activity in a MG cell line devoid of functional endogenous NFI proteins. Initially, we were concerned that our exogenous NFIs would also be rendered inactive by phosphorylation; however, if these NFI proteins are phosphorylated, this post-translational modification appears to have been significantly delayed so as to allow transcriptional activation upon transfection of NFI expression plasmids. Alternatively, it is possible that the exogenous NFI proteins were insufficiently phosphorylated and not rendered completely inactive. Previous studies from our lab suggest that there is a gradation in NFI phosphorylation whereby a nonphosphorylated NFI protein must be phosphorylated at several sites to acquire the hyperphosphorylated status found in T98 cells (Bisgrove *et al.*, 2000).

Of note, preliminary CAT studies were performed in the U251 cell line using the same conditions described for the CAT experiments presented in this thesis. However, these studies yielded insignificant alterations in CAT activity upon transfection of the NFI expression plasmids (data not shown). The explanation for this observation is likely twofold: i) the endogenous NFI proteins in the U251 cells generate a high level of background CAT activity, and ii) the small quantity of NFI expression plasmid used in these experiments produced a pool of NFI proteins that represented only a small minority of the active NFI proteins present in these cells. Therefore, to observe a significant alteration in CAT activity in these cells, it is likely that large quantities of NFI expression plasmid would need to be used. However, by titrating the amount of pCHNFI construct used to transfect the T98 cells, we found that levels of NFI expression plasmid higher than 1 μg produced a non-specific inhibitory effect on CAT activity (data not shown). While titration experiments have not yet been performed on U251 cells, we predict that this inhibitory effect will also be observed in these cells.

It is not surprising that the transfection of a large quantity of an NFI expression plasmid can have a dramatic effect on the cell given the variety of genes that are responsive to NFI. Adjustment in the phosphorylation status of NFI proteins likely represents a mechanism by which a cell can mediate the activity of NFI proteins to exert global effects on gene expression. In regards to the progression of MG, the phosphorylation of NFI proteins may result in the decreased activation of glial cell-specific genes such as *B-FABP* and *GFAP* which, in turn, may lead to decreased cellular differentiation.

5.1.4. B-FABP and GFAP Regulation in Glial Cells and Malignant Glioma

Even though *B-FABP* and *GFAP* expression appears to be mediated by similar NFI family members (*i.e.* NFI-A and NFI-X), in light of their expression in different glial cell types it is difficult to conceive that these genes are regulated solely by NFI transcription factors. Rather, the localized expression of NFI-A and NFI-X in glial cells of the human CNS (Krebs *et al.*, 1996; Sumner *et al.*, 1996) may contribute to the activation of numerous glial cell-specific genes, with other factors specific to each population of glial cells being necessary for the activation of specific genes by NFIs. For example, as described in section 1.2.2, the *GFAP* promoter may only become responsive to specific NFI proteins when cAMP levels are elevated (Kaneko *et al.*, 1994; Takanaga *et al.*, 2004), such as has been described during astrocyte differentiation (Vallejo and Vallejo, 2002). It has been hypothesized that when cAMP levels are low, a repressor binds to the CRE in the -240/-170 bp region of the *GFAP* promoter (Kaneko *et al.*, 1994). Then, as cAMP levels increase a cAMP-modulating factor (non cell-type specific) inactivates the repressor and a positive regulatory factor (glial cell-type specific) binds to the CRE in the -170/-110 bp region of the *GFAP* promoter. In addition, Kaneko and coworkers (1993) suggest that GFAP expression is tightly regulated in glial cells by the presence of both a neural-specific expression element and a glial-specific expression element.

Cell-specific expression elements have also been identified in the *B-FABP* promoter that may confine *B-FABP* expression to the radial glial cell population in the glial cell lineage. Feng *et al.* (1995) have identified a single radial glial enhancer (RGE) element that is localized to the -800/-300 bp region of the *B-FABP* promoter. This region was further characterized by Josehpson and colleagues (1998) who demonstrated that a POU protein binding site and an HRE element may be functionally significant in mediating *B-FABP* expression. The role of these sites has not been further characterized but one could envision a coordinate requirement for specific NFI and POU proteins in order to activate *B-FABP* expression in radial glial cells. Although we did not previously report a DNA-protein interaction at the POU site in the human *B-FABP* promoter using T98 or U251 nuclear extracts (Bisgrove *et al.*, 2000), upon closer examination of the DNase I footprint data a protein interaction at the POU-binding region was evident. Thus, it is possible that the POU site is essential for *B-FABP* expression in MG.

In regards to the coordinate expression of *B-FABP* and *GFAP* in MG, one would expect that the factors necessary to permit *B-FABP* or *GFAP* expression in separate cell populations of the glial cell lineage are present within a single cell in MG. Our northern blot data (Figure 3.1) indicate that all four *NFI* genes were typically expressed in the MG cell lines, and that *NFI-A* and *NFI-X* are present at somewhat higher levels in the B-FABP/GFAP-positive cell lines compared to the B-FABP/GFAP-negative cell lines. Thus, the two NFI proteins that have been implicated in the activation of *B-FABP* and *GFAP* in this study are also expressed at higher levels in B-FABP/GFAP-expressing cells lines. However, since the B-FABP/GFAP-negative lines also express these NFIs, alternate mechanisms must be present within these cells to inhibit *B-FABP* and *GFAP* expression. We contend that the coordinate loss of B-FABP and GFAP in MG cell lines is primarily due to the phosphorylation of NFI; however, we do not exclude the possibility that other factors may also be involved. For instance, the complexity of the role of NFI proteins *in vivo* is likely enhanced by the modulated affinity of NFI proteins for certain promoter contexts (*i.e.* chromatin structure) (Alevizopoulos *et al.* 1995) and/or the presence of NFI heterodimers (Kruse and Sippel, 1994).

5.2. Role of B-FABP and GFAP in Malignant Glioma

The co-expression of B-FABP and GFAP in MG and their coordinate regulation by specific NFI family members implies that the cell of origin of MG may normally express both proteins or may be altered as the result of tumor formation. Interestingly, both B-FABP and GFAP function as differentiation markers for specific cell types in the glial cell lineage. B-FABP is involved in the establishment and maintenance of radial glial cell differentiation in the developing brain (Feng *et al.*, 1994), while GFAP is expressed in mature astrocytes. It is therefore likely that B-FABP and GFAP expression in MG is indicative of a more differentiated state. In support of this idea, several researchers have shown that there is an inverse correlation between GFAP expression and the degree of MG anaplasia, with the more malignant tumours expressing lower levels of GFAP (Eng and Rubinstein, 1978; van der Meulen *et al.*, 1978; Velasco *et al.*, 1980). Furthermore, Rutka and colleagues (1994) have shown that the reduction of GFAP in GFAP-positive MG cell lines by overexpressing antisense *GFAP* cDNA generates cells that have an increased growth and invasive potential.

These results indicate that the loss of GFAP may serve as an important event in MG progression. Moreover, since B-FABP and GFAP are co-expressed in MG cell lines (Godbout *et al.*, 1998), the loss of B-FABP expression may also represent an important event in the progression of malignant glioma. Members of the FABP family have been implicated in modulating cell growth and differentiation, and their role in these events suggests that they could also be used as tumor markers (reviewed in Zimmerman and Veerkamp, 2002).

5.2.1. B-FABP Reduces the Growth and Invasive Potential of Malignant Glioma Cells

As described in Chapter 4, we stably transfected the T98 and U87 B-FABP/GFAP-negative MG cell lines with B-FABP expression constructs. In contrast to the controls, which typically formed large and numerous colonies in soft agar, the B-FABP transfectants for both the U87 and T98 cell lines demonstrated a marked reduction in colony size and number (Figures 4.15 and 4.16). Of particular note, the level of B-FABP detected by western blot analysis tended to correlate inversely with colony formation. The reduction in colony size for the U87-B-FABP transfectants can be explained, at least in part, by their dramatically reduced proliferation rate (Figure 4.13). However, the proliferation rate of the T98-B-FABP transfectants was similar to that of the controls (Figure 4.12), so the reduction in colony size observed for T98 is most likely due to a loss in anchorage-independent growth capacity. Overall, the decreased ability of the U87 and T87 B-FABP transfectants to grow in soft agar suggests that the restoration of B-FABP expression to B-FABP/GFAP-negative MG cells reduces their tumourigenicity.

The ability of B-FABP to decrease the proliferation rate of U87 cells, but not T98 cells, is intriguing. Several researchers have suggested that the function of specific FABPs is cell-type specific (reviewed in Zimmerman and Veerkamp, 2002). For example, L-FABP expression in hepatoma cells leads to a higher proliferation rate (Keler *et al.*, 1992), while in embryonic stem cells L-FABP inhibits proliferation (Schroeder *et al.*, 2001). Since many genetic alterations have been associated with MG progression and different MG tumours arise via different genetic alterations, it is likely that the ability of B-FABP to mediate proliferation in the U87 and T98 MG cell lines may differ based on their molecular genetics. Importantly though, we never observed an increase in proliferation due to B-FABP expression, so B-FABP remains, in regards to its affect on proliferation, a good candidate for MG therapy.

Our experiments where B-FABP levels were reduced in the U251 B-FABP/GFAP-positive cell line support our suggestion that B-FABP may be a good candidate for MG therapy. In the U251 cell line, a ~90% reduction in B-FABP levels did not result in a significant change in colony formation or proliferation rate (Figures 4.14 and 4.17). These results suggest that even very low levels of B-FABP in U251 are sufficient in maintaining the phenotypic characteristics of these cells. Moreover, colony formation in soft agar revealed the importance of B-FABP as reduced B-FABP levels allowed the formation of small cell clusters. Apparently the lower levels of B-FABP permitted the cells to divide a few times, but ultimately these cells did not become anchorage-independent.

The mechanism through which B-FABP inhibits the growth potential of MG tumour cells is unclear; however, other FABPs have also demonstrated an anti-proliferative activity in cancer cells (review in Zimmerman and Veerkamp, 2002). For example, the expression of heart (H)-FABP is decreased in human breast cancer cells and the transfection of *H-FABP* cDNA into these cells results in a reduction in proliferation (Huynh *et al.*, 1995; Wang and Kurtz, 2000). These and other studies (Lehmann *et al.*, 1989; Yang *et al.*, 1994) on H-FABP have led to its classification as a tumour suppressor (reviewed in Hohoff and Spener, 1998). Further support for H-FABPs classification as a tumour suppressor comes from the finding that *H-FABP* maps to chromosomal position 1p33-p35, which is often lost in sporadic breast cancer (Phelan *et al.*, 1996).

Interestingly, several studies on gliomas have reported both genomic losses and rearrangements in the long arm of chromosome 6 (Rey *et al.*, 1987; Jenkins *et al.*, 1989; Burton *et al.*, 2002; Huang *et al.*, 2003), the region to which the *B-FABP* gene is maps (6q22-23) (Godbout *et al.* 1998). In fact, Burton and coworkers (2002) have found that 6q loss, 10q loss and 19q gain, separately or in combination, are most closely associated with the aggressive clinical behaviour of GBM. Furthermore, the recurrent and exclusive loss of chromosome 6q in primary ependymomas has led Rearden and colleagues (1999) to suggest that a tumour suppressor lies in this region. Taken together, these observations and the findings presented here suggest that, similar to H-FABP which serves as a tumour suppressor for human breast cancer, B-FABP may serve as a tumor suppressor for MG. However, to date, there is no *in vivo* evidence confirming that the *B-FABP* gene is one of the consequential genes lost within the 6q region.

To further characterize the effects of B-FABP expression in MG cell lines, we examined the invasiveness of our B-FABP transfected T98 and U87 cells using Matrigel™ invasion chambers. We found that the T98 and U87 B-FABP transfected clones demonstrated a significantly decreased invasive potential compared to controls (Figures 4.19, 4.23 and 4.27). From this work, the mechanism by which B-FABP reduces the invasive potential of MG cells is unclear. Tumour cell invasion is a complex process involving intricate cell-ECM interactions, ECM degradation, and the migration of cells through the degraded ECM. One could postulate that since FABPs have been implicated in mediating gene transcription by either directly interacting with PPARs and/or by delivering FA ligands to PPARs (reviewed in Duplus *et al.*, 2000; Tan *et al.*, 2002), FABPs may mediate the transcription of PPAR-responsive genes. Interestingly, several recent reports have demonstrated a reduction in MMP expression by PPARs (Shu *et al.*, 2000; Hetzel *et al.*, 2003; Francois *et al.*, 2004), including MMP-9, which has been implicated in glioma invasion (reviewed in Ware *et al.*, 2003). Thus, possibly by activating specific PPARs, B-FABP may reduce the expression of MMPs in MG tumour cells, in turn decreasing their invasive capacity.

Due to the suggested role of FABPs in mediating transcription (reviewed in Zimmerman and Veerkamp, 2002) and because B-FABP and GFAP are co-expressed in MG, we had initially thought that B-FABP might induce GFAP expression. However, we did not detect GFAP in either our T98 or U87 B-FABP transfected clones by immunofluorescence or western blot. This result is not surprising as we have since shown that B-FABP and GFAP may be coordinately regulated by the NFI family of transcription factors (discussed in section 5.1).

5.2.2. GFAP Reduces the Growth and Invasive Potential of Malignant Glioma Cells

While this is the first report describing a role for B-FABP in reducing the growth and invasive potential of MG cell lines, Rutka and Smith (1993) have reported the inhibitory effects of GFAP expression on growth and invasion in the SF-126 astrocytoma cell line. In addition, these researchers have discovered that the reduction of GFAP in the U251 MG cell line produces cells with enhanced growth and invasive properties (Rutka *et al.*, 1994). While the mechanism through which GFAP mediates its effects on proliferation, growth in soft agar and invasion was not determined in these studies, it was suggested that alterations in cell/cell and cell/ECM interactions were at least partly responsible. As it is well known that the plasma membrane receptors that mediate cell/cell and cell/ECM interactions have structural links to the cytoskeleton, the authors proposed that the loss of GFAP may lead to cytoskeletal collapse and a decreased expression of important cell surface molecules. In turn, the loss of these cell surface molecules would promote growth in soft agar and cell piling at confluence.

In our study, we investigated the effect of GFAP expression in the T98 B-FABP/GFAP-negative MG cell line. Complementary to the findings of Rutka and Smith (1993), the expression of GFAP in T98 cells led to a reduced growth capacity in soft agar as demonstrated by a reduction in colony size and number compared to controls (Figure 4.15). Similar to our B-FABP transfected U87 cells, much of the reduction in colony size may be due to the anti-proliferative effect of GFAP in these cells (Figure 4.12). However, combined with the reduction in colony number, these results suggest that the restoration of GFAP expression in T98 cells reduces their tumourigenicity. This conclusion is supported by the observation that both colony formation and proliferation rate inversely correlate with GFAP levels.

The mechanism whereby GFAP expression reduces the proliferation rate of T98 cells is unclear. It has been suggested that GFAP expression in MG cell lines may alter the proliferation rate of these cells by decreasing the accessibility of kinases to substrates involved in the cell cycle (Wilhelmsson *et al.*, 2003). Since IFs are phosphorylated during depolymerization (reviewed in Ku *et al.*, 1996), a greater abundance of IFs may require that a higher number of phosphorylation events take place prior to cell division. Thus, kinases such as protein kinase C and cdc2, which are involved in both cell cycle regulation and the phosphorylation of IF proteins (discussed in Wilhelmsson *et al.*, 2003) may be sequestered and unavailable for the phosphorylation of cell cycle substrates in cells that overexpress GFAP. This would explain the inverse correlation observed between GFAP levels and the proliferation rate of the T98-GFAP transfectants, and the even greater reduction in proliferation observed with our T98-B/G clones.

In this study, the expression of GFAP in T98 cells resulted in an inhibition of invasion compared to the controls (Figures 4.19 and 4.23). Interestingly, several studies have shown that IF proteins can contribute to the motility and invasion of different cancer types (reviewed in Hendrix *et al.* 1996; Rutka *et al.*, 1999; Crowe *et al.*, 1999; Singh *et al.*, 2003). Of particular note, vimentin has been associated with a dedifferentiated malignant phenotype due to its ability to increase cell motility and invasion (reviewed in Hendrix *et al.*, 1996; Rutka *et al.*, 1999). Rutka and coworkers (1999) have shown that the co-expression of vimentin and nestin in MG cell lines results in enhanced motility and invasion, while MG cell lines with high levels of GFAP are less invasive. In addition, it has been shown that a decrease in

GFAP in U251 cells leads to an increased expression of vimentin (Rutka *et al.*, 1998). From these observations, we can hypothesize that overexpression of GFAP in our GFAP transfectants may have led to a corresponding decrease in vimentin which, in turn, resulted in a reduction in invasive potential.

Even though the role of the each of the type III IF proteins expressed in the glial cell lineage (nestin, vimentin and GFAP) is not well understood, it has been postulated that vimentin may mediate its effects on invasion through CD44. CD44 is a cell surface adhesion molecule that has been implicated in tumour cell invasion and metastasis (reviewed in Jothy, 2003). Of interest, in antisense GFAP transfected U251 cells, the elimination of GFAP was found to correlate with an increase in both vimentin and CD44 (Rutka *et al.*, 1998). These results suggest that vimentin, but not GFAP, can mediate invasion via the CD44 receptor. With this in mind, it would be interesting to determine whether vimentin and CD44 levels are decreased in our GFAP expressing T98 cells.

5.2.3. Alterations in Morphology

The most dramatic alteration observed in our B-FABP-expressing T98 and U87 clones was the presence of long, thin cytoplasmic processes (Figures 4.8 and 4.9). Interestingly, Feng and coworkers (1994) have previously shown that the expression pattern of murine *B-FABP* mRNA in the developing CNS coincides with neuronal migration along radial glial fibers and that the addition of B-FABP antibodies blocks the extension of radial glial cell processes. From these experiments, the researchers concluded that B-FABP is intimately involved in the differentiation of radial glial cells. In fact, to this day, B-FABP remains one of the most potent differentiation markers of radial glial cells. Based on these results, we hypothesize that the ability of B-FABP to induce process formation in the T98 and U87 MG cell lines is indicative of a more differentiated phenotype.

While it has been shown that depletion of B-FABP can impair radial glial cell process formation (Feng *et al.*, 1994) and depletion of E-FABP can impair neurite outgrowth (Allen *et al.*, 2000), to our knowledge this is the first report to provide evidence that the sole expression of an FABP can induce process formation. In support of our conclusion that the induction of process formation is due specifically to the presence of B-FABP, we have shown that U251 cells with reduced B-FABP fail to develop processes. The mechanism through which B-FABP induces process formation in these studies is unclear; however, it is possible that a reduction in B-FABP enhances cell motility since the fan-like structures present in the B-FABP reduced U251 cells resemble the characteristic structure of the leading-edge in migrating cells.

Alternatively, the fan-like structures may not represent the leading-edge of migrating cells, but rather an improper maintenance of focal adhesion sites. It is well established that focal adhesions are intimately involved in cell spreading and migration (reviewed in Wehrle-Haller and Imhof, 2002). Focal adhesions provide a physical link between the extracellular substrate and the actin cytoskeleton. Within these focal adhesions, Rho-associated kinases (ROKs) appear to mediate the reorganization of cytoskeletal proteins (reviewed in Amano *et al.*, 2000). Interestingly, various ROKs are also involved in mediating axon outgrowth and the control of growth cone dynamics, likely through focal adhesions (Bito *et al.*, 2000). In addition, the fatty acid translocase (FAT/CD36) localizes to areas of cell adhesion (Stomski *et al.*, 1992), such as focal adhesions, and the cytoplasmic tail of CD36 has been shown to interact with H-FABP (Spitsberg *et al.*, 1995). These findings imply that H-FABP, and likely E- and B-FABP due to their sequence similarity with H-FABP, can be directly recruited to focal adhesions involved in migration and process/axon formation. At these sites they may function to increase FA uptake and transport to either the growing membrane or to the smooth endoplasmic reticulum (ER) where the FA can be incorporated into phospholipids. In support of this, the presence of smooth ER in growing axons has been reported (Deitch and Banker, 1993; reviewed in Futerman and Banker, 1996) and E-FABP has been shown to localize to retinal ganglion cell axons during differentiation and axon outgrowth (Allen *et al.*, 2001). Also, as mentioned in section 1.3.3, H-FABP (and likely E- and B-FABP) has an increased rate of FA transfer to membranes due to their ability to deliver FAs to the membrane via collision mediated transfer.

In many different cell types, process formation is indicative of a more differentiated phenotype (*i.e.* radial glial cells, neurons and retinal ganglion cells). The ability of specific FABPs to promote process formation likely depends on several factors including cell type, cellular milieu, extracellular environment and the presence of specific FA ligands. For example, while it has been proposed that E-FABP is involved in axon growth in retinal ganglion cells (Allen *et al.*, 2001), E-FABP is also expressed in cells that do not develop processes, such as fibroblasts. Thus, other differentiation factors must be required to promote/inhibit process formation in these cell types. Of particular note, as B-FABP expression was able to induce process formation in the T98 and U87 MG cell lines we believe that these cells must still retain the differentiation factors and machinery necessary for B-FABP to induce differentiation.

In this study we have also examined the effect of GFAP expression on the morphology of T98 cells. Compared to the T98 control clones which typically consist of flat, polygonal-shaped cells that demonstrate a high degree of cell crowding and piling at confluence, the GFAP transfected T98 cells have an elongated phenotype and markedly reduced levels of crowding and piling at confluence. However, in contrast with Rutka and Smith (1993) we did not observe process formation in our GFAP transfected T98 cells. By transfecting SF-126 astrocytoma cells with a GFAP expression construct, Rutka and Smith (1993) found that the stably transfected clones extended abundant, thin cytoplasmic processes. The apparent discrepancy in morphology among the GFAP transfected cells in the two studies may be related to B-FABP expression in these cell lines. It is possible that for GFAP to induce process formation in MG cells, B-FABP must be present for the reasons discussed earlier in this section. Unfortunately, the B-FABP expression status of the SF-126 astrocytoma cell line is not known so this hypothesis is purely speculative at this time. Alternatively, process formation may require a certain threshold of GFAP expression which was not reached in our T98-GFAP transfectants.

Our finding that GFAP does not induce process formation in MG cells is also in contrast to evidence provided by Liem and colleagues (Weinstein *et al.*, 1991; Chen and Liem, 1994). These researchers demonstrated, both by suppressing GFAP expression in U251 cells and then by reexpressing GFAP in these GFAP-depleted U251 cells, that GFAP is required for the formation of stable astrocytic processes. However, in accordance with our suggestion that B-FABP may be required for the induction of process formation by GFAP, these researchers performed their experiments using a B-FABP-positive MG cell line. Thus, it is possible that simply the presence of B-FABP in this cell line permitted GFAP to mediate its effects on process formation. However, we also recognize that these experiments were performed by co-culturing U251 cells with neurons. Thus, different environmental cues, rather than B-FABP, may have allowed GFAP to induce process formation. Importantly though, Rutka and Smith (1993) did not use co-culture experiments in their studies and they were able to demonstrate the induction of process formation by GFAP.

5.2.4. Importance of Subcellular Localization

Examination of the subcellular localization of B-FABP in the U87 transfectants revealed that B-FABP was present in the nucleus of each clone that exhibited alterations in morphology and reduced growth and invasive properties (Figure 4.11). In contrast, the B-FABP transfected clone where B-FABP was excluded from the nucleus (U87-B-FABP-5) displayed similar growth and invasive properties as the controls. While the function of B-FABP in the nucleus was not addressed in these studies, we postulate that B-FABP is able to modulate the effects of FAs on gene transcription by delivering specific FAs to the nucleus or by trafficking ligands to PPARs. As a result, B-FABP may actively participate in cell differentiation by altering gene transcription in MG cells.

The localization of FABPs to the nucleus has previously been reported for several FABPs (reviewed in Zimmerman and Veerkamp, 2002), including L-FABP in liver hepatocytes (Bordewick *et al.*, 1989) and B-FABP in gomori-positive astrocytes (Young *et al.*, 1996). The action of L-FABP in the nucleus has been extensively characterized by several researchers (Schroeder *et al.*, 2001; Wolfrum *et al.*, 2001; Huang *et al.*, 2004). Taken together, these reports show that in L-FABP expressing cells: i) L-FABP localizes to the nucleus, ii) L-FABP is able to interact with PPARα and shuttle FA ligands to this nuclear receptor, iii) L-FABP is itself a PPARα-responsive gene indicating that L-FABP is able to regulate its own transcription, and iv) L-FABP may affect the transcription of many genes involved in FA metabolism and cell differentiation by altering the intracellular distribution of FAs. Furthermore, it is interesting that when embryonic stem cells are transfected with either L-FABP or I-FABP, only L-FABP displays nuclear localization and induces differentiation (Athtaves *et al.*, 1998; Schroeder *et al.*, 2001). In combination with our results, these results suggest that the role of FABPs in mediating differentiation is FABP-type specific and for some FABPs nuclear localization may be essential to induce differentiation. As no studies have addressed the role of B-FABP in the nucleus or its interaction with PPARs, this would be an interesting topic for future investigations.

5.3. Future Directions

Future experiments will be required to address several questions that have arisen from this work. Of note, in light of the major differences in the effect of B-FABP expression in the U87-B-FABP transfectants and the association of these effects with the nuclear localization of B-FABP, it will be interesting to further characterize the role of B-FABP in the nucleus of MG cells. This work may involve the use of pull-down assays and immunoprecipitation experiments to identify specific PPAR family members (PPAR-α, -β, -γ) with which B-FABP can interact. Alternatively, confocal microscropy could be used to show the co-localization of B-FABP and PPAR in the nucleus. It will also be interesting to identify specific FA ligands which B-FABP is able to deliver to the nucleus or to other specific subcellular locations. Because B-FABP has such a high affinity for DHA (Balendiran *et al.*, 2000) it may be informative to examine the cellular concentration of fluorescent FAs, including DHA, in the presence and absence of B-FABP. The stable U87 transfectants generated in these experiments would be ideal cell lines to use for these studies. Lastly, it will be important to identify specific gene targets that mediate the differentiation effects observed in our B-FABP transfectants. One approach to discover genes that are differentially expressed in our B-FABP transfectants compared to our control transfectants is microarray analysis. Importantly, this work would likely identify candidate genes involved in mediating the reduction in growth and invasive potential observed in the B-FABP transfected T98 and U87 cells.

Another question that needs to be answered is whether or not B-FABP is localized to sites of focal adhesion, and if so what role it plays at these sites. The ability of B-FABP to induce process formation and the abundance of PUFAs in neural tissue membranes suggests that B-FABP may be involved in membrane biogenesis. It is possible that through interactions with FAT/CD36 or focal adhesion kinases, B-FABP is localized to sites of focal adhesion where it aids in the uptake of FAs and the delivery of FAs to the growing membrane. If this is the case, one could hypothesize that B-FABP is involved in cell migration. However, the fan-like structures observed in the B-FABP depleted U251 cells suggest that the loss of B-FABP results in increased migration and its presence may even inhibit migration. To clarify the role of B-FABP in cell motility, videomicroscopy and/or wound-healing assays (as described in Etienne-Manneville and Hall, 2001) could be performed using the U87 and/or T98 B-FABP transfectants and controls. As for the role of B-FABP at sites of focal adhesion, confocal microscopy and co-localization studies may shed some light on the involvement B-FABP at these sites.

One assumption that we made in this report was that the exogenous NFI proteins present in the nuclear extracts obtained from the T98 cells transfected with the pCHNFI expression plasmids were hypophosphorylated. This assumption should be addressed by examining the migration of these NFIs in gel shift assays before and after treatment with potato acid phosphatase (PAP). Furthermore, we have found that the NFIs that bind to the NFI-binding sites in the *GFAP* promoter are hypophosphorylated in U251 cells compared to those in T98 cells. It would be particularly interesting to identify the phosphatase and kinase that is responsible for mediating the phosphorylation status of the NFI proteins. One way this could be done is to fractionate the nuclear extracts from T98 and U251 cells using conventional liquid chromatography, identify the fraction capable of phosphorylating or dephosphorylating NFI using gel shift assays, and identify the phosphatase or kinase in this fraction by mass spectrometry.

5.4. Concluding Remarks

We have shown in these studies that the three NFI consensus sites in the *GFAP* promoter are able to bind NFI proteins. In addition, it appears that both NFI-A and NFI-X are potent activators of *B-FABP* and *GFAP* transcription. Thus, it is possible that in MG cells decreased levels of these NFIs may lead to lower levels of B-FABP and GFAP. However, probably the most important regulatory mechanism mediating the expression of B-FABP and GFAP is the phosphorylation status of the NFI proteins. We believe that B-FABP and GFAP may be good candidates for differentiation therapy as they both appear to reduce the tumourigenicity of MG cells, possibly by inducing differentiation. However, we recognize that the phosphatase and/or kinase that acts on the NFI proteins may directly or indirectly regulate the expression of numerous genes in MG. Thus, the identification of this phosphatase and/or kinase may lead to the identification of novel targets for MG therapy and, in turn, improve the treatment of MG.

CHAPTER SIX

References

Abumrad, N., Coburn, C., and Ibrahimi, A. (1999). Membrane proteins implicated in long-chain fatty acid uptake by mammalian cells: CD36, FATP, and FABPpm. *Biochim. Biophys. Acta* **144:** 4-13.

Alevizopoulos, A., Dusserre, Y., Tsai-Pflugfelder, M., von der Weid, T., Wahli, W., and Mermod, N. (1995). A proline-rich TGF-β-responsive transcriptional activator interacts with histone H3. *Genes Dev.* **9:** 3051-3066.

Allen, G.W., Liu, J., and De Leon, M. (2000). Depletion of a fatty acid-binding protein impairs neurite outgrowth in PC12 cells. *Mol. Brain Res.* **76:** 315-324.

Allen, G.W., Liu, J., Kirby, M.A., and De Leon, M. (2001). Induction and axonal localization of epithelial/epidermal fatty acid-binding protein in retinal ganglion cells are associated with axon development and regeneration. *J. Neurosci. Res.* **66**: 396-405.

Allore, R.J., Friend, W.C., O'Hanlon, D., Neilson, K.M., Baumal, R., Dunn, R.J., and Marks, A. (1990). Cloning and expression of the human S100 beta gene. *J. Biol. Chem.* **265:** 15537-15543.

Altmann, H., Wendler, W., and Winnacker, E. (1994). Transcriptional activation by CTF proteins is mediated by a bipartite low-proline domain. *Proc. Natl. Acad. Sci. U.S.A.* **91:** 3901-3905.

Alvarez-Buylla, A., Theelen, M., and Nottebohm, F. (1990). Proliferation "hot spots" in adult avian ventricular zone reveal radial cell division. *Neuron* **5:** 101-109.

Alvarez-Buylla, A., Garcia-Verdugo, J.M., and Tramontin, A.D. (2001). A unified hypothesis on the lineage of neural stem cells. *Nat. Rev. Neurosci.* **2:** 287-293.

Amano, M., Fukata, Y., and Kaibuchi, K. (2000). Regulation and functions of Rho-associated kinase. *Exp. Cell Res.* **261**: 44-51.

Amemiya, K., Traub, R., Durham, L., and Major, E.O. (1992). Adjacent nuclear factor-1 and activator protein binding sites in the enhancer of the neurotropic JC virus. *J. Biol. Chem.* **267**: 14204-14211.

Andræ, J., Bongcam-Rudloff, E., Hansson, I., Lendahl, U., Westermark, B., and Nistér, M. (2001). A 1.8 kb GFAP-promoter fragment is active in specific regions of the embryonic CNS. *Mech. Dev.* **107**: 181-185.

Anton, E.S., Marchionni, M.A., Lee, K.F., and Rakic, P. (1997). Role of GGF/neuregulin signaling in interactions between migrating neurons and radial glia in the developing cerebral cortex. *Development* **124**: 3501-3510.

Atshaves, B.P., Foxworth, W.B., Frolov, A.A., Roths, J.B., Kier, A.B., Oetama, B.K., Piedrahita, J.A., and Schroeder, F. (1998). Cellular differentiation and I-FABP protein expression modulate fatty acid uptake and diffusion. *Am. J. Physiol.* **274**: C633-C644.

Baillie, A.G., Coburn, C.T., and Abumrad, N.A. (1996). Reversible binding of long-chain fatty acids to purified FAT, the adipose CD36 homolog. *J. Membr. Biol.* **153**: 75-81.

Balcarek, J.M., and Cowan, N.J. (1985). Structure of the mouse glial fibrillary acidic protein gene: implications for the evolution of the intermediate filament multigene family. *Nucl. Acids Res.* **13**: 5527-5543.

Balendiran, G.K., Schnutgen, F., Scapin, G., Börchers, T., Xhong, N., Lim, K., Godbout, R., Spener, F., and Sacchettini, J.C. (2000). Crystal structure and thermodynamic analysis of human brain fatty acid-binding protein. *J. Biol. Chem.* **275**: 27045-27054.

Bandyooadhyay, S., and Gronostajski, R.M. (1994). Identification of a conserved oxidation-sensitive cysteine residue in the NFI family of DNA-binding proteins. *J. Biol. Chem.* **269:** 29949-29955.

Barres, B. (2003) What is a glial cell. *Glia* **43:** 4-5.

Bass, N.M, Raghupathy, E., Rhoads, D.E., Manning, J.A., and Ockner, R.K. (1984). Partial purification of molecular weight 12000 fatty acid binding proteins from rat brain and their effect on synaptosomal Na$^+$-dependent amino acid uptake. *Biochemistry* **23:** 6539-6544.

Behin, A., Hoang-Xuan, K., Carpentier, A.F., and Delattre, J.-Y. (2003). Primary brain tumours in adults. *Lancet* **361:** 323-31.

Benjamin, R., Capparella, J., and Brown, A. (2003) Classification of glioblastoma multoforme in adults by molecular genetics. *Cancer J.* **9:** 82-90.

Bennett, E., Stenvers, K.L., Lund, P.K., and Popko, B. (1994). Cloning and characterization of a cDNA encoding a novel fatty acid-binding protein from rat brain. *J. Neurochem.* **63:** 1616-1624.

Besnard, F., Brenner, M., Nakatani, Y., Chao, R., Purohit, H., and Freese, E. (1991). Multiple interacting sites regulate astrocytes-specific transcription of the human gene for glial fibrillary acidic protein. *J. Biol. Chem.* **266:** 18877-18883.

Bignami, A., Raju, T., and Dahl, D. (1982). Localization of vimentin, the non-specific intermediate filament protein, in embryonal glia and in early differentiating neurons. *In vivo* and *in vitro* immunofluoresence study of the rat embryo with vimentin and neurofilament antisera. *Dev. Biol.* **91:** 286-295.

Bigner, S.H., Bullard, D.E., Pegram, C.N., Wikstrand, C.J., and Bigner, D.D. (1981). Relationship of *in vitro* morphologic and growth characteristics of established human glioma-derived cell lines to their tumorigenicity in athymic nude mice. *J. Neuropathol. Exp. Neurol.* **40:** 390-409.

Bigner, S.H., Burger, P.C., Wong, A.J., Werner, M.H., Hamilton, S.R., Muhlbaier, L.H., Vogelstein, B., and Bigner, D.D. (1988). Gene amplification in malignant human gliomas: clinical and histopathological aspects. *J. Neuropath. and Exp. Neurol.* **47:** 191-205.

Bisgrove, D.A., Monckton, E.A., and Godbout, R. (1997). Involvement of AP-2 in regulation of the R-FABP gene in the developing chick retina. *Mol. Cell. Biol.* **17:** 5935-5945.

Bisgrove, D.A., Monckton, E.A., Packer, M.P., and Godbout, R. (2000). Regulation of Brain Fatty Acid-binding Protein Expression by Differential Phosphorylation of Nuclear Factor I in Malignant Glioma Cell Lines. *J. Biol. Chem.* **275:** 30668-30676.

Bito, H., Furuyashiki, T., Ishihara, H., Shibasaki, Y., Ohashi, K., Mizuno, K., Maekawa, M., Ishizaki, T., and Narumiya, S. (2000). A critical role for a Rho-associated kinase, p160ROCK, in determining axon outgrowth in mamalian CNS neurons. *Neuron* **26:** 431-441.

Böhmer, F.D., Lehmann, W., Schmidt, H.E., Langen, P., and Grosse, R. (1984). Purification of a growth inhibitor for Ehrlich ascites mammary carcinoma cells from bovine mammary gland. *Exp. Cell Res.* **150:** 466-476.

Bordewick, U., Heese, M., Borchers, T., Robenek, H., and Spener, F. (1989). Compartmentation of hepatic fatty-acid-binding protein in liver cells and its effect on microsomal phosphatidic acid biosynthesis. *Biol. Chem. Hoppe-Seyler* **370:** 229-238.

Bradford, M.M. (1976). A rapid and sensitive method for the quatitation of microgram quantities of protein utilizing the principle of protein-dye binding. *Anal. Biochem.* **72:** 248-254.

Brenner, M., Lampel, K., Nakatani, Y., Mill, J., Banner, C., Maerow, K., Dohadwala, M., Lipsky, R., and Freese, E. (1990). Characterization of human cDNA and genomic clones for glial fibrillary acidic protein. *Mol. Brain Res.* **7:** 277-286.

Brenner, M., Kisseberth, W.C., Su, Y., Besnard, F., and Messing, A. (1994). GFAP promoter directs astrocyte-specific expression in transgenic mice. *J. Neurosci.* **14:** 1030-1037.

Brummelkamp, T.R., Bernards, R., and Agami, R. (2002). A system for stable expression of short interfering RNAs in mammalian cells. *Science* **296:** 550-553.

Burger, P.C. (1983). Pathologic anatomy and CT correlations in the glioblastoma multiforme. *Appl. Neurophysiol.* **46:** 180-187.

Burrows, R.C., Lillien, L., and Levitt, P. (2000). Mechanisms of progenitor maturation are conserved in the stratium and cortex. *Dev. Neurosci.* **22:** 7-15.

Burton, E.C., Lamborn, K.R., Feuerstein, B.G., Prados, M., Scott, J., Forsyth, P., Passe, S., Jenkins, R.B., and Aldape, K.D. (2002). Genetic aberrations defined by comparative genomic hybridization distinguish long-term from typical survivors of glioblastoma. *Cancer Res.* **62:** 6205-6210.

Calver, A.R., Hall, A.C., Yu, W.P., Walsh, F.S., Heath, J.K., Betsholtz, C., and Richardson, W.D. (1998). Oligodendrocyte population dynamics and the role of PDGF *in vivo.* *Neuron* **20:** 869-882.

Celis, J.E., Ostergaard, M., Basse, B., Celis, A., Lauridsen, J.B., Ratz, G.P., Andersen, I., Hein., B., Wolf, H., Orntoft, T.F., and Rasmussen, H.H. (1996). Loss of adipocyte-type fatty acid binding protein and other protein biomarkers is associated with progression of human bladder transitional cell carcinomas. *Cancer Res.* **56:** 4782-4790.

Chanas-Sacre, G., Rogister, B., Moonen, G., and Leprince, P. (2000). Radial glia phenotype: Origin, regulation, and transdifferentiation. *J. Neurosci. Res.* **61:** 357-363.

Chaudhry, A.Z., Lyons, G.E., and Gronostajski, R.M. (1997). Expression patterns of the four nuclear factor I genes during mouse embryogenesis indicate a potential role in development. *Dev. Dyn.* **208:** 313-325.

Chaudry, A.Z., Vitullo, A.D., and Gronostajski, R.M. (1998). Nuclear factor I (NFI) isoforms differentially activate simple versus complex NFI-responsive promoters. *J. Biol. Chem.* **273:** 18538-18546.

Chen, A., Beno, D.W.A., and Davis, B.H. (1996). Suppression of stellate cell type I collagen gene expression involves AP-2 transmodulation of nuclear factor-1-depentent gene transcription. *J. Biol. Chem.* **271:** 25994-25998.

Chen, W.J., and Liem, R.K.H. (1994a). The endless story of the glial fibrillary acidic protein. *J. Cell Sci.* **107:** 2299-2311.

Chen, W.J., and Liem, R.H.K. (1994b). Reexpression of glial fibrillary acidic protein rescues the ability of astrocytoma cells to form processes in response to neurons. *J. Cell Biol.* **127:** 813-823.

Coe, N.R., and Bernlohr, D.A. (1998). Physiological properties and functions of intracellular fatty acid-binding proteins. *Biochim. Biophys. Acta* **1391:** 287-306.

Condorelli, D.F., Nicoletti, V., Barresi, V., Conticello, S.G., Caruso, A., Tendi, E.A., and Giuffrida Stella, A.M. (1999). Structural features of the rat GFAP gene and identification of a novel alternative transcript. *J. Neurosci. Res.* **56:** 219-228.

Cooke, D.W., and Lane, M.D. (1999). The transcription factor nuclear factor I mediates repression of the GLUT4 promoter by insulin. *J. Biol. Chem.* **274:** 12917-12924.

Corfas, G., Rosen, K.M., Aratake, H., Krauss, R., and Fischbach, G.D. (1995). Differential expression of ARIA isoforms in the rat brain. *Neuron* **14:** 103-115.

Crowe, D.L., Milo, G.E., and Shuler, C.F. (1999). Keratin 19 downregulation by oral squamous cell carcinoma lines increases invasive potential. *J. Dent. Res.* **78:** 1256-1263.

Culican, S.M., Baumrind, N.K., Yamamoto, M., and Pearlman, A.K. (1990). Cortical radial glia: identification in tissue culture and evidence for their transformation to astrocytes. *J. Neurosci.* **10:** 684-692.

Dahl, D., Rueger, D.C., Bignami, A., Weber, K., and Osborn, M. (1981). Vimentin, the 57,000 molecular weight protein of fibroblast filaments, is the major cytoskeletal component in immature glia. *Eur. J. Cell Biol.* **24:** 191-196.

Dai, C., and Holland, E.C. (2003). Astrocyte differentiation states and glioma formation. *Cancer J.* **9:** 72-81.

das Neves, L., Duchala, C.S., Godinho, F., Haxhiu, M.A., Colmenares, C., Macklin, W.B., Campbell, C.E., Butz, K.G., and Gronostajski, R.M. (1999). Disruption of the murine nuclear factor I-A gene (NFIa) results in perimatal lethality, hydrocephalus, and agenesis of the corpus callosum. *Proc. Natl. Acad. Sci. U.S.A.* **96:** 11946-11951.

Davidson, N.O., Ifkovits, C.A., Skarosi, S.F., Hausman, A.M.I., Llor, X., Sitrin, M.D., Montag, A., and Brasitus, T.A. (1993). Tissue and cell-specific patterns of expression of rat liver and intestinal fatty acid binding protein during development and in experimental colonic and small intestinal adenocarcinomas. *Lab. Invest.* **68:** 663-675.

Deitch, J.S., and Banker, G.A. (1993). An electron microscope analysis of hippocampal neurons developing in culture: early stages in the emergence of polarity. *J. Neurosci.* **13:** 4301-4315.

Dekker, J., , van Oosterhout, J.A.W.M., van der Vliet, P.C. (1996). Two regions within the DNA binding domain of nuclear factor I interact with DNA and stimulate adenovirus DNA replication independently. *Mol. Cell. Biol.* **16:** 4073-4080.

De Leon, M., Welcher, A.A., Liu, N.Y., Ruda, M.A., Shooter, E.M., and Molina, C.A. (1996). Fatty acid binding protein is induced in neurons of the dorsal root ganglia after peripheral nerve injury. *J. Neurosci. Res.* **44:** 283-292.

de Oliveira Sousa, V., Romão, L., Neto, V.M., Gomes, F.C.A. (2004). Glial fibrillary acidic protein promoter is differentially modulated by transforming growth factor-beta 1 in astrocytes from distinct brain regions. *Eur. J. Neurosci.* **19:** 1721-1730.

Dignam, J.D., Lebovitz, R.M. and Roeder, R.G. (1983). Accurate transcription initiation by RNA polymerase II in a soluble extract from isolated mammalian nuclei. *Nucleic Acids Res.* **11:** 1475-1489.

Duffy, P.E., Huang, Y.Y., and Rapport, M.M. (1982). The relationship of GFAP to cell shape, motility, and differentiation of human astrocytoma cells. *Exp. Cell Res.* **139:** 145-157.

Duplus, E., Glorian, M., and Forest, C. (2000). Fatty acid regulation of gene transcription. *J. Biol. Chem.* **275:** 30749-30752.

Edmondson, J.C. and Hatten, M.E. (1987). Glial-guided granule neuron migration *in vitro*: a high-resolution time-lapse video microscopic study. *J. Neurosci.* **7:** 1928-1934.

Edwards, M.A., Yamamoto, M., and Caviness, V.S. Jr. (1990). Organization of radial glia and related cells in the developing murine CNS. An analysis based upon a new monoclonal antibody marker. *Neuroscience* **36:** 121-144.

Elateri, I., Muller-Weeks, S., and Caradonna, S. (2003). The transcription factor, NFI/CTF plays a positive regulatory role in expression of the hSMUG1 gene. *DNA Repair* **2:** 1371-1385.

Eng, L.F., Gerstl, B., and Vanderhaeghen, J.J. (1970). A study of proteins in old multiple sclerosis plaques. *Trans. Am. Soc. Neurochem.* **1:** 42.

Eng, L.F., Vanderhaeghen, J.J., Bignami, A., and Gerstl, B. (1971). An acidic protein isolated from fibrous astrocytes. *Brain Res.* **28:** 351-354.

Eng, L.F., and Rubinstein, L.J. (1978). Contribution of immunohistochemistry to diagnostic problems of human cerebral tumors. *J. Histochem. Cytochem.* **26:** 513-522.

Eng, L.F. (1980). The glial fibrillary acidic (GFA) protein. *"Proteins of the Nervous System".* Bradshaw, R.A. and Schneider, D.M. eds., 2nd edition, pp. 85-117.

Eng, L.F., Ghirnikar, R.S., and Yuen, L.L. (2000). Glial fibrillary acidic protein: GFAP-thirty-one years (1969-2000). *Neurochem. Res.* **25:** 1439-1451.

Engelhard, H., Narang, C., Homer, R., and Duncan, H. (1996). Urokinase antisense oligonucleotides as a novel therapeutic agent for malignant glioma: *in vitro* and *in vivo* studies of uptake, effects and toxicity. *Biochem. Biophys. Res. Commun.* **227:** 400-405.

Etienne, M.C., Formento, J.L., Lebrun-Frenay, C., Gioanni, J., Chatel, M., Paquis, P., Bernard, C., Courdi, A., Bensadoun, R.J., Pignol, J.P., Francoual, M., Grellier, P., Frenay, M., and Milano, G. (1998). Epidermal growth factor receptor and labeling index are independent prognostic factors in glial tumor outcome. *Clin. Cancer Res.* **4:** 2383-2390.

Etienne-Manneville, S., and Hall, A. (2001). Integrin-mediated activation of cdc42 controls cell polarity in migrating astrocytes through PKCζ. *Cell* **106:** 489-498.

Feinstein, D.L., Weinmaster, G.A., and Milner, R.J. (1992). Isolation of cDNA clones encoding rat glial fibrillary acidic protein: expression in astrocytes and in Schwann cells. *J. Neurosci. Res.* **32:** 1-14.

Feng, L., Hatten, M.E., and Heintz, N. (1994). Brain lipid-binding protein BLBP: a novel signaling system in the developing mammalian CNS. *Neuron* **12:** 895-908.

Feng, L., and Heintz, N. (1995). Differentiating neurons activate transcription of the brain lipid-binding protein gene in the radial glia through a novel regulatory element. *Development* **121:** 1719-1730.

Fliesler, S.J., and Anderson, R.E. (1983). Chemistry and metabolism of lipids in the vertebrate retina. *Prog. Lipid Res.* 22: 79-131.

Francois, M., Richette, P., Tsagris, L., Raymondjean, M., Fulchignoni-Lataud, M.C., Forest, C., Savouret, J.F., and Corvol, M.T. (2004). Peroxisome proliferator activated receptor gamma down-regulates chondrocyte matrix metalloproteinases-1 via a novel composite element. *J. Biol. Chem.* [Epub ahead of print]

Freshney, R.I. (1983). *Culture of Animal Cells: A Manual of Basic Technique.* Alan R. Liss, Inc., New York. pp. 133-136, 174.

Fuchs, E., and Weber, K. (1994). Intermediate filaments: structure, dynamics, function, and disease. *Annu. Rev. Biochem.* **63:** 345-382.

Fuchs, E. (1996). The cytoskeleton and disease: Genetic disorders of Intermediate filaments. *Annu. Rev. Genet.* **30:** 197-231.

Futerman, A.H., and Banker G.A. (1996). The economics of neurite ougrowth: the addition of new membrane to growing axons. *TINS* **19**: 144-149.

Gage, F.H. (2000). Mammalian neural stem cells. *Science* **287:** 1433-1438.

Gao, W.Q., and Hatten, M.E. (1993). Neuronal differentiation rescued by implantation of weaver granule cell precursors into wild-type cerebellar cortex. *Science* **260:** 367-370.

Gao, W.Q., and Hatten, M.E. (1994). Immortalizing oncogenes subvert the establishment of granule cell identity in developing cerebellum. *Development* **120:** 1059-1070.

Gasser, U.E., and Hatten, M.E. (1990). Neuron-glia interactions of rat hippocampal cells *in vitro*: glial-guided neuronal migration and neuronal regulation of glial differentiation. *J. Neurosci.* **10:** 1276-1285.

Geisler, N., and Weber, K. (1983). Amino acid sequence data on glial fibrillary acidic protein (GFA); implications for the subdivision of intermediate filaments into epithelial and non-epithelial members. *EMBO J.* **2:** 2059-2063.

Gerber, H., Seipel, K., Georgiev, O., Höfferer, M., Hug, M., Rusconi, S., and Schaffner, W. (1994). Transcriptional activation modulated by homopolymeric glutamine and proline stretches. *Science* **263:** 808-811.

Gil, G., Smith, J.R., Goldstein, J.L., Slaughter, C.A., Orth, K., Brown, M.S., and Osborne, T.F. (1988). Multiple genes encode nuclear factor I-like proteins that bind to the promoter for 3-hydroxy-3-methylglutaryl-coenzyme A reductase. *Proc. Natl. Acad. Sci. U.S.A.* **85:** 8963-8967.

Gladson, C.L., Pijuan-Thompson, V., Olman, M.A., Gillespie, G.Y., and Yacoub, I.Z. (1995). Up-regulation of urokinase and urokinase receptor genes in malignant astrocytoma. *Am. J. Pathol.* **146:** 1150-1160.

Glatz, J.F.C., and Storch, J. (2001). Unraveling the significance of cellular fatty acid- binding proteins. *Curr. Opin. Lipid.* **12:** 267-274.

Godbout, R. (1993). Identification and characterization of transcripts present at elevated levels in the undifferentiated chick retina. *Exp. Eye Res.* **56:** 95-106.

Godbout, R., Bisgrove, D.A., Shkolny, D., and Day, R.S. (1998). Correlation of B-FABP and GFAP expression in malignant glioma. *Oncogene* **16:** 1955-1962.

Goldman, J.E., and Chiu, F.C. (1984). Growth kinetics, cell shape and the cytoskeleton of primary astrocytic cultures. *J. Neurochem.* **42:** 175-184.

Goldman, S. (2003). Glia as neural progenitor cells. *Trends Neurosci.* **26:** 590-596.

Gorman, C.M., Moffat, L.F. and Howard, B.H. (1982). Recombinant genomes which express chloramphenicol acetyltransferase in mammalian cells. *Mol. Cell Biol.* **2:** 1044-1051.

Gottschalk, J., and Szymas, J. (1987). Significance of immunohistochemistry for neuro-oncology VI. Occurrence, localization, and distribution of glial fibrillary acidic protein (GFAP) in 820 tumors. *Zentralblatt Fur Allgemeine Pathologie Und Pathologische Anatomie* **133:** 319-330.

Gounari, F., De Francesco, R., Schmitt, J., van der Vliet, P.C., Cortese, R., and Stunnenburg, H. (1990). Amino-terminal domain of NFI binds to DNA as a dimer and activates adenovirus DNA replication. *EMBO J.* **9:** 559-566.

Goyal, N., Knox, J., and Gronostajski, R.M. (1990). Analysis of multiple forms of nuclear factor I in human and murine cell lines. *Mol. Cell. Biol.* **10:** 1041-1048.

Graham, F.L., and van der Eb, A.J. (1973). A new technique for the assay of infectivity of human adenovirus 5 DNA. *Virology.* **52:** 456-467.

Green, J.B. (1994). Roads to neuralness: embryonic neural induction as derepression of a default state. *Cell* **77:** 317-320.

Gronostajski, R.M., Adhya, S., Nagata, K., Guggenheimer, R.A., and Hurwitz, J. (1985). Site-specific DNA binding of nuclear factor I: Analyses of cellular binding sites. *Mol. Cell. Biol.* **5:** 964-971.

Gronostajski, R.M. (1986). Analysis of nuclear factor I binding to DNA using degenerate oligonucleotides. *Nucleic Acids Res.* **14:** 9117-9132.

Gronostajski, R.M. (1987). Site-specific DNA binding of nuclear factor I: effect of the spacer region. *Nucleic Acids Res.* **15:** 5545-5559.

Gronostajski, R.M. (2000). Roles of the NFI/CTF gene family in transcription and development. *Gene* **249:** 31-45.

Hamilton, J.A., and Kamp, F. (1999). How are fatty acids transported in membrane? Is it by proteins or by free diffusion through the lipids. *Diabetes* **48:** 2255-2269.

Hansson, E., and Ronnback, L. (1994). Astroglial modulation of synaptic transmission. *Perspect. Dev. Neurobiol.* **2:** 217-223.

Hatten, M.E. (1999). Central nervous system neuronal migration. *Annu. Rev. Neurosci.* **22:** 511-539.

Hendrix, M.J., Seftor, E.A., Chu, Y.W., Trevor, K.T., and Seftor, R.E. (1996). Role of intermediate filaments in migration, invasion and metastasis. *Cancer Metastasis Rev.* **15:** 507-25.

Herr, F.M., Aronson, J., and Storch J. (1996). Role of portal lysine residues in electrostatic interactions between heart fatty acid binding protein and phospholipid membranes. *Biochemistry* **35:** 1296-1303.

Hetzel, M., Walcher, D., Grub, M., Bach, H., Hombach, V., and Marx, N. (2003). Inhibition of MMP-9 expression by PPARgamma activators in human bronchial epithelial cells. *Thorax* **58:** 778-783.

Heuckeroth, R.O., Birkenmeier, E.H, and Levin, M.S. (1987). Analysis of tissue-specific expression, developmental regulation, and linkage relationships of a rodent gene encoding heart fatty acid-binding protein. *J. Biol. Chem.* **262:** 9709-9717.

Hirt, B. (1967). Selected extraction of polyoma DNA from infected mouse cell cultures. *J. Mol. Biol.* **26:** 365-369.

Hohoff, C., and Spener, F. (1998). Fatty acid binding proteins and mammary-derived growth inhibitor. *Fett/Lipid* **100:** 252-263.

Hsu, K.T., and Storch, J. (1996). Fatty acid transfer from liver and intestinal fatty acid-binding proteins to membranes occurs by different mechanisms. *J. Biol. Chem.* **271:** 13317-13323.

Huang, B., Starostik, P., Schraut, H., Krauss, J., Sorensen, N., and Roggendorf, W. (2003). Human ependymomas reveal frequent deletions on chromosomes 6 and 9. *Acta Neuropathol.* **106:** 357-362.

Huang, R.P., Fan, Y., Hossain, M.Z., Peng, A., Zeng, Z.L., and Boynton, A.L. (1998). Reversion of the neoplastic phenotype of human glioblastoma cells by connexin 43 (cx43). *Cancer Res.* **58:** 5089-5096.

Hunter, K.E., and Hatten, M.E. (1995). Radial glial cell transformation to astrocytes is bidirectional: Regulation by a diffusible factor in embryonic forebrain. *Proc. Natl. Acad. Sci. U.S.A.* **92:** 2061-2065.

Huynh, H.T., Larsson, C., Narod, S., and Pollak, M. (1995). Tumor suppressor activity of the gene encoding mammary-derived growth factor inhibitor. *Cancer Res.* **55:** 2225-2231.

Imura, T., Kornblum, H.I., and Sofroniew, M.V. (2003). The predominant neural stem cell isolated from postnatal and adult forebrain but not early embryonic forebrain expresses GFAP. *J. Neurosci.* 23: 2824-2832.

Inoue, T., Tamura, T., Furuichi, T., and Mikoshiba, K. (1990). Isolation of complementary DNAs encoding a cerebellum-enriched nuclear factor I family that activates transcription from the mouse myelin basic protein promoter. *J. Biol. Chem.* **265:** 19065-19070.

Isaacs, A., Baker, M., Wavrant-De Vrièze, F., and Hutton, M. (1998). Determination of the gene structure of human GFAP and absence of coding region mutations associated with frontotemporal dementia with parkinsonism linked to chromosome 17. *Genomics* **51:** 152-154.

Jackson, S.P., and Tjian, R. (1988). O-glycosylation of eukaryotic transcription factors: Implications for mechanisms of transcriptional regulation. *Cell* **55:** 125-133.

Jackson, S.P., MacDonald, J.J., Lees-Miller, S., and Tjian, R. (1990). GC box binding induces phosphorylation of Sp1 by a DNA-dependent protein kinase. *Cell* **63:** 155-165.

Jakoby, M.G., Miller, K.R., Toner, J.J., Bayman, A., Cheng, L., Li, E., and Cistola, D.P. (1993). Ligand-protein electrostatic interactions govern the specificity of retinol- and fatty acid-binding proteins. *Biochemistry* **32:** 872-878.

Jenkins, R.B., Kimmel, D.W., Moertel, C.A., Schultz, C.G., Scheithauer, B.W., Kelly, P.J., and Dewald, G.W. (1989). A cytogenetic study of 53 human gliomas. *Cancer Genet. Cytogenet.* **39:** 253-279.

Jessell, T.M., and Melton, D.A. (1992). Diffusible factors in vertebrate embryonic induction. *Cell* **68:** 257-270.

Johnsingh, A.A., Johnston, J.M., Merz, G., Xu, J., Kotula, L., Jacobsen, J.S., and Tezapsidis, N. (2000). Altered binding of mutated presenilin with cytoskeleton-interacting proteins. *FEBS Lett.* **465:** 53-58.

Jones, K.A., Yamamoto, K.R., and Tjian, R. (1985). Two distinct transcription factors bind to the HSV thymidine kinase promoter *in vitro*. *Cell* **42:** 559-572.

Jones, K.A., Kadonaga, J.T., Rosenfeld, P.J., Kelly, T.J., and Tjian, R. (1987). A cellular DNA-binding protein that activates eukaryotic transcription and DNA replication. *Cell* **48:** 79-89.

Josephson, R., Müller, T., Pickel, J., Okabe, S., Reynolds, K., Turner, P.A., and Zimmer, A. (1998). POU transcription factors control expression of CNS stem cell-specific genes. *Development* **125:** 3087-3100.

Jothy, S. (2003). CD44 and its partners in metastasis. *Clin. Exp. Metastasis* **20:** 195-201.

Kamb, A., Gruis, N.A., Weaver-Feldhaus, J., Liu, Q., Harshman, K., Tavtigain, S.V., Stockert, E., Day, R.S. III, Johnson, B.E., and Skolnick, M.H. (1994). A cell cycle regulator potentially involved in genesis of many tumour types. *Science* **264:** 436-440.

Kane, R., Murtagh, J., Finlay, D., Marti, D., Jaggi, R., Blatchford, D., Wilde, C., and Martin, F. (2002). Transcription factor NFIC undergoes N-glycosylation during early mammary gland involution. *J. Biol. Chem.* **277:** 25893-25903.

Kaneko, R., and Sueoka, N. (1993). Tissue-specific versus cell type-specific expression of the glial fibrillary acidic protein. *Proc. Natl. Acad. Sci. U.S.A.* **90:** 4698-4702.

Kaneko, R., Hagiwara, N., Leader, K., and Sueoka, N. (1994). Glial-specific cAMP response of the glial fibrillary acidic protein gene in the RT4 cell lines. *Proc. Natl. Acad. Sci. U.S.A.* **91:** 4529-4533.

Kannius-Janson, M., Johansson, E.M., Bjursell, G., and Nilsson, J. (2002). Nuclear factor 1-C2 contributes to the tissue-specific activation of a milk protein gene in the differentiating mammary gland. *J. Biol. Chem.* **277:** 17589-17596.

Kaufmann, E., Weber, K., and Geisler, N. (1985). Intermediate filament forming ability of desmin derivatives lacking either the amino-terminal 67 or the carboxy-terminal 27 residues. *J. Mol. Biol.* **185:** 733-742.

Kawamura, H., Nagata, K., Masamune, Y., and Nakanishi, Y. (1993). Phosphorylation of NF-I by CDC2 kinase. *Biochem. Biophys. Res. Comm.* **192:** 1424-1431.

Keler, T., Barker, C.S., and Sorof, S. (1992). Specific growth stimulation by linoleic acid in hepatoma cell lines transfected with the target protein of a liver carcinogen. *Proc. Natl. Acad. Sci. U.S.A.* **89:** 4830-4834.

Kim, H.K., and Storch, J. (1992a). Mechanism of free fatty acid transfer from heart fatty acid binding protein to phospholipid membranes: Evidence for a collisional process. *J. Biol. Chem.* **267:** 20051-20056.

Kim, H.K., and Storch, J. (1992b). Free fatty acid transfer from rat liver fatty acid-binding protein to phospholipid vesicles: Effect of ligand and solution properties. *J. Biol. Chem.* **267:** 77-82.

Kim, T.K., and Roeder, R.G. (1994). Proline-rich activator CTF1 tragets the TFIIB assembly step during transcriptional activation. *Proc. Natl. Acad. Sci. U.S.A.* **91:** 4170-4174.

Kleihues, P., and Ohgaki, H. (1999). Primary and secondary glioblastomas: from concept to clinical diagnosis. *Neuro-oncology* **1:** 44-51.

Kleinfeld, A.M. (2000). Lipid phase fatty acid flip-flop, is it fast enough for cellular transport? *J. Membr. Biol.* **175:** 79-86.

Kondraganti, S., Mohanam, S., Chintala, S.K., Kin, Y., Jasti, S.L., Nirmala, C., Lakka, S.S., Adachi, Y., Kyritsis, A.P., Ali-Osman, F., Sawaya, R., Fuller, G.N., and Rao, J.S. (2000). Selective suppression of matrix metalloproteinase-9 in human glioblastoma cells by antisense gene transfer impairs glioblastoma cell invasion. *Cancer Res.* **60:** 6851-6855.

Kornblum, H.I., Hussain, R., Wiesen, J., Miettinen, P., Zurcher, S.D., Chow, K., Derynck, R., and Werb, Z. (1998). Abnormal astrocyte development and neuronal death in mice lacking the epidermal growth factor receptor. *J. Neurosci. Res.* **53:** 697-717.

Krebs, C.J., Dey, B., and Kumar, G. (1996). The cerebellum-enriched form of nuclear factor I is functionally different from ubiquitous nuclear factor I in glial-specidic promoter regulation. *J. Neurochem.* **66:** 1354-1361.

Kruse, U., and Sippel, A.E. (1994). Transcription factor nuclear factor I proteins form stable homo- and heterodimers. *FEBS Lett.* **348**: 46-50.

Kulkarni. S., and Gronostajski, R.M. (1996). Altered expression of the developmentally regulated NFI gene family during phorbol ester-induced differentiation of human leukemic cells. *Cell Growth Differ.* **7:** 501-501.

Kurtz, A., Zimmer, A., Schnütgen, F., Bruning, G., Spener, F., and Müller, T. (1994). The expression pattern of novel gene encoding brain-fatty acid binding protein correlates with neuronal and glial cell development. *Development* 120: 2637-2649.

Lakka, S.S., Jasti, S.L., Gondi, C., Boyd, D., Chandrasekar, N., Dinh, D.H., Olivero, W.C., Gujrati, M., and Rao, J.S. (2002). Downregulation of MMP-9 in ERK-mutated stable transfectants inhibits glioma invasion *in vitro*. *Oncogene* **21:** 5601-5608.

Laywell, E.D., Kukekov, V.G., and Steindler, D.A. (1999). Evidence that cultured astrocytes from diverse CNS areas of the mouse produce neurospheres *in vitro*. *Soc. Neurosci. Meet.* **25:** 554.

Lazarides, E. (1982). Intermediate filaments: a chemically heterogeneous developmentally regulated class of proteins. *Annu. Rev. Biochem.* **51:** 219-250.

Lee, J.C., Mayer-Proschel, M., and Rao, M.S. (2000). Gliogenesis in the central nervous system. *Glia* **30:** 105-121.

Leegwater, P.A.J., van der Vliet, P.C., Rupp, R.A.W., Nowock, J., and Sippel, A.E. (1986). Functional homology between the sequence-specific DNA-binding protein nuclear factor I from HeLa cells and the TGGCA protein from chicken liver. *EMBO J.* **5:** 381-386.

Lehmann, W., Widmairer, R., and Langen P. (1989). Response of different mammary epithelial cell lines to a mammary derived growth inhibitor (MDGI). *Biomed. Biochim. Acta* **48:** 143-151.

Levitt, P., and Rakic, P. (1980). Immunoperoxidase localization of glial fibrillary acidic protein in radial glial cells and astrocytes of the developing rhesus monkey brain. *J. Comp. Neurol.* **193:** 815-840.

Libermann, T.A., Nusbaum, H.R., Razon, N., Kris, R., Lax, I., Soreq, H., Whittle, N., Waterfield, M.D., Ullrich, A., and Schlessinger, J. (1985). Amplification, enhanced expression and possible rearrangement of EGF receptor gene in primary brain tumours of glial origin. *Nature* **313:** 144-147.

Liedtke, W., Edelmann, W., Bieri, P.L., Chiu, F.C., Cowan, N.J., Kucherlapati, R., and Raine, C.S. (1996). GFAP is necessary fir the integrity of CNS white matter architecture and long-term maintenance of myelination. *Neuron* **17:** 607-615.

Linskey, M.E., and Gilbert, M.D. (1995). Glial differentiation: A review with implications for new directions in neuro-oncology. *Neurosurgery* **36:** 1-22.

Liou, H., and Storch, J. (1998). The helical cap domain is important for fatty acid transfer from adipocyte and heart fatty acid-binding proteins to membranes. *FASEB J.* **12:** A514.

Liu, Y., Molina, C.A., Welcher, A.A., Longo, L.D., and De Leon, M. (1997). Expression of DA11, an neuronal-injury-induced fatty acid binding protein, coincides with axon growth and neuronal differentiation during central nervous system development. *J. Neurosci. Res.* **48:** 551-562.

Liu, Y., Longo, L.D., and De Leon, M. (2000). In situ and immunocytochemical localization of E-FABP mRNA and protein during neuronal migration and differentiation. *Brain Res.* **852:** 16-27.

Louis, D.N., Holland, E.C., and Cairncross, J.G. (2001). Glioma classification: a molecular repraisal. *Am. J. Pathol.* **159:** 779-786.

MacPherson, I., and Montagnier, L. (1964). Agar suspension culture for the selective assay of cells transformed by polyoma virus. *Virology.* **23:** 291-294.

Malatesta, P., Hartfuss, E., and Götz, M. (2000). Isolation of radial glial cells by fluorescent-activated cell sorting reveals a neuronal lineage. *Development* **127:** 5253-5263.

Martin, G.G., Huang, H., Atshaves, B.P., Binas, B., and Schroeder, F. (2003). Ablation of the liver fatty acid binding protein gene decreases fatty acyl CoA binding capacity and alters fatty acyl CoA pool distribution in mouse liver. *Biochemistry* **42:** 11520-11532.

Masood, K., Besnard, F., Su, Y., and Brenner, M. (1993). Analysis of a segment of the human glial fibrillary acidic protein gene that directs astrocytes-specific transcription. *J. Neurochem.* **61:** 160-166.

Matrisian, L.M. (1992). The matrix-degrading metalloproteinases. *BioEssays* **14:** 455-463.

Meisterernst, M., Gander, I., Rogge, L., and Winnacker, E.L. (1988a). A quantitative analysis of nuclear factor I/DNA interactions. *Nucleic Acids Res.* **16:** 4419-4435.

Meisterenst, M., Rogge, L., Donath, C., Gander, I., Lottspeich, F., Mertz, R., Dobner, T., and Fockler, R. (1988b). Isolation and characterization of the porcine nuclear factor I (NFI) genes. *FEBS Lett.* **236:** 27-32.

Meisterernst, M., Rogge, L., Foeckler, R., Karaghiosoff, M., and Winnacker, E. L. (1989). Structural and functional organization of a porcine gene coding for nuclear factor I. *Biochemistry* **28:** 8191-8200.

Menet, V., Gimenez y Ribotta, M., Sandillon, F., and Privat, A. (2000). GFAP null astrocytes are a favourable substrate for neuronal survival and neurite growth. *Glia* **31:** 267-272.

Mermod, N., O'Neill, E.A., Kelly, T.J., and Tjian, R. (1989). The proline-rich transcriptional activator of CTF/NF-I is distinct from the replication and DNA binding domain. **58:** 741-753.

Messing, A., and Brenner, M. (2003). GFAP: Functional implications gleaned from studies of genetically engineered mice. *Glia* **43:** 87-90.

Miake, H., Tsuchiya, K., Nakamura, A., Ikeda, K., Levesque, L., Fraser, P.E., St-George Hyslop, P.H., Mizusawa, H., and Uchihara, T. (1999). Glial expression of presenilin epitopes in human brain with cerebral infarction and in astrocytoma. *Acta Neuropathol.* **98:** 337-340.

Misson, J-P., Edwards, M.A., Yamamoto, M., and Caviness, V.S. Jr. (1988a). Identification of radial glial cells within the developing murine central nernous system: studies based upon a new immunohistochemical marker. *Brain Res. Dev. Brain Res.* **44:** 95-108.

Misson, J-P., Edwards, M.A., Yamamoto, M., and Caviness, V.S. Jr. (1988b). Mitotic cycling of radial glial cells of the murine cerebral wall: a combined autoradiographic and immunohistochemical study. *Dev. Brain Res.* **38:** 183-190.

Miura, M., Tamura, T., and Mikoshiba, K. (1990). Cell-specific expression of the mouse glial fibrillary acidic protein gene: Identification of the cis- and trans-acting promoter elements for astrocyte-specific expression. *J. Neurochem.* **55:** 1180-1188.

Mohanam, S., Wang, S.W., Rayford, A., Yamamoto, M., Sawaya, R., Nakajima, M., Liotta, L.A., Nicolson, G.L., Stetler-Stevenson, W.G., and Rao, J.S. (1995). Expression of tissue inhibitors of metalloproteinases negative regulators of human glioblastoma invasion *in vivo*. *Clin. Exp. Metast.* **13:** 57-62.

Mohanam, S., Jasti, S.L., Kondraganti, S.R., Chandrasekar, N., Kin, Y., Fuller, G.N., Lakka, S.S., Kyritsis, A.P., Dinh, D.H., Olivero, W.C., Gujrati, M., Yung, W.K., and Rao, J.S. (2001). Stable transfection of urokinase-type plasminogen activator antisense construct modulates invasion of human glioblastoma cells. *Clin. Cancer Res.* **7:** 2519-2526.

Murphy, K.G., Hatton, J.D., and Sang U, H. (1998). Role of glial fibrillary acidic protein expression in the biology of human glioblastoma U-373MG cells. *J, Neurosurg.* **89:** 997-1006.

Nagata, K., Guggenheimer, R.A., Enomoto, T., Lichy, J.H., and Hurwitz, J. (1982). Adenovirus DNA replication *in vitro*: Identification of a host factor that stimulates synthesis of the preterminal protein-dCMP complex. *Proc. Natl. Acad. Sci. U.S.A.* **79:** 6438-6442.

Nakagawa, T., Kubota, T., Kabuto, M., Sato, K., Kawano, H., Hayakawa, T., and Okada, Y. (1994). Production of matrix metalloproteinases and tissue inhibitor of metalloproteinases-1 by brain tumors. *J. Neurosurg.* **81:** 69-77.

Nakanishi, K., Okouchi, Y., Ueki, T., Asai, K., Isobe, I., Eksioglu, Y.Z., Kato, T., Hasegawa, Y., and Kuroda, Y. (1994). Astrocytic contribution of functioning synapse formation estimated by spontaneous neuronal intracellular $Ca2^+$ oscillations. *Brain Res.* **659:** 169-178.

Nakashima, K., Yanagisawa, M., Arakawa, H., Kimura, N., Hisatsune, T., Kawabata, M., Miyazono, K., and Taga, T. (1999). Synergistic signaling in fetal brain by STAT3-Smad1 complex bridged by p300. *Science* **284:** 479-482.

Nakatani, Y., Brenner, M., and Freese, E. (1990a). An RNA polymerase II promoter containing sequences upstream and downstream from the RNA startpoint that direct initiation of transcription from the same site. *Proc. Natl. Acad. Sci. U.S.A.* **87:** 4289-4293.

Nakatani, Y., Horikoshi, M., Brenner, M., Yamamoto, T., Besnard, F., Roeder, R.G., and Freese, E. (1990b). A downstream initiation element required for efficient TATA box binding and *in vitro* function of TFIID. *Nature* **348:** 86-88.

Nebl, G., and Cato, A. (1995). NFI/X proteins: a class of NFI family of transcription factors with positive and negative regulatory domains. *Cell. Mol. Biol. Res.* **41:** 85-95.

Nehls, M.C., Rippe, R.A., Veloz, L., and Brenner, D.A. (1991). Transcription factors nuclear factor I and Sp1 interact with the murine collagen α1(I) promoter. *Mol. Cell. Biol.* **11:** 4065-4073.

Newcomb, E.W., Cohen, H., Lee, S.R., Bhalla, S.K., Bloom, J., Hayes, R.L., and Miller, D.C. (1998). Survival of patients with glioblastoma multiforme is not influenced by altered expression of p16, p53, EGFR, MDM2 or Bcl-2 genes. *Brain Pathol.* **8:** 655-656.

Nielsen, A.L., Holm, I.E., Johansen, M., Bonven, B., Jørgensen, P., Jørgensen, A.L. (2002). A new splice variant of glial fibillary acidic protein, GFAPε, interacts with the presenilin proteins. *J. Biol. Chem.* **277:** 29983-29991.

Noctor, S.C., Flint, A.C., Weissman, T.A., Dammerman, R.S., and Kriegstein, A.R. (2001). Neurons derived from radial glial cells establish radial units in neocortex. *Nature* **409:** 714-720.

Novak, A., Goyal, N., and Gronostajski, R.M. (1992). Four consersved cysteine residues are required for the DNA binding activity of nuclear factor I. *J. Biol. Chem.* **267:** 12986-12990.

Nowock, J., and Sippel, A.E. (1982). Specific protein-DNA interaction at four sites flanking the chicken lysozyme gene. *Cell* **30:** 607-615.

O'Brien, R.M., Noisin, E.L., Suwanichkul, A., Yamasaki, T., Lucas, P.C., Wang, J.-C., Powell, D.R. and Granner, D.K. (1995). Hepatic nuclear factor 3 and hormone-regulated expression of phosphoenolpyruvate carboxykinase and insulin-like growth factor-binding protein-1 genes. *Mol. Cell. Biol.* **15:** 1747-1758.

Ochiai, W., Yanagisawa, M., Takizawa, T., Nakashima, K., and Taga, T. (2001). Astrocyte differentiation of fetal neuroepithelial cells involving cardiotrophin-1-induced activation of STAT3. *Cytokine* **14:** 264-271.

Ockner, R.K., Manning, J.A., Poppenhausen, R.B., and Ho, W.K.L. (1972). A binding protein for fatty acids in cytosol of intestinal mucosa, liver, myocardium, and other tissues. *Science* **177:** 56-58.

Ockner, R., Manning, J.A., and Kane, J.P. (1982). Fatty acid binding protein. Isolation from rat liver, characterization, and immunochemical quantification. *J. Biol. Chem.* **257:** 7872-7878.

Okano-Uchida, T., Himi, T., Komiya, Y., and Ishizaki, Y. (2004). Cerebellar granule cell precursors can differentiate into astroglial cells. *Proc. Natl. Acad. Sci. U.S.A.* **101:** 1211-1216.

Osada, S., Ikeda, T., Xu, M., Nishihara, T., and Imagawa, M. (1997). Identification of the transcriptional repression domain of nuclear factor 1-A. *Biochem. Biophys. Res. Commun.* **238:** 744-747.

Osada, S., Matsubara, T., Daimon, S., Terazu, Y., Xu, M., Nishihara, T., and Imagawa, M. (1999). Expression, DNA-binding specificity and transcriptional regulation of nuclear factor 1 family proteins from rat. *Biochem. J.* **342:** 189-198.

Owada, Y., Yoshimoto, T., and Kondo, H. (1996). Spatiotemporally differential expression of genes for three members of fatty acid-binding proteins in developing and mature rat brains. *J. Chem. Neuroanat.* **12:** 113-122.

Owada, Y., Utsunomiya, A., Yoshimoto, T., and Kondo, H. (1997). Changes in gene expression for skin-type fatty acid binding protein in hypoglossal motor neurons following nerve crush. *Neurosci. Letters* **223:** 25-28.

Paonessa, G., Gounari, F., Frank, R., and Cortese, R. (1988). Purification of a NFI-like DNA binding protein from rat liver and cloning of the corresponding cDNA. *EMBO J.* **7:** 3115-3123.

Parnavelas, J.G., and Nadarajah, B. (2001). Radial glial cells: Are they really glia? *Cell* **31:** 881-884.

Pekney, M, Stanness, K.A., Eliasson, C., Betsholtz, C., and Janigro, D. (1998). Impaired induction of blood-brain barrier properties in aortic endothelial cells by astrocytes from GFAP-deficient mice. *Glia* **22:** 390-400.

Pekney, M., Johansson, C.B., Eliasson, C., Stakeberg, J., Wallen, A., Perlmann, T., Lendahl, U., Betsholtz, C., Berthold, C.H., and Frisen, J. (1999). Abnormal reaction to central nervous system injury in mice lacking glial fibrillary acidic protein and vimentin. *J. Cell. Biol.* **145:** 503-514.

Phelan, C.M., Larsson, C., Baird, S., Futreal, P.A., Ruttledge, M.H., Morgan, K., Tonin, P., Hung, H., Korneluk, R.G., Pollak, M.N., and Narod, S.A. (1996). The human mammary-derived growth inhibitor (MDGI) gene: genomic structure and mutation analysis in human breast tumors. *Genomics* **34:** 63-68.

Pontén, J., and MacIntyre, E.H. (1968). Long term culture of normal and neoplastic human glia. *Acta. Pathol. Microbiol. Scand.* **74:** 465-486.

Prada, C., Puga, J., Pérez-Méndez, L., López, R., and Ramírez, G. (1991). Spatial and temporal patterns of nerogenesis in the chick retina. *Eur. J. Neurosci.* **3:** 559-569.

Prado, F., Vicent, G., Cardalda, C., and Beato, M. (2002). Differential role of the proline-rich domain of nuclear factor 1-C splice variants in DNA binding and transactivation. *J. Biol. Chem.* **277:** 16383-16390.

Prinsen, C.F.M., and Veerkamp, J.H. (1998). Transfection of L6 myoblasts with adipocyte fatty acid-binding protein cDNA does not affect fatty acid uptake but disturbs lipid metabolism and fusion. *Biochem. J.* **329:** 265-273.

Qian, F, Kruse, U., Lichter, P., and Sippel, A.E. (1995). Chromosomal localization of the four genes (NFIA, B, C, and X) for the human transcription factor I by FISH. *Genomics* **28:** 66-73.

Quinlan, R.A., Hatzfeld, M., Franke, W.W., Lustig, A., Schulthess, T., and Engel, J. (1986). Characterization of dimer subunits of intermediate filament proteins. *J. Mol. Biol.* **192:** 337-349.

Quinlan, R.A., Moir, R.D., and Stewart, M. (1989). Expression in *Escherichia coli* of fragments of glial fibrillary acidic protein: characterization, assembly properties and paracrystal formation. *J. Cell Sci.* **93:** 71-83.

Rafty, L.A., Santiago, F.S., and Khachigan, L.M. (2002). NFI/X represses PDGF A-chain transcription by interacting with Sp1 and antagonizing Sp1 occupancy of the promoter. *EMBO J.* **21:** 334-343.

Rakic, P. (1971). Neuron-glia relationship during granule cell migration in developing cerebellar cortex. A Golgi and electronmicroscopic study in Macacus Rhesus. *J. Comp. Neurol.* **141:** 282-312.

Rakic, P. (1972). Mode of cell migration to superficial layers of fetal monkey cortex. *J. Comp. Neurol.* **145:** 61-84.

Rao, M.S., and Mayer-Proschel, M. (1997). Glial-restricted precursors are derived from multipotent neuroepithelial stem cells. *Dev. Biol.* **188:** 48-63.

Rao, J.S. (2003). Molecular mechanisms of glioma invasiveness: the role of the proteases. *Nat. Rev. Cancer* **3:** 489-501.

Reardon, D.A., Entrekin, R.E., Sublett, J., Ragsdale, S., Li, H., Boyett, J., Kepner, J.L., and Look, A.T. (1999). Chromosome arm 6q loss is the most common recurrent autosomal alteration detected in primary pediatric ependymoma. *Genes Chromosomes Cancer* **24:** 230-237.

Reeves, S.A., Helman, L.J., Allison, A., Isreal, M.A. (1989). Molecular cloning and primary structure of human glial fibrillary acidic protein. *Proc. Natl. Acad. Sci. U.S.A.* **86:** 5178-5182.

Rey, J.A., Bello, M.J., de Campos, J.M., Kusak, M.E., Ramos, C., and Benitez, J. (1987). Chromosomal patterns in human malignant astrocytomas. *Cancer Genet. Cytogenet.* **29:** 201-221.

Rickman, D.S., Bobek, M.P., Misek, D.E., Kuick, R., Blaivas, M., Kurnit, D.M., Taylor, J., and Hanash, S.M. (2001). Distinctive molecular profiles of high-grade and low-grade gliomas based on oligonucleotide microarray analysis. *Cancer Res.* 61: 6885-6891.

Roulet, E., Armentero, M-T., Krey, G., Corthésy, B., Dreyer, C., Mermod, N., and Wahli, W. (1995). Regulation of the DNA-binding and transactivational activities of *Xenopus laevis* NFI-X by a novel C-terminal domain. *Mol. Cell. Biol.* **15:** 5552-5562.

Rutka, J.T., and Smith, S.L. (1993). Transfection of himan astrocytoma cells with glial fibrillary acidic protein complementary DNA: Analysis of expression, proliferation, and tumorigenicity. *Cancer Res.* **53:** 3624-3631.

Rutka, J.T., Hubbard, S.L., Fukuyama, K., Matsuzawa, K., Dirks, P.B., and Becker, L.E. (1994). Effects of antisense glial fibrillary acidic protein complementary DNA on the growth, invasion, and adhesion of human astrocytoma cells. *Cancer Res.* **54:** 3267-3272.

Rutka, J.T., Ackerley, C., Hubbard, S.L., Tilup, A., Dirks, P.B., Jung, S., Ivanchuk, S., Kurimoto, M., Tsugu, A., and Becker, L.E. (1998). Characterization of glial filament-cytoskeletal interactions in human astrocytomas: an immuno-ultrastructural analysis. *Eur. J. Cell Biol.* **76:** 279-87.

Rutka, J.T., Ivanchuk, S., Mondal, S., Taylor, M., Sakai, K., Dirks, P., Jun, P., Jung, S., Becker, L.E., and Ackerley, C. (1999). Co-expression of nestin and vimentin intermediate filaments in invasive human astrocytoma cells. *Int. J. Dev. Neurosci.* **17:** 503-15.

Sambrook, J., Fritsch, E.F., and Maniatis, T. (1989). *Molecular Cloning: a laboratory manual.* Cold Spring Harbor Press, pp. 1.29 – 1.46 and pp. 18.64-18.66.

Santoro, C., Mermod, N., Andrews, P., and Tjian, R. (1988). A family of human CCAAT-box-binding proteins active in transcription and DNA replication: cloning and expression of multiple cDNAs. *Nature* **334:** 218-224.

Schaap, F.G., Binas, B., Danneberg, H., Van der Vusse, G.L., and Glatz, J.F.C. (1999). Impaired long-chain fatty acid utilization by cardiac myoctyes isolated from mice lacking the heart-type fatty acid binding protein. *Circ. Res.* **85:** 329-337.

Schaap, F.G., van der Vusse, G.J., and Glatz, J.F.C. (2002). Evolution of the family of intracellular lipid binding proteins in vertebrates. *Mol. Cell. Biochem.* **239:** 69-77.

Schmechel, D., and Rakic, P. (1979). A Golgi study of radial glial cells in developing monkey telencephalon: morphogenesis and transformation into astrocytes. *Anat. Embryol.* **156:** 115-152.

Schmid, C.W., and Jelinek W.R. (1982). The alu family of dispersed repetitive sequences. *Science* **216:** 1065-1070.

Schroeder, F., Atshaves, B.P., Starodub, O., Boedeker, A.L., Smith, R.R., Roths, J.B., Foxworth, W.B., and Kier, A.B. (2001). Expression of liver fatty acid binding protein alters growth and differentiation of embryonic stem cells. *Mol. Cell. Biochem.* **219:** 127-138.

Sehgal, A., Ricks, S., Warrick, J., Boynton, A.L., and Murphy, G.P. (1999). Antisense human neuroglia related cell adhesion molecule hNr-CAM, reduces the tumorigenic properties of human glioblastoma cells. *Anticancer Res.* **19:** 4947-4953.

Seipel, K., Georgiev, O., and Schaffner, W. (1992). Different activation domains stimulate transcription from remote ('enhancer') and proximal ('promoter') positions. *EMBO J.* **11:** 4961-4958.

Sellner, P. (1994). Developmental regulation of fatty acid binding protein in neural tissue. *Dev. Dynam.* **200:** 333-339.

Sellner, P.A., Chu, W., Glatz, J.F.C., and Berman, N.E.J. (1995). Developmental role of fatty acid-binding proteins in mouse brain. *Dev. Brain Res.* **89:** 33-46.

Shibuki, K., Gomi, H., Chen, L., Bao, S., Kim, J.J., Wakatsuki, H., Fujisaki, T., Fujimoto, K., Katoh, A., Ikeda, T., Chen, C., Thompson, R.F., and Itohara, S. (1996). Deficient cerebellar long-term depression, impaired eyeblink conditioning, and normal motor coordination in GFAP mutant mice. *Neuron* **16:** 587-599.

Shimizu, F., Watanabe, T.K., Shinomiya, H., Nakamura, Y., and Fujiwara, T. (1997). Isolation and expression of a cDNA for human brain fatty acid-binding protein (B-FABP). *Biochim. Biophys. Acta* **1354:** 24-28.

Shin, S.-I., Freedman, V.H., Risser, R., and Pollack, R. (1975). Tumorigenicity of virus-transformed cells in nude mice is correlated specifically with anchorage independent growth *in vitro*. *Proc. Natl. Acad. Sci. U.S.A.* **72:** 4435-4439.

Shiota, C. Miura, M., and Mikoshiba, K. (1989). Developmental profile and differential localization of mRNAs of myelin proteins (MBP and PLP) in oligodendrocytes in the brain and in culture. *Dev. Brain Res.* **45:** 83-94.

Shu, H., Wong, B., Zhou, G., Li, Y., Berger, J., Woods, J.W., Wright, S.D., and Cai, T.Q. (2000). Activation of PPARalpha or gamma reduces secretion of matrix metalloproteinase 9 but not interleukin 8 from human monocytic THP-1 cells. *Biochem. Biophys. Res. Commun.* **267:** 345-349.

Shu, T., Butz, K.G., Plachez, C., Gronostajski, R.M., and Richards, L.J. (2003). Abnormal development of forebrain glia and commissural projections in NFIa knock-out mice. *J. Neurosci.* **23:** 203-212.

Singh, M.V., and Ntambi, J.M. (1998). Nuclear factor 1 is essential for the expression of stearoyl-CoA desaturase 1 gene during preadipocyte differentiation. *Biochim. Biophys. Acta* **1398:** 148-156.

Singh, S., Sadacharan, S., Su, S., Belldegrun, A., Persad, S., and Singh, G. (2003). Overexpression of vimentin: role in the invasive phenotype in an androgen-independent model of prostate cancer. *Cancer Res.* **63:** 2306-2311.

Smith, E.R., and Storch, J. (1999). The adipocyte fatty acid-binding protein binds to membranes by electrostatic interactions. *J. Biol. Chem.* **274:** 35325-35330.

Song, M., and Ghosh, A. (2004). FGF2-induced chromatin remodeling regulates CNTF-mediated gene expression and astrocytes differentiation. *Nat. Neurosci.* **7:** 229-235.

Spitsberg, V.L., Matitashvili, E., and Gorewit, R.C. (1995). Association and coexpression of fatty acid-binding protein and glycoprotein CD36 in the bovine mammary gland. *Eur. J. Biochem.* **230**: 872-878.

Stein G.H. (1979). T98G: An anchorage-independent human tumor cell line that exhibits stationary phase G1 arrest *in vitro*. *J. Cell Physiol.* **99:** 43-54.

Stomski, F.C., Gani, J.S., Bates, R.C., and Burns, G.F. (1992). Adhesion to thrombosponin by human fibroblasts is mediated by multiple receptors and includes a role for glycoprotein 88 (CD36). *Exp. Cell Res.* **198**: 85-92.

Storch, J., and Thumser, A.E.A. (2000). The fatty acid transport function of fatty acid-binding proteins. *Biochim. Biophys. Acta* **1486:** 28-44.

Sumner, C., Shinohara, T., Durham, L., Traub, R., Major, E.O., Amemiya, K. (1996). Expression of multiple classes of the nuclear factor-1 family in the developing human brain: differential expression of two classes of NF-1 genes. *J. Neurovirol.* **2:** 87-100.

Takanaga, H., Yoshitake, T., Hara, S., Yamasaki, C., and Kunimoto, M. (2004). cAMP-induced astrocytic differentiation of C6 glioma cells is mediated by autocrine interleukin-6. *J. Biol. Chem.* **279:** 15441-15447.

Tamura, T., Miura, M., Ikenaka, K., and Mikoshiba, K. (1988). Analysis of transcription control elements of the mouse myelin basic protein gene in HeLa cell extracts: demonstration of a strong NFI-binding motif in the upstream region. *Nucleic Acids Res.* 16: 11441-11459.

Tan, N.S., Shaw, N.S., Vinckenbosch, N., Liu, P., Yasmin, R., Desvergne, B., Wahli, W., and Noy, N. (2002). Selective cooperation between fatty acid binding proteins and peroxisome proliferator-activated receptors in regulating transcription. *Mol. Cell. Biol.* **22:** 5114-5127.

Thompson, J., Winter, N., Terwey, J., Bratt, J., and Banaszak, L. (1997). The crystal structure of the liver fatty acid-binding protein. A complex with two bound oleates. *J. Biol. Chem.* **272:** 7140-7150.

Toda, M., Miura, M., Asou, H., Toya, S., and Uyemura, K. (1994). Cell growth suppression of astrocytoma C6 cells by GFAP cDNA transfection. *J. Neurochem.* **63:** 1975-1978.

Toda, M., Miura, M., Asou, H., Sugiyama, I., Kawase, T., and Uyemura, K. (1999). Suppression of glial tumor growth by expression of glial fibrillary acidic protein. *Neurochem. Res.* **24:** 339-343.

Toresson, H., Mata, D.U., Fagerstrom, C., Perlmann, T., and Campbell, K. (1999). Retinoids are produced by glia in the lateral ganglionic eminence and regulate striatal neuron differentiation. *Development* **126:** 1317-1326.

Tsujimura, K., Tanaka, J., Ando, S., Matsuoka, Y., Kusubata, M., Sugiura, H., Yamauchi, T., and Inagaki, M. (1994). Identification of phosphorylation sites on glial fibrillary acidic protein for cdc2 kinase and Ca(2+)-calmodulin-dependent protein kinase II. *J. Biochem.* (Tokyo) **116:** 426-434.

Vallejo, I., and Vallejo, M. (2002). Pituitary adenylate cyclase-activating polypeptide induces astrocyte differentiation of precursor cells from developing cerebral cortex. *Mol. Cell. Neurosci.* **21:** 671-683.

van der Meulen, J.D.M., Houthoff, H.J., and Ebels, E.J. (1978). Glial fibrillary acidic protein in human gliomas. *Neuropathol. App. Neurobiol.* **4:** 177-190.

Veerkamp, J.H., and Zimmerman, A.W. (2000). Fatty acid-binding proteins of the nervous tissue. *J. Mol. Neurosci.* **16:** 133-142.

Velasco, M.E., Dahl, D., Roessmann, U., and Gambetti, P. (1980). Immunohistochemical localization of glial fibrillary acidic protein in human glial neoplasms. *Cancer* **45:** 484-494.

Wang, H.L., and Kurtz, A. (2000). Breast cancer growth inhibition by delivery of the MDGI-derived peptide P108. *Oncogene* **19:** 2455-2460.

Wang, H., Wang, H., Shen, W., Huang, H., Hu, L., Ramdas, L., Zhou, Y.H., Liao, W.S., Fuller, G.N., and Zhang, W. (2003). Insulin-like growth factor binding protein 2 enhances glioblastoma invasion by activating invasion-enhancing genes. *Cancer Res.* **63:** 4315-4321.

Ware, M.L., Berger, M.S., and Binder, D.K. (2003). Molecular biology of glioma tumorigenesis. *Histol. Histolpathol.* **18:** 207-216.

Weinstein, D.E., Shelanski, M.L., and Liem, R.H. (1991). Suppression by antisense mRNA demonstrates a requirement for the glial fibrillary acidic protein in the formation of stable astrocytic processes in response to neurons. *J. Cell Biol.* **112:** 1205-1213.

Westermark, B., Pontén, J., and Hugosson, R. (1973). Determinants for the establishment of permanent tissue culture lines from human gliomas. *Acta. Pathol. Microbiol. Scand.* **81:** 791-805.

Wehrle-Haller, B., and Imhof, B.A. (2002). The inner lives of focal adhesions. *Trends Cell Biol.* **12**: 382-389.

Wilhelmsson, U., Eliasson, C., Bjerkvig, R., and Pekny, M. (2003). Loss of GFAP expression in high-grade astrocytomas does not contribute to tumor development or progression. *Oncogene* **22:** 3407-3411.

Wolfrum, C., Borrmann, C.M., Borchers, T., and Spener, F. (2001). Fatty acids and hypolipidemic drugs regulate peroxisome proliferator-activated receptors α- and γ-mediated gene expression via liver fatty acid binding protein: A signaling path to the nucleus. *Biochemistry* **98:** 2323-2328.

Wootan, M.G., Bernlohr, J., and Storch, J. (1993). Mechanism of fluorescent fatty acid transfer from adipocyte fatty acid binding protein to membrane. *Biochemistry* **32:** 8622-8627.

Wootan, M.G., and Storch, J. (1994). Regulation of fluorescent fatty acid transfer from adipocyte and heart fatty acid binding proteins by acceptor membrane lipid composition and structure. *J. Biol. Chem.* **269:** 10517-10523.

Xiang, M., Gan, L., Zhou, L., Klein, W.H., and Nathans, J. (1996). Targeted deletion of the mouse POU domain gene Brn-3a causes selective loss of neurons in the brainstem and trigeminal ganglion, uncoordinated limb movement, and impaired suckling. *Proc. Natl. Acad. Sci. U.S.A.* **93:** 11950-11955.

Xu, L.Z., Sanchez, R., Sali, A., and Heintz, N. (1996). Ligand specificity of brain lipid-binding protein. *J. Biol. Chem.* **271:** 24711-24719.

Yanagisawa, M., Nakashima, K., and Taga, T. (1999). STAT3-mediated astrocytes differentiation from mouse fetal neuroepithelial cells by mouse oncostatin M. *Neurosci. Lett.* **269:** 169-172.

Yang, B-S., Gilbert, J.D., and Freytag, S.O. (1993). Overexpression of Myc suppresses CCAAT transcription factor/nuclear factor 1-dependent promoters *in vivo*. *Mol. Cell. Biol.* **13:** 3093-3102.

Yang, Y., Spitzer, E., Kenny, N., Zshiesche, W., Li, M., Kromminga, A., Muller, T., Spener, F., Lezius, A., Veerkamp, J.H., Smith, G.H., Salomon, D.S., and Grosse, R. (1994). Members of the fatty acid binding protein family are differentiation factors for the mammary gland. *J. Cell. Biol.* **127:** 1097-1109.

Young, J.K., Baker, J.H., and Müller, T. (1996). Immunoreactivity for brain-fatty acid binding protein in Gomori-postive astrocytes. *Glia* **16:** 218-226.

Zamorano, A., Lamas, M., Vergara, P., Naranjo, J.R., and Segovia, J. (2003). Transcriptionally mediated gene targeting of *gas*1 to glioma cells elicits growth arrest and apoptosis. *J. Neurosci. Res.* **71:** 256-263.

Zelenika, D., Grima, B., Brenner, M., and Pessac, B. (1995). A novel glial fibrillary acidic protein mRNA lacking exon I. *Mol. Brain Res.* **30:** 251-258.

Zhang, W., Han, S.W., McKeel, D.W., Goate, A., and Wu, J.Y. (1998). Interaction of presenilins with the filamin family of actin-binding proteins. *J. Neurosci.* **18:** 914-922.

Zhang, X., and Miskimins, R. (1993). Binding at an NFI site is modulated by cyclic AMP-dependent activation of myelin basic protein gene expression. *J. Neurochem.* **60:** 2010-2017.

Zhang, Y., Zhao, W., Zhang, H.J., Domann, F.E., and Oberley, L.W. (2002). Overexpression of copper zinc superoxide dismutase suppresses human glioma cell growth. *Cancer Res.* **62:** 1205-1212.

Zhuo, L., Theis, M., Alvarez-Maya, I., Brenner, M., Willecke, K., and Messing, A. (2001). hGFAP-cre transgenic mice for manipulation of glial and neuronal function *in vivo. Genesis* **31:** 85-94.

Zhou, R., and Skalli, O. (2000). TGF-α differentially regulates GFAP, vimentin, and nestin gene expression in U-373 MG glioblastoma cells: Correlation with cell shape and motility. *Exp. Cell Res.* **254:** 269-278.

Zhou, X.P., Li, Y.J., Hoang-Xuan, K., Laurent-Puig, P., Mokhtari, K., Longy, M., Sanson, M., Delattre, J.Y., Thomas, G., and Hamelin, R. (1999). Mutational analysis of the

PTEN gene in gliomas: molecular and pathological correlations. *Int. J. Cancer* **84:** 150-154.

Zimmerman, A.W., and Veerkamp, J.H. (2002). New insights into the structure and function of fatty acid-binding proteins. *Cell. Mol. Life Sci.* **59:** 1096-1116.

Zorbas, H, Rein, T., Krause, A., Hoffmann, K., and Winnacker, E.-L. (1992). Nuclear factor I (NFI) binds to an NFI-type site but not to the CCAAT site in the human α-globin gene promoter. *J. Biol. Chem.* **267:** 8478-8484.